Planar graphs : non-aligned drawings, power domination and enumeration of Eulerian orientations

Claire Pennarun

THÈSE

PRÉSENTÉE À

L'UNIVERSITÉ DE BORDEAUX

ÉCOLE DOCTORALE DE MATHÉMATIQUES ET D'INFORMATIQUE

par **Claire Pennarun**

POUR OBTENIR LE GRADE DE

DOCTEUR

SPÉCIALITÉ : INFORMATIQUE

Planar graphs: non-aligned drawings, power domination and enumeration of Eulerian orientations

---

Date de soutenance : 14 juin 2017

Devant la commission d'examen composée de :

Nicolas BONICHON	Maître de conférences, Université de Bordeaux	Directeur
Mireille BOUSQUET-MÉLOU	Directrice de recherche, CNRS	Examinatrice
Nadia BRAUNER-VETTIER .	Professeur, Université Joseph Fourier	Présidente du jury
Paul DORBEC	Maître de conférences, Université de Bordeaux	Directeur
Éric FUSY	Chargé de recherches, École Polytechnique ...	Rapporteur
Michael HENNING	Professeur, University of Johannesburg	Rapporteur

– 2017 –

Graphes planaires : dessins non-alignés, domination de puissance et énumération d'orientations Eulériennes

Dans cette thèse, nous étudions trois problèmes concernant les graphes planaires.

Nous travaillons tout d'abord sur les dessins planaires non-alignés, c'est-à-dire des dessins planaires de graphes sur une grille sans que deux sommets se trouvent sur la même ligne ou la même colonne. Nous caractérisons les graphes planaires possédant un tel dessin sur une grille à n lignes et n colonnes, et nous présentons deux algorithmes générant un dessin planaire non-aligné avec arêtes brisées sur cette grille pour tout graphe planaire, avec $n-3$ ou $\min(\frac{2n-5}{3}, \#\{\text{triangles séparateurs}\}+1)$ brisures au total. Nous proposons également deux algorithmes dessinant un dessin planaire non-aligné sur des grilles d'aire $O(n^4)$. Nous donnons des résultats spécifiques concernant les graphes 4-connexes et de type triangle-emboîté.

Le second sujet de cette thèse est la domination de puissance dans les graphes planaires. Nous exhibons une famille de graphes ayant un nombre de domination de puissance γ_P au moins égal à $\frac{n}{6}$. Nous montrons aussi que pour tout graphe planaire maximal G à $n \geq 6$ sommets, $\gamma_P(G) \leq \frac{n-2}{4}$. Enfin, nous étudions les grilles triangulaires T_k à bord hexagonal de dimension k et nous montrons que $\gamma_P(T_k) = \lceil \frac{k}{3} \rceil$.

Nous étudions également l'énumération des orientations planaires Eulériennes. Nous proposons tout d'abord une nouvelle décomposition de ces cartes. Puis, en considérant les orientations des dernières $2k-1$ arêtes autour de la racine, nous définissons des sous- et sur-ensembles des orientations planaires Eulériennes paramétrés par k. Pour chaque classe, nous proposons un système d'équations fonctionnelles définissant leur série génératrice, et nous prouvons que celle-ci est toujours algébrique. Nous montrons ainsi que la constance de croissance des orientations planaires Eulériennes est comprise entre 11.56 et 13.005.

Liste des mots-clés: graphe planaire, algorithme, dessin planaire, domination de puissance, énumération

Planar graphs: non-aligned drawings, power domination and enumeration of Eulerian orientations

In this thesis, we present results on three different problems concerning planar graphs.

We first give some new results on planar non-aligned drawings, i.e., planar grid drawings where vertices are all on different rows and columns. We show that not every planar graph has a non-aligned drawing on a grid with n rows and columns, but we present two algorithms generating a non-aligned polyline drawings on such a grid requiring either $n-3$ or $\min(\frac{2n-5}{3}, \#\{\text{separating triangles}\}+1)$ bends in total. Concerning non-minimal grids, we give two algorithms drawing a planar non-aligned drawing on grids with area $O(n^4)$. We also give specific results for 4-connected graphs and nested-triangle graphs.

The second topic is power domination in planar graphs. We present a family of graphs with power dominating number γ_P at least $\frac{n}{6}$. We then prove that for every maximal planar graph G of order n, $\gamma_P(G) \leq \frac{n-2}{4}$, and we give a constructive algorithm. We also prove that for triangular grids T_k of dimension k with hexagonal-shape border, $\gamma_P(T_k) = \lceil \frac{k}{3} \rceil$.

Finally, we focus on the enumeration of planar Eulerian orientations. After proposing a new decomposition for these maps, we define subsets and supersets of planar Eulerian orientations with parameter k, generated by looking at the orientations of the last $2k-1$ edges around the root vertex. For each set, we give a system of functional equations defining its generating function, and we prove that it is always algebraic. This way, we show that the growth rate of planar Eulerian orientations is between 11.56 and 13.005.

List of keywords: planar graph, algorithm, graph drawing, power domination, enumeration

Contents

Remerciements

Ces trois ans de thèse ont été une belle et incroyable expérience, pendant laquelle j'ai rencontré des personnes formidables, voyagé énormément, appris des milliers de choses, à la fois en théorie des graphes et sur moi-même. Cette période de ma vie n'aurait pas été aussi fructueuse sans l'aide de nombreuses personnes que je veux remercier ici (et aussi sûrement quelques unes que j'aurais malencontreusement oublié, qu'elles me pardonnent).

En premier lieu, j'aimerais remercier mes (fabuleux, il faut bien le dire) directeurs de thèse, Nicolas et Paul. Ce fut un grand plaisir de travailler avec eux, et j'espère que beaucoup d'autres doctorants auront la chance de profiter de leur encadrement et de leurs conseils. Merci pour votre confiance et votre soutien pendant ces trois ans !

Merci à Mike Hennning et à Eric Fusy, d'avoir accepté d'être rapporteurs pour ma thèse. C'est un grand plaisir de vous compter dans ce jury. Merci également à mes deux examinatrices, Nadia Brauner et Mireille Bousquet-Mélou. Mireille, tu as été comme ma "marraine" de thèse pendant ces trois ans, et j'espère que nous discuterons encore souvent de féminisme et de vélo !

J'ai eu la chance d'effectuer ma thèse dans un cadre idéal, au LaBRI, et je suis déjà triste à l'idée de quitter un jour cet endroit. L'équipe CombAlgo a été une merveilleuse équipe d'accueil, et je tiens à remercier tous les membres des groupes de travail de combinatoire du vendredi matin et celui de théorie des graphes du vendredi après-midi. Grâce à vous tous, les fins de semaines étaient toujours studieuses, joyeuses et pleines de victuailles ! Des remerciements particuliers à tous les collègues (pas nécessairement "grapheux" ou "combinatoriciens") avec qui j'ai discuté de la recherche ou d'autres choses (souvent), rigolé (régulièrement), bavardé en réunion (un peu) ou partagé des repas (beaucoup, aussi bien au Bleu qu'au Haut-Carré). Merci aussi à toute l'équipe administrative, qui a permis que cette thèse se déroule de la meilleure manière sur le plan de la paperasse diverse et variée. Je tiens également à remercier tous les doctorants et anciens doctorants avec qui j'ai traversé la thèse, et bien sûr mes co-bureaux, Matthieu (râleur mais on l'aime bien) et Tristan (et son régime de bananes), ce fut très agréable de partager ce grand bureau avec vous !

Merci à mes collègues de l'IUT, avec qui ce fut si agréable de travailler pendant mes trois ans de monitorat. Merci notamment à Isabelle, Romain et Olivier, qui

ont suivi mon parcours d'enseignante pendant cette thèse et qui ont toujours été disponibles et à l'écoute. Je remercie aussi mes étudiants, qui ont fait que ces cours n'ont jamais été monotones. Grâce à vous tous, j'ai appris beaucoup sur l'enseignement (et j'ai gagné une carte à mon effigie).

Pendant ma thèse, j'ai eu la chance de beaucoup voyager et j'ai rencontré des personnes formidables. Merci à Aline, Valentin, Daniel, Lucas et Louis de m'avoir accueilli et d'avoir partagé leur bureau et leurs connaissances avec moi pendant mes séjours en métropole. Thank you to Jit, for inviting me for three great months in Canada, and for your neverending scientific curiosity, to Therese, for being the first person to show interest in my results and trusted me to work together, to all the members of the Computational Geometry group in Ottawa (in particular Carsten and Sander, for being positive and helpful when needed, and dreadfully research-efficient too!), to Liz, Buddy and Sarah for welcoming me with such warmth during Canada's bitter winter (I now have a Canadian family, mind you!).

Faire de la recherche, ce n'est possible que si vous avez des guides. Alors merci à tous les professeurs que j'ai eu la chance de rencontrer sur mon chemin, avec un merci en particulier à Marc Erb, Sylvia Ramond, Claire Sageaux et François Maricourt, qui ont été des guides formidables. Merci aussi à mes encadrants de stage de recherche pendant mes études, Lisl Weynans, Anne Canteaut, Anca Muscholl, Sylvain Salvati et David Auber, qui m'ont vu progresser en recherche depuis le début de ma licence.

Ces trois ans ont aussi été l'occasion de faire d'autres activités que l'enseignement et la recherche, et c'était parfois primordial. Alors merci à mes collègues de Maths à Modeler (et leurs vieilles cigognes), à mes amies de Femmes et Sciences, à mes camarades des ateliers du samedi et des différentes chorales où j'ai pu chanter, à mes anciens professeurs et leurs collègues pour m'avoir accueilli au lycée Pape Clément si souvent. Un grand merci à Jean-Laurent, qui a su transformer mon énergie en chant pendant cette thèse !

Merci à tous les potes et tous les proches, d'ici et d'ailleurs, qui ont partagé des bières, des blagues, des soirées... Ces remerciements sont l'occasion de vous dire à quel point vous êtes importants pour moi. Vous savoir derrière moi m'a toujours aidé à progresser (notamment parce que j'ai peur de vous des fois). Merci en particulier à Arnaud, Arno, Alexandre, Alexis B. et Alexis C., Antoine, Benjamin, Boris, Clara, Germain, Grégoire, Jaufré, Lena, Lucas, Jean-Laurent, Nina et Valentine (last but not least!). La vie serait bien triste sans vous tous !

Merci à ma famille, avec une mention très spéciale à mes parents et ma soeur, qui m'ont toujours aidé, supporté et permis de m'épanouir, et qui sont les personnes les plus extraordinaires et drôles du monde. Je vous aime :)

Surtout, merci à Alex, pour tout. Grâce à toi, je sais mieux qui je suis et qui je veux être.

Résumé (en français)

> *Je ne connais pas les réponses, mais il y a quelques jours je ne savais pas qu'il y avait des questions.*
>
> Terry Pratchett, *Nation*

Ce chapitre consiste en une traduction directe de l'introduction en anglais vers le français.

Les résultats présentés dans cette thèse, bien que très différents les uns des autres, appartiennent tous au domaine de la *théorie des graphes*. Ce résumé est donc pour moi une bonne opportunité de présenter le concept des graphes, et en quoi la théorie des graphes est une manière de penser intéressante quand on essaie de résoudre certains types de problèmes.

Afin d'illustrer cela, prenons un exemple simple, mais parlant. Si vous faites régulièrement de la pâtisserie, il vous est sûrement déjà arrivé la chose suivante : vous aviez prévu de faire des crèpes, et vous réalisez que vous n'avez plus de beurre. Qu'à cela ne tienne, la recette indique justement que vous pouvez remplacer le beurre par de l'huile d'olive (et vous en avez, ça tombe bien), donc tout va pour le mieux. Maintenant, supposez que votre placard et votre frigo sont assez réduits, et que vous oubliez souvent de faire les courses avant de préparer votre repas. Quels sont les ingrédients "clé" que vous devriez toujours avoir sous la main afin de pouvoir faire n'importe quel plat (en substituant peut-être des ingrédients à ceux prévus dans la recette) sans avoir besoin d'aller faire les courses? En d'autres termes, quel est le nombre minimum d'ingrédients que vous devriez avoir de telle sorte que tout ingrédient que vous n'avez pas peut être remplacé par un ingrédient que vous avez ? (Attention : ceci n'est pas un livre de cuisine. Nous ne garantissons pas que le résultat soit bon, ou même consommable.) On pourra considérer que deux ingrédients sont interchangeables si au moins une recette autorise à remplacer l'un par l'autre. Une première façon de faire est de noter les noms de chaque paire d'ingrédients interchangeables, comme dans la Figure 1a. Mais cette solution rend la lecture des relations entre les ingrédients difficiles, et ne semble donc pas efficace pour résoudre ce problème.

Une autre manière de voir notre problème de "placard minimal" est d'essayer de se concentrer sur le coeur du problème, c'est-à-dire séparer l'information pertinente

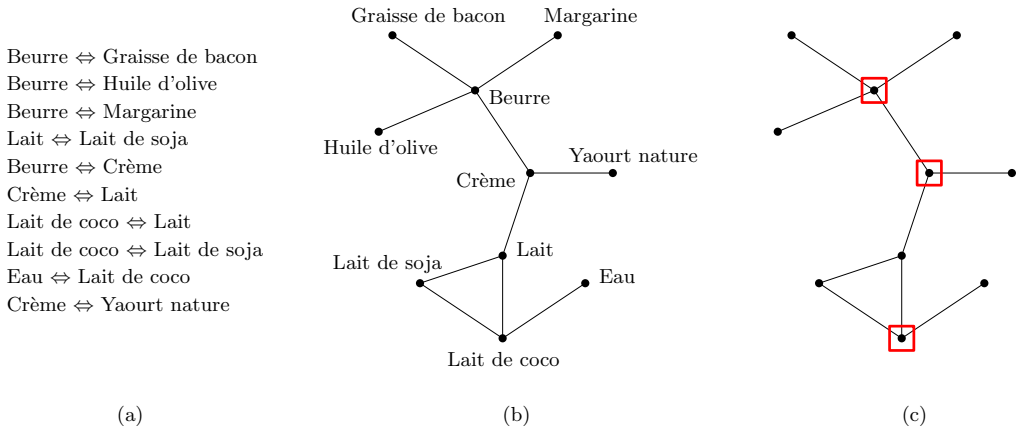

Figure 1: (a) La liste des substitutions potentielles. (b) Le graphe correspondant. (c) Les sommets sélectionnés (encadrés en rouge) sont voisins de tous les sommets non-sélectionnés du graphe.

de la superflue, qui peut être supprimée sans changer le problème. Dans notre cas, ce qui est important n'est pas vraiment le nom des ingrédients, mais plutôt leurs *relations*. L'objet mathématique qui permet de modéliser les relations deux-à-deux d'un ensemble d'entités donné est un *graphe*.

Le graphe correspondant à notre problème (voir Figure 1b) contient des *sommets*, qui représentent les ingrédients, et des *arêtes*, symbolisant les relations d'"échange potentiel" entre deux ingrédients [1]. Résoudre notre problème revient maintenant en fait à trouver ce qu'on appelle un *ensemble dominant minimum* dans le graphe. Dans notre exemple, il est facile de voir qu'acheter du lait de coco, de la crème et du beurre suffit à couvrir toutes les possibilités d'échange nécessaires, alors qu'on ne peut pas trouver seulement deux ingrédients suffisants pour permettre toutes les substitutions. Cela peut également être vu directement en étudiant la structure du graphe (see Figure 1c) : comme il y a trois sommets n'ayant qu'un voisin (et que tous ces sommets sont distincts), l'ensemble dominant minimum du graphe ne peut pas être de taille inférieure à trois.

Beaucoup de problèmes de la vie courante, ainsi que de nombreux problèmes industriels, peuvent être modélisés par des graphes, une fois que l'information superflue a été supprimée. La transformation d'un problème en un problème de graphe nous permet donc d'appliquer des algorithmes et/ou des résultats de la théorie des graphes pour le résoudre.

Certains graphes ayant des propriétés particulières sont spécialement étudiés. C'est le cas des *graphes planaires* ; un graphe planaire est un graphe qui peut être représenté dans le plan (c'est-à-dire dessiné) sans que ses arêtes ne se croisent (comme le graphe de la Figure 1). En tant qu'objets mathématiques, les graphes planaires ont beaucoup de belles propriétés, comme la formule d'Euler. Ces pro-

[1] Un graphe très similaire dans sa conception, appelé le *flavor network* ou *graphe des saveurs*, a été utilisé pour trouver des motifs distinctifs dans différentes traditions culinaires [AABB11]. Dans ce graphe, les sommets sont aussi les ingrédients, tandis qu'il existe une arête entre deux ingrédients qui partagent un même composé aromatique.

priétés peuvent aider à prouver un résultat, puisque ajouter des contraintes sur les objets limite le degré de liberté de la solution recherchée. Cependant, la planarité peut également empêcher un problème de devenir simple à résoudre ; par exemple, certains problèmes de décision restent NP-complets, même en étant restreints à la classe des graphes planaires. Ainsi, les graphes planaires forment une classe intéressante : la complexité des problèmes peut soit chuter drastiquement ou rester très élevée quand on les restreint à eux. Les graphes planaires sont également présents dans de nombreux contextes scientifiques autres que les mathématiques et l'informatique ; en analyse d'image par exemple, les pixels ou les régions de couleurs d'une image peuvent être représentés par des sommets, créant une représentation de l'image par un graphe planaire. Des algorithmes s'appliquant sur les graphes planaires servent notamment pour résoudre des problèmes de segmentation d'image. En chimie, la caractérisation de molécules planaires permet de d'apparier des structures chimiques en temps polynomial, et certains graphes planaires spécifiques peuvent représenter des structures carbonées complexes, comme les fullerènes.

Cette thèse traite de problèmes concernant trois sujets différents (le dessin de graphes, la domination de puissance et l'énumération de certaines cartes) dans lesquels la planarité joue un rôle important. Nous donnons maintenant le contexte global de chaque problème, et présentons nos contributions. Pour chacun de ces sujets, les définitions nécessaires et un état de l'art détaillé sont donnés en introduction du chapitre correspondant. Pour cette raison (et pour éviter les redites), nous omettons de nombreuses définitions dans ce résumé. Pour familiariser le lecteur avec les notions et les objets utilisés tout le long de ce manuscrit, le Chapitre 1 contient des définitions, notations et exemples basiques sur les graphes et les cartes, ainsi qu'une introduction générale aux méthodes de la combinatoire énumérative.

Le premier sujet de cette thèse est le *dessin planaire de graphes*. Comme dans notre problème du "placard minimal", dessiner un graphe est une manière naturelle de représenter l'information qu'il contient. De plus, les dessins de graphes comportant peu de croisements d'arêtes sont en général plus agréables et plus simples à comprendre que ceux avec beaucoup de croisements. Par définition, tout graphe planaire a un dessin planaire, c'est-à-dire un placement des sommets et un dessin des arêtes avec des courbes tels que les courbes représentant les arêtes ne se croisent pas. Cependant, savoir qu'un graphe est planaire ne suffit pas à savoir *comment* le dessiner planairement ; il faut donc des algorithmes, qui, à partir d'un graphe planaire, produisent un dessin également planaire. On peut en fait imposer que le dessin final n'utilise que des segments de droites pour les arêtes, comme l'ont prouvé (indépendamment) Wagner [Wag36], Fáry [Fá48] et Stein [Ste51]. De plus, on peut considérer que les algorithmes de dessin assignent à tous les sommets des coordonnées entières, et donc que les dessins sont faits sur une grille régulière, où les sommets sont placés aux intersections des lignes et des colonnes. Evidemment, on veut éviter que le dessin final prenne trop de place, et il est donc naturel d'essayer d'estimer la largeur et la hauteur de la grille de taille minimale contenant un dessin planaire avec segments (c'est-à-dire dans lequel les arêtes sont des segments de droite) de n'importe quel graphe planaire. Schnyder [Sch90] a notamment exhibé une construction permettant de dessiner tout graphe planaire à n sommets sur une

grille de taille $(n-2) \times (n-2)$, et il est conjecturé que la taille minimale d'une telle grille est $\lceil \frac{2n}{3} \rceil \times \lceil \frac{2n}{3} \rceil$. Remarquons qu'il est suffisant de prouver des résultats pour les graphes planaires maximaux, qui sont les graphes auxquels aucune arête ne peut être ajoutée sans perdre la planarité. En effet, on peut transformer n'importe quel graphe planaire en un graphe planaire maximal en ajoutant des arêtes, puis dessiner ce nouveau graphe et enfin supprimer les arêtes ajoutées précédemment. Les algorithmes de dessin concernant les graphes planaires maximaux reposent généralement sur une structure ajoutée au graphe, comme les forêts de Schnyder ou des orientations obtenues par un ordre canonique.

Dans le chapitre 2, nous étudions les *dessins planaires non-alignés*, dans lesquels chaque ligne et colonne de la grille contient au plus un sommet du graphe (voir Figure 7a, b, c). Cette contrainte aditionnelle provient de considérations de visualisation, et permet au dessin d'avoir de bonnes propriétés, par exemple en termes de préservation de la carte mentale. Il est clair que tout graphe planaire à n sommets requiert ce que nous appelons une grille minimale (de taille $(n-1) \times (n-1)$, donc avec n lignes et n colonnes) pour admettre un dessin non-aligné planaire. En comparaison avec le résultat de Schnyder décrit plus haut, cette addition d'une ligne et une colonne est-elle suffisante pour compenser (en un sens) la contrainte "non-aligné" ?

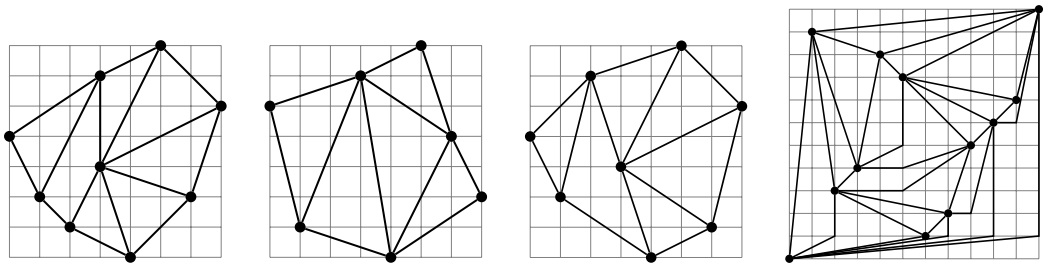

Figure 2: (a) Un dessin planaire sur une grille, mais pas non-aligné. (b et c) Deux dessins planaires non-alignés avec segments. (d) Un dessin planaire non-aligné avec brisures.

Malheureusement, nous montrons qu'en fait, parmi tous les graphes planaires maximaux à n sommets, un seul admet un dessin *planaire non-aligné avec segments* sur une grille de taille $(n-1) \times (n-1)$. Nous progressons alors suivant deux axes : ajouter des brisures aux arêtes et conserver un dessin sur une grille minimale (voir Figure 7d), ou autoriser plus de lignes et/ou de colonnes. Nous considérons tout d'abord les dessins planaires non-alignés *avec brisures*, en essayant de minimiser le nombre de ces dernières. Nous présentons un algorithme linéaire utilisant les propriétés des forêts de Schnyder des graphes planaires maximaux, et garantissant $n-3$ brisures dans le dessin final. Nous montrons également que les graphes 4-connexes ont un dessin non-aligné planaire sur la grille minimale avec au plus une brisure, et nous utilisons ce résultat comme élément central d'un algorithme calculant un dessin non-aligné planaire sur la grille minimale de n'importe quel graphe planaire. Cet

algorithme s'effectue en temps polynomial, et le nombre de brisures final dépend du nombre de triangles séparateurs du graphe d'entrée. Dans un second temps, nous nous intéressons aux dessins non-alignés planaires avec segments dans des grilles de taille supérieure, et nous proposons deux algorithmes polynomiaux générant de tels dessins sur des grilles d'aire $O(n^4)$. Ces deux algorithmes sont des extensions de constructions classiques du dessin de graphe : la méthode de "shift" de de Fraysseix et al. [DFPP90] et la méthode des réaliseurs de Schnyder [Sch89; Sch90]. Pour finir, nous montrons que les graphes dits triangle-emboîtés possèdent un dessin planaire non-aligné avec segments sur une grille de taille $(n-1) \times O(n)$.

Les problèmes d'optimisation combinatoire (c'est-à-dire, étant donné un paramètre p, quelle est la valeur de p pour un graphe donné ? pour une famille de graphes ?) sont un second domaine dans lequel les graphes planaires jouent un rôle important. Pour certains problèmes, l'hypothèse de planarité est suffisante pour obtenir des résultats importants, comme par exemple dans le cas du très célèbre Théorème des quatre couleurs (qui dit que tout graphe planaire possède une coloration de ses sommets utilisant quatre couleurs et telle que deux sommets adjacents sont colorés différemment). Dans d'autres cas, les propriétés de planarité ne sont pas suffisantes pour conclure, et l'on doit soit restreindre encore la classe de graphe étudiée, soit renforcer le graphe avec une structure, pour que des résultats apparaissent. C'est par exemple le cas du problème de *domination* (aussi appelé "problème du placard minimal" dans cette introduction). Etant donné un graphe, un ensemble de sommets sélectionnés est dit *ensemble dominant* du graphe si tout sommet non-sélectionné est voisin d'un sommet sélectionné. L'ordre minimal d'un tel ensemble est le *nombre de domination* du graphe (le nombre de domination du graphe de la Figure 1c est trois, comme vu plus haut). Décider si le nombre de domination d'un graphe est au plus un entier donné est un exemple de problème NP-complet sur les graphes planaires [GNR08]. Une borne générale concernant le nombre de domination des graphes planaires (et plus précisément des graphes planaires maximaux) est celle donnée par Matheson et Tarjan [MT96] : pour n suffisamment grand, tout graphe planaire maximal à n sommets a un ensemble dominant de taille au plus $\frac{n}{3}$ (et ils conjecturent que cette borne supérieure est en fait égale à $\frac{n}{4}$). Le problème de *domination de puissance* est une variante de la domination comprenant des étapes de propagation, permettant à un sommet de monitorer non seulement ses voisins mais aussi des sommets à une distance non-bornée de lui (voir Figure 8). L'étude de la domination de puissance fut originellement motivée par des préoccupations de surveillance de réseaux électriques, puis le problème transposé en termes de graphes par Haynes et al. [HHHH02]. Comme pour la domination, le problème de décision associé à la domination de puissance est NP-complet pour les graphes planaires, et presque tous les résultats connus sur cette classe travaillent avec des hypothèses supplémentaires sur le graphe d'entrée, comme par exemple un petit diamètre ou une largeur arborescente bornée.

Dans le chapitre 3, nous montrons de nouveaux résultats concernant la domination de puissance dans les graphes planaires. Nous présentons tout d'abord des configurations spéciales permettant de construire une famille de graphes avec un nombre de sommets n arbitrairement grand et un nombre de domination valant

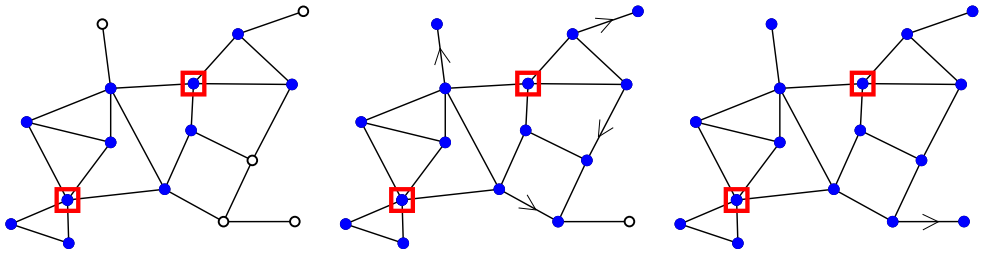

(a) (b) (c)

Figure 3: (a) Deux sommets sont sélectionnés (entourés par un carré rouge), et leur voisinage fermé est monitoré (en bleu). (b) Certains sommets se propagent vers leur seul voisin non-monitoré. (c) Après deux étapes de propagation, tous les sommets sont monitorés : l'ensemble de départ est un ensemble dominant de puissance du graphe comprenant deux sommets.

toujours $\frac{n}{6}$. Nous prouvons ensuite que tout graphe planaire maximal avec $n \geq 6$ sommets a un ensemble de domination de puissance à au plus $\frac{n-2}{4}$ sommets. Notre algorithme est constructif et est divisé en trois étapes. La preuve de cet algorithme repose essentiellement sur la structure des graphes planaires maximaux et sur les propriétés de planarité. Dans un dernier temps, nous continuons l'étude de la domination de puissance dans les treillis réguliers ; des valeurs exactes du nombre de domination de puissance ont déjà été données pour certaines familles, comme les grilles carrées, les grilles hexagonales ou les graphes toriques. Nous considérons donc les grilles triangulaires de dimension k à bord hexagonal, et nous prouvons que leur nombre de domination de puissance vaut exactement $\lceil \frac{k}{3} \rceil$.

Le troisième sujet abordé dans cette thèse est l'*énumération de certaines cartes planaires*. Les cartes sont des objets plus spécifiques que les graphes : en plus des sommets et des arêtes, une carte contient également un ordre cyclique des arêtes autour de chaque sommet. Dans le cas des cartes planaires, cet ordre assure directement un dessin planaire du graphe sous-jacent. Nous considérons des cartes enracinées, c'est-à-dire qu'un coin (une incidence face-sommet) de la carte est choisi (voir Figure 9a). L'énumération des cartes planaires, très étudiée depuis les travaux fondateurs de Tutte [Tut68; Tut63a], a de nombreuses applications (notamment via les méthodes bijectives), aussi bien pour trouver des codages compacts de structures combinatoires, aider à analyser la complexité en moyenne d'algorithmes, ou pour générer des structures aléatoires plus efficacement. Enumérer des cartes est également intéressant pour les physiciens statisticiens. L'ajout aux cartes planaires d'une structure (par exemple un arbre couvrant, une coloration propre des sommets, une orientation particulière des arêtes...) est une approche particulièrement fructueuse, menant souvent à de belles bijections avec d'autres classes d'objets combinatoires.

Une classe de cartes planaires comportant de nombreuses propriétés est celle des cartes planaires *Eulériennes*. La notion de graphes Eulériens provient du problème connu sous le nom de problème des "Septs ponts de Königsberg". Vers 1730, la ville

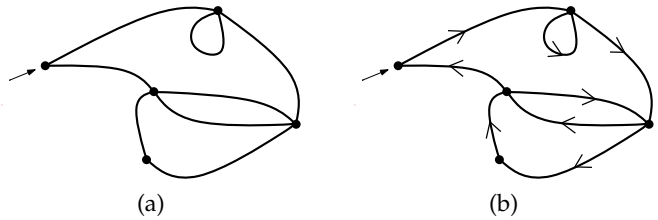

(a) (b)

Figure 4: (a) Une carte planaire avec sommet-racine v. (b) Une de ses orientations Eulériennes.

de Königsberg, en Prusse [2] était séparée en quatre quartiers, reliés entre eux par des ponts qui enjambaient la rivière Pregel (voir Figure 10a). Le problème en question était le suivant : "*Y a-t-il un parcours passant par chacun des ponts exactement une fois, et revenant à son point de départ ?*". Evidemment, cette question se traduit directement en termes de graphes (voir Figure 10b): "*Y a-t-il un cycle dans le graphe sous-jacent qui passe par chaque arête exactement une fois ?*".

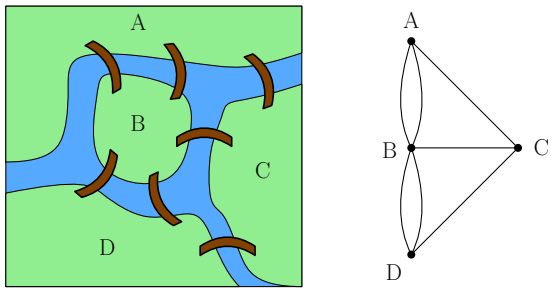

(a) (b)

Figure 5: (a) Un (rapide) plan de la ville de Königsberg avec ses sept ponts et ses quatre quartiers A, B, C et D. (b) Le graphe sous-jacent.

Le mathématicien de génie Leonhard Euler travailla sur ce problème et généralisa la question à tout graphe connexe, en posant la définition suivante : si un graphe admet un cycle (appelé cycle Eulérien) contenant chaque arête exactement une fois, alors ce graphe est un *graphe Eulérien*. Il montra ensuite que dans tout graphe Eulérien, les sommets ont un degré pair [Eul41][3]. En particulier, le graphe de la Figure 10b possède des sommets de degré impair, et n'est donc pas un graphe Eulérien.

Le nombre de cartes planaires Eulériennes est connu pour avoir une expression simple, et cette famille est reliée à beaucoup d'autres objets combinatoires (comme certaines permutations, ou certains arbres) par de belles bijections. Enrichir les cartes planaires Eulériennes d'orientations spécifiques (telles que tout sommet possède autant d'arêtes entrantes que sortantes) conduit à une nouvelle famille de cartes planaires, les *orientations planaires Eulériennes*, qui ont une structure de treillis.

[2] maintenant appelée Kaliningrad, en Russie

[3] En fait, si le graphe est connexe, posséder un cycle Eulérien et avoir seulement des sommets de degré pair sont deux propriétés équivalentes.

Dans le chapitre 4, nous étudions l'énumération des orientations planaires Eulériennes enracinées (voir Figure 9b). Nous présentons tout d'abord une variante de la décomposition standard des orientations, qui nous permet de calculer le nombre d'orientations Eulériennes à n arêtes pour $n \leq 15$. La résolution de la série génératrice étant difficile, nous définissons des familles de sous- et sur-ensembles des orientations planaires Eulériennes et étudions ces familles. Pour chaque ensemble, nous calculons un système d'équations fonctionnelles définissant sa série génératrice ; pour les sous-ensembles, ces systèmes et les séries génératrices associées sont algébriques, et leurs coefficients possèdent un comportement asymptotique classique des arbres. Quant aux sur-ensembles, les systèmes définissent des séries algébriques à deux variables et impliquent des différences divisées, ce qui ajoute de la difficulté à leur résolution. Nous prouvons cependant que les séries qui en résultent sont également algébriques en faisant appel à un théorème d'algèbre de Popescu. De cette manière, nous montrons que le taux de croissance des orientations planaires Eulériennes est compris entre 11.56 et 13.005.

Notre travail a donné lieu à de nombreuses questions et pistes de recherches que nous trouvons intéressantes. Certaines questions soulevées par nos résultats sont présentées dans la dernière section de chaque chapitre, et des perspectives de recherche plus globales sont données dans le dernier chapitre de ce manuscrit.

Certains des résultats présentés dans cette thèse ont donné naissance aux articles suivants :

- *Rook-drawing for plane graphs*, avec David Auber, Nicolas Bonichon et Paul Dorbec, Journal of Graph Algorithms and Applications, Vol. 21(1), 103–120, 2017 (présenté à la conférence Graph Drawing'15).
- *On the number of planar Eulerian orientations*, avec Nicolas Bonichon, Mireille Bousquet-Mélou et Paul Dorbec, European Journal of Combinatorics, Vol. 65, 59–91, 2017.
- *Non-aligned drawings of planar graphs*, avec Therese Biedl, Journal of Graph Algorithms and Applications, sous presse. ArXiv preprint: arXiv:1606.02220 [cs.CG] (presented at the Graph Drawing'16 conference).
- *Power domination in triangulations*, avec Antonio González et Paul Dorbec, manuscrit.
- *Power domination in triangular grids*, avec Prosenjit Bose et Sander Verdonschot, accepté à la Canadian Conference on Computational Geometry.

Introduction

> *Sometimes, if you pay real close attention to the pebbles you find out about the ocean.*
>
> Terry Pratchett, *Lords and Ladies*

The results presented in this thesis, although very different one from another, all belong to the field of *graph theory*. This introduction is thus a good opportunity for me to present the concept of graphs and why graph theory is an interesting way of thinking when trying to solve problems.

In order to illustrate that, let us take a simple, yet expressive example. If you often cook or bake, you may have already experienced the following: after planning to make some pancakes, you realize that there is no butter left. Never mind, the recipe indicates that you can replace it with olive oil (which you have!), and everything is fine. Now suppose your pantry is small, and you often forget to plan the ingredients before cooking. What are the key ingredients you shall keep in your pantry in order to be able to cook any recipe (with potential substitutions) without needing to go to the grocery store? In other words, what is the minimum number of ingredients you should possess such that every ingredient you do not have can be replaced by one you do? (Warning: this is not a cooking book: we do not guarantee that the result is always good or even edible.) We consider that two ingredients are exchangeable if at least one recipe allows to replace one with the other. A first idea is to note the names of all pairs of ingredients that are exchangeable, as in Figure 6a. But it is difficult to see the relations between the ingredients and this does not seem to be an efficient way to solve this problem.

Another way to look at our minimal pantry problem is to try and find the core of it, which means separating the pertinent information from the superfluous one, that can be deleted from the analysis. In this case, what matters is not in fact the names of the ingredients, but the *relations* between them. The mathematical object modeling pairwise relationships within a given set is called a *graph*. The graph corresponding to our problem (see Figure 6b) contains *vertices*, which represent the ingredients, and *edges*, corresponding to the "potential substitution" relationship

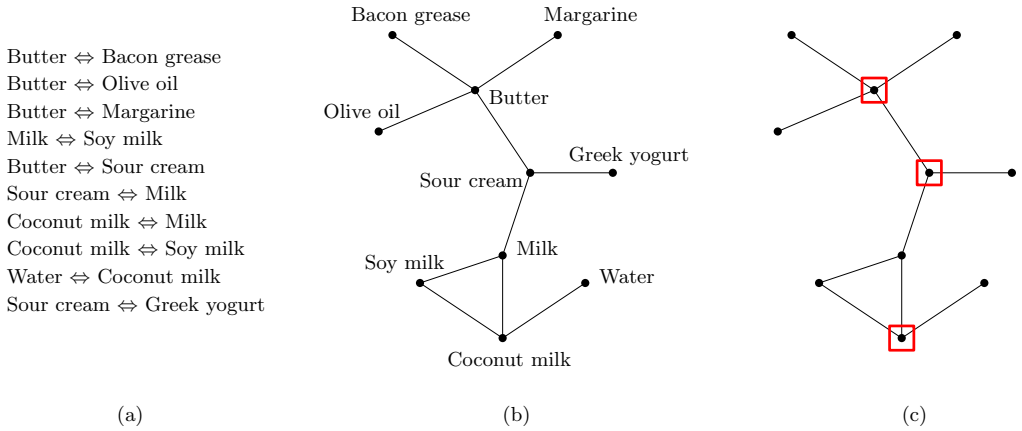

Figure 6: (a) A list of potential substitutions. (b) The corresponding graph. (c) The (red-framed) selected vertices are neighbors from every non-selected vertex of the graph.

between them [4], and solving our problem consists in fact in finding a *minimum dominating set* in the graph. In our example, it is easy to see that buying coconut milk, sour cream and butter is enough to cover all possibilities, whereas one can not find only two ingredients sufficient to get all potential substitutions. This can also be seen directly on the graph (see Figure 6c): since it has three vertices with only one neighbor and all are distinct, then the minimum dominating set of the graph can not have size less than three. Many problems from the day-to-day life, as well as industrial ones, can be modeled by graphs once the superfluous information has been removed. Converting the problem into a graph-theoretical one allows us to directly apply graph algorithms and/or known results to solve it.

Some graphs with particular properties are of special interest, like *planar graphs*. A planar graph is a graph which can be represented on the plane without crossing edges (like the graph of Figure 6). As mathematical objects, planar graphs have many beautiful properties, like the Euler formula. These properties can be helpful when trying to prove a result (since additional hypotheses limit the degrees of liberty of the solution). However, planarity can also prevent a problem to become simple to solve: for example, some decision problems are still NP-complete even when restricted to planar graphs. That way, planar graphs form an interesting class: the complexity of the problems can either drop drastically or stay very high when restricted to them. Planar graphs are also encountered in a number of contexts other than mathematics and computer science. For example, in image analysis, pixels or regions of an image can be represented by vertices, and algorithms on planar graphs have applications for image segmentation or planar shape matchings, among other problems. In chemistry, characterizing planar molecules allows to match chemical structures in polynomial time, and specific planar graphs can represent complex

[4] A very similar graph, called *flavor network*, has been used to find general distinctive patterns in different culinary traditions [AABB11]. In this graph, vertices are also ingredients, and there are edges between ingredients sharing a flavor compound.

carbon structures like fullerenes.

This thesis deals with problems on three different topics (graph drawing, power domination and enumeration of specific maps) in which planarity plays an important role. We now present the global context of each problem and state our contributions. For each of these topics, a detailed state of the art and the necessary definitions are given in the introduction of the corresponding chapter. For this reason (and to avoid redundancy), we omit many definitions here. In order to familiarize the reader with the notions and objects used throughout this thesis, Chapter 1 contains definitions, notations and basic examples on graphs and maps, as well as a general introduction to the methods of enumerative combinatorics.

The first topic of this thesis is *planar graph drawing*. Drawing graphs is a natural way to represent the information they contain. Moreover, drawings with a small number of crossings are generally more pleasing and easier to apprehend. By definition, each planar graph has a planar drawing, i.e., a placement of vertices and drawing of edges with curves on the plane, such that the edges do not cross. However, knowing that a graph is planar is not sufficient to know *how* to draw it planarly. Algorithms producing a planar drawing of a given planar graph are thus required. One can even require the final drawing to use only straight-lines for the edges, as it was proved (independently) by Fáry [Fá48], Stein [Ste51] and Wagner [Wag36]. Moreover, we can consider the drawings to be done on a regular grid, with vertices placed at the intersections of the grid rows and columns. Clearly, we do not want the drawing to be too big, and it is thus natural to try and estimate the length and width of the minimal grid allowing a straight-line drawing of any planar graph. In particular, Schnyder [Sch90] showed a construction to draw any planar graph with n vertices on an $(n-2) \times (n-2)$-grid, and it is conjectured that the minimal grid has size $\lceil \frac{2n}{3} \rceil \times \lceil \frac{2n}{3} \rceil$. Remark that it is sufficient to prove results for maximal planar graphs, i.e., graphs in which no edge can be added without losing planarity. Indeed, we can turn any planar graph into a maximal one by adding some edges, apply a drawing algorithm on the maximal planar graph obtained, and finally remove the previously added edges. Drawing algorithms for maximal planar graphs usually rely on some structure added to the graph, such as Schnyder woods or orientations given by a canonical ordering.

In Chapter 2, we study *planar non-aligned drawings* of planar graphs,, in which each row and column contains at most one vertex of the graph (see Figure 7a, b, c). This additional constraint originates from visualization considerations, and enables the drawing to have good properties, for example in terms of mental map preservation. It is clear that any planar graph with n vertices requires a so-called minimal grid of size $(n-1) \times (n-1)$ (with n rows and columns) to admit a planar non-aligned drawing. Compared to the result of Schnyder stated above, is this addition of one row and one column sufficient to compensate (in a way) for the added "non-aligned" constraint?

Alas, we show that in fact, among all maximal planar graphs with n vertices, only one admits a planar *straight-line* non-aligned drawing on an $(n-1) \times (n-1)$-grid. We thus investigate along two axes: adding bends to the drawing (and keep it on a minimal grid, see Figure 7d), or allowing more rows and/or columns. We

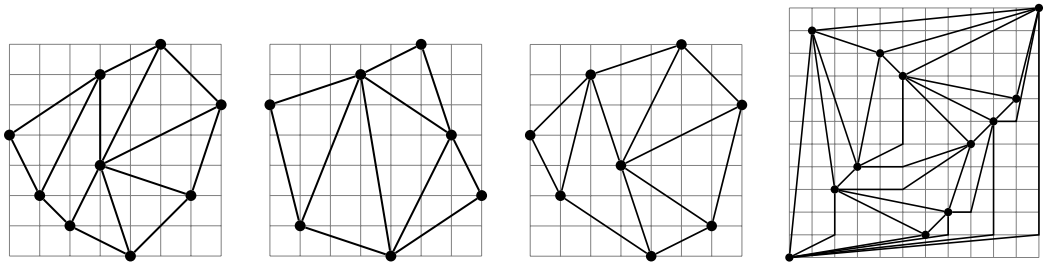

(a) (b) (c) (d)

Figure 7: (a) A planar grid drawing, but not non-aligned. (b and c) Two planar non-aligned drawings. (d) A planar polyline non-aligned drawing.

first consider planar *polyline* non-aligned drawings on the minimal grid, with a small number of bends. We present a linear algorithm using properties of Schnyder woods of maximal plane graphs, and ensuring $n-3$ bends in the final drawing. We also show that 4-connected graphs have a planar non-aligned drawing on the $(n-1)\times(n-1)$-grid with at most one bend, and we use this result as the central part of an algorithm computing a planar non-aligned drawing of any planar graph. This algorithm runs in polynomial time, and the final number of bends depends on the number of separating triangles in the input graph. In a second time, we consider straight-line non-aligned planar drawings in larger grids, and we propose two polynomial-time algorithms generating such drawings on grids with $O(n^4)$ area. They both are extensions of classical constructions in graph drawing, namely the shift method of de Fraysseix et al. [DFPP90] and the realizer method of Schnyder [Sch89; Sch90]. Finally, we show that nested-triangle graphs have a planar non-aligned straight-line drawing on an $(n-1)\times O(n)$-grid.

Combinatorial optimization is another topic in which planar graphs play a large role. In some problems, planarity is a sufficient hypothesis to get important results, as for example in the widely-known Four Color Theorem (stating that every planar graph has a coloring of its vertices using four colors and such that no adjacent vertices have the same color). In other cases, planarity properties are not enough to conclude, and one needs either to restrict the class of graphs considered or to backbone the input graph with a structure for results to emerge. This is for example the case of the problem of *domination* (also called the "small pantry problem" in this introduction). A set of selected vertices of a graph such that every non-selected vertex is a neighbor of a selected vertex is a *dominating set*. The smallest order of such a set is the *domination number* of the graph (the domination number of the graph of Figure 6c is three, as we saw previously). Deciding if the domination number of a graph is at most a given integer is an example of a problem remaining NP-complete when restricted on planar graphs [GNR08]. One general bound on the domination number of planar graphs or maximal planar graphs is the one given by Matheson and Tarjan: for n sufficiently large, every n-vertex maximal planar graph has a dominating set of size at most $\frac{n}{3}$ (and they conjecture that this upper bound is in

fact $\frac{n}{4}$). The problem of *power domination* is a variant of domination with additional propagation steps, allowing a selected vertex to monitor not only its neighbors but also vertices at a non-bounded distance from it (see Figure 8). The study of power domination was, at first, motivated by electrical monitoring problems, and later translated into a graph problem by Haynes et al. [HHHH02]. As for domination, the decision problem associated to power domination is NP-complete on planar graphs, and almost every known result on planar graphs considers an additional hypothesis, such as a small diameter or a bounded tree-width.

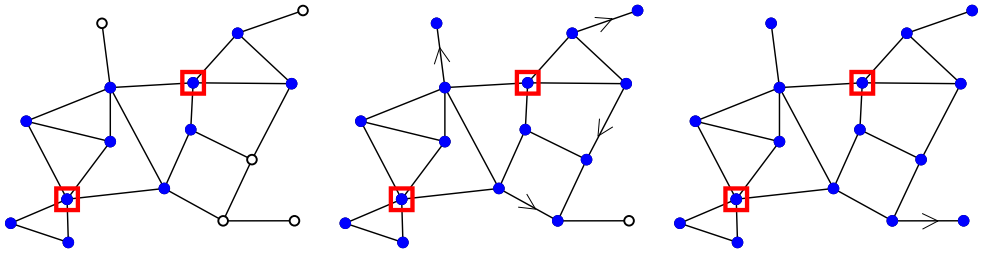

Figure 8: (a) Two vertices are selected and their closed neighborhood is monitored (in blue). (b) Some vertices propagate to their only non-monitored neighbor. (c) After two rounds of propagation, all vertices are monitored: the selected set is a power dominating set of the graph with size two.

In Chapter 3, we show new results concerning power domination in planar graphs. We first present special configurations allowing us to construct graphs with arbitrarily large n and power domination number $\frac{n}{6}$. Then, we prove that a power dominating set of any maximal planar graph with n vertices has at most $\frac{n-2}{4}$ vertices. Our algorithm is constructive and is divided in three steps. The proof relies heavily on the structure of maximal planar graphs and on planarity properties. Exact values for the power domination number of some families of regular lattices (such as square grids, hexagonal meshes or torus graphs) have been given, and we carry on with this study by considering triangular meshes of dimension k with an hexagonal-shaped border. We subsequently prove that their power domination number is exactly $\lceil \frac{k}{3} \rceil$.

The third subject considered in this thesis is the *enumeration of particular planar maps*. Maps are more refined objects than graphs: in addition to vertices and edges, a map also contains a cyclic order of the edges around each vertex. In the case of planar maps, this order directly ensures a planar drawing of the underlying graph. We here consider rooted maps, i.e., one corner of the map is chosen (see Figure 9a). The enumeration of planar maps, well studied since the seminal work of Tutte [Tut68; Tut63a], has many applications: it can be used to find compact encodings of combinatorial structures, help the average-case complexity analysis of algorithms, or generate random structures more efficiently. Enumerating maps is also of interest for statistical physicists. Equipping planar maps with an additional structure (such as a spanning tree, a proper colouring, a particular orientation...) has

been particularly investigated, and this approach often led to beautiful bijections with other classes.

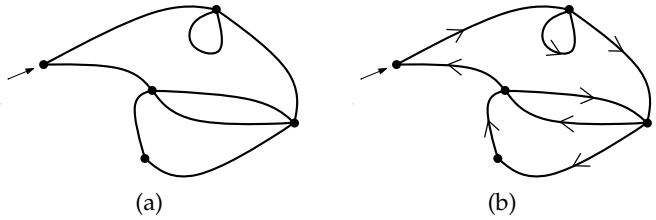

Figure 9: (a) A planar map with root-vertex v. (b) One of its Eulerian orientations.

One class of planar maps with many nice properties is the family of planar *Eulerian* maps. The notion of Eulerian graphs emerged via the problem known as the "Seven Bridges of Königsberg". Around 1730, the city of Königsberg in Prussia [5] was split into four districts, connected by bridges over the Pregel river (see Figure 10a). The problem was the following: "*Is there a walk going through all bridges exactly once, starting and ending at the same place?*". Of course, this question translates directly in terms of graphs (see Figure 10b): "*Is there a cycle in the underlying graph going through every edge exactly once?*".

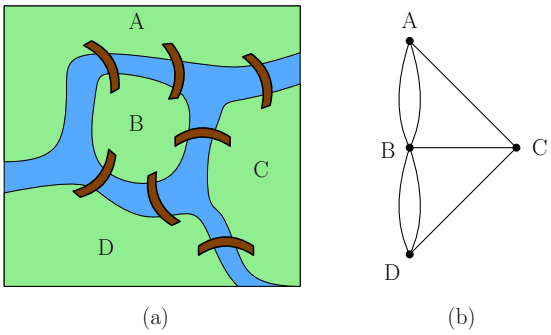

Figure 10: (a) A (rough) plan of the city of Königsberg along with its seven bridges and its four districts. (b) The underlying graph.

Leonhard Euler worked on this problem and generalized the question for any connected graph: if a graph admits a cycle (called Eulerian cycle) containing every edge exactly once, then this graph is an *Eulerian graph*. He proved that if a graph is Eulerian, then every vertex of that graph has an even degree [Eul41][6]. In particular, since the graph of Figure 10b has vertices of odd degree, it is not an Eulerian graph.

The number of planar Eulerian maps is well-known to have a simple expression, and this class relates to many other combinatorial objects (such as certain permutations and trees) by nice bijections. Backboning planar Eulerian maps with specific

[5] now Kaliningrad in Russia

[6] In fact, for connected graphs, having an Eulerian cycle and having only even degree vertices is equivalent [HW73].

orientations (such that for each vertex, the in-going and out-going degrees are equal) leads to the set of *planar Eulerian orientations*, which has a lattice structure.

In Chapter 4, we study the enumeration of planar rooted Eulerian orientations (see Figure 9b). We present a variant of the standard decomposition of orientations which allows us to compute the number of Eulerian orientations having n edges for $n \leq 15$. Not being able to solve the generating function exactly, we define families of subsets and supersets of planar Eulerian orientations and study these families instead. For each set, we compute a system of functional equations defining its generating function: for the subsets, these systems are algebraic, the associated generating functions are algebraic series, and their coefficients have a tree-like asymptotic behaviour. For the supersets, the systems define bivariate series and involve divided differences, which adds difficulty to their solving. However, we are able to prove that the resulting series are also algebraic by using a deep algebra theorem due to Popescu. This way, we show that the growth rate of planar Eulerian orientations is between 11.56 and 13.005.

Our studies gave birth to many questions and leads of research that we find interesting to pursue. Some questions raised by our results are presented in the last section of each chapter, and more global research perspectives are given in the general concluding chapter of this manuscript.

Some of the results presented in this thesis can be found in the following articles:

- *Rook-drawing for plane graphs*, with David Auber, Nicolas Bonichon and Paul Dorbec, Journal of Graph Algorithms and Applications, Vol. 21(1), 103–120, 2017 (presented at the Graph Drawing'15 conference).
- *On the number of planar Eulerian orientations*, with Nicolas Bonichon, Mireille Bousquet-Mélou and Paul Dorbec, European Journal of Combinatorics, Vol. 65, 59–91, 2017.
- *Non-aligned drawings of planar graphs*, with Therese Biedl, Journal of Graph Algorithms and Applications, in press. ArXiv preprint: arXiv:1606.02220 [cs.CG] (presented at the Graph Drawing'16 conference).
- *Power domination in triangulations*, with Antonio González and Paul Dorbec, work in progress.
- *Power domination in triangular grids*, with Prosenjit Bose and Sander Verdonschot, accepted to Canadian Conference on Computational Geometry.

1
Preliminaries

In this chapter, we give the reader the basic definitions concerning the objects considered in this thesis. In Section 1.1, we give definitions and notations on graphs and maps, whereas in Section 1.2 we present some notions of enumerative and analytic combinatorics.

1.1 Graphs and maps

1.1.1 Graphs

A *graph* $G = (V, E)$ is an object composed of a set of *vertices* $V(G)$, and a multiset $E(G)$ of unordered pairs of vertices called *edges*. One easy way to represent a graph is to depict the vertices as points and the edges as lines connecting them [1].

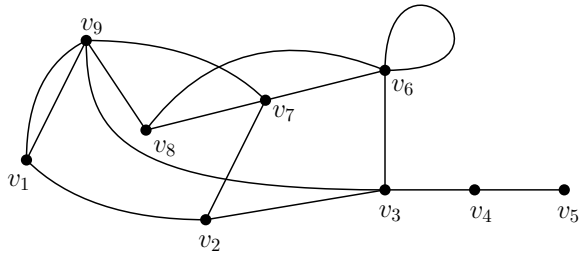

Figure 1.1: A graph with nine vertices $v_1, \cdots, v_9$ and fifteen edges. Vertices v_7 and v_8 are adjacent, but v_9 and v_4 are not. We have $d(v_3) = 4$ and $d(v_6) = 5$. The distance between v_1 and v_4 is three.

An edge e formed from vertices u and v is denoted by $e = (uv)$. Vertices u and v are said to be the *ends* of (uv), and *adjacent* to or *neighbors* of each other. An edge and its endpoints are said to be *incident* to each other. An edge is a *loop* if its endpoints are the same (e.g. v_6 is incident to a loop). Edges sharing both their endpoints (i.e. $e = (uv), e' = (uv)$ with $e \neq e'$) are called *multiple edges*. The graph is called *simple* if it contains neither multiple edges nor loops. The number of vertices of a graph is its

[1] The specific preoccupations of *graph drawing* will be see in more details in the following chapter.

order $|V(G)|$. In this thesis, all graphs are considered *finite*, i.e. their order is a finite number.

The *degree* $d(v)$ of a vertex v is the number of distinct edges incident to v, counting loops twice. If the graph is simple, $d(v)$ is also the number of distinct neighbors of v. In simple graphs, a vertex with degree 1 is called a *leaf*. A graph is said to be k*-regular* if all vertices of G have degree k.

A graph G is *connected* if for any pair of vertices $u, v \in V(G)$, there is a path along the edges of $E(G)$ connecting u to v. If a graph G is not connected, then each connected component of G can be considered individually. If removing fewer than k vertices (along with their incident edges) does not disconnect the graph, then G is said to be k*-connected*.

The *distance* between two vertices u and v in a graph G is the length of a shortest path from u to v, i.e. the minimum number of edges to follow to reach v from u. The *diameter* of G is the maximum of all vertex pairs v, v' of the distance between v and v' in the graph.

Matchings and independent sets A set $S \subseteq V(G)$ of vertices is *independent* if no two vertices of S are adjacent. Similarly, a set $A \subseteq E(G)$ of edges is a *matching* if no two edges of A are incident to a same vertex. A matching is said to be *perfect* if every vertex of the graph is incident to exactly one edge of the matching.

Paths, cycles, bipartite and complete graphs Some specific graphs have their own notations (see Figure 1.2). A *path* on k vertices $u_1, \cdots, u_k$ (and $k-1$ edges) is denoted by $P_k = (u_1, \cdots, u_k)$. A *cycle* on k vertices $v_1, \cdots, v_k$ (and k edges) is denoted by $C_k = (v_1 \cdots v_k)$. If the set of vertices V of a graph can be partitioned into two independent sets U_1 and U_2, then the graph is called a *bipartite graph*. The *complete graph* K_m is the simple graph on m vertices along with all possible edges. The *complete bipartite graph* $K_{m,\ell}$ is the graph composed of two independent sets of order m and ℓ, and of all possible edges between these sets.

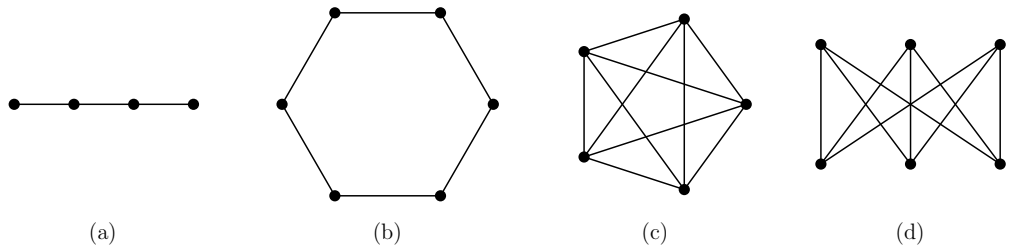

Figure 1.2: (a) The path P_4. (b) The cycle C_6. (c) The complete graph K_5. (d) The complete bipartite graph $K_{3,3}$.

Subgraphs and subdivisions A graph H is said to be a *subgraph* of a graph G if H can be obtained by selecting a set S of vertices of G along with some of the edges whose both ends are in S (see Figure 1.3a). More formally, H is a subgraph of G if $V(H) \subseteq V(G)$ and $E(H) \subseteq E(G) \cap (V(H) \times V(H))$.

H is an *induced subgraph* of G if H can be obtained by selecting a set S of vertices of G along with all edges whose both ends are in S (see Figure 1.3b). The subgraph of G induced by a set $S \subseteq V(G)$ of vertices is denoted by $G[S]$, and $G - S$ denotes the subgraph $G[V(G) \setminus S]$.

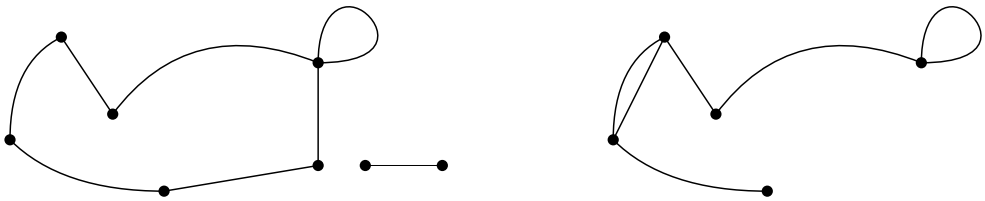

(a) (b)

Figure 1.3: (a) A subgraph of the graph in Figure 1.1. (a) Another subgraph of the graph in Figure 1.1, this time induced by vertices v_1, v_2, v_6, v_8 and v_9.

A graph G' is a *subdivision* of a graph G if G' can be obtained by replacing some edges of G by paths (see Figure 1.4). On the contrary, a *path contraction* is the replacement of successive vertices of degree two by a single edge.

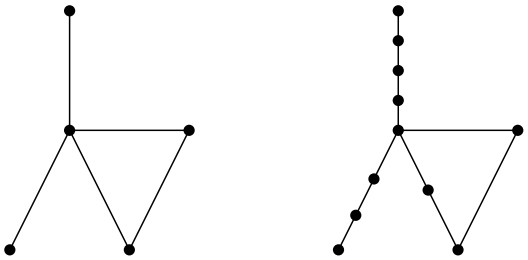

(a) (b)

Figure 1.4: The graph (b) is a subdivision of (a): one edge has been subdivided once, one edge has been subdivided twice, and an other has been subdivided three times.

Directed graphs A graph is a *directed graph*, or *digraph*, if its edges possess an orientation (see Figure 1.5). We here consider that all edges have exactly one orientation. Any vertex v of a directed graph is incident to *in-edges*, directed toward v, and *out-edges*, directed outward v. The number of in-edges (resp. out-edges) of a vertex v is the *in-degree* (resp *out-degree*) of v. Of course, these two parameters add up to the degree of v.

A vertex of a directed graph with only in-edges is called a *sink*, whereas one with only out-edges is a *source*.

Neighborhood We define the *open neighborhood* of any vertex $u \in V(G)$ as $N_G(u) = \{v \in V(G) \mid (uv) \in E(G)\}$, and its *closed neighborhood* as $N_G[u] = N_G(u) \cup \{u\}$. Given

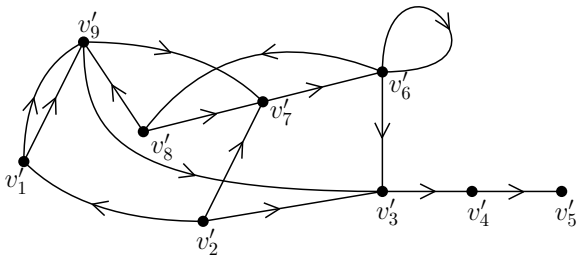

Figure 1.5: This directed graph is an orientation of the graph of Figure 1.1. There is an out-edge from v'_4 to v'_5. Vertex v'_6 has in-degree two and out-degree three. Vertex v'_2 is a source, and v'_5 is a sink.

a subset $S \subseteq V(G)$, the *open* (resp. *closed*) *neighborhood of* u *in* S is $N_S(u) = N_G(u) \cap S$ (resp. $N_S[u] = N_S(u) \cup \{u\}$). The *open* (resp., *closed*) *neighborhood of* a subset of vertices S is $\bigcup_{v \in S} N_G(v)$ (resp. $S \cup \bigcup_{v \in S} N_G(v)$).

Without other indication, the graphs considered in this thesis are simple, finite, connected and undirected.

1.1.2 Planar graphs and maps

A *planar graph* is a graph admitting a *planar drawing*, i.e. a drawing on the plane in which no two edges cross.

A well-known mathematical puzzle, called the *three houses problem*, goes as follows (see Figure 1.6): "There are three houses: A, B and C. Each house needs to be connected to gas, electricity and water at the same time. Is it possible to connect all houses to the utilities without the pipes to cross?". The underlying graph appearing is in fact the complete bipartite graph $K_{3,3}$, and so this problem translates directly to graph theory in these terms: "Is $K_{3,3}$ a *planar* graph?".

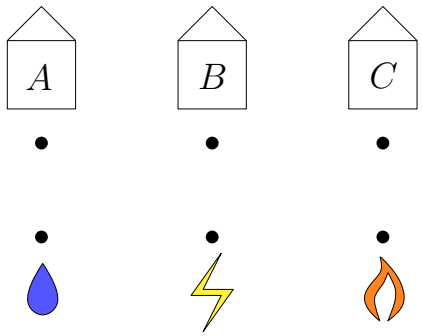

Figure 1.6: The three houses problem. There are three houses and three utility services (water, electricity and gas). Can you connect each house to every utility without crossings?

If a subgraph H of a graph G is non-planar, then G is also non-planar: adding edges and/or vertices to a non-planar graph only increase the potential constraints.

For example, the complete graph K_m ($m \geq 6$) is not planar because K_5 is an induced subgraph and is also non-planar. Subdividing a graph also do not change its planarity. However, some graphs (like K_5 and $K_{3,3}$) are non-planar even if all their subgraphs and path contractions are planar [2]. In fact, $K_{3,3}$ and K_5 are the only such obstacles to planarity [3]:

> **Theorem 1.1.** *(Kuratowski's theorem [Kur30]) A finite graph is planar if and only if it has no subgraph isomorphic to a subdivision of K_5 or $K_{3,3}$.*

To prove that a given graph G is not planar, it then suffices to show that after possible contractions of paths, there is a subgraph of G isomorphic to either K_5 or $K_{3,3}$.

Trees A *tree* is a simple graph without cycles (see Figure 1.7). Trees are planar since K_5 and $K_{3,3}$ both contain cycles as subgraphs. One of the vertices of a tree is often distinguished and called the *root*. In a tree, a vertex u is a *descendant* of a vertex v (or v is an *ancestor* of u) if v is on the path from the root to u. Moreover, if v is connected to u, we say that v is the *parent* of u (and u is a *child* of v). Two vertices are said to be *unrelated* if one is neither ancestor nor descendant of the other. The *depth* of a tree is the length of the longest path from a leaf to the root in the tree. Given a tree T and a vertex u, the *subtree* of u, denoted by $T(u)$, is the tree induced by u and all of its descendants.

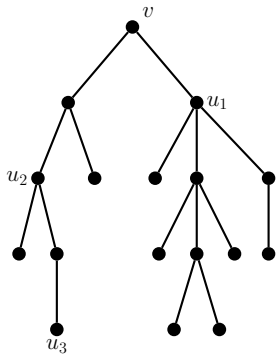

Figure 1.7: A tree with seventeen vertices and depth four. Vertex v is the root. u_2 is an ancestor of u_3 (but not its parent), whereas u_3 and u_1 are unrelated. Vertex u_3 is a leaf.

Plane graphs An *embedding* of a planar graph G on the plane is a placement of the vertices and edges in 2D-space, assigning coordinates to vertices and curves to

[2] In fact, any planar embedding of K_5 violates Euler's formula given below, whereas for $K_{3,3}$ one needs to combine Euler's formula with the fact that each face of a planar embedding of $K_{3,3}$ would have at least four edges to reach conclusion.

[3] Wagner's theorem [Wag36], which makes a characterization of planar graphs via *minors*, is equivalent to Kuratowski's (however, the equivalence is not trivial).

edges, such that the latter do not cross (see Figure 1.8). A planar graph together with an embedding is called a *plane graph*.

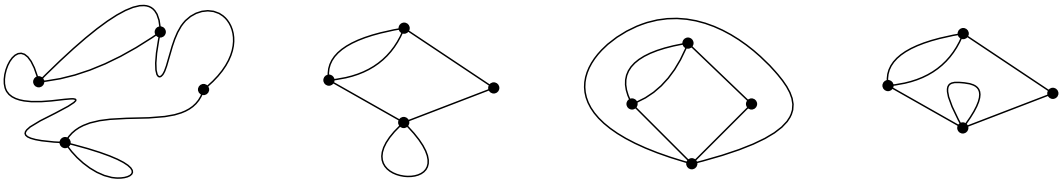

Figure 1.8: Four plane graphs that are different embeddings of the same planar graph. They all have four faces. The outer face of the second graph has size five.

Given a plane graph G, the edges partition the plane into regions called *faces*. The only unbounded face is called the *outer face* of G, and the vertices of G are called respectively *outer* or *inner* vertices depending on whether or not they belong to the outer face. Similarly, *outer edges* are edges belonging to the outer face, the other edges are called *inner edges*.

The *size* of a face is the number of edges on its boundary (if the plane graph is simple, this is equivalent to the number of vertices on the boundary).

The numbers of vertices, edges and faces of a plane graph are related by the following formula:

Theorem 1.2. *(Euler's formula) If $G = (V, E)$ is a finite connected plane graph with f faces, then $|V(G)| - |E(G)| + f = 2$.*

Given a plane graph G, its *dual graph* G' can be obtained by creating a vertex in G' for each face of G, and two vertices of G' are adjacent if and only if the corresponding faces in G share an edge. This relation of duality is symmetric: the dual of G' is G.

A triangle composed of vertices $u, v, w \in V(G)$, denoted by $[uvw]$, is said *facial* if it is the boundary of some face of G. A triangle is said to be a *separating triangle* if the removal of its vertices along with their adjacent edges disconnects the graph (i.e., there are vertices of the graph both inside and outside the triangle).

For any set $S \subseteq V(G)$, the graphs $G[S]$ and $G - S$ can be viewed as plane graphs with the embedding inherited from the embedding of G.

A *maximal plane graph* or *triangulation* is a plane graph with maximal number of edges, implying that every face (including the outer face) is a triangle if the graph has at least three vertices.

Given a plane tree T, the clockwise *preorder* of T is a list of the vertices of T in the order of a clockwise depth-first search algorithm on T. The clockwise *postorder* of T is a list of the vertices of T in the order of their last visit in a clockwise depth-first search algorithm of T. Counterclockwise preorder and postorder are defined similarly.

Planar maps Two plane graphs are equivalent if one can be obtained from the other by continuous deformation on the sphere: in Figure 1.8, the first three plane

graphs are equivalent, but they are not equivalent to the last one. Informally, two plane graphs are equivalent if, along with having the same set of edges and vertices, their corresponding vertices also have the same neighbors in clockwise order.

The equivalence class of equivalent plane graphs, called a *planar map*, is thus not determined by the exact position of the vertices or the specific equations satisfied by the curves representing the edges, but by the topological information contained in an embedding. More precisely, a planar map is a planar graph with some additional information, namely the ordered cyclic list of edges incident to each vertex in counterclockwise order (see Figure 1.9).

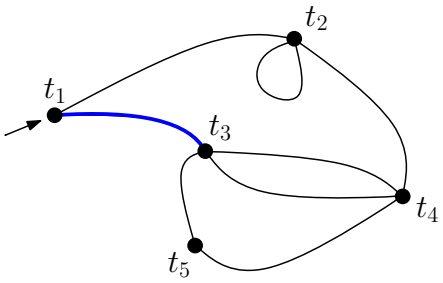

Figure 1.9: A rooted planar map. Vertex t_1 is the root vertex, and the edge (t_1t_3) is the root edge.

Remark that planar maps have no distinguished face, on the contrary to plane graphs, which always have an outer face. Planar maps are then often *rooted*, i.e. one corner (an incidence between a vertex and a face) of the map is distinguished, and called the *root corner*. The vertex and face incident to this corner are respectively the *root vertex* (or simply *root*) and the *root face*. By convention, the *root edge* is the edge following the root corner in counterclockwise order around the root vertex. Throughout this thesis, we indicate in figures the root corner with an arrow, and the root face as the infinite face.

By convention, we include among rooted maps the *atomic map* having one vertex and no edge.

1.2 Enumerative combinatorics

How many ways are there to arrange a group of people around a table? How many planar graphs are there with a given number of edges ? Answering these questions (and many more!) is the goal of a specific branch of combinatorics called *enumerative combinatorics*. More precisely, enumerative combinatorics is dedicated to counting the number of discrete objects (here, arrangements of people, or graphs) having a specific property (e.g. being planar), with respect to one or more parameters (the size of the group, the number of edges in the graph).

In this thesis, we focus on the enumeration of some specific planar maps, and we count them according to their number of edges. The goal is then, given a property $\mathcal{P}$, to find the exact values (or the asymptotic behavior of the values) of the *counting sequence* $(a_n) = a_1, a_2, \ldots$, where a_n is the number of planar maps with n edges and

property $\mathcal{P}$.

1.2.1 An example: the enumeration of rooted plane trees

We first present some general notions of enumerative combinatorics on-the-fly, illustrated by the classical example of rooted (plane) trees; the question asked is thus the following: *Given an integer n, how many rooted trees with n edges exist?* The rooted trees with at most three edges are shown in Figure 1.10.

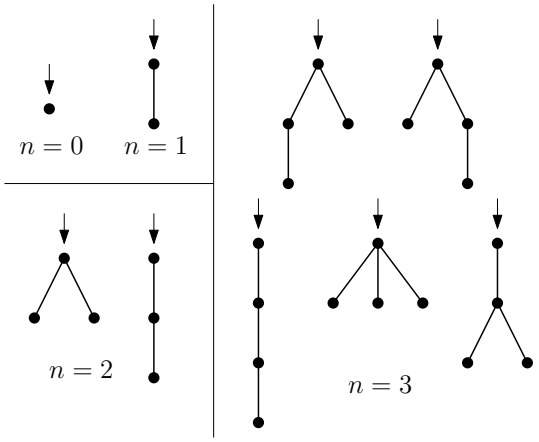

Figure 1.10: The rooted plane trees with at most three edges.

Simple recursion and enumeration

One way to count rooted trees (other than drawing them all and counting, which can quickly become tedious), is to make some use of their recursive nature. Indeed, given a tree with root vertex v, either it has no edges (and there is only one tree possible), or it has at least one edge. In that case, we can delete the root edge, and two trees remain: one whose root is the left-most child of v, and one whose root is v (see Figure 1.11). Since we delete only an edge from the initial tree, we are sure that each of the remaining parts are trees (even if they may be restricted to a single vertex).

We thus have the following description, called *specification*[4], of the class $\mathcal{T}$ of rooted plane trees:

$$\mathcal{T} = \circ \cup (\mathcal{T} \times e \times \mathcal{T}) , \tag{1.1}$$

where $\circ$ represents the atomic tree with one vertex and no edges, and e is an edge. Let a_n be the number of trees with n edges. The specification given by Equation (1.1) translates into the following recurrence relation on the coefficients:

$$a_n = \sum_{i+j=n-1} a_i a_j , \qquad a_0 = 1 .$$

[4]It is also sometimes called the *grammar* of the class, by analogy with formal languages descriptions.

This recurrence on the coefficients allows us to compute the counting sequence (a_n) iteratively: $a_0 = 1$, $a_1 = a_0a_0 = 1$, $a_2 = a_0a_1 + a_1a_0 = 2$, $a_3 = a_1a_1 + a_0a_2 + a_2a_0 = 5$...

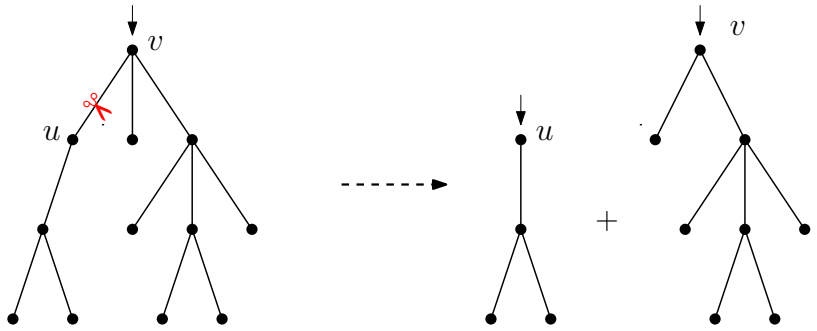

Figure 1.11: Deleting the root edge of a tree creates two new trees.

In the case of rooted trees, we know in fact a simple general formula for a_n:

$$a_n = \frac{1}{n+1}\binom{2n}{n}. \tag{1.2}$$

The counting sequence (a_n) is in fact the sequence of well-known Catalan numbers, which also count many recursively-defined objects, such as well-parenthesized expressions, full binary trees, triangulations of a convex polygon... When two classes happen to have the same counting sequence, it is generally interesting to look for *bijections*, i.e. one-to-one correspondences between objects of the two families. These bijections often allow to better understand underlying properties of one of the families.

Generating functions

In many cases, we do not know nice formulas (such as the one of Equation (1.2)) providing the value of the a_n directly; in that case one might try to get information about the class of objects via the analysis of its generating function. The *generating function* $A(t)$ of a sequence (a_n) (and by extension, of a class $\mathcal{A}$ having counting sequence (a_n)) is the formal power series

$$A(t) = \sum_{n\geq 0} a_n t^n,$$

where t is the *variable* accounting for the number n of edges.

The specification of a class directly translates into equations satisfied by its generating function. In this thesis, we use (mainly implicitly) the following translations:

- (Disjoint union.) $\mathcal{A} = \mathcal{B} \cup \mathcal{C} \Rightarrow A(t) = B(t) + C(t)$,
- (Cartesian product.) $\mathcal{A} = \mathcal{B} \times \mathcal{C} \Rightarrow A(t) = B(t) \cdot C(t)$,
- (Sequence.) $\mathcal{A} = \mathrm{SEQ}(\mathcal{B}) \Rightarrow A(t) = \dfrac{1}{1 - B(t)}$,

where $\mathcal{A}$, $\mathcal{B}$, and $\mathcal{C}$ are combinatorial classes, and $A(t)$, $B(t)$, $C(t)$ are their respective generating functions with parameter t.

Let us apply this to our example of rooted trees; Equation (1.1) turns into the following one on the generating function $A(t)$ of rooted trees:

$$A(t) = 1 + tA(t)^2 \,. \tag{1.3}$$

This translation of the specification of the class gives thus a *functional equation* of the generating function [5]. The functional equation (1.3) is quadratic and can therefore be solved:

$$A(t) = \frac{1 - \sqrt{1-4t}}{2t} \,,$$

which gives the closed formula for the coefficients (a_n) presented in Equation (1.2).

1.2.2 Using more variables: the enumeration of planar maps

It happens that in order to compute the generating function of a class, one parameter is not sufficient and one needs to take other parameters into account, which yields the use of new variables into the generating function. These additional variables are called *catalytic* variables, following Zeilberger's terminology [Zei00]. If $x_1, \ldots, x_\ell$ are catalytic variables, the generating function is often denoted as $A(t; x_1, \ldots, x_\ell)$. To illustrate such a case, we now turn to the enumeration of *planar maps*.

Consider a planar map M, not reduced to the atomic map, and its root edge e. If e is a loop, then M is obtained from two smaller maps M_1 and M_2 by joining M_1 and M_2 at their root vertices and adding a loop surrounding M_1 (Figure 1.12a).

If the root edge e is not a loop, then we contract it, which gives a smaller map M'. Note however that several maps give M' after contracting their root edge. All such maps can be obtained from M' as follows (see Figure 1.12b): we split the root vertex v of M' into two vertices v and v' joined by an edge (which will be the root edge), and distribute the edges adjacent to v between v and v'. Note that if v has degree d in M', then v has degree between 1 and $d+1$ in M: there are $d+1$ possible distributions of the edges of v.

Since the number of possible splits of a planar map depends on the degree of the root, then we need a catalytic variable taking this degree into account.

Let $M(t; x)$ be the generating function of planar maps, counted by their number of edges $\mathrm{e}(M)$ (variable t) and by the degree $d(M)$ of the root (variable x):

$$M(t; x) = \sum_{M \in \mathcal{M}} t^{\mathrm{e}(M)} x^{d(M)} = \sum_{d \geq 0} x^d M_d(t) \,,$$

where $\mathcal{M}$ is the set of planar maps and $M_d(t)$ denotes the generating function of planar maps with root vertex degree d, counted by number of edges.

[5] In fact, the functional equation satisfied by the generating function of every (*constructible*) class can be found by translating its specification.

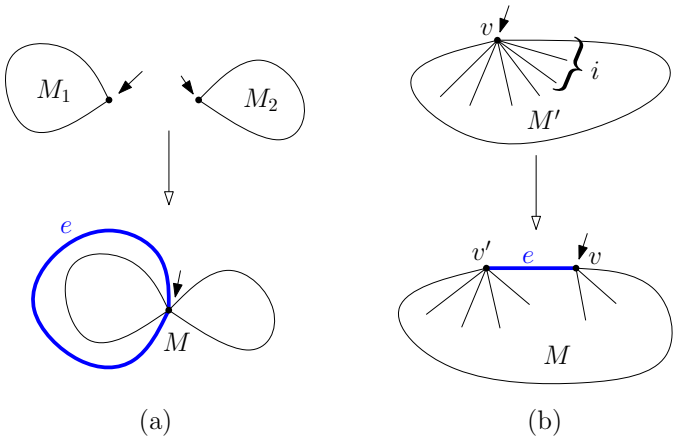

Figure 1.12: Construction of a planar map with n edges: (a) merge an ordered pair of maps M_1, M_2 with n_1 and n_2 edges ($n_1 + n_2 = n - 1$) and add a loop around M_1, or (b) split the root-vertex of a map with $n - 1$ edges. The new edge (here thicker) is the root edge of M.

The above construction translates into the following functional equation satisfied by the generating function $M(t; x)$:

$$\begin{aligned} M(t;x) &= 1 + tx^2 M(t;x)^2 + t \sum_{d \geq 0} M_d(t)(x + x^2 + \cdots + x^{d+1}) \\ &= 1 + tx^2 M(t;x)^2 + t \sum_{d \geq 0} M_d(t) \frac{x^{d+2} - x^2}{x - 1} \\ &= 1 + tx^2 M(t;x)^2 + \frac{tx}{x-1}(xM(t;x) - M(t;1)). \end{aligned} \tag{1.4}$$

The term 1 accounts for the atomic map, the next term for maps obtained by merging two smaller maps, and the third term for maps obtained from a split of the root vertex.

1.2.3 Analyzing the generating function

The analytic study of the generating function of a combinatorial class gives information about its counting sequence: for example, the behavior of the generating function in the area near its singularities (i.e. the values where the generating function ceases to be differentiable) often tells something about the asymptotic approximation of the coefficients. The following is known [FS09, Sec.IV.1]: the *location* of a function's singularities dictates the *exponential growth* of its coefficients, and the *nature* of the singularities determines their associate *subexponential factor*. More precisely, if $F(z)$ is a function analytic at 0 such that the dominant singularities (the nearest to the origin) have modulus R, then the coefficient f_n of z at order n satisfies $f_n \bowtie (1/R)^n$, i.e. $f_n = R^{-n}\theta(n)$ with $\limsup |\theta(n)|^{1/n} = 1$. The value $1/R$ is generally called the *growth rate* (often also denoted by μ) of the generating function.

If there exist non-zero constants α, β such that $F(t) = \alpha - \beta(\sqrt{1 - t/r})(1 + o(1))$, as $t \to r$, one says that r is a *square-root singularity* of $F(t)$ (for example, the generating function $A(t)$ of rooted plane trees has a square-root singularity at $t = \frac{1}{4}$). Square-root singularities always induce a behavior of the form $R^{-n}n^{-3/2} = \mu^n n^{-3/2}$ for the coefficients (f_n). This $-3/2$ exponent is typically found in the behavior of coefficients of classes with a tree-like structure.

Generating functions are often classified by their *nature*, i.e. the type of equation satisfied by the generating function (and its derivatives, if need be). We say that a generating function is:

- *Rational* if it can be expressed as a ratio of two polynomials,
- *Algebraic* if it satisfies a polynomial equation,
- *Holonomic* (or *differentially finite* or *D-finite*) if there is a linear combination relating the generating function and its derivatives, with polynomial coefficients in the variable t,
- *Differentially algebraic* if there is a polynomial equation relating the generating function and its derivatives, with polynomial coefficients in t.

Indeed, these families of generating functions are subsets of each other:

$$\text{Rational} \to \text{Algebraic} \to \text{Holonomic} \to \text{Differentially algebraic}$$

Algebraic functions have nice properties: since they can be seen geometrically as plane algebraic curves, the possible values of their singularities are known (using the Newton-Puiseux theorem [Pui50] allowing to describe locally any branch of an algebraic curve) and algebraicity of the generating function always yields rational exponents in the asymptotic behavior of coefficients. Moreover, the singularities of an algebraic function can be found among the roots of the discriminant of its minimal polynomial (plus the zeros of the dominant coefficient).

For more information on analytic combinatorics, we refer the reader to the excellent homonymous book by Flajolet and Sedgewick [FS09].

2

Non-aligned drawings of graphs

There are various ways of conveying the information a graph contains; one can for example provide the list of vertices and the list of edges, or the list of neighbors for each vertex. But one very effective way to grasp the overall structure of the information contained in a graph is to draw it. Graphs appear in lots of different contexts: they can represent atoms and their connections in molecules in chemistry, interactions between people in sociology and social networks analysis, cities and roads in geography... In each of these domains, graphs tend to have different properties, and one needs to draw them in order to perform specific tasks, such as identifying groups of highly connected individuals in a social network, or visualizing cycles in a metabolic network. This leads to the conception of a wide range of graph *drawing* algorithms, each one ensuring particular properties of the final drawing and representing the vertices and edges in a specific way (see Figure 2.1). Generally, the vertices are rendered as points, and the edges (which are relations between two vertices) as curves or segments between their endpoints.

Many different visual properties (often called *aesthetics criteria*) may be considered when drawing a graph, such as optimizing the area of the drawing, having an aspect ratio close to 1:1, minimizing the number of edge crossings, increasing the angular resolution (i.e. the minimum angle between two edges incident to the same vertex)... These criteria have been widely studied and assessed throughout the years (see for example [CP96; Pur97; Pur02; PCJ95; TDBB88]). Of course, it is difficult to create a drawing having all these properties at the same time, and it is sometimes difficult to be sure that even one of these properties is fully satisfied (for example, minimizing the number of crossings in the drawing of a given graph is an NP-complete problem [GJ83a]). This is why most drawing algorithms focus on one (or a few) of these properties. For more details on the different possibilities of graph drawings, we refer the reader to the books of di Battista et al. [BGETT99] and Kaufmann and Wagner [KW03], and to the review of Bennett et al. [BRSG07] concerning aesthetics in graph visualization.

In this chapter, we are interested in generating drawings without any edge crossings. A drawing of a graph G is said to be *planar* if the curves representing the edges of G do not cross each other. Of course, such a drawing is possible only if the input graph is itself planar. The interest for planar drawings arose when the

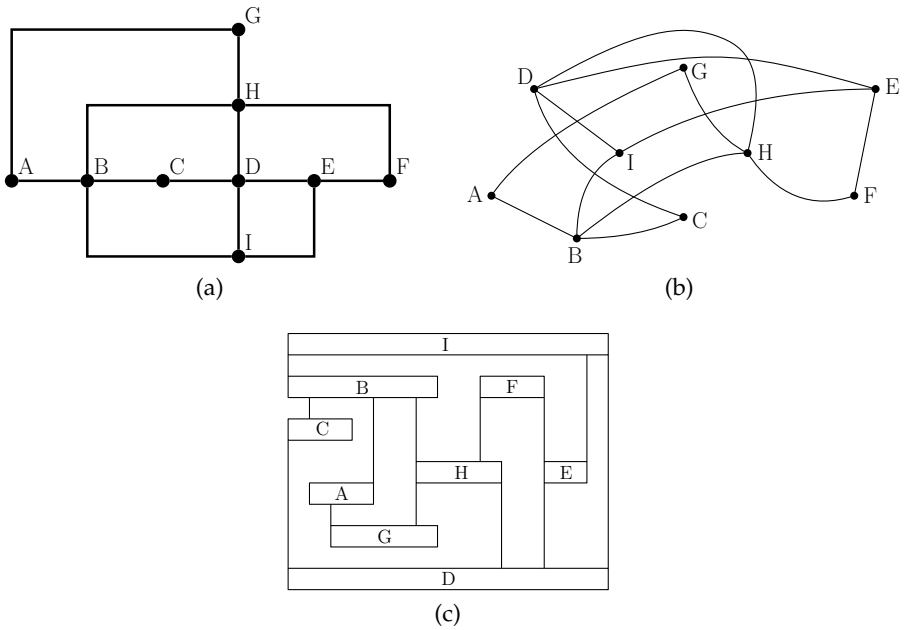

Figure 2.1: Different drawings of the same graph. The vertices can be represented as points like in (a) and (b), or as rectangles (c). Edges can be vertical and horizontal segments (a), curves (b) or vertical-only segments (c).

need for automatic design of electrical circuits became larger. For example, in the context of VLSI electronic circuits (for which the placement of modules on the chip can be represented as a graph), one needs to draw the graph without crossings and as few bends as possible [Ull84; Val81]. By definition, finding a planar drawing of a planar graph G is always possible with edges as curves. Wagner [Wag36], Fáry [Fá48], and Stein [Ste51] independently proved that if a graph is planar then it admits a planar drawing with *straight-lines*. Various drawing algorithms ([CYN84; Rea87; Tut63b]) were proposed to draw planar graphs with straight-lines, but these methods generally involve high precision arithmetic, and tend to form areas with a high vertex density.

In order to control the minimum and maximum distances between vertices in the drawing, one can force them to have integer coordinates on a grid of polynomial size, i.e. to draw the graph planarly on a grid, by placing the vertices at the intersection of the rows and columns. Formally, a *grid drawing* of a graph G is a drawing in which the vertices of G are mapped to intersections of a regular grid. A $k \times \ell$-grid is a grid of width k and height ℓ (i.e. with $k+1$ columns and $\ell+1$ rows). Throughout this chapter, the position of a vertex u on a grid is given by the couple $(x(u), y(u))$, where x and y are functions taking values in $\{1, \ldots, k+1\}$ and $\{1, \ldots, \ell+1\}$ respectively.

It is natural to try to find the minimal size of a grid supporting a planar straight-line drawing for any graph of order n. De Fraysseix et al. [DFPP90] showed that every planar graph with n vertices admits a straight-line drawing on a $(2n-4) \times (n-2)$ grid (using the so-called *shift* method, which takes advantage of a canonical ordering

of the graph). Schnyder [Sch90] improved this result by proving the existence of such a drawing on an $(n-2)\times(n-2)$-grid, with the use of the well-known *realizer* method (see Figure 2.2). Some time later, Chrobak and Nakano [CN98] proposed a linear-time algorithm which, given a plane graph with n vertices, generates a straight-line grid drawing of width at most $\lfloor\frac{2(n-1)}{3}\rfloor$ and of height at most $4\lfloor\frac{2(n-1)}{3}\rfloor-1$. This drawing has optimal width, since nested-triangle graphs with $\frac{n}{3}$ triangles need a grid of size at least $\lceil\frac{2(n-1)}{3}\rceil\times\lceil\frac{2(n-1)}{3}\rceil$ to support a straight-line drawing [CN98; DLT84]. Note that nested-triangle graphs are also critical constructions for polyline drawings, for which they yield the same minimum grid-size [BLSM02]. It is conjectured that a $\lceil\frac{2n}{3}\rceil\times\lceil\frac{2n}{3}\rceil$-grid can support a straight-line drawing of any plane graph.

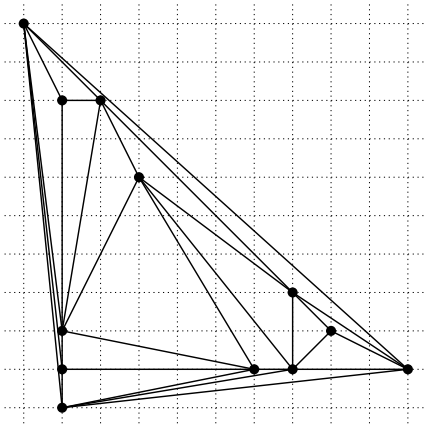

Figure 2.2: A Schnyder-like drawing of a triangulation with 12 vertices on a 10×10-grid.

In the context of interactive drawings or dynamic graphs, the graph one wants to visualize *evolves* through time, i.e. vertices and/or edges are added or deleted from the graph. In that case, one may want to consider additional properties of the drawing (sometimes called dynamic aesthetics [CP96]), among which the following general property, stated by Coleman and Parker [CP96]: *Placement of existing vertices and edges should change as little as possible when a change is made to the graph*. This property is often referred to as the *preservation of the mental map* [ELMS91], or, less often, as layout stability [PT90]. This was refined to three properties of the drawing when changes are made to it: the position of vertices present in consecutive steps should ensure preservation of the orthogonal ordering (their relative positions with respect to the x- and y-order should not change), of the topology (they should induce the same combinatorial map), and of the neighborhood (they should keep the same neighbors) [AP13; CP96; MELS95].

In this chapter, we study a specific constraint on the placement of vertices, which ensures the preservation of the mental map for all three properties: the graph is drawn on a regular grid, with at most one vertex of the graph on each row or column of the grid. This way, the addition or deletion of a vertex from the drawing only impacts the row and column the vertex is on (see Fig. 2.3), and the orthogonal

ordering, the neighborhood and the topology of the graph induced by the common vertices are all preserved. Formally, a *non-aligned drawing* of a graph G is a grid drawing of G with an additional constraint: no two vertices must be placed on the same line or column. This notion was introduced by Alamdari and Biedl [AB12] in the context of rectangle-of-influence drawings (in which the rectangle defined by two adjacent vertices is empty).

Non-aligned drawings are also used as an intermediate step during the construction of orthogonal drawings (where edges are composed of vertical and horizontal segments, see Figure 2.1a) of arbitrary graphs [BK97], and in the construction of orthogonal overloaded drawings introduced by Kornaropoulos [KT11], in which edges may overlap if they have a common endpoint. Orthogonal overloaded drawings are used in the DAGView framework [KT12], which provides drawings with nice properties in the context of large graphs visualization, since they tend to cluster strongly connected components, and are readable even when the size of the graph or the edge density increase. The orthogonal overloaded drawings show significantly better results than other representations of directed graphs to perform visualization-based tasks [DMPT14]. Angelini et al. [Ang+16] also used non-aligned drawings to generate so-called L-Drawings, which allows them to draw non-ambiguous drawings of directed graphs: each edge leaves the source vertically and enter the destination horizontally.

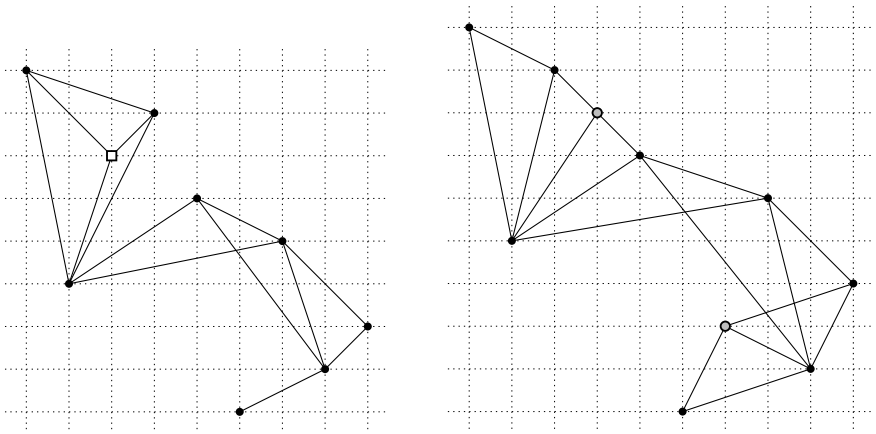

(a) (b)

Figure 2.3: (a) A non-aligned drawing of a graph. (b) Modifying the graph: deleting the square-shaped vertex and adding two vertices (in gray); the general aspect of the drawing does not change much.

We now stir the problems of planar drawing and non-aligned drawing together and study the problem of generating non-aligned drawings of planar graphs.

We first explore the existence of minimal non-aligned drawings for planar graphs in Section 2.1. A *minimal non-aligned drawing* is a non-aligned drawing on a $(n-1) \times (n-1)$-grid. It is clear that no smaller grid could be the support of a non-aligned drawing. The first question that comes to mind is: *Does every planar graph admit a*

planar straight-line minimal non-aligned drawing, *i.e. a minimal non-aligned drawing in which each edge is represented by a segment and no two edges cross?*

Unfortunately, we show using geometrical arguments that among maximal planar graphs with $n \geq 3$ vertices, only one (namely the tower graph of order n) admits such a drawing. We thus relax the straight-line constraint and present two algorithms creating *polyline* planar minimal non-aligned drawings for maximal plane graphs on n vertices, in which edges are drawn as polylines with bends placed on grid intersections (with at most one bend per edge). The first algorithm (see Sect. 2.1.2) makes use of the Schnyder wood of a maximal plane graph, and the coordinates of the vertices are given by depth-first search in two of the trees of the Schnyder wood. This algorithm runs in linear time and generates a drawing with exactly $n - 3$ bends in total. The second algorithm (see Sect. 2.1.3), running in polynomial time, uses a completely different approach: we begin by making the given maximal plane graph 4-connected, and we then generate a rectangle-of-influence drawing of this new graph, which is a planar straight-line drawing. This drawing is in turn slightly modified to become a planar polyline non-aligned drawing of the original graph. The total number of bends depends directly on the number of separating triangles in the original graph.

Another interesting problem is to increase the number of lines and columns allowed to some function of n and see if every graph can be drawn on such a grid. This leads to the following question: *What are the smallest f and g such that every plane graph G has a straight-line planar non-aligned drawing on the $f(n) \times g(n)$-grid?* Note that a step in the construction of upward-rightward drawings presented by Di Giacomo et al. [DG+14] is to (unknowingly) create a planar non-aligned straight-line drawing of the input graph on an $O(n^2) \times O(n^2)$-grid.

In Section 2.2, we study non-aligned drawings on larger grids. We begin by presenting two algorithms generating a non-aligned planar straight-line drawing of a given plane graph on a grid with area $O(n^4)$. The first algorithm (see Section 2.2.1) is based on the *shift* method of de Fraysseix et al. [DFPP90] and gives a drawing on an $(n-1) \times O(n^3)$-grid. However, as opposed to the original algorithm or the method described in [DG+14], we pre-compute the x-coordinates of all vertices using only a canonical ordering of the graph and thus we do not require any shifting. Our algorithm has also a slightly smaller area than the one obtained in [DG+14]. The second algorithm (see Section 2.2.2) is a slight modification of the realizer method proposed by Schnyder [Sch90] and gives a drawing on an $O(n^2) \times O(n^2)$-grid. Finally, we give a general configuration on an $(n-1) \times (\frac{4}{3}n - 1)$-grid to draw a planar straight-line drawing of graphs composed of nested triangles.

The results presented in Sections 2.1.1 and 2.1.2 are joint work with David Auber, Nicolas Bonichon and Paul Dorbec [ABDP15; ABDP17]. The results of Sections 2.1.3 and 2.2 are joint work with Therese Biedl [BP; BP16].

For simplicity, throughout this chapter, the term *non-aligned drawing* denotes a straight-line non-aligned drawing unless otherwise stated. Moreover, we assume throughout the chapter that the input graph is a maximal plane graph; we can achieve this in linear time by adding edges and delete them in the obtained drawing.

2.1 On the minimal grid

By definition, a graph with n vertices can not have a non-aligned drawing on a grid smaller than the $(n-1) \times (n-1)$-grid (with n rows and columns), which we call the *minimal grid*. The question here is to know if there exist graphs needing at least $n+1$ rows or columns in their non-aligned drawing. Alas, we show in Theorem 2.1 that almost every maximal plane graph has no non-aligned drawing on the minimal grid.

2.1.1 Existence of a minimal non-aligned drawing

We define the *tower graph* $\mathcal{T}_n$ of order $n \geq 3$ as the plane join graph $K_2 + P_{n-2}$ (i.e. a complete graph K_2 and a path on $n-2$ vertices P_{n-2} together with all the edges joining vertices from K_2 to vertices of P_{n-2}) drawn in such a way that the vertices of K_2 are on the outer face (see Fig. 2.4 for a drawing of $\mathcal{T}_6$).

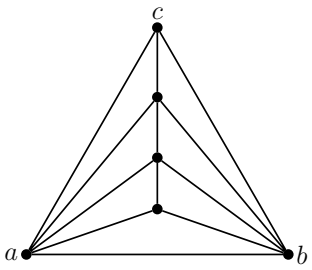

Figure 2.4: The tower plane graph $\mathcal{T}_6$.

Theorem 2.1. *There exists a unique maximal plane graph on $n \geq 3$ vertices admitting a planar minimal non-aligned drawing, namely the tower plane graph $\mathcal{T}_n$.*

Proof. Suppose we have a planar minimal non-aligned drawing of a maximal plane graph G. We prove that G is the tower plane graph $\mathcal{T}_n$.

Let a, b, c be the three outer vertices of G. To maintain planarity and keep the embedding, the inner vertices are at coordinates inside the area defined by the edges (ab), (bc) and (ca). Thus the outer vertices must occupy altogether the four borders of the grid, and one of them has to be placed in a corner. Without loss of generality, assume that a occupies the bottom-left corner.

Consider the positions of the two other outer vertices of G. Suppose one of them (without loss of generality, say b) is in the top-right corner. If the third vertex c is placed below the edge (ab) (see Fig. 2.5a), then the second column on the left can not contain a vertex: the coordinates $(2, k)$ are outside the area delimited by the edges (ab), (bc) and (ca) for all $k > 2$. The point $(2, 2)$ is covered by (ab) and the point $(2, 1)$ can not contain a vertex because a is already on the first row. If c is above (ab), then for similar reasons the column left to b can not contain a vertex. Thus b is not in the top-right corner. Without loss of generality, assume b is on the top row and c on the rightmost column of the grid.

Let α be the angle between the column containing b and the edge (bc) and β be the angle between the row containing c and the edge (bc) (see Fig.2.5b). Consider the row just below b: the angle between the edge (ab) and the column containing b is less or equal to $45°$ thus no vertices can be placed at the left of b on the row below it. No vertex can be placed on the same column as b either. No vertex can be placed at the right of the intersection between the edge (bc) and the row below b. Thus for the row under b to contain a vertex we must have $\alpha \geq 45°$. With similar arguments concerning the column on the left of c, $\beta \geq 45°$. Since $\alpha + \beta = 90°$, we infer $\alpha = \beta = 45°$. Suppose c is not the vertex placed on the row below b. Then the edge (bc) would prevent this row to be occupied. Thus, c is the vertex placed on the row below b and b is placed on the column left to c, i.e. $x(b) = y(c) = n - 1$. Finally, the inner vertices must be placed on coordinates (i, i) for $2 \leq i \leq n - 2$, i.e. along a diagonal of the grid (see Fig. 2.5c).

Now that the positions of the vertices are determined, there is only one way to complete the drawing into a maximal plane graph, forming the graph $\mathcal{T}_n$. □

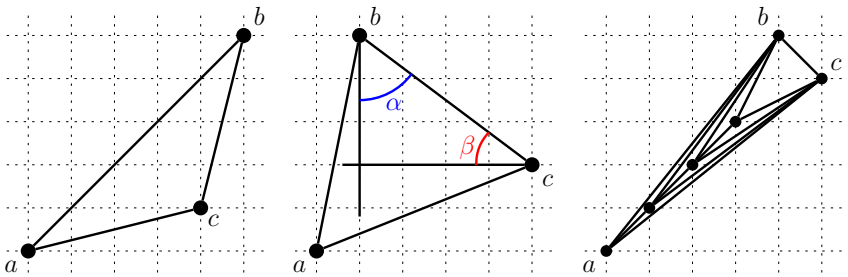

Figure 2.5: (a) and (b) Illustrations of the proof of Theorem 2.1. (c) A planar minimal non-aligned drawing of $\mathcal{T}_6$.

Another way to see Theorem 2.1 is the following: if G is a plane graph with a triangle as outer face and such that some of its inner vertices form a cycle, then G has no planar minimal non-aligned drawing.

Remark that the property of having a minimal planar non-aligned drawing is not closed by taking subgraphs: if we add a leaf on the outer face of an octahedron with n vertices (which can not be drawn on the minimal grid by Theorem 2.1), then this new graph can be drawn on an $n \times n$ grid (see Figure 2.6).

2.1.2 Linear-time algorithm creating $n - 3$ bends

Since we proved that in general, planar graphs do not have a planar non-aligned straight-line drawing, we now allow a small number of edges to be bent, i.e. to be drawn as polylines with a bend placed on a grid intersection (obviously, this intersection must not contain a vertex of the graph). Such drawings are called *polyline* drawings. The natural question arising is the minimum number of edges bent in such a drawing.

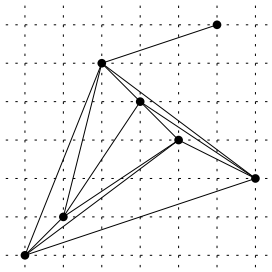

Figure 2.6: A minimal non-aligned drawing of a graph containing an octahedron as subgraph.

We here describe an algorithm producing a planar polyline minimal non-aligned drawing of a maximal plane graph with $n-3$ bends in linear time. Before presenting the algorithm, we give some definitions concerning the Schnyder wood of a maximal plane graph.

Schnyder woods

Definition 2.1 (Schnyder [Sch90])**.** A *Schnyder wood* of a maximal plane graph G is a partition of the inner edges of G into three directed trees T_0, T_1, T_2 with the following properties:

- each tree T_i is rooted on a distinct outer vertex v_i;
- the edges of each tree are directed toward the root;
- each inner vertex u of G has exactly one parent in each T_i, denoted $P_i(u)$;
- in counterclockwise order around each inner vertex, the out-edges are in T_0 then T_1 then T_2;
- each in-edge belonging to the tree T_i is placed after the out-edge in $T_{i+1 \bmod 3}$ and before the out-edge in $T_{i-1 \bmod 3}$ in counterclockwise order around an inner vertex.

The orientation of edges around an inner vertex is given in Fig. 2.7a. A Schnyder wood of a maximal plane graph is shown in Fig. 2.7b. Throughout the section, we call a 0-edge (respectively 1-edge, 2-edge) an edge belonging to the tree T_0 (resp. T_1, T_2). We denote by $\overline{T}_i$ the tree formed by T_i and the edges $(v_{i-1}v_i)$ and $(v_{i+1}v_i)$.

This tool, introduced by Schnyder in 1989 [Sch89] has been widely used since: directly in [Sch90], or to produce optimal drawings of planar graphs with bends [BLSM02], or with an extension to *orderly spanning trees* [CLL01] (for plane graphs not necessarily maximal), with many applications to graph drawings, such as visibility and 2-visibility drawings [CLL01; LLS04] or floor-planning [LLY03].

Let us recall some useful properties of Schnyder woods:

Lemma 2.2 ([Sch90, Section 8])**.** *Every maximal plane graph with n vertices admits at least one Schnyder wood, and it can be computed in $O(n)$ time.*

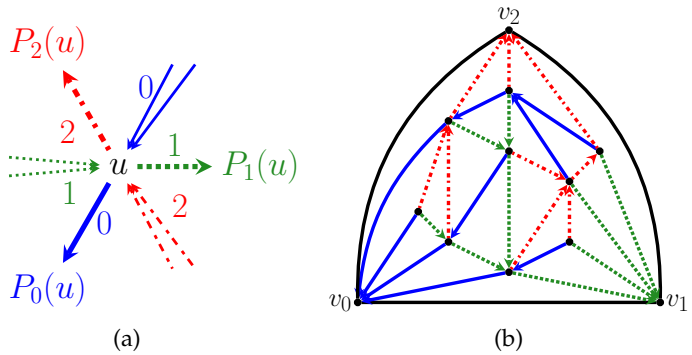

Figure 2.7: (a) Orientation around an inner vertex u in a Schnyder wood. (b) A Schnyder wood of a maximal plane graph. T_0 is drawn plain, T_1 is drawn dotted, and T_2 is drawn dotted-dashed.

Lemma 2.3 ([BGH11, Lemma 4]). *For every inner vertex u, $P_{i-1}(u)$ and $P_{i+1}(u)$ are unrelated to u in $\overline{T}_i$. Moreover $P_{i-1}(u)$ (resp. $P_{i+1}(u)$) appears before (resp. after) u in the clockwise preorder and postorder of $\overline{T}_i$.*

Linear algorithm for polyline non-aligned drawing

Our algorithm is inspired by the algorithm for polyline drawings proposed in [BLSM02]. The original algorithm was designed to minimize the grid size and thus many rows and columns support several vertices. This new algorithm shares with the former the edge bending strategy, but the vertex placement is different.

Theorem 2.4. *Every maximal plane graph G with n vertices admits a polyline planar minimal non-aligned drawing Γ, which can be computed by Algorithm 2.1 in linear time. This drawing has $n-3$ bends.*

In Algorithm 2.1 and later, $ll_0(u)$ denotes the last descendant met in a clockwise preorder of u in T_0.

An example of the result of Algorithm 2.1 on a maximal plane graph is presented in Fig. 2.8. Since the vertices are placed according to their position in a preorder and a postorder, each row and column contains exactly one vertex. Thus Γ is a minimal non-aligned drawing.

Number of bends

Let k be the number of leaves in T_0. By construction, T_0, T_1 and T_2 contain each $n-3$ edges and $n-2$ vertices. Recall that T_i does not contain v_{i-1} and v_{i+1}. The edges of T_0 are all bent, except one for each non-leaf vertex in T_0. Thus $n-3-(n-2-k)$ 0-edges are bent. The edges of T_1 are all bent, except k. Thus $n-3-k$ 1-edges are bent. Finally, the edges of T_2 are not bent. The edges (v_0v_2) and (v_2v_1) are not bent, and the

Algorithm 2.1: Planar polyline minimal non-aligned drawing for a maximal plane graph G

$(T_0, T_1, T_2) \leftarrow$ Schnyder wood of G
column order $C \leftarrow$ clockwise preorder of $\overline{T}_0$
row order $R \leftarrow$ clockwise postorder of $\overline{T}_1$
for *u vertex of G* **do**
  $(x(u), y(u)) = (C(u), R(u))$
for *u inner vertex of G* **do**
  if $x(u) \neq x(P_0(u)) + 1$ **then**
    Bend edge $(uP_0(u))$ at $(x(u), y(P_0(u)) + 1)$
  if $u \neq ll_0(u)$ **then**
    Bend edge $(uP_1(u))$ at $(ll_0(u), y(u))$
Bend edge (v_1v_0) at $(x(v_1), 2)$

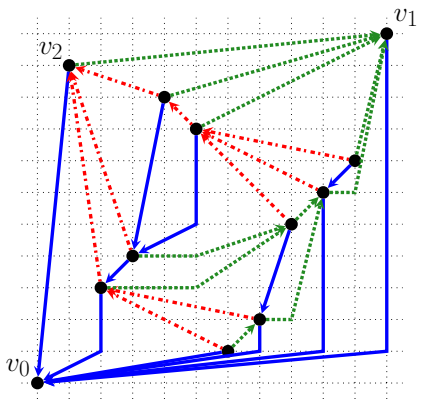

Figure 2.8: The polyline drawing obtained by Algorithm 2.1 applied on the graph G of Fig. 2.7b.

edge (v_0v_1) is bent. Thus there are exactly $n-3-(n-2-k)+(n-3-k)+1 = n-3$ bends in the drawing of G.

Planarity

We now present some structural properties of the drawing Γ in Lemmas 2.5 and 2.7.

Lemma 2.5. *In Γ, for each inner vertex u:*

- *$x(P_0(u)) < x(u)$ and $y(P_0(u)) < y(u)$: $P_0(u)$ is left and below u.*
- *$x(P_1(u)) > x(u)$ and $y(P_1(u)) > y(u)$: $P_1(u)$ is right and above u.*
- *$x(P_2(u)) < x(u)$ and $y(P_2(u)) > y(u)$: $P_2(u)$ is left and above u.*

Proof. Recall that the x-coordinates are given by a clockwise preorder of T_0 and that the y-coordinates are given by a clockwise postorder of T_1. Hence $x(P_0(u)) < x(u)$ and $y(P_1(u)) > y(u)$. Applying Lemma 2.3 with $i = 1$ we get that $P_0(u), u$ and

$P_2(u)$ appear in that order in the clockwise postorder of T_1. Hence $y(P_0(u)) < y(u)$ and $y(P_2(u)) > y(u)$. Applying again Lemma 2.3 but this time with $i = 0$ we get that $P_2(u), u$ and $P_1(u)$ appear in that order in the clockwise preorder of T_0. Hence $x(P_2(u)) < x(u)$ and $x(P_1(u)) > x(u)$. □

Remark 2.6. From Lemma 2.5 and the coordinates of bends chosen for the edges in Algorithm 2.1, we observe that the configuration around an inner vertex follows the scheme illustrated in Fig. 2.9.

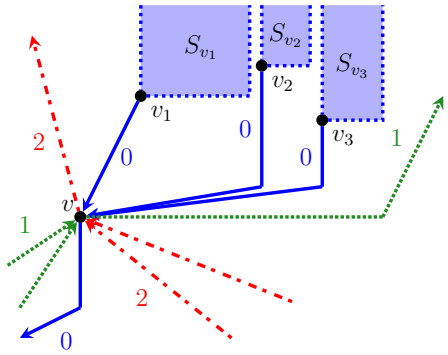

Figure 2.9: Edges orientation around an inner vertex v in Γ. The area S_{v_i} at the top-right hand side of v_i is the area in which the subtree of v_i in T_0 is drawn.

We now show that the relative positions of the vertices in the drawing Γ give information about their relation in the different trees:

Lemma 2.7. *The following holds for every inner vertex u :*

(i) every vertex v such that $x(P_0(u)) < x(v) < x(u)$ is a descendant of $P_0(u)$ in T_0.
(ii) if v is a vertex such that $x(u) < x(v) < x(P_1(u))$, then either v is a descendant of u in T_0, or $y(v) < y(u)$ in Γ.
(iii) if w is a vertex such that $x(P_2(u)) < x(w) < x(u)$, then either w is a descendant of $P_2(u)$ in T_0, or $y(w) < y(u)$ in Γ.

Proof. The first property is a direct consequence of the fact that the x-coordinates are given by the clockwise preorder of T_0.

Let v be a vertex such that $x(u) < x(v) < x(P_1(u))$. By Remark 2.6, either v is a descendant of u in T_0, or it is in the area $\mathcal{A}$ delimited in the original graph G by the T_0-paths (u, v_0) and $(P_1(u), v_0)$, and the edge $(uP_1(u))$ in T_1 (see Fig. 2.10a). Note that v may belong to the path $(P_1(u), v_0)$. We consider the path P in T_2 from v to v_2. Considering the relative orientations of the edges in the Schnyder wood, since v_2 is outside area $\mathcal{A}$, P has to intersect the border (u, v_0) of $\mathcal{A}$ to reach v_2 (even if v belongs to the T_0-path $(P_1(u), v_0)$, its out-edge in T_2 heads into $\mathcal{A}$). Let t denote the vertex at the intersection. There is a path in T_2 from v to t and a path in T_0 from u to t. By Lemma 2.5, $y(v) < y(t)$ and $y(t) < y(u)$, and thus $y(v) < y(u)$.

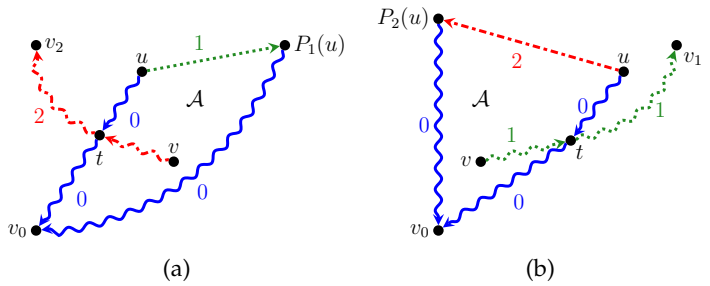

Figure 2.10: Illustrations of the proof of Lemma 2.7.(ii) and Lemma 2.7.(iii).

A similar argument, exchanging the roles of T_1 and T_2 (see Fig. 2.10b), proves the third statement. □

We now prove that the edges of Γ do not cross. Lemmas 2.8 and 2.9 state such for the edges inside each tree $\overline{T}_0$ and T_1. Then we prove that edges from different trees do not cross with Lemmas 2.10, 2.11 and 2.12. After that, we show that edges from T_2 do not cross pairwise with Lemma 2.13. Finally, drawing the edge (v_1v_2) with a straight line does not create any crossing, since all vertices and bends are placed on the same side of the straight-line defined by the vertices v_1 and v_2.

For each vertex u of G, recall that we denote $ll_0(u)$ the last descendant met in the clockwise preorder of u in $\overline{T}_0$. We define the subgrid $[a, b] \times [c, d]$ as the grid with $b - a + 1$ columns and $d - c + 1$ lines, such that the vertex in the bottom-left corner has coordinates (a, c) and the one in the top-right corner has coordinates (b, d).

Lemma 2.8. *The edges of $\overline{T}_0$ do not cross in Γ.*

Proof. We prove by induction on the depth k of subtrees in $\overline{T}_0$ the following proposition: in Γ, the subtree of a vertex u in $\overline{T}_0$, denoted $\overline{T}_0(u)$, is drawn planarly in the subgrid $[x(u), x(u) + (|\overline{T}_0(u)| - 1)] \times [y(u), n]$ (see Fig. 2.11).

The proposition clearly holds when $k = 0$.

Assume the proposition holds for subtrees of depth at most k in $\overline{T}_0$. Let u be a vertex of G such that $\overline{T}_0(u)$ has depth $k+1$. Let $u_1, \dots, u_m$ be the children of u (taken in clockwise order around u). Vertices of $\overline{T}_0(u)$ are consecutive in the clockwise preorder of $\overline{T}_0$ and by Lemma 2.5, $y(v) > y(u)$ for every vertex v of $\overline{T}_0(u)$. Thus the drawing of the union of subtrees $\overline{T}_0(u_\ell)$ lies in $[x(u), x(u) + (|\overline{T}_0(u)| - 1)] \times [y(u), n]$.

By the induction hypothesis the edges of these subtrees are drawn in disjoint areas, hence the drawing of the union of the subtrees is planar. Moreover, by construction the edges joining u to $u_1, \dots, u_m$ do not cross each other and lie in a region free of edges from the subtrees (each vertex u_ℓ lies in the bottom row of its dedicated area). Hence the drawing of $\overline{T}_0(u)$ is planar. By construction of the bends for the edges joining u to $u_1, \dots, u_m$, $\overline{T}_0(u)$ is also drawn in the subgrid $[x(u), x(u) + (|\overline{T}_0(u)| - 1)] \times [y(u), n]$. □

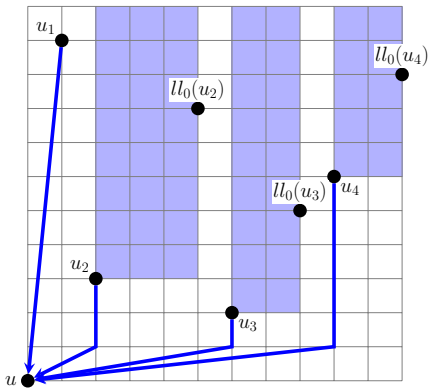

Figure 2.11: Illustration of the proof of Lemma 2.8. The area at the top-right hand side of u_i is the area in which the subtree of u_i in $\overline{T}_0$ is drawn.

Lemma 2.9. *The edges of T_1 do not cross in Γ.*

Proof. We prove by induction on the depth k of subtrees in T_1 the following proposition: in Γ, the subtree of a vertex u in T_1, denoted $T_1(u)$, is drawn planarly in the subgrid $[1, x(u)] \times [y(u) - (|T_1(u)| - 1), y(u)]$ (see Fig. 2.12).

The proposition clearly holds when $k = 0$.

Assume the proposition holds for subtrees of depth at most k in T_1. Let u be a vertex of G such that $T_1(u)$ has depth $k + 1$. Let $u_1, \ldots, u_m$ be the children of u (in clockwise order around u). Vertices of $T_1(u)$ are consecutive in the clockwise postorder of T_1 and by Lemma 2.5, $x(v) < x(u)$ for every vertex v of $T_1(u)$. Thus the drawing of the union of subtrees $T_1(u_\ell)$ lies in $[1, x(u)] \times [y(u) - (|T_1(u)| - 1), y(u)]$.

By the induction hypothesis, the edges of these subtrees are drawn in disjoint areas, hence the drawing of their union is planar.

Let now prove that the edges joining u and $u_1, \ldots, u_m$ do not cross each other. Recall that the edge $(u_\ell u)$ is bent at coordinates $(x(ll_0(u_\ell)), y(u_\ell))$. Let u_ℓ and $u_{\ell+1}$ be two consecutive children of u. Let us show that the bends (uu_ℓ) and $(uu_{\ell+1})$ are placed at positions with increasing y-coordinates and decreasing x-coordinates. By Lemma 2.5, $y(u_\ell) < y(u_{\ell+1})$, thus the bends have increasing y-coordinates. We now prove that $x(ll_0(u_{\ell+1})) \leq x(ll_0(u_\ell))$. By definition of the x-coordinates, all descendants of a vertex t in T_0 are placed on consecutive columns at the right of t. Since $y(u_\ell) < y(u_{\ell+1})$, by contrapositive of Lemma 2.7.(ii), either $u_{\ell+1}$ is a descendant of u_ℓ in T_0 or $x(u_{\ell+1}) < x(u_\ell)$. If $u_{\ell+1}$ is a descendant of u_ℓ in T_0, then by Lemma 2.5 and the definition of the x-coordinates, $x(ll_0(u_{\ell+1})) \leq x(ll_0(u_\ell))$. If $x(u_{\ell+1}) < x(u_\ell)$, then all descendants of $u_{\ell+1}$ in T_0 have abscissas between $x(u_{\ell+1})$ and $x(u_\ell)$, hence $x(ll_0(u_{\ell+1})) \leq x(ll_0(u_\ell))$.

Then the bends for the edges (uu_ℓ) are placed at positions with increasing y-coordinates and decreasing x-coordinates. Thus the edges joining u and $u_1, \ldots, u_m$ do not cross each other. These edges can not cross edges of a subtree of u_ℓ in $\overline{T}_0$ either, as each vertex u_ℓ lies in the bottom row of the area dedicated to the drawing

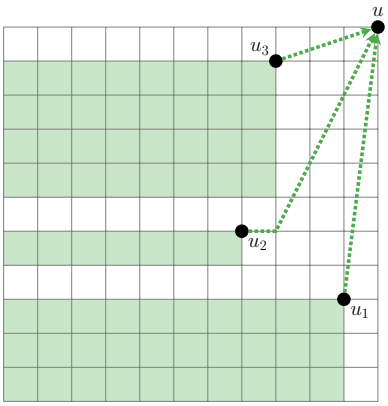

Figure 2.12: Illustration of the proof of Lemma 2.9. The area at the bottom-left hand side of u_i is the area in which the subtree of u_i in T_1 is drawn.

of $\overline{T}_0(u)$ and the bent of the edge $(u_\ell u)$ lies in the right-most column of this area. Hence the drawing of $T_1(u)$ is planar. □

Lemma 2.10. *The edges of $\overline{T}_0$ and T_1 do not cross in Γ.*

Proof. Let (wt) be a 1-edge. By Lemma 2.5, $x(w) < x(t)$ and $y(w) < y(t)$. Let (uv) be an edge of $\overline{T}_0$. If $x(w) > x(u)$ or $y(w) > y(u)$, then the edges (wt) and (uv) can not cross each other. Assume $x(w) < x(u)$ and $y(w) < y(u)$.

Suppose $x(t) > x(u)$. Since $x(w) < x(u) < x(t)$ and $y(w) < y(u)$, then by Lemma 2.7.(ii), u is a descendant of w in $\overline{T}_0$. Thus v is also a descendant of w in $\overline{T}_0$. But then the bend of (wt) avoids any crossing.

Suppose $x(t) < x(u)$. If $y(v) < y(w)$, then the bend of (uv) avoids any crossing. Thus assume $y(v) > y(w)$. By Lemma 2.7.(i), if $x(v) < x(w)$, then w is a descendant of v in T_0, contradicting $y(v) > y(w)$. So $x(w) < x(v) < x(t)$ and by Lemma 2.7.(ii), v is a descendant of w in $\overline{T}_0$, and so is u. By definition of the x-coordinates, all descendants of w in $\overline{T}_0$ are consecutive to w and before t in the x-order, a contradiction with $x(t) < x(u)$. □

Lemma 2.11. *The edges of $\overline{T}_0$ and T_2 do not cross in Γ.*

Proof. Let (wt) be a 2-edge. By Lemma 2.5, $x(t) < x(w)$ and $y(t) > y(w)$. Let (uv) be an edge of $\overline{T}_0$. If $x(w) < x(v)$ or $y(v) > y(t)$, then the edges (uv) and (wt) do not cross each other. Similarly, if $x(u) < x(t)$ or $y(u) < y(w)$, the edges do not cross either. So assume that $x(v) < x(w)$, $y(v) < y(t)$, $x(t) < x(u)$ and $y(w) < y(u)$.

If $x(u) < x(w)$, then by Lemma 2.7.(iii), u is a descendant of t in $\overline{T}_0$. Since v is the parent of u in $\overline{T}_0$, v is also a descendant of t in $\overline{T}_0$. Hence by Lemma 2.5, $y(v) > y(t)$; a contradiction.

If $x(u) > x(w)$, then $x(v) < x(w) < x(u)$ and by Lemma 2.7.(i), w is a descendant of v in $\overline{T}_0$. Thus (uv) avoids w and there is no crossing. □

Lemma 2.12. *The edges of T_1 and T_2 do not cross in Γ.*

Proof. Let (uv) be a 2-edge and (wt) a 1-edge. By Lemma 2.5, $x(u) > x(v)$, $y(u) < y(v)$, $x(t) > x(w)$ and $y(t) > y(w)$. Assume $x(t) > x(v)$, $y(t) > y(u)$, $x(w) < x(u)$ and $y(w) < y(v)$, or (uv) and (wt) may not cross.

If $x(t) < x(u)$ (see Fig. 2.13a), then $x(v) < x(t) < x(u)$. Since $y(t) > y(u)$, by the contrapositive of Lemma 2.7.(iii), t is a descendant of v in $\overline{T}_0$. Then the orientation of the edges around t implies that either (uv) and (wt) do not cross, or (wt) also crosses the T_0-path (t, v), contradicting Lemma 2.10.

If $x(u) < x(t)$, then $x(w) < x(u) < x(t)$. u is not a descendant of w in $\overline{T}_0$ (otherwise the bend of (wt) would prevent the crossing). Thus by definition of $x(u)$, u is in the area $\mathcal{A}$ delimited in the original graph G by the paths (w, v_0) and (t, v_0) in $\overline{T}_0$, and the edge (wt) in T_1 (see Fig.2.13b). Note that u may belong to the path (t, v_0) in $\overline{T}_0$. We consider the path $\mathcal{P}$ in T_2 from u to v_2. Considering the relative orientations of the edges in the Schnyder wood, since v_2 is outside $\mathcal{A}$, then $\mathcal{P}$ has to intersect the border (w, v_0) of $\mathcal{A}$ to reach v_2 (even if u is on the path (t, v_0), its out-edge in T_2 heads into $\mathcal{A}$). Let z denote the intersection. By Lemma 2.5, $y(z) < y(w)$. z is a parent of u in T_2 and thus a parent of v in T_2 (we may have $z = v$). Thus by Lemma 2.5, $y(z) \geq y(v)$ and thus $y(w) > y(v)$, which is a contradiction. □

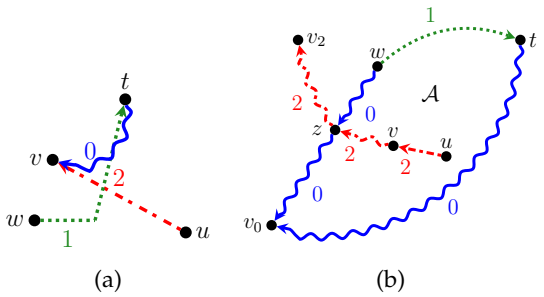

Figure 2.13: Illustration of the two cases for the proof of Lemma 2.12.

Lemma 2.13. *The edges of T_2 do not cross in Γ.*

Proof. Let (uv) and (wt) be edges of T_2. Suppose they cross each other. Thus $x(w) > x(v)$, $y(w) < y(v)$, $x(t) < x(u)$ and $y(t) > y(u)$. Since the two edges play similar roles, we can suppose without loss of generality that $x(t) > x(v)$ (see Fig.2.14. Then $x(v) < x(t) < x(u)$ and $y(t) > y(u)$, and by Lemma 2.7.(iii), t is a descendant of v in $\overline{T}_0$. But then the edge (wt) would cross a 1-edge in the path of T_1 joining v to v_1, contradicting Lemma 2.12. □

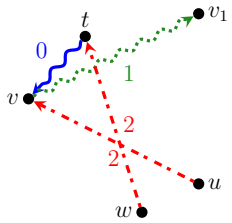

Figure 2.14: Illustration for the proof of Lemma 2.13.

2.1.3 Polynomial-time algorithm creating at most $\frac{2n-5}{3}$ bends

Even if there is a lower bound of $\lceil \frac{2(n-1)}{3} \rceil$ for the width and height of a minimal grid supporting a straight-line planar drawing for any plane graph [CN98; DFPP90], some restricted classes of graphs only need a much smaller grid. For example, some 4-connected plane graphs (i.e. graphs without separating triangle) have more compact straight-line grid drawings: He [He97] showed that any 4-connected plane graph with an outer face of degree at least 4 has a straight-line planar drawing on an $\left(\frac{n+3}{2}\right) \times \left(\frac{2(n-1)}{3}\right)$-grid. Later, Miura, Nakano and Nishizeki [MNN01] improved this result to an $(\lceil \frac{n}{2} \rceil - 1) \times \lfloor \frac{n}{2} \rfloor$-grid. Both algorithms use a 4-canonical ordering of the vertices of the graph, and run in linear time. 4-connected plane graphs are thus good candidates to have non-aligned planar drawings on grids of small dimensions.

We now present a second algorithm creating minimal non-aligned drawings with bends; as before we do this only for maximal plane graphs. We first recall the notion of rectangle-of-influence drawings. After giving some results on non-aligned drawings for 4-connected graphs, we present our algorithm. The main idea is the following: we convert any maximal plane graph into a 4-connected maximal plane graph by subdividing few edges and re-triangulating, we draw a rectangle-of-influence drawing of this new graph, and we argue that the obtained drawing, modified suitably, gives a minimal non-aligned drawing with a small number of bends. More precisely, the total number of bends directly depends on the number of separating triangles of the original plane graph.

Rectangle-of-influence drawings

A *rectangle-of-influence (RI) drawing* (introduced by Ichino and Sklansky [IS85]) is a straight-line drawing such that for any edge (uv), the minimum axis-aligned rectangle containing u and v and denoted by $R(uv)$ is *empty*, i.e. contains no other vertex of the drawing in its relative interior (we call it the *RI property*). An example of rectangle-of-influence drawing is given in Figure 2.15a. In the literature there are four kinds of RI-drawings, depending on whether points on the boundary of the rectangle are allowed or not (open vs. closed RI-drawings), and whether an edge (uv) must exist if $R(uv)$ is empty (strong vs. weak RI-drawings). The section here only deals with open weak RI-drawings.

RI-drawings are useful because they can be deformed (within limits) without introducing crossings. We say that two drawings Γ and Γ' of a graph have *the same*

relative coordinates if for any two vertices v and w, we have $x_\Gamma(v) < x_\Gamma(w)$ if and only if $x_{\Gamma'}(v) < x_{\Gamma'}(w)$, and $y_\Gamma(v) < y_\Gamma(w)$ if and only if $y_{\Gamma'}(v) < y_{\Gamma'}(w)$, where $x_\Gamma(v)$ (resp. $y_\Gamma(v)$) denotes the x-coordinate (resp. y-coordinate) of v in Γ. The following result appears to be folklore; we sketch a proof for completeness.

> **Observation 1.** *Let Γ be an RI-drawing. If Γ' is a straight-line drawing with the same relative coordinates as Γ, then Γ' is an RI-drawing, and it is planar if and only if Γ is.*

Proof. The claim that Γ' is also a RI-drawing was shown by Liotta et al. [LLMW98]. It remains to argue planarity. Assume that edge (uv) crosses edge (wz) in an RI-drawing. Since all rectangles-of-influence are empty, this happens if and only if (up to renaming) we have $x(w) \leq x(u) \leq x(v) \leq x(z)$ and $y(u) \leq y(w) \leq y(z) \leq y(v)$. This only depends on the relative orders of u, v, w, z, and hence a transformation maintaining relative coordinates also maintains planarity. □

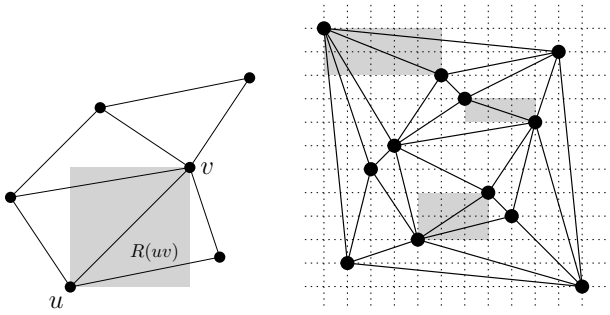

Figure 2.15: (a) The rectangle-of-influence $R(uv)$ of two vertices u and v. (b) An RI-drawing of a maximal 4-connected plane graph (without one of its outer edges) satisfying the conditions of Theorem 2.14.

In fact, some RI-drawings of maximal plane 4-connected graphs (minus one outer edge) are planar *non-aligned* drawings with specific properties:

> **Theorem 2.14** ([BBM99]). *Let G be a maximal plane 4-connected graph and e one of its outer edges. Then $G - e$ has a planar RI-drawing Γ such that Γ is non-aligned and on a minimal grid with n rows and columns, the ends of e are at $(1, n)$ and $(n, 1)$, and the other two vertices on the outer face of $G - e$ are at $(2, 2)$ and $(n - 1, n - 1)$.*

Figure 2.15b illustrates such a drawing. The latter part of the claim is not specifically stated in [BBM99], but can easily be inferred from the construction (see also a simpler exposition in [BD16], Section 4.2). The constructions given in [BBM99] and [BD16] both use canonical ordering or a variation of it.

We need a slight strengthening of Theorem 2.14 to deal with maximal plane graphs:

Lemma 2.15. *Let G be a maximal plane graph, let $e \in E$ be an edge on the outer face, and assume all separating triangles of G contain e. Then $G - e$ has a planar RI-drawing. Moreover, the drawing is non-aligned and on a minimal grid, the ends of e are at $(1, n)$ and $(n, 1)$, and the other two vertices on the outer face are at $(2, 2)$ and $(n - 1, n - 1)$.*

Proof. We proceed by induction on the number of separating triangles of G. In the base case, G is 4-connected and the claim holds by Theorem 2.14. For the inductive step, assume that $T = [uxw]$ is a separating triangle. By assumption it contains e, say $e = (uw)$. Let G_1 be the graph consisting of T and all vertices inside T, and let G_2 be the graph obtained from G by removing all vertices inside T. Apply induction to both graphs. In drawing Γ_2 of $G_2 - e$, vertex x is on the outer face and hence (after possible reflection) placed at $(2, 2)$. Now insert a (scaled-down) copy of the drawing Γ_1 of G_1, minus vertices u and w, in the square $(1, 2] \times (1, 2]$ (see Figure 2.16). Since x was (after possible reflection) in the top-right corner of $\Gamma_1 - \{u, w\}$, the two copies of x can be identified. One easily verifies that this gives an RI-drawing, because within each drawing the relative coordinates are unchanged, and the two drawings have disjoint x-range and y-range except at u and w. Finally, re-assign coordinates to the vertices while keeping relative coordinates intact so that they are placed on a $(n - 1) \times (n - 1)$-grid; by Observation 1 this gives a planar RI-drawing. □

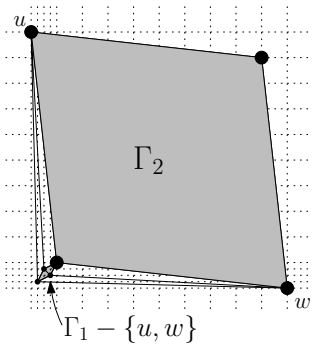

Figure 2.16: Combining two RI-drawings if all separating triangles contain the edge (uw).

Finally, we show that some vertices of a RI-drawing may be moved around locally without breaking planarity or RI property:

Lemma 2.16. *Let Γ be a planar RI-drawing. Let x be an inner vertex of degree 4 with neighbours u_1, u_2, u_3, u_4 forming a cycle. If none of x, u_1, u_2, u_3, u_4 share a grid-line, then we can move x to a point on grid-lines of its neighbours and still have a planar RI-drawing.*

Without loss of generality, u_1, u_2, u_3, u_4 are the neighbours of x in counterclockwise order, forming the cycle $C_u = (u_1u_2u_3u_4)$. Consider the five columns supporting x, u_1, u_2, u_3, and u_4; we denote these columns by $1, \ldots, 5$ (from left to right), even though their actual x-coordinates may be different (and in particular, the vertices

may not belong to consecutive columns). Likewise let $1, \dots, 5$ be the five rows supporting x, u_1, u_2, u_3, u_4.

Quadrants Q_i ($i = 1, 2, 3, 4$) are defined as follows (see Fig. 2.17):

$$\begin{cases} Q_1 & := \{(4,4), (4,5), (5,4), (5,5)\} \\ Q_2 & := \{(1,4), (1,5), (2,4), (2,5)\} \\ Q_3 & := \{(1,1), (1,2), (2,1), (2,2)\} \\ Q_4 & := \{(4,1), (4,2), (5,1), (5,2)\}\,. \end{cases}$$

Each neighbour of x shares no grid-line with x and hence belongs to some quadrant Q_i. We claim that without loss of generality u_i is in Q_i for $i = 1, 2, 3, 4$. In fact, if any quadrant is empty, then either two consecutive vertices of u_1, u_2, u_3, u_4 are in diagonally opposite quadrants (and x is inside their rectangle-of-influence, a contradiction), or all four of u_1, u_2, u_3, u_4 are within two consecutive quadrants (and x is outside cycle C_u, violating planarity). So each quadrant contains at least one of the four vertices, implying that each contains exactly one of them.

Since x has a neighbour in each quadrant, x must be placed at $(3, 3)$. The open rectangle $R\big((2,2)(4,4)\big)$ contains none of u_1, u_2, u_3, u_4, so the cycle C_u goes around it. The only vertex inside C_u is x, thus no vertex other than u_3 or u_4 can be at $(2, 2)$ or $(4, 2)$. But not both u_3 and u_4 can be in row 2. Without loss of generality, point $x' := (2, 2)$ contains no vertex. We can then move x to x'.

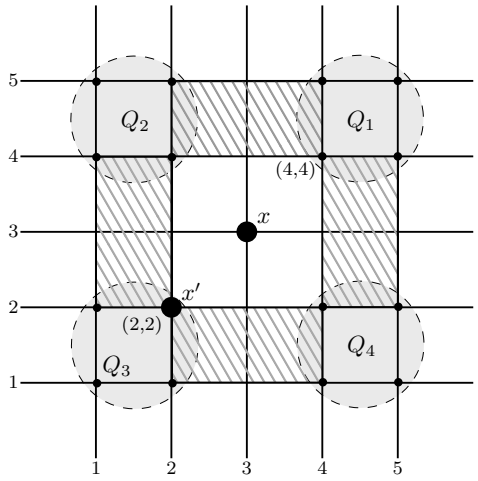

Figure 2.17: Moving x locally in an RI-drawing to point x'. Q_i represents the possible locations of the u_i. Since the vertices $u_1, \dots, u_4$ are in non-aligned position, the hatched areas are empty.

We claim that we obtain an RI-drawing, and verify the conditions for the four edges (xu_i) separately:

- Vertex u_3 is in Q_3, but not at $(2, 2)$ (by choice of x'). In any case, rectangle $R(xu_3)$

has x' inside or on the boundary, and since (xu_3) is an edge in an RI-drawing, $R(x'u_3) \subset R(xu_3)$ is empty.

- Vertices u_3 and u_4 are on rows 1 and 2, but not on the same row, so $R(u_3u_4)$ contains points that are between rows 1 and 2. By definition of the positions of the u_i, $R(u_3u_4)$ includes $R\big((2,1)(4,2)\big)$. So the empty rectangle $R(u_3u_4)$ contains point $(2,2) = x'$ and therefore includes rectangle $R(x'u_4)$.
- Similarly one shows that $R(x'u_2)$ is empty.
- It remains to show that $R(x'u_1)$ is empty, regardless of the position of u_1 within Q_1. We already saw that $R_1 := R\big((2,2)(4,4)\big)$ is empty. Since u_1 and u_2 are on rows 4 and 5 (but not on the same row), $R_2 := R\big((2,4)(4,5)\big)$ is within $R(u_1u_2)$ and is thus empty. Similarly one shows that $R_3 := R\big((4,2)(5,4)\big)$ is empty. Notice that $R_1 \cup R_2 \cup R_3$ contains $R(x'u_1)$, unless u_1 is at $(5,5)$. But in the latter case $R_4 := R\big((4,4)(5,5)\big) \subset R(xu_1)$ is empty. So either way $R(x'u_1)$ is contained within the union of empty rectangles and therefore is empty. □

Non-aligned drawings for 4-connected planar graphs

Combining Theorem 2.14 with Observation 1, we immediately obtain:

> **Theorem 2.17.** *Let G be a maximal 4-connected plane graph. Then G has a planar minimal non-aligned drawing with at most one bend.*

Proof. Fix an arbitrary edge e on the outer face, and apply Theorem 2.14 to obtain an minimal RI-non-aligned drawing Γ of $G - e$. It remains to add in the edge $e = (uv)$. One end u of e is in the top-left corner, and the leftmost column contains no other vertex. The other end v is in the bottom-right corner, and the bottom-most row contains no other vertex. We route (uv) by going vertically from u and horizontally from v, with the bend in the bottom-left corner. □

Corollary 1. *Let G be a 4-connected planar graph. Then G has a minimal non-aligned drawing with at most one bend, and with no bend if G is not maximal.*

Proof. If G is maximal then the result was shown above, so assume G has at least one face of degree 4 or more. Since G is 4-connected, one can add edges to G such that the obtained graph G' is maximal and 4-connected [BKK97]. Pick a face incident to an added edge e as outer face of G', and apply Theorem 2.14 to obtain an RI-drawing of $G' - e$. Deleting all edges in $G' - G$ gives the result. □

Since we have only (at most!) one bend in the drawing of a 4-connected planar graph, and the ends of the bent edge are at the top-left and bottom-right corners, we can remove the bend by stretching, if necessary. This gives us the following theorem:

> **Theorem 2.18.** *Every 4-connected planar graph has a non-aligned planar drawing on an $(n-1) \times (n^2 - 3n + 3)$-grid and on a $(2n-3) \times (2n-3)$-grid.*

Proof. Let Γ be the RI-drawing of $G - (uv)$ with u at $(1,n)$ and v at $(n,1)$. Relocate u to point $(1, n^2 - 3n + 4)$. The resulting drawing is still a planar RI-drawing by

Observation 1. Now $y(u) - y(v) = (n-2)(n-1)+1$, hence the line segment from u to v has a slope

$$\frac{y(u)-y(v)}{x(u)-x(v)} = \frac{(n-2)(n-1)+1}{-(n-1)} < -(n-2) = 2-n\,,$$

and is above point $(n-1, n-1)$ (and also above all other vertices of the drawing). So we can add this edge without violating planarity, and obtain a non-aligned straight-line drawing of G (see Figure 2.18a).

For the other result, start with the same drawing Γ. Relocate u to coordinates $(1, 2n-2)$ and v to $(2n-2, 1)$. The line segment from u to v has slope -1 and crosses Γ only between points $(n-1, n)$ and $(n-1, n)$, where no points of Γ are located. So we obtain a non-aligned planar straight-line drawing (see Figure 2.18b). □

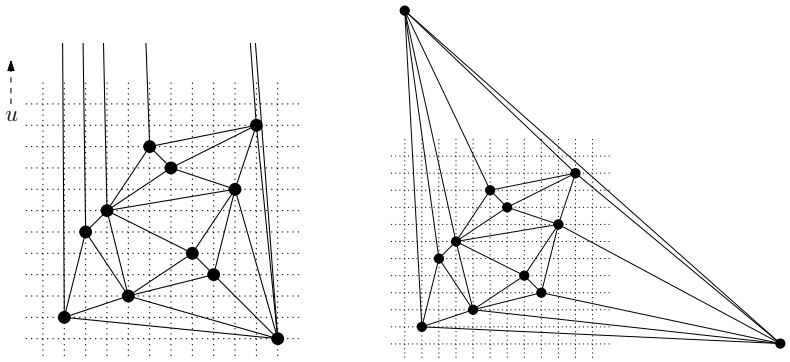

(a) (b)

Figure 2.18: Transformation of the drawing of Figure 2.15a into: (a) a non-aligned drawing of G of with n columns, where the top-left corner was moved sufficiently high, and (b) a non-aligned drawing of G on a $(2n-3) \times (2n-3)$-grid.

Constructing minimal non-aligned drawings with few bends

We now explain the construction of a polyline minimal non-aligned drawing for a maximal plane graph G with at least five vertices.

A *filled triangle* [BBM99] of G is a triangle that has vertices strictly inside it. A maximal plane graph has at least one filled triangle, namely the outer face, and every separating triangle is also a filled triangle. We use f_G to denote the number of filled triangles of the graph G.

As presented before, our construction is based on the following steps: make G 4-connected (while remembering the changes made to it), use Lemma 2.15, and undo the changes while keeping a planar non-aligned RI-drawing.

We proceed as follows:

1. Find a small independent-filled-hitting set E_f.

Here, an *independent-filled-hitting set* of a plane graph G is a set of edges $E' \subset E(G)$ such that (i) every filled triangle has at least one edge in E' (we say that E' *hits* all filled triangles), and (ii) every face of G has at most one edge in E' (we say that E' is *independent*).

Precisions about the size of this set are given later, in Lemma 2.19. For now, simply assume that E_f exists (see Figure 2.19a).

2. Since the outer face is a filled triangle, there exists one edge $e_o \in E_f$ that belongs to it. Define $E_s := E_f - \{e_o\}$ and notice that since E_f is independent, E_s contains no outer edges.
3. As done in some previous papers [Car+15; KW02], remove separating triangles by subdividing all edges $e \in E_s$, and re-triangulate by adding edges from the subdivision vertex (see Figure 2.19b). Let V_x be the new set of vertices, and let G_1 be the new graph. Observe that G_1 may still have separating triangles, but all those separating triangles contain e_o since E_f hits all filled triangles.
4. By Lemma 2.15, $G_1 - e_o$ has a non-aligned RI-drawing Γ where the ends of e_o are at the top-left and bottom-right corner (see Figure 2.15a).
5. Transform Γ into drawing Γ' so that the relative orders stay intact, the original vertices (i.e., vertices of G) are on an $(n-1) \times (n-1)$-grid and the subdivision vertices (i.e., vertices in V_x) are inbetween.

   This can be done by enumerating the vertices in according to their x-coordinates, and assigning new x-coordinates by increasing to the next integer for each original vertex and increasing by $\frac{1}{|V_x|+1}$ for each subdivision vertex. The y-coordinates are updated similarly (see Figure 2.19c). The drawing Γ' is still a non-aligned RI-drawing, and the ends of e_o are still on the top-left and bottom-right corner.
6. Let e be an edge in E_s with subdivision vertex x_e. Since e is an inner edge of G, x_e is an inner vertex of G_1. By Lemma 2.16, we can move x_e to some grid point nearby. Note that the neighbours of x_e are not in V_x, since E_s is independent. So we can apply this operation independently to all subdivision vertices.
7. Now replace each subdivision vertex x_e by a bend, connected to the ends of e along the corresponding edges from x_e (see Figure 2.19d). (Sometimes, as in the example, we could also simply delete the bend and draw the edge e with a segment. Such optimization is not dealt with here.) None of the shifting changed positions for vertices of G, so we now have a minimal non-aligned drawing of $G - e_o$ with bends. The above shifting of vertices does not affect outer vertices, so the ends of e_o are still in the top-left and bottom-right corner. Finally, draw e_o by drawing vertically from one end and horizontally from the other; these segments are not occupied by the minimal non-aligned drawing.

We added one bend for each edge in E_f. We now give some precisions on this independent-filled-hitting set in the following lemma:

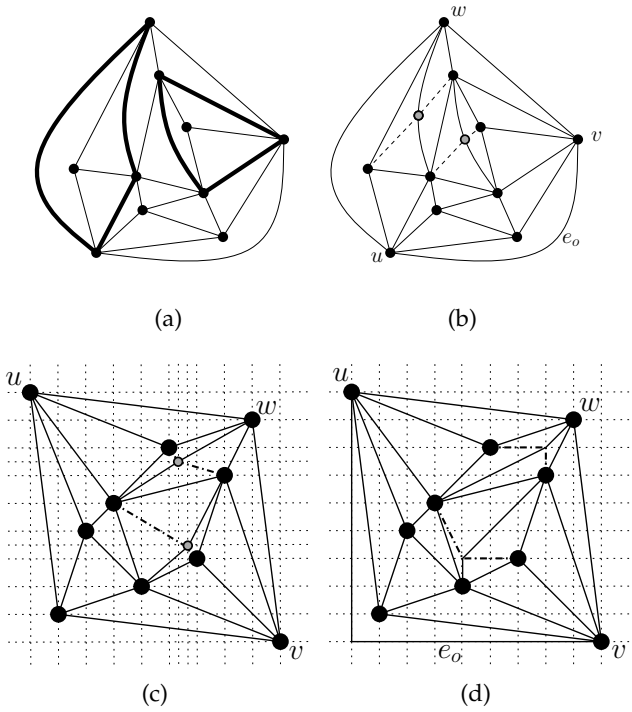

Figure 2.19: (a) A maximal plane graph G. Edges of the separating triangles are drawn thicker. (b) Creating G_1. The subdivision vertices are drawn in gray, and subdivision edges are dashed. (c) The RI-drawing of $G_1 - e_o$ reordered such that subdivision vertices are not at integer coordinates. (d) Drawing the same graph, with subdivision vertices shifted to integer gridpoints, and adding e_o.

Lemma 2.19. *Any maximal plane graph G of order n has an independent-filled-hitting set of size at most*

- *f_G (where f_G is the number of filled triangles of G), and it can be found in $O(n)$ time,*
- *$\frac{2n-5}{3}$, and it can be found in $O((n \log n)^{1.5}\sqrt{\alpha(n,n)})$ time (where α is the slow-growing inverse Ackermann function).*

The proof of this lemma requires detours into matchings and coloring; to keep the flow of the explanation, we defer it to the next section.

By Lemma 2.19, we can find a set E_f with $|E_f| \leq f_G$ and $|E_f| \leq \frac{2n-5}{3}$ (neither bound is necessarily smaller than the other), and hence have:

Theorem 2.20. *Any planar graph G of order n has a planar minimal non-aligned drawing with at most b bends, with $b \leq \min\{\frac{2n-5}{3}, f_G\}$.*

2.1.4 Proof of Lemma 2.19

Recall that we want to find a set E_f that *hits* all filled triangles (i.e., contains at least one edge of each filled triangle) and is *independent* (i.e., no face contains two edges of E_f).

Let us first show that every maximal plane graph has a independent-filled-hitting set. Since G is maximal, its dual graph G^* is 3-regular and 3-connected, and by Petersen's theorem [Pet91] it has a perfect matching; it can be found in linear time [BBDL01]. We call an edge set E_f a *dual matching* if the dual edges of E_f form a matching in G^*, and a *dual perfect matching* if its dual edges form a perfect matching in G^*.

> **Observation 2.** *Every dual matching is independent. Every dual perfect matching hits all triangles of G (in particular therefore all filled triangles).*

So we can find an independent-filled-hitting set E_f by computing a perfect matching in G^* and taking the corresponding dual perfect matching. Since G has $2n-4$ faces, this gives $|E_f| = n-2$. The rest of this section deals with improving this bound.

We give two proofs that show how to find independent-filled-hitting sets that are smaller than $n-2$ edges; the first is quite simple and takes linear time; the second gives a better bound, but is more complicated and requires computation of a minimum-weight perfect matching.

Our first result shows how to find a matching of size at most f_G in linear time. The existence of such a matching could easily be proved using the four color theorem (see below for more details), but with a different approach we can find it in linear time.

> **Lemma 2.21.** *Any maximal plane graph G has an independent-filled-hitting set E_f of size at most f_G. It can be found in linear time.*

Proof. We prove a slightly stronger statement, namely, that we can find such a set E_f and additionally (i) we can prescribe which edge e_o on the outer face is in E_f, and (ii) every separating triangle has exactly one edge in E_f.

We proceed by induction on the number of filled triangles. If G has only one (the outer face), then set $E_f = \{e_o\}$; this satisfies all claims. Now assume G has multiple filled triangles, and let $T_1, \dots, T_k$ (for $k \geq 1$) be the maximal separating triangles in the sense that no other separating triangle contains T_i inside. Let G_i (for $i = 1, \dots, k$) be the graph induced by T_i and all vertices inside it. Since we chose maximal separating triangles, the graphs $G_1, \dots, G_k$ are disjoint. Let the *skeleton* G^{skel} of G be the graph obtained from G by removing the interior of $T_1, \dots, T_k$, and $(G^{\text{skel}})^*$ the dual graph of G^{skel} (see Figure 2.20). Since G^{skel} is maximal, its dual graph is 3-regular and 3-connected, and therefore has a perfect matching M by Petersen's theorem [Pet91], which can be found in linear time (see e.g. [BBDL01]). We can assume that the dual edge e_o^* of e_o is in M: if not, then find an alternating cycle that contains e_o^* and swap matching with non-matching edges so that e_o^* is in

M. For every maximal separating triangle T_i of G, exactly one edge e_i of T_i has its dual edge in matching M, since T_i forms a face in G^{skel}.

Now, apply the induction step: find an independent-filled-hitting set $E_{f,i}$ of each G_i while prescribing e_i to be within E_i. Combine all these independent-filled-hitting sets into one set and add e_o to it (if it is not already in it); the result is the set $E_f = \{(\bigcup_{i=1}^{k} E_{f,i}) \cup \{e_o\}\}$.

Every filled triangle of G is either the outer face or a filled triangle of one of the subgraphs G_i, so E_f hits all filled triangles. Also, every filled triangle contains exactly one edge of E_f, so E_f has the right size. Finally, if f is a face of G, then it is either an inner face of one of the subgraphs G_i or a face of G^{skel}. Either way at most one edge of f is in E_M, and thus E_f is independent.

The time complexity is dominated by splitting the graph into its 4-connected components at all separating triangles, which can be done in linear time [Kan97], and by finding the perfect matching in the dual graph, which can also be done in linear time [BBDL01]. □

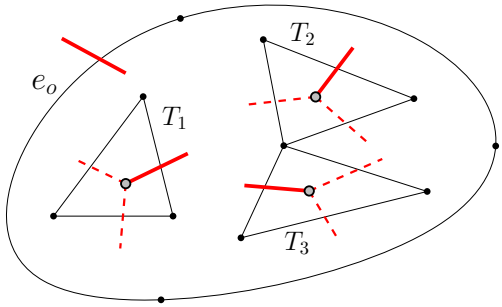

Figure 2.20: Skeleton G^{skel} of a maximal plane graph. The dual of G^{skel} is shown with grey vertices and red edges. The edges of the perfect matching are heavier.

We now give the second result, which gives a different (and sometimes better) bound at the price of being slower to compute.

Recall that the four color theorem for planar graphs states that we can assign colors $\{1, 2, 3, 4\}$ to vertices of G such that no edge has the same color at both endpoints [AH77]. Define M_1 to be all edges whose ends are colored $\{1, 2\}$ or $\{3, 4\}$, M_2 to be all edges whose ends are colored $\{1, 3\}$ or $\{2, 4\}$, and M_3 to be all edges whose ends are colored $\{1, 4\}$ or $\{2, 3\}$. Since every face of G is a triangle and colored with three different colors, then for $i = 1, 2, 3$, each edge set M_i contains exactly one edge of each triangle. Thus each M_i is an independent-filled-hitting set. Now, define E_i to be the set of edges obtained by deleting from M_i all edges that do not belong to a filled triangle. Each E_i is also an independent-filled-hitting set, and since it contains exactly one edge of each filled triangle, its size is at most f_G. The biggest of these three disjoint independent-filled-hitting sets E_1, E_2, E_3 contains at most $\frac{2n-5}{3}$ edges, due to the following:

Lemma 2.22. *Any maximal planar graph G with $n \geq 4$ has at most $2n-5$ edges belonging to a filled triangle.*

We would like to mention first that Cardinal et al. [Car+15] gave a very similar result, namely that every maximal planar graph contains at most $2n-7$ edges belonging to a separating triangle (immediately implying that at most $2n-4$ edges belong to a filled triangle). Since their proof was not given in [Car+15], and ours is quite short, we give it below despite the rather minor improvement.

Proof. For every edge e that belongs to a filled triangle, fix an arbitrary filled triangle T containing e and assign to e the face that is incident to e and inside triangle T. We claim that no face f can have been assigned to two edges e_1 and e_2. Assume for contradiction that it did, so there are two distinct filled triangles T_1 and T_2, both having f inside and with e_i incident to T_i for $i = 1, 2$. Since face f is inside both T_1 and T_2, one of the two triangles (say T_2) is inside the other (say T_1). Since e_1 belongs to f, it is on or inside T_2, but since it is also on T_1 (which contains T_2 inside) it therefore must be on T_2. But then T_2 contains both e_1 and e_2, and these two (distinct) edges hence determine the three vertices of T_2. But these three vertices also belong to the triangular face f, and so T_2 is an inner face and hence not a filled triangle by $n \geq 4$; this is a contradiction. Thus we can assign a unique inner face to every edge of a filled triangle, therefore in total there are at most $2n-5$ of them. □

We could find the smallest edge set among E_1, E_2, E_3 by 4-coloring the graph (which can be done in $O(n^2)$ time [RSST97]), but we propose a slightly more efficient approach. Compute the dual graph G^*, and assign weight 1 to an edge e^* if its dual edge e in G belongs to a filled triangle; else assign weight 0 to e^*. We now need to find a minimum-weight perfect matching M in G^*; this can be done in $O((n \log n)^{1.5}\sqrt{\alpha(n,n)})$ time [GT91] since we have $m \in O(n)$ and maximum weight 1. Since M is a perfect matching, by Observation 2, the dual edges of M (in G) form an independent-filled-hitting set in G. Deleting then from M all edges of weight 0 gives a smaller independent-filled-hitting set E_f, with size at most $\min\{f_G, \frac{2n-5}{3}\}$ since one of the three perfect matchings of G^* induced by a 4-coloring would have at most this weight. We hence conclude:

Corollary 2. *Every plane graph G has an independent-filled-hitting set of size at most $\frac{2n-5}{3}$. It can be found in $O((n \log n)^{1.5}\alpha(n,n))$ time.*

This proves Lemma 2.19.

2.2 Increasing the grid size

The second lead to study the non-aligned drawing problem is to find some bounds on the size of the grid which can support a planar non-aligned straight-line drawing of any planar graph. In this section, we study upper bounds: we show in Section 2.2.1 and Section 2.2.2 respectively that an $(n-1) \times O(n^3)$-grid and a $O(n^2) \times O(n^2)$-grid both support this kind of drawing, for any given planar graph. Finally, in Section 2.2.3, we give an upper bound of $(n-1) \times (\frac{4}{3}n - 2)$ for the size of a grid

supporting the planar non-aligned straight-line drawing of any so-called *nested-triangle* graph.

2.2.1 Drawing on an $(n-1) \times O(n^3)$-grid

In this section, we show how to build non-aligned straight-line drawings for which the width is $n-1$, and the height is around $\frac{1}{2}n^3$. We use the well-known canonical ordering for *maximal plane graphs*.

Canonical ordering

Definition 2.2. [DFPP90] A *canonical ordering* of a maximal plane graph G is a vertex order $v_1, \ldots, v_n$ such that:
- $\{v_1, v_2, v_n\}$ is the outer face of G,
- for any $3 \leq k \leq n$, the graph G_k induced by $v_1, \ldots, v_k$ is 2-connected and its outer face is a cycle containing the vertex v_k and the edge $(v_1 v_2)$.

This implies that v_k has at least 2 *predecessors* (i.e., neighbours in G_{k-1}), and its predecessors form an interval on the outer face of G_{k-1}. We assume (after possible renaming) that v_1 is the neighbor of v_2 found in clockwise order on the outer face, and enumerate the outer face of graph G_{k-1} in clockwise order as $c_1, \ldots, c_L$ with $c_1 = v_1$ and $c_L = v_2$. Then the predecessors of v_k consist of $c_\ell, \ldots, c_r$ for some $1 \leq \ell < r \leq L$; we call c_ℓ and c_r the *leftmost* and *rightmost* predecessors of v_k (see also Figure 2.21a). An example of a canonical ordering of a graph is given in Figure 2.21b.

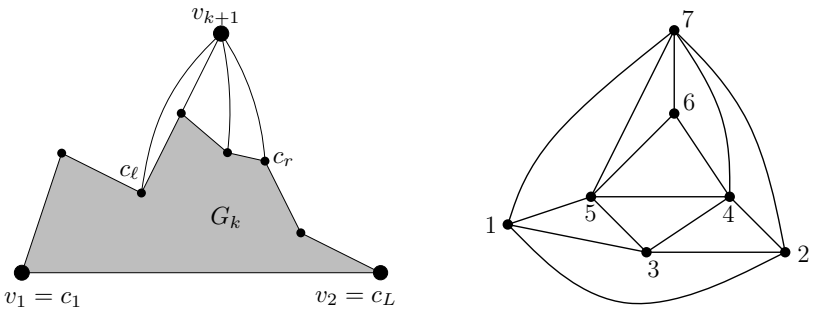

(a) (b)

Figure 2.21: (a) Structure of a canonical ordering; v_{k+1} has here four predecessors; the left-most one is c_ℓ and the right-most one is c_r. (b) A canonical ordering of a maximal plane graph.

A canonical ordering of a given graph can be found in linear time [DFPP90]. An algorithmic method to compute such an ordering is to construct it backwards; the outer face of each graph G_k contains a vertex which is not adjacent to a chord of this outer face. We can select this vertex as v_k and remove it from the graph,

thus obtaining G_{k-1}. Remark that this construction is not deterministic: in fact, a maximal plane graph often has multiple canonical orderings. In the following, we consider any of these orderings as valid.

Distinct x-coordinates

We first give a construction achieving distinct x-coordinates in $\{1, \dots, n\}$ (but y-coordinates may coincide). Let $v_1, \dots, v_n$ be a canonical ordering of G. The goal is to build a planar straight-line drawing of the graph G_k induced by $v_1, \dots, v_k$ using induction on k. The key idea is to define *all* x-coordinates beforehand. Define an orientation of the edges of G as follows. Direct (v_1v_2) as $v_1 \to v_2$. For $k \geq 3$, if c_r is the rightmost predecessor of v_k, then direct all edges from predecessors of v_k towards v_k, with the exception of (v_kc_r), which is directed $v_k \to c_r$.

By induction on k, one can show that the orientation of G_k is acyclic, with unique source v_1 and unique sink v_2, and the outer-face directed $c_1 \to \cdots \to c_L$; the base case $k = 2$ is clear, and when adding a vertex v_k, if a cycle is created, it contains the path $c_i \to v_k \to c_r$, with $\ell < i < r - 1$. By the orientation of the outer face of G_{k-1}, G_{k-1} also has a cycle, which contradicts the induction hypothesis. Since G is acyclic, we can find a topological order $x : V \to \{1, \dots, n\}$ of the vertices, i.e., if $u \to v$ then $x(u) < x(v)$. We use this topological order as our x-coordinates, and hence have $x(v_1) = 1$ and $x(v_2) = n$. We thus use two distinct vertex-orderings: one defined by the canonical ordering, which is used to compute y-coordinates, and one defined by the topological ordering derived from the canonical ordering, which directly gives the x-coordinates.

We now build a planar straight-line drawing of G_k respecting these x-coordinates by induction on k (see also Figure 2.22). Start by placing v_1 at coordinates $(1, 2)$, v_3 at $(x(v_3), 2)$ and v_2 at $(n, 1)$.

For $k \geq 3$, let c_ℓ and c_r be the leftmost and rightmost predecessors of v_{k+1}. Notice that $x(c_\ell) < \cdots < x(c_r)$ due to our orientation, which in particular implies that for any $\ell \leq j \leq r$, the upward ray from c_j intersects no other vertex or edge. Let y^* be the smallest integer value such that any c_j, for $\ell \leq j \leq r$, can "see" the point $p^* = (x(v_{k+1}), y^*)$, in the sense that the line segment from c_j to p^* intersects no other vertices or edges. Such a y^* exists since the upward ray from c_j is empty: by tilting this ray slightly, c_j can also see all sufficiently high points on the vertical line $\{x = x(v_{k+1})\}$. Placing v_{k+1} at p^* hence gives a planar straight-line drawing of G_{k+1}.

To analyze the height of this construction, we bound the value of the slopes of the segments representing the edges.

> **Lemma 2.23.** *All edges on the outer face of the constructed drawing of G_k have slope at most $s_k := k - 3$ for $k \geq 3$.*

Proof. It clearly holds for $k = 3$ and $s_3 = 0$: one slope is 0, and the other two are negative. Now assume it holds for some $k \geq 3$, and let $c_\ell, \dots, c_r$ be the predecessors of v_{k+1}. Since the y-coordinates are given by the topological order defined above, $x(c_\ell) < \cdots < x(v_{k+1}) < x(c_r)$. Fix one predecessor c_j for $\ell \leq j < r$, and consider

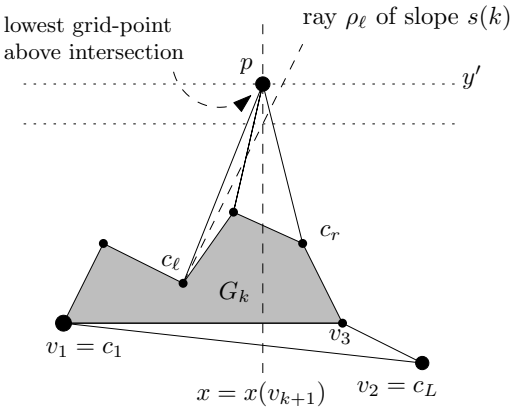

Figure 2.22: Finding a y-coordinate for v_{k+1}.

the ray ρ_j of slope s_k starting from c_j. Since all edges of the outer face of G_k have slope at most s_k, vertex c_j can see all points that are above ρ_j and to the right of c_j. In particular, consider the point where the ray ρ_ℓ intersects the vertical line $\{x = x(v_{k+1})\}$, and set y' to be the smallest integer y-coordinate that is strictly above this intersection. By construction, point $p = (x(v_{k+1}), y')$ is above ρ_j and to the right of c_j for $j = \ell, \ldots, r-1$, and hence can see all of them. Since the edge $(c_{r-1}c_r)$ has also slope at most s_k, point p is above $(c_{r-1}c_r)$, and can be connected to both of them without creating any crossings. Also note that the segment (pc_r) therefore has a smaller slope than the one of the edge $(c_{r-1}c_r)$, and in particular has a slope smaller than s_k.

So the point $p = (x(v_{k+1}), y')$ can see all vertices $c_\ell, \ldots, c_r$, and the value of $y^* = y(v_{k+1})$ is hence no bigger than y'. We already argued that the edge $(v_{k+1}c_r)$ has slope at most $s_k \leq s_{k+1}$, so it only remains to compute the value of the slope of the other new outer face edge $(c_\ell v_{k+1})$. Since y' is the smallest integer y-coordinate above the intersection of ρ_ℓ and the line $\{x = x(v_{k+1})\}$, we have

$$y^* \leq y' \leq y(c_l) + (x(v_{k+1}) - x(c_l)) \cdot s_k + 1. \tag{2.1}$$

Since $x(v_{k+1}) - x(c_l) \geq 1$, the slope of $(c_l v_{k+1})$ is at most

$$\frac{y^* - y(c_l)}{x(v_{k+1}) - x(c_l)} \leq s_k + \frac{1}{x(v_{k+1}) - x(c_l)} \leq s_k + 1 = s_{k+1}$$

as desired. □

In the final drawing, $x(v_n) \leq n-1$, and the edge from v_1 to v_n has slope at most $s_n = n-3$. This shows that the y-coordinate of v_n is at most $2 + (n-2) \cdot (n-3)$. Since the triangle $[v_1 v_2 v_n]$ bounds the drawing, we have the following:

Theorem 2.24. *Every maximal plane has a planar straight-line drawing on an* $(n-1) \times (1 + (n-2)(n-3))$*-grid such that all vertices have distinct* x*-coordinates.*

While this theorem is not useful per se for non-aligned drawings, we find it interesting from a didactic point of view: It proves that polynomial coordinates can

be achieved for straight-line drawings of planar graphs, and requires for this only the canonical ordering, but neither the properties of Schnyder trees [Sch90], nor the details of how to "shift" that is needed for other methods using the canonical ordering (e.g. [CK97; DFPP90]). However, we believe that our bound on the height is much too big, and that the height achieved by this construction is $o(n^2)$ and possibly $O(n)$.

Distinct x- and y-coordinates

We now modify the above construction slightly to achieve both distinct $x-$ and y-coordinates. Define the exact same x-coordinates as in the previous setting and place v_1 and v_2 as before. To place vertex v_{k+1}, let y^* be the smallest y-coordinate such that point $(x(v_{k+1}), y^*)$ can see all predecessors of v_{k+1}, and such that none of $v_1, \dots, v_k$ is in row $\{y = y^*\}$. Clearly this gives a non-aligned drawing. It remains to bound how much it increases the total height of the drawing.

Lemma 2.25. *Define $s'_k := \sum_{i=1}^{k-2} i = \frac{1}{2}(k-1)(k-2)$ for $k \geq 2$. All edges on the outer face of the constructed non-aligned drawing of G_k have slope at most s'_k for $k \geq 2$.*

Proof. The claim clearly holds for $k = 2$, since (v_1v_2) has negative slope. Now consider the step consisting in adding v_{k+1} (with predecessors $c_\ell, \dots, c_r$), and define ρ' to be the ray of slope s'_k emanating from c_ℓ. Let y' be the smallest integer coordinate above the intersection of ρ' with the vertical line $\{x = x(v_{k+1})\}$. As in Lemma 2.23, we can show that $p' = (x(v_{k+1}), y')$ can see all vertices $c_\ell, \dots, c_r$.

We may or may not be able to use point p' for v_{k+1}, depending on whether there is an other vertex with y-coordinate y' (there is at most one, since the graph G_k is already drawn with the non-aligned constraint). If it is the case, then we add 1 to the value of y' (which means moving p' one row higher) and check again. Since $y(c_\ell) \geq 2$ and $s'_k \geq 1$, then $y' \geq 3$. Therefore neither v_1 nor v_2 has y-coordinate y' and at most $k-2$ rows are considered when trying to find the y-coordinate of v_{k+1}. Thus we have:

$$y^* \leq y' + (k-2) \leq y(c_\ell) + (x(v_{k+1}) - x(c_\ell)) \cdot s'_k + 1 + (k-2) \tag{2.2}$$

Reformulating as before shows that the slope of $(c_\ell v_{k+1})$ is at most

$$\frac{y^* - y(c_l)}{x(v_{k+1}) - x(c_l)} \leq s'_k + \frac{k-1}{x(v_{k+1}) - x(c_l)} \leq s'_k + k - 1 = s'_{k+1}. \quad \square$$

The maximal slope on the outer face of $G_n = G$ is hence at most $\frac{1}{2}(n-1)(n-2)$, and achieved at edge (v_1v_n). Since $x(v_n) - x(v_1) \leq n-2$ and $y(v_1) = 2$, the y-coordinate of v_n is at most $2 + \frac{1}{2}(n-1)(n-2)^2$. This gives the following theorem:

Theorem 2.26. *Every planar graph has a non-aligned straight-line drawing in an $(n-1) \times \left(1 + \frac{1}{2}(n-1)(n-2)^2\right)$-grid.*

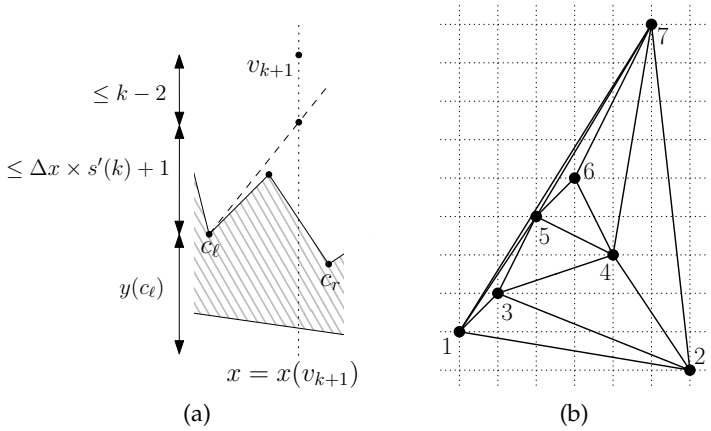

Figure 2.23: (a) Illustration of the bounding of y^* in Equation 2.2. (b) Result of our construction on the graph given in Figure 2.21b; all vertices have distinct coordinates.

We suspect that the method results in a smaller height than the proved upper bound: Equation (2.2) is generally not tight, and so a smaller slope-bound (implying a smaller height) is very likely to hold.

2.2.2 Drawing on an $O(n^2) \times O(n^2)$-grid

We now show how to construct non-aligned drawings on a grid with quadratic width and height. by scaling and perturbing a so-called *weak barycentric representation*.

In the following, a vertex v is assigned to a triplet of non-negative integer coordinates $(p_0(v), p_1(v), p_2(v))$.

Definition 2.3. For two vertices u, v and $i = 0, 1, 2$, we say that $(p_i(u), p_{i+1}(u)) <_{\text{lex}} (p_i(v), p_{i+1}(v))$ if either $p_i(u) < p_i(v)$, or $p_i(u) = p_i(v)$ and $p_{i+1}(u) < p_{i+1}(v)$ ($<_{\text{lex}}$ denotes the lexicographic order).

Note that in this section, addition on the subscripts is done modulo 3.

Definition 2.4 (Weak barycentric representation [Sch90])**.** A *weak barycentric representation* of a graph G is an injective function $\mathcal{P}$ that maps each $v \in V(G)$ to a point $(p_0(v), p_1(v), p_2(v)) \in \mathbb{N}_0^3$ such that:

- $p_0(v)+p_1(v)+p_2(v) = c$ for every vertex v, where c is a constant independent of the vertex,
- for each edge (uv) and each vertex $z \neq \{u, v\}$, there exists some $k \in \{0, 1, 2\}$ such that:
  - $(p_k(u), p_{k+1}(u)) <_{\text{lex}} (p_k(z), p_{k+1}(z))$ and
  - $(p_k(v), p_{k+1}(v)) <_{\text{lex}} (p_k(z), p_{k+1}(z))$.

Weak barycentric representations are of particular interest in graph drawing,

since they can be used directly to generate a straight-line planar embedding of a planar graph:

> **Theorem 2.27** ([Sch90]). *Let $\mathcal{P} = \big((p_0(v), p_1(v), p_2(v))_{v\in V}\big)$ be a weak barycentric representation of a planar graph G. Then mapping each vertex $v \in V(G)$ to the point $(p_0(v), p_1(v))$ gives a planar straight-line drawing of G.*

In Schnyder's original drawing algorithm, the vertices coordinates can be determined by counting combinatorial objects of the graph (e.g. the number of vertices in a certain region $R_i(v)$ for each tree T_i and each inner vertex v). He shows in particular the following result [1]:

> **Theorem 2.28** ([Sch90]). *Every planar graph with n vertices has a weak barycentric representation with $c = n - 1$. Furthermore, $0 \leq p_i(v) \leq n - 2$ for all vertices $v \in V$ and all $i \in \{0, 1, 2\}$, and the outer vertices v_0, v_1, v_2 respectively receive coordinates $(n - 2, 1)$, $(1, 0)$, and $(0, n - 2)$.*

Observe that weak barycentric representations are preserved under scaling, i.e., if we have a weak barycentric representation $\mathcal{P}$ (say with constant c), then we can scale all assigned coordinates by the same factor N and obtain another weak barycentric representation (with constant $c \cdot N$). We need to do slightly more, namely scale and "twist", as detailed in the following lemma.

> **Lemma 2.29.** *Let $\mathcal{P} = \big((p_0(v), p_1(v), p_2(v))_{v\in V}\big)$ be a weak barycentric representation of a graph G. Let $N \geq 1 + \max_{v\in V}\{\max_{i=0,1,2} p_i(v)\}$ be a positive integer. Define $\mathcal{P}'$ to be the assignment $p'_i(v) := N \cdot p_i(v) + p_{i+1}(v)$ for $i = 0, 1, 2$. Then $\mathcal{P}'$ is also a weak barycentric representation of G.*

Proof. Let c_P be the constant of $\mathcal{P}$. Then for each vertex v, $p'_1(v) + p'_2(v) + p'_3(v) = N\,(p_1(v) + p_2(v) + p_3(v)) + p_1(v) + p_2(v) + p_3(v) = N \cdot c_P + c_P$, which is also a constant.

Let $\{u, v\}$ be two vertices of G, $u \neq v$. Since $\mathcal{P}$ is injective, we know that there exists $i \in \{0, 1, 2\}$ such that $p_i(u) \neq p_i(v)$. Without loss of generality, $p_i(u) > p_i(v)$. Since all coordinates p_i are integers, $p_i(u) \geq p_i(v)+1$. Thus $N \cdot p_i(u) \geq N \cdot p_i(v)+N > N \cdot p_i(v) + p_{i+1}(v) - p_{i+1}(u)$ by $p_{i+1}(v) < N$ and $p_{i+1}(u) \geq 0$. Thus $p'_i(u) > p'_i(v)$ and $\mathcal{P}'$ is injective.

Finally, we need to check the second property of a weak barycentric representation. Let (uv) be an edge of G and $z \neq \{u, v\}$ a vertex of G. Since $\mathcal{P}$ is a weak barycentric representation, there is some $k \in \{0, 1, 2\}$ such that $(p_k(u), p_{k+1}(u)) <_{\text{lex}} (p_k(z), p_{k+1}(z))$ and $(p_k(v), p_{k+1}(v)) <_{\text{lex}} (p_k(z), p_{k+1}(z))$. We only show the claim for u, and there are two cases:

- $p_k(u) < p_k(z)$: As in the preceding paragraph, $p'_k(u) < p'_k(z)$.

[1] In Schnyder's grid drawing algorithm, the coordinates of vertices begin at 0. Although this may seem in contradiction with the definitions given in this thesis, we see later that our final drawing has correct coordinates.

- $p_k(u) = p_k(z)$: Then $p_{k+1}(u) < p_{k+1}(z)$ and $p'_k(u) = Np_k(u) + p_{k+1}(u) = Np_k(z) + p_{k+1}(u) < Np_k(z) + p_{k+1}(z) = p'_k(z)$.

So either way $p'_k(u) < p'_k(z)$ and then $(p'_k(u), p'_{k+1}(u)) <_{\text{lex}} (p'_k(z), p'_{k+1}(z))$. □

We can now apply this shift to the coordinates given by Schnyder's weak barycentric representation:

Theorem 2.30. *Every planar graph has a non-aligned straight-line planar drawing on an $(n(n-2)-1) \times (n(n-2)-1)$-grid.*

Proof. Let $\mathcal{P} = \big((p_0(v), p_1(v), p_2(v))_{v \in V}\big)$ be the weak barycentric representation of Theorem 2.28; we know that $0 \leq p_i(v) \leq n-2$ for all v and all i. Now apply Lemma 2.29 with $N = n-1$ to obtain a weak barycentric representation $\mathcal{P}'$ with $p'_i(v) = (n-1)p_i(v) + p_{i+1}(v)$. Observe that $p'_i(v) \leq (n-1)(n-2) + (n-2) = n(n-2)$. Also, $p'_i(v) \geq 1$ since not both $p_i(v)$ and $p_{i+1}(v)$ can be 0. (More precisely, $p_i(v) = 0 = p_{i+1}(v)$ would imply $p_{i+2}(v) = n-1$, contradicting $p_{i+2}(v) \leq n-2$.)

As shown by Schnyder [Sch90], mapping each vertex v to point $(p'_0(v), p'_1(v))$ gives a planar straight-line drawing of G. By the above, this drawing has the desired grid-size. It remains to show that it is non-aligned, namely that, for any two vertices u, v and any $i \in \{0, 1\}$, we have $p'_i(u) \neq p'_i(v)$. Assume after possible renaming that $p_i(u) \leq p_i(v)$. We have two cases:

- If $p_i(u) < p_i(v)$, then $p_i(u) \leq p_i(v) - 1$ since $\mathcal{P}$ assigns integers. Thus $N \cdot p_i(u) \leq N \cdot p_i(v) - N < N \cdot p_i(v) - p_{i+1}(u) + p_{i+1}(v)$ since $p_{i+1}(u) < N$ and $p_{i+1}(v) \geq 0$. Therefore $p'_i(u) < p'_i(v)$.
- If $p_i(u) = p_i(v)$, then $p_{i+1}(u) \neq p_{i+1}(v)$ (else the three coordinates of u and v would be the same, which is impossible since $\mathcal{P}$ is an injective function). Then $p'_i(u) = N \cdot p_i(u) + p_{i+1}(u) \neq N \cdot p_i(v) + p_{i+1}(v) = p'_i(v)$. □

2.2.3 The special case of nested triangles

We now turn to non-aligned drawings of a special graph class. A *nested-triangle graph* G (first named by Dolev et al. [DLT84]) is formed as follows. G has $3k$ vertices for some $k \geq 1$, say $\{u_i, v_i, w_i\}$ for $i = 1, \ldots, k$. Vertices $\{u_i, v_i, w_i\}$ form a triangle (for $i = 1, \ldots, k$). We also have paths $(u_1, u_2, \ldots, u_k)$, $(v_1, v_2, \ldots, v_k)$, and $(w_1, w_2, \ldots, w_k)$. With this the graph is 3-connected; we assume that its outer face is the triangle $[u_1 v_1 w_1]$. All inner faces that are not triangles may or may not have a diagonal in them, and there are no restrictions on which diagonal (if any).

Theorem 2.31. *Any nested-triangle graph with n vertices has a non-aligned straight-line drawing on an $(n-1) \times (\frac{4}{3}n - 2)$-grid.*

Proof. The cycle $(w_k v_k v_{k-1} w_{k-1})$ may or may not have a chord; after possible exchange of $w_1, \ldots, w_k$ and $v_1, \ldots, v_k$, we assume that there is no edge between v_{k-1} and w_k. For $i = 1, \ldots, k$, place u_i at (i, i), vertex v_i at $(3k + 1 - i, k + i)$, and w_i at

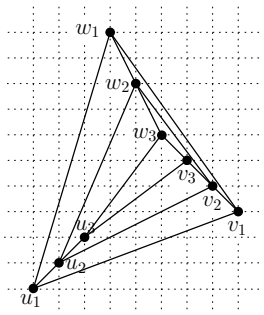

Figure 2.24: A non-aligned straight-line drawing of a nested-triangle graph with $k = 3$ on an 8×10-grid.

$(k + i, 4k + 1 - 2i)$ (see Figure 2.24). The x- and y-coordinates are all distinct. The x-coordinates range from 1 to n, and the maximal y-coordinate is $4k - 1 = \frac{4}{3}n - 1$.

For each of the points u_i, v_i, w_i, the edges to the set $\{u_{i+1}, v_{i+1}, w_{i+1}\}$ must not intersect or overlap. Here are the coordinates of the different vectors:

- $\overrightarrow{u_iu_{i+1}} = (1, 1)$, $\overrightarrow{u_iv_{i+1}} = (3k - 2i, k + 1)$, $\overrightarrow{u_iw_{i+1}} = (k + 1, 3k + 2 - 3i)$
- $\overrightarrow{v_iu_{i+1}} = (-3k + 2i, 2i - k + 1)$, $\overrightarrow{v_iv_{i+1}} = (-1, 1)$, $\overrightarrow{v_iw_{i+1}} = (-2k + 2i, 3k - 3i - 1)$
- $\overrightarrow{w_iu_{i+1}} = (-k + 1, -4k + 3i)$, $\overrightarrow{w_iv_{i+1}} = (2k - 2i, -3k + 3i)$, $\overrightarrow{w_iw_{i+1}} = (1, -2)$.

All inner faces are drawn strictly convex, with the exception of the face with vertices $\{v_k, v_{k-1}, w_{k-1}, w_k\}$, which has a $180°$ angle at v_k (but our choice of naming ensured that there is no edge $(v_{k-1}w_k)$). Thus any diagonal inside these cycles can be drawn without overlap. Since G is planar, two edges joining vertices of different triangles cannot cross. Thus G is drawn without crossing on an $(n - 1) \times \left(\frac{4}{3}n - 2\right)$-grid. □

Nested-triangle graphs are of interest in graph drawing because they are lower-bound graphs for the area of straight-line drawings [DFPP90; DLT84], as well as for the one of polyline drawings [BLSM02]. We conjecture that this is also the case for the area of straight-line non-aligned drawings:

> **Conjecture 2.32.** Any non-aligned planar straight-line drawing of a nested-triangle graph with n vertices and $k = \frac{n}{3}$ triangles on a grid of width $n - 1$ has height at least $\frac{4}{3}n - 2 = 4k - 2$.

This conjecture holds for $k = 2$: our construction gives a planar non-aligned straight-line drawing of the octahedron on a 5×6-grid (with 6 columns and 7 lines). This is clearly optimal since it has no straight-line minimal non-aligned drawing (as seen in Section 2.1.1). We think that some geometrical arguments similar to those used to prove Theorem 2.1 could be used to prove this conjecture. It seems that the nested triangles are forced to be placed such that the more they are in the "center" of the drawing, the worse their aspect ratio is. The constraints coming from the potential edges between two nested-triangles seem to be quite strong.

2.3 Conclusion and outlook

In this chapter, we studied a special type of grid drawing, namely non-aligned planar drawing, motivated by both theoretical problems and visualization considerations. We observed that in general, maximal planar graphs do not admit a planar straight-line minimal non-aligned drawing, except in the case of tower graphs. On the other hand, we showed that every 4-connected graph admits a planar straight-line minimal non-aligned drawing if it has a face of degree four.

We showed that every plane graph admits a planar polyline minimal non-aligned drawing with at most $n-3$ bent edges, which can be constructed in linear time. We also constructed planar minimal non-aligned drawings with at most $\frac{2n-5}{3}$ bends; the number of bends can also be bounded by the number of filled triangles. However, this latter algorithm only runs in polynomial time.

We considered drawings that allow more rows and columns while keeping vertices on distinct rows and columns; we proved by two different methods that such non-aligned planar straight-line drawings always exist and have area $O(n^4)$. We also conjecture that the $(n-1) \times (\frac{4}{3}n-2)$-grid achieved for nested-triangle graphs is optimal for planar straight-line non-aligned drawings with width $n-1$.

As for open problems, the most prominent question following the work presented in this chapter is to find lower bounds on the area of the minimal grid supporting the non-aligned planar straight-line drawing of any planar graph. No planar graph is known that needs more than one bend in a planar minimal non-aligned drawing, and no planar graph is known that needs more than $2n+1$ grid-lines in a planar non-aligned straight-line drawing. The "naive" approach of taking multiple copies of the octahedron fails because the property of having a minimal non-aligned drawing is not closed under taking subgraphs.

Since separating triangles seem to be structural obstacles for straight-line planar drawings on small grids, graphs with many separating triangles may be examples reaching such lower bounds. Two families of graphs are potential candidates: Apollonian networks (also called 3-trees), which are 3-degenerated, and nested-triangle graphs, already seen in Section 2.2.3. Both these classes have nice structural properties which could be used to create recursive drawing algorithms. Results on classical minimum-area drawings for these classes have been shown [MNRA11] and could be extended to non-aligned drawings.

3

Power domination of planar graphs

This chapter is dedicated to the study of power domination in graphs, which is a variant of the better-known domination problem.

The domination problem first appeared in the context of chess: in 1862, de Jaenisch [Jae62] studied how many queens one can place on a chessboard such that every square of the board is threaten by at most one queen[1]. In 1962, both Berge [Ber62] and Ore [Ore62] proposed, in their respective books, a formalization of this problem on graphs, and the subject has become widely studied since then. Given a graph G, a set $S \subset V(G)$ is a *dominating set* of G if every vertex of G is either in S or in the neighborhood of S (see Figure 3.1)[2]. In the example studied by de Jaenisch, vertices are the squares of the board, two vertices are adjacent in the graph if placing a queen on one of the squares threatens the other, and selecting a vertex means placing a queen on the corresponding square. The minimum number of vertices in any dominating set of G is the *domination number* of G, denoted by $\gamma(G)$.

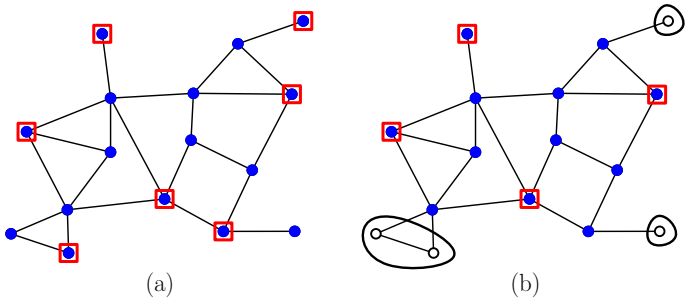

Figure 3.1: Vertices of S are framed with a red square, vertices of M are colored blue. (a) Each vertex is either in S or has a neighbor in S: S is a dominating set, and $\gamma(G) \leq 7$. (b) Some vertices are not neighbors of the set S: it is not a dominating set.

[1] In fact, de Jaenisch was interested in the more specific *independent domination* problem: he also required the queens not to be self-attacking.

[2] Berge usually refered to a dominating set as "externally stable" or "absorbent".

Domination has many applications, providing tools to solve optimal location problems (such as assignment of frequencies to radio stations, location of fire stations or other facilities...), scheduling problems, or for example to decide the optimal number of representatives of a group of people, ensuring that each person in the group is represented by someone he/she knows.

The corresponding decision problem DOMINATING SET (i.e. "Given a graph G and an integer k, does $\gamma(G) \leq k$?") is a classical NP-complete problem, and is particularly interesting because it remains NP-complete when restricted to planar graphs [GJ79]. However, this problem admits a PTAS (Polynomial-time approximation scheme) for planar graphs [Bak94]. One of the most prominent results on domination in planar graphs is the bound given by Matheson and Tarjan [MT96]: for sufficiently large n, every maximal planar graph with n vertices has a dominating set containing at most $\frac{n}{3}$ vertices. They also show that any maximal planar graph containing $\frac{n}{4}$ disjoint copies of K_4 needs at least $\frac{n}{4}$ vertices in any dominating set. They conjectured that $\frac{n}{4}$ is the best possible upper bound on the power domination number of maximal planar graphs, and this has been confirmed for triangulations with maximum degree 6 [KP10]. Results considering additional hypotheses on the minimum degree of the triangulation have also been proved: if a graph (non-necessarily planar) with n vertices has minimum degree respectively 3, 4 or 5, then it admits a dominating set of size at most respectively $\frac{3n}{8}$, $\frac{5n}{14}$ or $\frac{4n}{11}$ (see [Ree96; SX09; XSC06]). However, there is still a gap between these bounds and the one of Matheson and Tarjan for triangulations. For more information on the domination problem, we refer the reader to two books on the topic [HHS98a; HHS98b].

Many variants of domination have been studied through the years, as for example connected domination (the vertices of S must induce a connected graph) or total domination (every vertex of G must be adjacent to a vertex of S). Here we focus on another variant, namely *power domination*. This problem arose in the context of monitoring an electrical network [BMBA93; MBA90; PTK86]. Monitoring an electrical system means knowing the state of each component (like the voltage magnitude at loads) by measuring some variables, e.g. currents and voltages. The measurements are done by placing Phasor Measurement Units (PMUs) at selected locations. PMUs monitor the state of the adjacent components, and then one may make use of electrical laws to determine the state of components further away in the network. For example, Kirschoff's second law states that, in an electrical circuit, the sum of currents around any node is zero: if there are k branches around that node, knowing the current for $k-1$ of them allows to deduce the value of the current in the last branch. Since PMUs are costly, the goal is to minimize their number.

This monitoring problem was then transposed in graph-theoretical terms by Haynes et al. [HHHH02] and given the name of power domination. Originally, the definition of power domination presented in [HHHH02] ensured the monitoring of the edges as well as of the vertices, and contained many propagation rules. We present an equivalent definition [BH05] that only requires monitoring the vertices, which we use throughout the thesis. Given a graph G and a set $S \subseteq V(G)$, we build a set M as follows: at first, $M = N[S]$, and then iteratively a vertex u is added to M if u has a neighbor v in M such that u is the only neighbor of v not in M (we

say that v *propagates* to u). At the end of the process, we say that M is the set of vertices *monitored* by S. The *non-monitored* vertices are vertices of the set $V(G) \setminus M$. We say that G is *monitored* when all its vertices are monitored. The set S is a *power dominating set* of G if $M_G(S) = V(G)$ (see Figure 3.2), and the minimum cardinality of such a set is the *power domination number* of G, denoted by $\gamma_P(G)$.

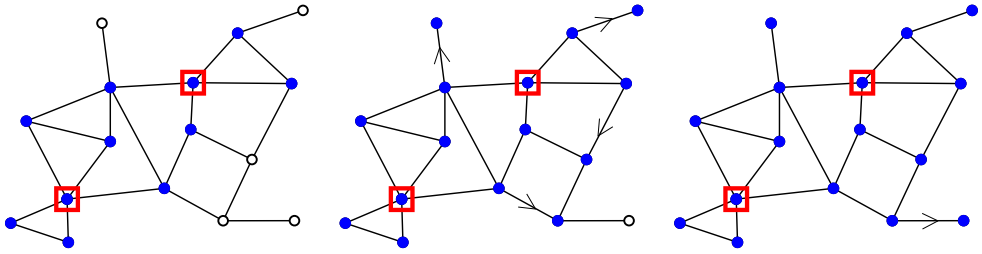

Figure 3.2: (a) Two vertices are chosen in the set S. Their closed neighborhood is monitored (in blue) (b) Some vertices propagate to their (only) non-monitored neighbor. (c) After two rounds of propagation, all vertices of G are monitored: S is a power dominating set of G of size two.

Power domination can be seen as a somewhat global version of domination. Indeed, given a graph G and a set of vertices S, checking if S is a dominating set of G can be done by checking around each vertex of $V(G)$ whether its closed neighborhood contains a vertex of S. However, to check if S is *power dominating* the graph G, this local approach is not sufficient and one needs to retrace the propagation process of S. Another way to apprehend the intrinsic difference between these two problems is to remark the following: a vertex of a dominating set only monitors its direct neighbors, whereas a vertex of a power dominating set could monitor vertices far from him through propagation. A typical and simple example is the path P_k: $\gamma(P_k) = \lceil k/3 \rceil$, but $\gamma_P(P_k) = 1$ (see Figure 3.3). Since it is clear that any dominating set is also power dominating, we have $1 \leq \gamma_P(G) \leq \gamma(G)$ for every graph G, and both bounds are tight. Examples of graphs with $\gamma_P(G) = \gamma(G)$ were given by Haynes et al. [HHHH02] (for example, the graph formed by k distinct triangles joined by a path), whereas the lower bound is reached in particular for paths and cycles.

Figure 3.3: (a) A dominating set of P_5 with two vertices. (b) One vertex is enough to power dominate P_5: ultimately, propagation allows to monitor all vertices.

The decision problem POWER DOMINATING SET naturally associated to power domination (i.e. "Given a graph G and an integer k, does G have a power dominating set of order at most k?") was proven NP-complete, by reductions from the 3-SAT

problem [HHHH02; LL05] (giving NP-completeness of the problem on bipartite graphs, chordal graphs and split graphs), as well as from DOMINATING SET [GNR08; KMRR06], which implies the NP-completeness also when restricted to planar graphs or circle graphs. Linear or polynomial algorithms were proposed to compute the power domination number of a graph if it is a tree [GNR08; HHHH02], a block graph [XKSZ06], an interval graph [LL05], or a circular-arc graph [LL05; LL13].

The tree-width of a graph seems to be a parameter of interest to better understand the complexity of POWER DOMINATING SET: there exists a k-approximation algorithm on graphs with tree-width k [AS09] (which yields a $O(\sqrt{n})$-approximation algorithm for planar graphs), and if a tree decomposition of width k of the graph is part of the input, then Guo et al. propose a linear time algorithm [GNR08].

Tight upper bounds on $\gamma_P(G)$ are also known for particular classes: $\gamma_P(G) \leq \frac{n}{3}$ if G is connected [ZKC06] or a tree [HHHH02], whereas cubic graphs satisfy $\gamma_P(G) \leq \frac{n}{4}$ [Dor+13; ZKC06]. There are also results when G is planar and has diameter two or three [ZK07].

The reduction from DOMINATING SET to POWER DOMINATING SET, proving the NP-completeness of the latter [GNR08], is based on the addition of neighbors of degree one to every vertex of a graph G to create a new graph G'. Thus finding a power dominating set S' of G' with size at most k is equivalent to finding a dominating set of G with size at most k. Clearly, this construction can not be applied if we restrict the instances of the problems to maximal planar graphs. Maximal planar graphs are thus an interesting class of graphs on which to study power domination.

In Section 3.1, we first prove that there exist maximal planar graphs with arbitrarily large number n of vertices and admitting no power dominating set of size less than $\frac{n}{6}$. This bound can be seen as the counterpart to the $\frac{n}{4}$ bound showed by Matheson and Tarjan for domination in maximal planar graphs [MT96]. Moreover, we prove that every maximal planar graph with n vertices admits a power dominating set of size at most $\frac{n-2}{4}$. We present a constructive algorithm reaching this bound.

Power domination has also been well studied on regular grids and their generalizations: the exact power domination number has been determined for the square grid [DH06] and other products of paths [DMKŠ08], for the hexagonal grid [FVV11], as well as for cylinders and tori [BF11]. These results are particularly interesting in comparison with the ones on the same classes for (classical) domination: for example, the problem of finding the domination number of grid graphs $P_n \times P_m$ for any value of n and m was an open problem until recently [GPRT11]. They also rely heavily on propagation: it is generally sufficient to monitor (with adjacency alone) a small portion of the graph in order to propagate to the whole graph.

We thus continue the study of power domination in grid-like graphs by focusing on triangular grids with hexagonal-shaped border. In Section 3.2, we show that $\gamma_P(G) = \lceil \frac{k}{3} \rceil$, where G is a triangular grid with diameter $2k-1$. Showing the upper bound is donc by exhibing a construction, whereas the proof of the lower bound relies on the study of an invariant (which is a classical way to prove lower bounds for this problem in regular lattices, see [DMKŠ08; DH06]).

The results presented in Section 3.1 are joint work with Paul Dorbec and Antonio González [DGP17]. The results of Section 3.2 are joint work with Prosenjit Bose and Sander Verdonschot [BPV17].

3.1 Power domination in triangulations

In the following, we consider maximal planar graphs with a fixed embedding, i.e. triangulations. Note that power dominating sets are independent of the embedding of the graph as they only depend on vertex adjacencies. We prove the following theorem:

Theorem 3.1. *Let G be a triangulation of order $n \geq 6$.*
Then $\gamma_P(G) \leq \frac{n-2}{4}$.

The proof of Theorem 3.1 is done in three steps, each one detailed in a constructive algorithm. In Section 3.1.1, Algorithm 3.1 produces a set S_1 monitoring some special configurations with a small number of vertices. Then, Algorithm 3.2 of Section 3.1.3 builds a set S_2 by expanding the set S_1 iteratively, while keeping certain properties. If the graph G is not fully monitored after that, we show in Section 3.1.4 that G has a characterized structure, which guarantees that our last Algorithm 3.3 maintains the wanted bound while adding some well chosen vertices to S_2 to build the required set S.

Given a plane graph G (i.e. a planar graph with an embedding, but not necessarily a triangulation), a subgraph $G' \subseteq G$ is an *induced triangulation* of G if $G[V(G')]$ is a triangulation.

We introduce the following property, which we maintain throughout the process of the construction of the power dominating set S in G.

Property $(*)$**.** *We say that a subset S of vertices of a plane graph G has* Property $(*)$ *in G whenever, for each induced triangulation $G' \subseteq G$ of order at least 4, if G' is monitored by S then one of the following holds:*

(a) one vertex of the outer face of G' has its closed neighborhood in G monitored by S,
(b) or, we have $|S \cap V(G')| \leq \frac{|V(G')|-2}{4}$.

In the following, G refers to a triangulation with order $n \geq 6$.

3.1.1 Monitoring special configurations

In the first part of the algorithm, we need to monitor some *special configurations* that might cause trouble later.

A subgraph of a triangulation G is said *facial* if all of its faces but the outer face are also faces of G.

In Figure 3.4, the three special configurations we consider are given. If one of these configurations H is a facial subgraph of G, then one of the vertices of H has to be selected in a power dominating set of G (otherwise, even if some of the outer vertices are monitored, they can not propagate to any of the inner vertices of H).

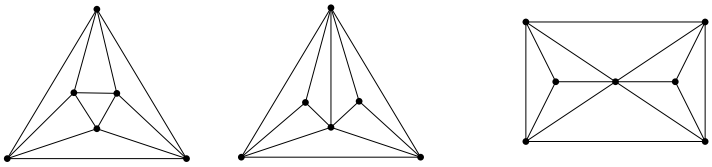

Figure 3.4: The good (the octahedron), the bad and the ugly configurations in a triangulation.

Thus $\gamma_P(G)$ is at least the number of disjoint facial special configurations of G. An example for which equality holds (inspired by a similar example in [MT96]) is given in Figure 3.5.

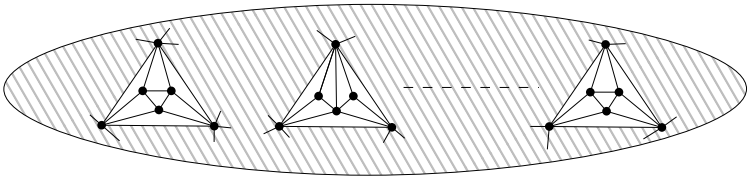

Figure 3.5: A class of maximal planar graphs for which $\gamma_P(G) = \frac{n}{6}$. The hatched area is triangulated arbitrarily.

This leads naturally to the following result, which is a counterpart of the one by Matheson and Tarjan [MT96] on domination in maximal planar graphs:

> **Theorem 3.2.** *For sufficiently large n, every maximal planar graph with n vertices has a power dominating set containing at most εn vertices, with $\varepsilon \geq \frac{1}{6}$.*

For this reason, the first step of our global algorithm is Algorithm 3.1, which takes care of monitoring vertices creating special configurations. But first, we have to check how these configurations may intersect: during Algorithm 3.1, intersecting configurations are monitored with a common vertex. Note that octahedra can not intersect with other special configurations.

We call *3-vertex* a vertex of G with degree 3, i.e. its neighborhood induces a K_4. We call *b-vertex* a vertex u of G with exactly two 3-neighbors v and v' and such that $N[u] = N[v] \cup N[v']$ (see Figure 3.6). In all figures of this section and the following one, b-vertices are depicted with blue squares, and 3-vertices are shown white.

The following lemma gives a characterization of the possible intersections of special configurations. Since its proof is basically a case analysis, we defer it to Section 3.1.2.

> **Lemma 3.3.** *If G contains a special configuration as facial subgraph, either G is a small graph (characterized in Section 3.1.2) and $\gamma_P(G) \leq \frac{n-2}{4}$, or each maximal component of b-vertices of G belongs to one of the induced configurations (1 to 7) depicted in Figure 3.7, or G contains a facial octahedron (configuration 8 in Figure 3.7).*

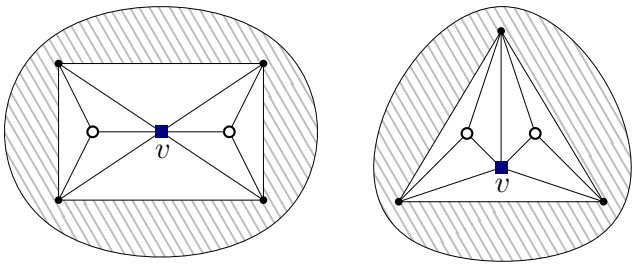

Figure 3.6: The two possible neighborhoods of a b-vertex v. Blue-square vertices are the b-vertices, white vertices are 3-vertices.

Observation 3.4. If a vertex belongs to two facial subgraphs isomorphic to configurations from Figure 3.7, then it is a vertex from the outer face for both configurations.

Proof. Let v be a vertex that belongs to two configurations of Figure 3.7. If v is a b-vertex, then none of the two configurations is an octahedron. Then by maximality of the components of b-vertices in each configuration, the two configurations must rely on the same set of b-vertices, so they are the same configuration. Now suppose v is a 3-vertex. In both configurations it must be an internal vertex, and have an adjacent b-vertex. So the configurations also share a b-vertex and the same argument concludes. Finally, if v is a vertex of degree 4, it is an internal vertex of an octahedron. Since two octahedra cannot intersect on internal vertices and no internal vertex of an octahedron may be adjacent to a 3-vertex, v does not belong to any other configuration. The observation follows. □

Now that the configurations containing b-vertices have been characterized, we propose an algorithm that successively considers each of them. During Algorithm 3.1 (and during its analysis), we consider configurations 1 to 7 to be *monitored* by S_1 only if all their inner b-vertices are in $M(S_1)$. An octahedron is said to be monitored if all its vertices are in $M(S_1)$.

Note that the output of Algorithm 3.1 is the empty set whenever G does not contain b-vertices nor facial octahedra. We prove the following lemma:

Lemma 3.5. *Let S_1 be the set obtained by application of Algorithm 3.1 to G. The following statements hold:*

(i) All b-vertices and all facial octahedra are monitored by S_1.
(ii) If S_1 is non empty, $|S_1| \leq \frac{|M(S_1)|-2}{4}$.
(iii) S_1 has Property $(*)$ in G.

Proof. (i) Every b-vertex in the graph belongs to one of the configurations of Figure 3.7. The selected vertices in each configuration monitors all the b-vertices of the configuration. The algorithm thus monitors every such vertices. Taking any vertex of a facial octahedron monitors the whole octahedron, thus all facial octahedra are monitored as well.

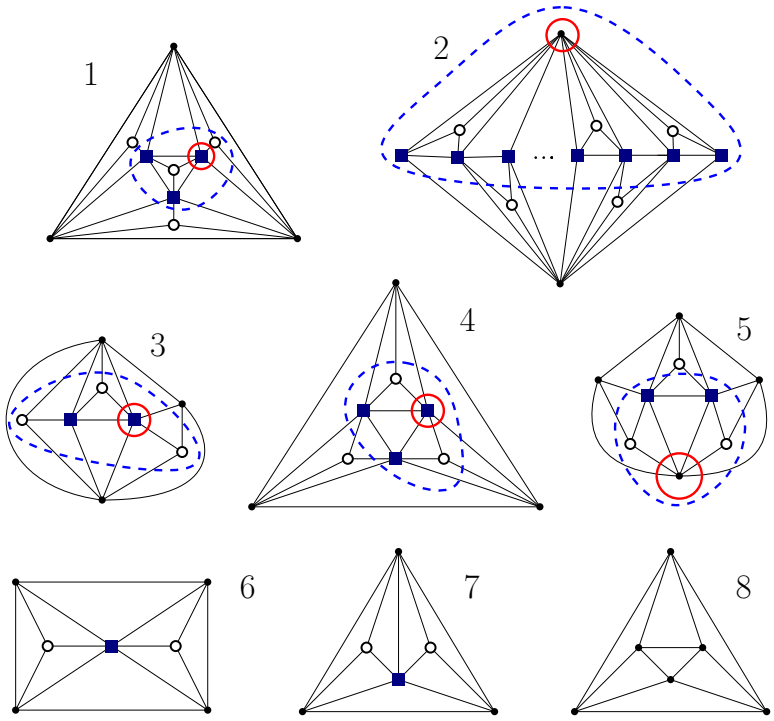

Figure 3.7: The different configurations containing a b-vertex, and the octahedron. So-called "special" vertices of configurations 1 to 5 are circled in red. For each configuration 1 to 5, vertices circled with a blue dotted curve form a set relative to the special vertex of the configuration. We call them the circled vertices of the configuration.

(ii) If the graph is dealt with in the first *if*s, the statement is straightforward. Otherwise, we first ensure that for each vertex $u \in S_1$, there are indeed at least five vertices labeled with u. For configurations 1, 3, 4 and 5, this is clear by definition of the circled vertices. For configuration 2, the vertex taken plus the (at least) three b-vertices of the path plus at least one 3-vertex make (at least) five labeled vertices. For every vertex u added in the second *while* loop, there are at least two vertices labeled with u in each of the two configurations, which together with u itself makes five vertices. For vertices added in the last *while* loop, at least six vertices are labeled with u each time.

Now, by Observation 3.4, only vertices on the outer face of some configuration may receive two labels, and so in only two cases: they may receive their own label when they are themselves added to S_1, or they may receive a label during the last *while* loop if they are in a non-monitored configuration 6, 7 or 8 disjoint from all remaining non-monitored configurations. Since last configurations are monitored by any vertex of their outer face, all vertices are labeled at most once.

If S_1 contains two or more vertices at the end of the algorithm, the statement is proved. If S_1 is reduced to a singleton, since the chosen vertex is of degree at least five, the statement holds.

(iii) Let G' be an induced triangulation of G monitored after Algorithm 3.1. If

Algorithm 3.1: Monitoring special configurations

Input: A triangulation G of order $n \geq 6$.
Output: A set $S_1 \subseteq V(G)$ monitoring all b-vertices and all vertices of facial octahedra.

$S_1 := \emptyset$
if *G has a vertex u of degree at least $n-2$* **then**
  Label $N[u]$ with u
  Return $\{u\}$
if *G is a triakis tetrahedron (as in Figure 3.9)* **then**
  u, v: two b-vertices of G at distance 2
  Label u, its 3-neighbors and two of its adjacent b-vertices with u
  Label all other vertices of G with v
  Return $\{u, v\}$
while $\exists$ *a non-monitored configuration H from Figure 3.7(1,2,3,4,5)* **do**
  u: the special vertex of H
  $S_1 \leftarrow S_1 \cup \{u\}$
  Label u and the circled vertices of H with u
while $\exists$ *non-monitored configurations H, H' from Figure 3.7(6,7,8) with a common vertex u* **do**
  $S_1 \leftarrow S_1 \cup \{u\}$
  Label u and the inner vertices of H and H' adjacent to u with u
while $\exists$ *a non-monitored configuration H from Figure 3.7(6,7,8)* **do**
  u: any outer vertex of H
  $S_1 \leftarrow S_1 \cup \{u\}$
  Label all vertices of H with u
Return S_1

$|S_1 \cup V(G')| = 0$, then Property $(*)$.(b) holds. Assume then $|S_1 \cup V(G')| > 0$. If there is a vertex $v \in S_1$ such that some vertices labeled with v are not in G', then v is a vertex of the outer face of G' and Property $(*)$.(a) holds. Otherwise, for every vertex $v \in S_1 \cap V(G')$, all vertices with label v are in G'. If $|S_1 \cap V(G')| \geq 2$, then this is sufficient to deduce that Property $(*)$.(b) holds. Otherwise, we observe that the set of vertices bearing a same label u either does not form an induced triangulation or is of size at least six, so G' contains at least six vertices and the statement also holds. □

In the following, S_1 denotes the output of Algorithm 3.1 applied to the graph G. Note that we can now forget the labels put on vertices during Algorithm 3.1.

3.1.2 Structure of special configurations

This section is dedicated to the proof of Lemma 3.3. Note that a b-vertex has degree at most six.

Observation 3.6. Let u, u' be two b-vertices. Vertices u and u' are adjacent if and only if there exists a 3-vertex $v \in N(u) \cap N(u')$.

Proof. ($\Rightarrow$) By definition of the neighborhood of a b-vertex u, every neighbor of u is also adjacent to a 3-vertex v adjacent to u.

($\Leftarrow$) Since v has degree 3, then all neighbors of v are pairwise adjacent. □

Lemma 3.7. *If G contains two 3-vertices v_1, v_2 with two common b-neighbors, then G is isomorphic to one of the graphs depicted in Figure 3.8.*

Proof. Either v_1 and v_2 have three common neighbors (inducing the first subgraph), or they have distinct third neighbors (inducing the second subgraph). In the first subgraph, all triangles are incident to a 3-vertex, so they are facial and there is no possibility for more vertices in the graph. In the second subgraph, the only faces not incident to a 3-vertex are incident to a b-vertex, which can not have other neighbors. Again, all triangles must then be facial. □

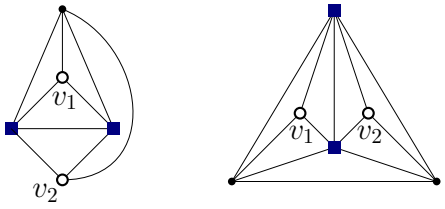

Figure 3.8: The two possible configurations of G if two 3-vertices v_1 and v_2 have two common b-neighbors. In both cases, G is exactly restricted to these graphs, and $\gamma_P(G) = 1$.

Lemma 3.8. *If all the neighbors of a 3-vertex are b-vertices, then G is isomorphic to a graph depicted in Figure 3.8 or contains the configuration depicted in Figure 3.9.*

Proof. Let v be a 3-vertex adjacent to three b-vertices u_1, u_2 and u_3, that necessarily form a triangle. Each u_i has another 3-neighbor v_i. If the vertices v_i are not all distinct, then there exist two b-vertices sharing two adjacent 3-vertices, and Lemma 3.7 concludes the graph is depicted in Figure 3.8. So assume the v_i are distinct. Let w_1 and w_2 be the neighbors of v_1 distinct from u_1. They are both adjacent to u_1. Since u_1 may not have any other neighbor, we infer without loss of generality that w_2 is adjacent to u_2 (and w_1 to u_3), and therefore that w_2 is also adjacent to v_2 (and w_1 to v_3). Similarly, v_2 and v_3 must have some vertex w_3 as a common neighbor, also adjacent to u_2 and u_3. Now, since the neighborhoods of 3-vertices and b-vertices are fully determined, we get a facial triakis tetrahedron, as depicted in Figure 3.9. □

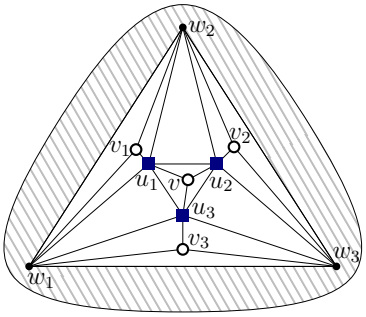

Figure 3.9: A facial triakis tetrahedron.

Lemma 3.9. *If G contains three b-vertices forming a three cycle with no common 3-neighbor, then G contains the first configuration depicted in Figure 3.10, or is isomorphic to one of the last two graphs depicted in Figure 3.10.*

Proof. Let $[u_1u_2u_3]$ be three b-vertices forming a cycle, with no common 3-neighbor. By Observation 3.6, every two of these vertices have a 3-vertex as a common neighbor, and they are distinct by hypothesis. Let v_1, v_2, v_3 be the 3-vertices adjacent respectively to u_1 and u_2, u_2 and u_3, and u_1 and u_3. Let z_1, z_2, z_3 be the third neighbors of respectively v_1, v_2 and v_3. Note that they are not necessarily distinct. Suppose two z_i are distinct, say z_1 and z_3 are. Observe that the neighbors of u_1 are exactly $\{u_2, u_3, v_1, v_3, z_1, z_3\}$. Therefore, if $[u_1u_2u_3]$ separates z_1 from z_3, then z_3 is adjacent to u_2 and z_1 is adjacent to u_3. Now, by definition of b-vertices, this implies that v_2 is adjacent to z_3 and to z_1, a contradiction. So $[u_1u_2u_3]$ does not separate any two z_i and is facial. Moreover, if say z_1 and z_3 are distinct, they must be adjacent, since u_1 has no other neighbor. So depending on whether the z_i are distinct or not, G contains the first configuration depicted in Figure 3.10, or is isomorphic to one of the last two graphs depicted in Figure 3.10. All faces incident to a 3-vertex or a b-vertex in these drawings are facial. □

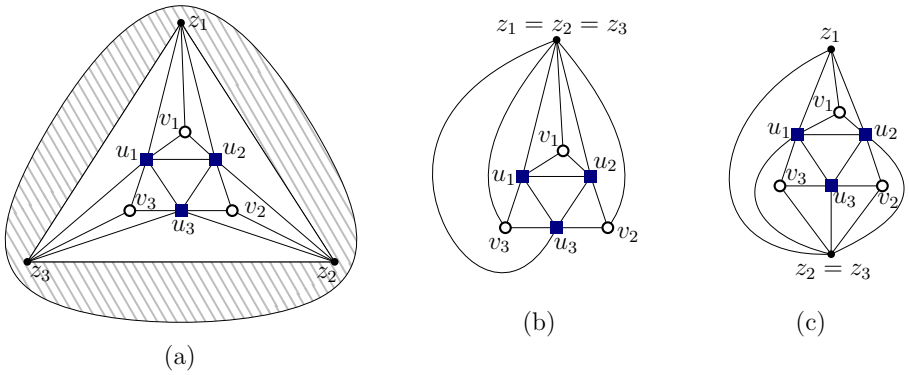

Figure 3.10: The possible configurations of G if there is a face composed of b-vertices. (a) A facial Sapphire graph, and (b and c) its contracts, satisfying $\gamma_P(G) = 1$.

Proposition 3.10. Let $u_1u_2u_3$ be a path on three b-vertices. Let v_1 be the 3-vertex adjacent to u_1 and let v_2 be the 3-vertex adjacent to u_2 and u_3. If u_1 is not adjacent to u_3, then there exist distinct vertices x and x' such that $\{u_1, u_2, u_3, v_1\} \subseteq N(x)$, $\{u_1, u_2, u_3, v_2\} \subseteq N(x')$, and $[xu_2u_3]$ and $[x'u_1u_2]$ are facial (see Figure 3.11).

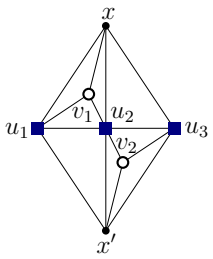

Figure 3.11: There are two distinct vertices both adjacent to $\{u_1, u_2, u_3\}$. All triangles are facial.

Observe that the above proposition together with Lemmas 3.8 and 3.9 covers all possibilities of three connected b-vertices.

Corollary 3. *Suppose a set of $k \geq 3$ b-vertices form a path $(u_1, \ldots, u_k)$ (where u_1 and u_k may be adjacent when $k > 3$). Let $v_1, \ldots, v_{k-1}$ be the 3-vertices with v_i being adjacent to u_i and u_{i+1}, and let v_0 be the 3-vertex adjacent to v_1 but not to v_2. Then there exists a vertex x adjacent to all u_i, $1 \leq i \leq k$ and to v_0 and v_2. (see Figure 3.12).*

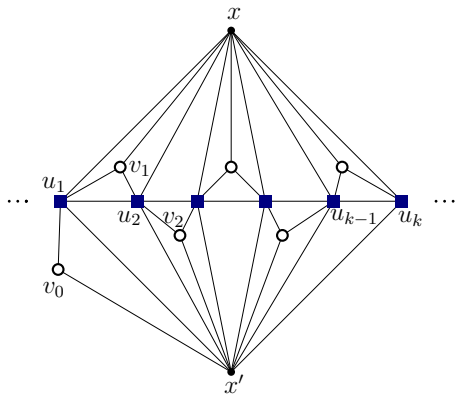

Figure 3.12: There are two vertices universal to the path $(u_1, u_2, u_3, \ldots, u_k)$. Vertex x' is also adjacent to v_0 and v_2.

Proof. Applying Proposition 3.10 to vertices u_1, u_2, u_3, there exist distinct vertices x, x' such that $\{u_1, u_2, u_3, v_1\} \subseteq N(x)$, $\{u_1, u_2, u_3, v_2\} \subseteq N(x')$, and $[xu_2u_3]$ and $[x'u_1u_2]$ are facial. Since x is adjacent to the b-vertex u_3, x must be adjacent to v_3 and thus to x_4. Then x_4 is also adjacent to x' as x_3 has no other neighbor. Iterating this argument, we infer that x and x' are adjacent to all u_i. Now, since x' is adjacent to u_1 but not to v_1, by definition of a b-vertex it is adjacent to v_0, and the corollary follows. □

Lemma 3.11. *If G contains a maximal component of b-vertices isomorphic to P_2, then G is isomorphic to one of the graphs on Figure 3.13, or it contains as a facial subgraph isomorphic to one of the graphs of Figure 3.14.*

Proof. Let u_1, u_2 be the b-vertices. Let v_1 be the 3-vertex adjacent to u_1 and u_2, and z the third neighbor of v_1. Let v_0 and v_2 be the second 3-neighbors of respectively u_1 and u_2, we can assume they are distinct by Lemma 3.7. Since v_0 is a 3-vertex and is not adjacent to u_2, v_0 has a neighbor t which is adjacent to u_1 and u_2. By definition of b-vertices, v_2 must also be adjacent to t. Let z_1 and z_2 be the third neighbors of respectively v_0 and v_2. Depending on which of z, z_1 and z_2 are distinct, we get one of the drawings of Figures 3.13 or 3.14. In Figure 3.13 all triangles are facial, so the whole graph is reduced to the drawing, while on in Figure 3.14, the outer face of the drawing may not be facial. □

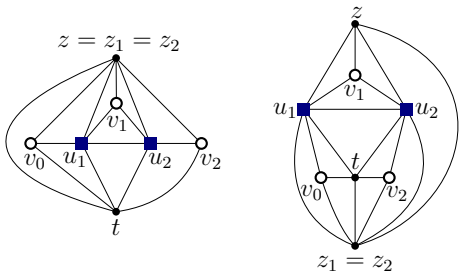

Figure 3.13: Possible configurations of G if there is a P_2 component of b-vertices. All triangles of the drawing are facial and $\gamma_P(G) = 1$.

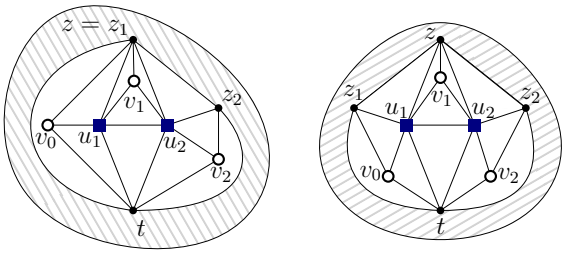

Figure 3.14: Other possible configurations of G if there is a P_2 component of b-vertices. The outer face is not necessary facial. All other triangles of the drawing are facial.

Finally, if there is an isolated b-vertex in G, then it belongs to one of the subgraphs depicted in Figure 3.6. This concludes the proof of Lemma 3.3.

3.1.3 Expansion of S_1

The next step consists in selecting greedily any vertex that increases the set of monitored vertices by at least four. We first make a small observation.

In the following, the graphs of the form $P_2 + P_k$ (i.e. formed by two vertices both adjacent to all vertices of a path P_k) for some $k \geq 1$ are called *tower graphs*. Remark that the only maximal planar graphs of order $n \leq 6$ are the complete graphs K_3 and K_4, the graphs $P_2 + P_3$ and $P_2 + P_4$, the octahedron, and the flip-octahedron (see Figure 3.15).

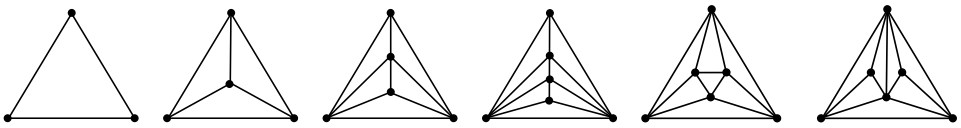

Figure 3.15: The maximal planar graphs of order $n \leq 6$.

Observation 3.12. Let G be a triangulation. Unless G is an octahedron or a tower graph $P_2 + P_k$ (for some $k \geq 1$), one inner vertex of G has degree at least 5.

Proof. Suppose G is not an octahedron or a tower graph. If G is the flip-octahedron (the last graph of Figure 3.15), then one of its inner vertices has degree five. Otherwise, by the preceding observation, G contains at least seven vertices. Suppose by way of contradiction that all inner vertices of G have degree at most 4. Denote by u the outer vertex of G with maximum degree, v, w the other two outer vertices of G, and $u_1, \ldots, u_k$ the inner neighbors of u ($k \geq 2$ or G is K_4), so that $(vu_1 \ldots u_k w)$ form a cycle. Without loss of generality, we assume that v is adjacent to no less vertices among $u_1, \ldots, u_k$ than w is.

Let ℓ be the maximum integer such that for all $i \leq \ell$, u_i is adjacent to v. Since G is not a tower graph, $\ell < k$. Observe that since v is not adjacent to $u_{\ell+1}$, u_ℓ and v have a common neighbor t (that is neither $u_{\ell-1}$ nor u) to make another face on the edge vu_ℓ. If $\ell > 1$, v, t, u, $u_{\ell-1}$ and $u_{\ell+1}$ make five neighbors to u_ℓ, a contradiction.

So $\ell = 1$ and since u_2 is not adjacent to v, $t \neq u_2$. (Note that $t \neq w$ or v would have only one neighbor among $u_1, \ldots, u_k$ while w has at least two, contradicting our assumption.) Thus u_1 has at least four neighbors: u, v, u_2 and t. By our initial assumption, $[u_1 u_2 t]$ is a facial triangle. Now if $k \geq 3$, u_2 also already has four neighbors so $[u_2 u_3 t]$ form a facial triangle. But then t and u_3 are already of degree four, so it is not possible to form another facial triangle containing the edge tu_3, a contradiction. So $k = 2$, and $[u_2 w t]$ is facial. But then we get an induced octahedron where the only non facial triangle is $[vtw]$, in which adding a vertex would raise the degree of t to more than 4, a contradiction. This concludes the proof. □

Let us now proceed with the algorithm defining a power dominating set. Assume that after Algorithm 3.1, $M(S_1) \neq V(G)$. We apply Algorithm 3.2 that builds a set of vertices $S_2 \subset V(G)$ by iteratively expanding S_1 in such a way that each addition of a vertex increases by at least four the number of monitored vertices. Moreover, at each round, the vertex added to S_2 has maximal degree in G among all candidate vertices.

We now prove the following lemma:

Algorithm 3.2: Greedy selection of vertices to expand S_1

Input: A triangulation G of order $n \geq 6$
Output: A set $S_2 \subseteq V(G)$ with $|S_2| \leq \frac{|M(S_2)|-2}{4}$
$S_2 :=$ Algorithm 3.1(G)
$M := M(S_2)$
while $\exists\, u$ *in* $V(G) \setminus S_2$ *such that* $|M(S_2 \cup \{u\})| \geq |M| + 4$ **do**
  Select such a vertex u of maximum degree in G.
  $S_2 \leftarrow S_2 \cup \{u\}$
  $M \leftarrow M(S_2)$
Return S_2

Lemma 3.13. *Let S_2 be the output of Algorithm 3.2 applied to G. The following statements hold:*

(i) $|S_2| \leq \frac{|M(S_2)|-2}{4}$.
(ii) S_2 *has Property* $(*)$ *in* G.

Proof. **(i)** Let ℓ denote the number of rounds of Algorithm 3.2 (i.e the number of vertices added during the "while" loop). For $0 \leq i \leq \ell$, we denote by $S_2^{(i)}$ the set of selected vertices after the i-th round of Algorithm 3.2, and by $M^{(i)}$ the set $M(S_2^{(i)})$ of vertices monitored by $S_2^{(i)}$. The algorithm ensures that for all $0 \leq i \leq \ell - 1$, $|S_2^{(i+1)}| = |S_2^{(i)}| + 1$ and $|M^{(i+1)}| \geq |M^{(i)}| + 4$. So provided we can establish the base case, Statement (i) holds by induction. If the result of Algorithm 3.1 applied on G is the empty set, then $1 \leq |S_2^{(0)}| \leq \frac{|M^{(0)}|}{6}$, and thus $|S_2^{(0)}| \leq \frac{|M^{(0)}|-2}{4}$. Otherwise, by Remark 3.12, the first vertex added to S_2 is of degree at least 5 so $|M^{(1)}| \geq 6$. Thus this time $\frac{|M^{(1)}|-2}{4} \geq 1 = |S_2^{(1)}|$, and the induction allows to conclude.

(ii) Let $G' \subseteq G$ be an induced triangulation monitored by S_2 after Algorithm 3.2. First assume G' is isomorphic to a tower graph. Note that no vertex added during Algorithm 3.1 is an inner vertex of a tower graph. Observe that for each inner vertex v of a tower graph, there exists an outer vertex v' such that $N[v] \subseteq N[v']$ and $d(v') \geq d(v)$. Then at any given round i, Algorithm 3.2 would rather select v' instead of any inner vertex v, and thus no inner vertex of G' is in S_2. Since G' is monitored, then at least one of the outer vertices of G' (say u) is in S_2 or has propagated to an inner vertex of G', so $N[u] \subseteq M$ and Statement (a) of Property $(*)$ holds for S_2 in G. If G' is isomorphic to the octahedron or to the flip-octahedron, then one of the outer vertices of G' is in S_1 thanks to Algorithm 3.1, and Property $(*)$.(a) also holds.

Assume now that $|V(G')| \geq 6$, and suppose that Property $(*)$.(a) does not hold for G'. Then some vertices of G' belong to S_2, and vertices of $V(G') \cap S_2$ only monitor vertices of G' (no propagation may occur from a vertex of the outer face of G'). Then the same proof as for **(i)** above restricted to G' shows that Property $(*)$.(b) holds. This proves that Property $(*)$ holds for S_2 in G. □

In the following, S_2 denotes the output of Algorithm 3.2 on the graph G.

3.1.4 Monitoring the remaining components

After Algorithm 3.2, some vertices of the graph may still remain non-monitored. Algorithm 3.3 thus completes the set S_2 into a power dominating set of G, while keeping the wanted bound. In order to succeed, we need to have a better understanding of the structure of the graph around these non-monitored vertices. More precisely, we show that the graph can be described in terms of *splitting structures* (see Figure 3.16): they are structures composed of a set $C = \{u_1, u_2, u_3\}$ of three non-monitored vertices and of two *associated triangulations* G_1 and G_2 whose outer vertices are monitored.

We make use of the following lemma, that is proved in Section 3.1.5. Denote by $\overline{M}_G(S)$ the set of vertices not monitored by S in G (i.e. $V(G) \setminus M_G(S)$).

> **Lemma 3.14.** *Let G be a triangulation, S a subset of vertices of G monitoring all b-vertices and facial octahedra. Let G' an induced triangulation of G. If $\overline{M}_G(S) \cap V(G') \neq \emptyset$, and for any $v \in V(G)$, $|M_G(S \cup \{v\})| \leq |M_G(S)| + 3$ (i.e. Algorithm 3.2 stopped), then G' is isomorphic to one of the splitting structures depicted in Figure 3.16.*

Observe that the triangulations associated to a splitting structure may contain non-monitored vertices, in which case we can again apply the above lemma and deduce that they are in turn isomorphic to a splitting structure.

Denote by S_2 the output of Algorithm 3.2 applied to G. If $M(S_2) = V(G)$, then by Lemma 3.13, S_2 is a power dominating set of G with at most $\frac{n-2}{4}$ vertices. Otherwise, Algorithm 3.3 recursively goes down to splitting structures whose associated triangulations are completely monitored, in which case it adds a vertex to S to monitor the remaining vertices.

Algorithm 3.3: Monitoring the last vertices

Input: A triangulation G of order $n \geq 6$ and an induced triangulation $G' \subseteq G$
Output: A set $S \subseteq V(G')$ monitoring G' and such that $|S| \leq \frac{|V(G')|-2}{4}$
$S \leftarrow V(G') \cap$Algorithm 3.2(G)
if $\exists\, u \notin M_G(S)$ **then**
  $G_1, G_2 \leftarrow$ triangulations associated to the splitting structure of G' containing u
  $S' \leftarrow$ Algorithm 3.3(G, G_1)
  $S'' \leftarrow$ Algorithm 3.3(G, G_2)
  $S \leftarrow S' \cup S'' \cup \{u\}$
Return S

We now prove that after the addition of vertices during Algorithm 3.3, the wanted bound still holds.

> **Lemma 3.15.** *Let G' be an induced triangulation of G and C a splitting structure in G' with G_1 and G_2 its associated triangulations. Let u be a vertex of C. Let S' denote the set $S \cap V(G_1)$ and S'' the set $S \cap V(G_2)$. If G_1 and G_2 are monitored and S' and S'' have Property $(*)$, then $S' \cup S'' \cup \{u\}$ also has Property $(*)$ and G' is monitored.*

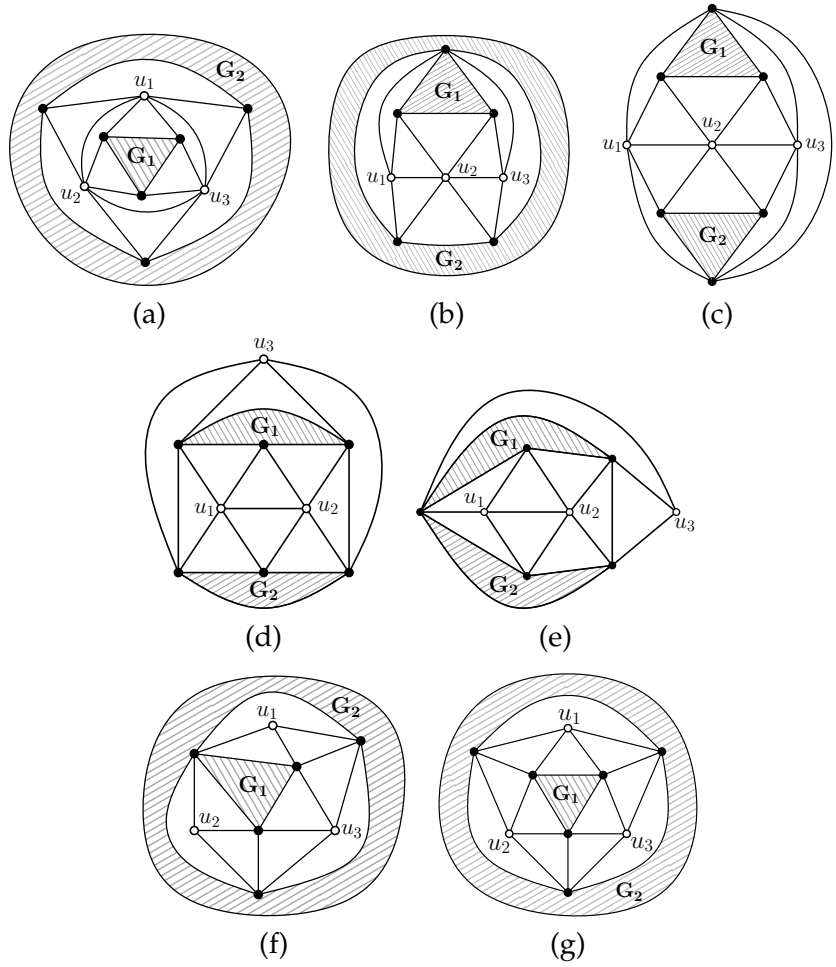

Figure 3.16: The seven different splitting structures and their associated triangulations G_1 and G_2. White vertices are non monitored. All triangles are facial except for G_1 and G_2.

Proof. First recall that after application of Algorithm 3.2, any vertex in $M_G(S)$ has at most three non-monitored neighbors. Therefore, in the induced triangulation G', a vertex adjacent to a vertex in C may not be adjacent to vertices from another configuration C' in G, or it would have two non-monitored neighbors in C and two in C', a contradiction. Thus if a vertex can propagate in G', then it can also propagate in G.

We know that S' and S'' have Property $(*)$, and so G_1 and G_2 both satisfy either Property $(*)$.(a) or (b). Since all vertices of the outer face of G_1 and G_2 have non-monitored neighbors, then in fact, G_1 and G_2 satisfy Property $(*)$.(b). Thus $|S'| \leq \frac{|V(G_1)|-2}{4}$ and $|S''| \leq \frac{|V(G_2)|-2}{4}$. Remark that $|V(G')| \geq |V(G_1)| + |V(G_2)| + 2$ in every splitting structure. After adding a vertex $u \in C$, we have:

$$|S' \cup S'' \cup \{u\}| \leq \frac{|V(G_1)|-2}{4} + \frac{|V(G_2)|-2}{4} + 1 = \frac{|V(G_1| + |V(G_2)|}{4} \leq \frac{|V(G')|-2}{4}.$$

Moreover, the outer vertices of induced triangulations of G' all have only monitored neighbors (the outer vertices of G' excepted) and thus G' satisfies Property $(*)$.

To prove that the addition of one vertex of C is sufficient to monitor G', we consider different cases depending on the splitting structure.

- For splitting structures (a), (b) and (c), adding u_2, then u_1 and u_3 are monitored by adjacency.
- For splitting structures (d) and (e), adding u_1, then u_2 is monitored by adjacency, and then any vertex of the outer face of G_1 or G_2 propagates to u_3.
- For splitting structures (f) and (g), adding u_1, then two vertices of the outer face of G_1 propagate independently to the other two vertices of C.

Thus G' is monitored, which concludes the proof. □

We can now use Lemma 3.15 to prove by direct induction on the splitting structures that at the end of Algorithm 3.3, Property $(*)$ holds for S in G. Moreover, the proof of Lemma 3.15 shows that for the set S, G satisfies Property $(*)$.(b). Thus the output S of Algorithm 3.3 satisfies the wanted bound and the graph is completely monitored. We thus get the following corollary that concludes the proof of Theorem 3.1.

Corollary 4. *At the end of Algorithm 3.3, $M(S) = V(G)$ and $|S| \leq \frac{|V(G)|-2}{4}$.*

In the following section, we finally prove Lemma 3.14.

3.1.5 Proof of Lemma 3.14

In the following, we work under the assumption of Lemma 3.14, i.e. that the set S monitors all octahedra and b-vertices, and that the addition of any vertex v to S would extend the set of vertices monitored by S by at most three. Any vertex contradicting the second part of the assumption is called a *contradicting vertex*.

For simplicity, when G and S are clear from context, we denote $M = M_G(S)$ and $\overline{M} = V(G) \setminus M_G(S)$.

As a direct consequence of the definition of power domination, we get the following observation:

Observation 3.16. Let S be a set of vertices of G such that for every vertex $v \in V(G)$, $|M_G(S \cup \{v\})| \leq |M_G(S)| + 3$. Then the following properties hold:

(i) Each vertex of M has either zero, two or three non-monitored neighbors.
(ii) Each vertex of $\overline{M}$ has at most 2 neighbors in $\overline{M}$.
(iii) For every vertex $u \in M \setminus S$, there exists $v \in M \cap N(u)$ such that $N[v] \subset M$ (that propagated to u).

We now make the following statement.

Lemma 3.17. *If v is of degree at least five, then for every two neighbors u_1 and u_2 of v, there exists a neighbor w of v adjacent to u_1 or u_2, but not both, and the corresponding triangle $[vu_iw]$ is facial.*

Proof. We partition the set of neighbors of v into two paths from u_1 to u_2: a path $(w'_1, \dots, w'_k)$ of length at least three (i.e. $k \geq 2$) and another path $(w_1, \dots, w_\ell)$, possibly empty. We have $w'_1 \neq w'_k$. By way of contradiction, assume both w'_1 and w'_k are adjacent to both u_1 and u_2. Contracting the path $(w'_1, \dots, w'_{k-1})$ into w'_1 and the path $(u_1, w_1, \dots, w_\ell)$ into u_1, we get that u_1, u_2, v, w'_1, w'_k induce a K_5 in the resulting graph, contradicting planarity of G. Thus w'_1 is not adjacent to u_2 (and $[w'_1u_1v]$ is facial) or w'_k is not adjacent to u_1 (and $[w'_ku_2v]$ is facial). □

Remark that Lemma 3.17 applies in particular to the case where v is in M with at least two neighbors in $\overline{M}$. Indeed, by Observation 3.16(iii), v has a neighbor v' that propagated to it. Then v' only has monitored neighbors, and two of them are also adjacent to v. Thus v has degree at least five.

Lemma 3.18. *Connected components of $G[\overline{M}]$ are of order at most three.*

Proof. Let C be a connected component of $G[\overline{M}]$. By Observation 3.16(ii), each vertex of $\overline{M}$ has degree at most two in $\overline{M}$, so C is a path or a cycle. Then adding any vertex of C to S would monitor all of C. Since we work under the assumption of Lemma 3.14, C is of order at most three. □

Thus each connected component of $G[\overline{M}]$ is isomorphic to either K_3, P_3, P_2, or K_1. Lemmas 3.19, 3.20 and 3.21 deal successively with the first three cases, whereas Lemma 3.22 goes through the case where $\overline{M}$ is an independent set in the induced triangulation considered.

Lemma 3.19. *Let G and M satisfy the assumption of Lemma 3.14. If an induced triangulation G' contains a component of $G[\overline{M}]$ isomorphic to K_3, then G' is isomorphic to the splitting structure depicted in Figure 3.17.*

Proof. Let C be a component of $G[\overline{M}]$ isomorphic to K_3 with $V(C) = \{x_1, x_2, x_3\}$. Let u be a vertex of M, adjacent to at least one of the vertices of C.

We first consider the case when u has neighbors in $\overline{M} \setminus C$. If u is adjacent to two vertices in C, then by Observation 3.16(i), u has exactly one neighbor in $\overline{M} \setminus C$, say v. Then $M(S \cup \{u\}) \supseteq M(S) \cup \{x_1, x_2, x_3, v\}$, and u is a contradicting vertex. So u has only one neighbor in C, say x_1. Within the neighborhood of x_1, the path from x_2 to x_3 going through u must contain at least three inner vertices, so x_1 is of degree at least five. Applying Lemma 3.17 on x_1, we get that a neighbor w of x_1 is adjacent to x_2 or x_3 but not both. Since w is adjacent to two vertices in C, it has no other neighbors in $\overline{M}$ or the above case would apply. Hence, adding u to S, all neighbors of u in $\overline{M}$ get monitored, then w propagates to x_2 or x_3 which can in turn propagate to the last vertex of C. So u is a contradicting vertex.

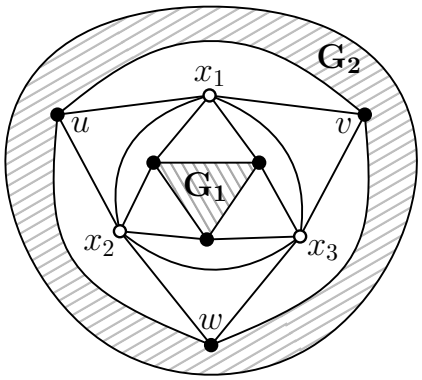

Figure 3.17: The configuration for G' containing a non-monitored component isomorphic to K_3. G_1 and G_2 are triangulations. All other triangles of the drawing are facial.

We assume now that any vertex of M adjacent to C has only vertices of C as neighbors in $\overline{M}$. Note that such a vertex must be adjacent to at least two vertices in C. Let u be a common neighbor of x_1 and x_2 such that $[ux_1x_2]$ is facial. By Lemma 3.17, there is a neighbor v of u that is adjacent to only one of $\{x_1, x_2\}$ (say x_1) and $[uvx_1]$ is facial. The vertex v must have a second non-monitored neighbor, that must be in C, so v is adjacent to x_3. Observe that the triangle $[vx_1x_3]$ must be facial. Otherwise, there is a vertex $t \neq v$ such that $[tx_1x_3]$ is facial and t is separated from x_2 by (vx_1x_3). Then by Lemma 3.17, t has a neighbor t' with only one neighbor among $\{x_1, x_3\}$ also separated from x_2 by (vx_1x_3), and thus with only one non-monitored neighbor, a contradiction. Now, v and x_3 have a common neighbor w outside the triangle $[vx_1x_3]$, such that $[vwx_3]$ is facial. By definition of v, we have $w \neq x_2$. We also have $w \neq u$ or v would be of degree three contradicting Observation 3.16(iii). The cycle (uvx_3x_2) separates w from x_1, so the second non-monitored neighbor of w (different from x_3) must be x_2. Unless an additional edge uw form a facial triangle $[uwx_2]$, there is another neighbor of x_2 that is separated from both x_1 and x_3 by the cycle $(uvwx_2)$, a contradiction. So u is adjacent to w in a facial triangle $[uwx_2]$.

In a similar way that we proved that $[vx_1x_3]$ is facial, we infer that $[wx_2x_3]$ is facial. By construction, $[ux_1x_2]$, $[uvx_1]$, $[vwx_3]$ are facial, and we proved $[vx_1x_3]$, $[uwx_2]$ and $[wx_2x_3]$ also are. If the triangle $[x_1x_2x_3]$ is facial, then the graph induced by the vertices u, v, w, x_1, x_2, x_3 is a facial octahedron, contradicting the assumption of Lemma 3.14. Thus $[x_1x_2x_3]$ is not facial, and applying the same line of reasoning inside $[x_1x_2x_3]$ shows that G' is isomorphic to the splitting structure depicted in Figure 3.17. □

Lemma 3.20. *Let G and M satisfy the assumption of Lemma 3.14. If an induced triangulation G' contains a component of $G[\overline{M}]$ isomorphic to P_3, then G' is isomorphic to one of the splitting structures depicted in Figure 3.18.*

Proof. Let C be a component of $G[\overline{M}]$ isomorphic to P_3 with $V(C) = \{x_1, x_2, x_3\}$.

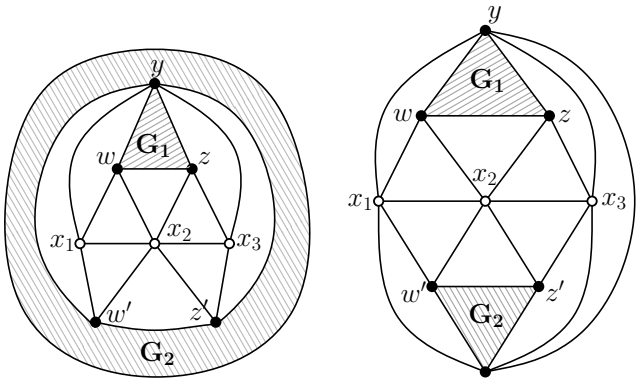

Figure 3.18: The two possible configurations for G' containing a non-monitored component isomorphic to P_3. G_1 and G_2 are triangulations. All other triangles of the drawing are facial.

Let u be a vertex adjacent to C. We first prove that all neighbors of u in $\overline{M}$ are vertices of C. By Observation 3.16(i), u has at most two neighbors in $\overline{M} \setminus V(C)$. If u has exactly one neighbor v in $\overline{M} \setminus V(C)$, then x_2 is a contradicting vertex, since u propagates to v. Assume then that u has two neighbors in $\overline{M} \setminus V(C)$ and thus only one neighbor in C. If u is adjacent to x_1 or x_3, then u is a contradicting vertex. Suppose that u is adjacent to x_2 only, which must then be of degree at least five. We apply Lemma 3.17 on x_2 and get a neighbor v of x_2 adjacent to x_1 or x_3 but not both. Taking u in S, v then propagates so u is a contradicting vertex. Thus neighbors of C may not be adjacent to vertices in $\overline{M}$ that are not in C.

We now prove that there is no vertex of M adjacent to all vertices of C. Suppose by way of contradiction that u is a vertex in M adjacent to x_1, x_2 and x_3. By Lemma 3.17, u has a neighbor $z \in M$ with exactly one neighbor in $\{x_1, x_3\}$ (say x_1) and $[uzx_1]$ is facial. Note that by the above statement, z is also adjacent to x_2.

Again, we can apply Lemma 3.17 to find a neighbor z' of z adjacent to x_1 or x_2 but not both. z' must have a second non-monitored neighbor, namely x_3. So z' cannot be adjacent to x_1 which is separated from x_3 by (ux_2z), so z' is adjacent to x_2 and x_3 and $[x_2zz']$ is facial. Now u is necessarily adjacent to z' forming a facial triangle $[ux_3z']$ or some vertex would have a single neighbor in C.

Observe that the triangle $[zx_1x_2]$ must be facial. Otherwise, there is a vertex $t \neq z$ such that $[tx_1x_2]$ is facial and t is separated from x_3 by (zx_1x_2). Then by Lemma 3.17, t has a neighbor t' with only one neighbor among $\{x_1, x_2\}$ also separated from x_3 by (zx_1x_2), and thus with only one non-monitored neighbor, a contradiction. With a similar argument, we get that $[z'x_2x_3]$, $[ux_1x_2]$ and $[ux_2x_3]$ are facial. But then x_2 is a b-vertex (as in the bad configuration of Figure 3.4), a contradiction.

Let $w, w', z, z' \in M$ such that $[x_1x_2w], [x_1x_2w'], [x_2x_3z], [x_2x_3z']$ are faces, by the above statement, all these vertices are distinct. Suppose that there is a neighbor u of x_2 different from the above vertices. u has a second neighbor in C, say x_1. The cycle (ux_1x_2) separates w or w' from x_3, say w. By Lemma 3.17, w has a neighbor with exactly one neighbor in $\{x_1, x_2\}$, and that cannot be adjacent to x_3, a contradiction. Thus x_2 has no other neighbor. Renaming vertices if necessary, we suppose $[x_2wz]$

and $[x_2w'z']$ are facial triangles.

Note that x_1 or x_3 must have another neighbor. Otherwise, w is adjacent to w' and$z$ is adjacent to z', which implies that x_2 is a b-vertex (as in the ugly configuration of Figure 3.4), a contradiction. Let $y \in M$ be a neighbor of x_1 such that $[x_1wy]$ is facial. The second neighbor of y in C is necessarily x_3. Similarly, z has a neighbor z_1 such that $[x_3z_1z]$ is facial and adjacent to x_1 and x_3. Note that $z_1 \neq w$ or w would be adjacent to three vertices in C. Then $y = z_1$ or the cycle (x_3ywz) would separate z_1 from x_1. We prove with similar arguments that there is a vertex y' such that $[x_1w'y']$ and $[x_3z'y']$ are facial.

If $y = y'$, then G' is isomorphic to the first splitting structure of Figure 3.18. Otherwise, suppose first that x_1 has another neighbor t. It also has to be adjacent to x_3. Then applying Lemma 3.17 to t, we find a vertex adjacent to only one vertex in C, a contradiction. So y and y' are adjacent, and $[x_1yy']$ and $[x_3yy']$ are facial. Thus G' is isomorphic to the second splitting structure of Figure 3.18. □

Lemma 3.21. *Let G and M satisfy the assumption of Lemma 3.14. If an induced triangulation G' contains a non-monitored component isomorphic to P_2, then G' is isomorphic to one of the graphs depicted in Figure 3.19.*

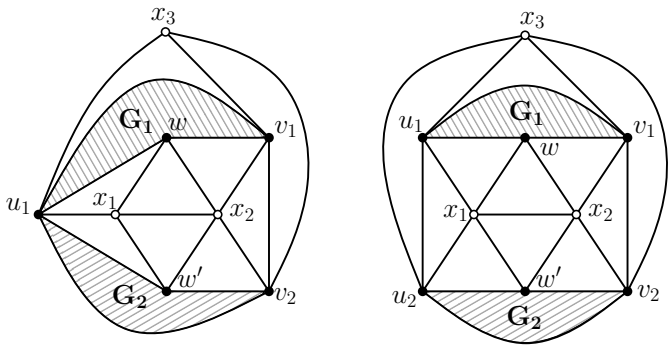

Figure 3.19: The two possible configurations of G if $G[\overline{M}]$ has a connected component isomorphic to P_2. G_1 and G_2 are triangulations. All other triangles of the graph are facial.

Proof. Let $C = \{x_1, x_2\}$ with $x_1x_2 \in E(G)$. Let w and w' be the vertices such that $[x_1x_2w]$ and $[x_1x_2w']$ are facial.

Claim 1. There is exactly one vertex of $\overline{M}$ at distance 2 of C.

Proof. Suppose there is no vertex of $\overline{M}$ at distance 2 from C. By Lemma 3.17, w has a neighbor $t \in M$ adjacent to only one vertex among $\{x_1, x_2\}$. Then t has only one neighbor in $\overline{M}$, which contradicts Observation 3.16(i). Thus there is a vertex of $\overline{M}$ at distance 2 from C. Suppose that there is $u' \in \overline{M} \setminus V(C)$ neighbor of $u \in N(C)$ and $v' \in \overline{M} \setminus V(C)$ neighbor of $v \in N(C)$. Then u is a contradicting vertex (whether it is distinct from v or not). (□)

Let x_3 be the only vertex of $\overline{M}$ at distance 2 of C.

Claim 2. The vertices adjacent to x_3 are exactly the vertices of $(N(x_1) \cup N(x_2)) \setminus \{w, w'\}$.

Proof. Suppose there is a vertex $w'' \in M, w'' \neq \{w, w'\}$ adjacent to x_1 and x_2. The cycle(x_1x_2w'') separates x_3 from either w or w', say w. By Lemma 3.17, there exists a vertex v adjacent to w and to only one vertex among $\{x_1, x_2\}$. By Observation 3.16(i), v has a second non-monitored neighbor, that cannot be x_3, which contradicts Claim 1. Thus w and w' are the only common neighbors of x_1 and x_2. Therefore, all vertices adjacent to only one of x_1 and x_2 (i.e. in $N(x_1) \cup N(x_2) \setminus \{w, w'\}$) are adjacent to x_3 (and there is at least one such vertex).

Suppose there exists some vertex v adjacent to x_3 but not in $N(x_1) \cup N(x_2)$. Then v is in $\overline{M}$ or it has another neighbor $x_4 \in \overline{M} \setminus \{x_1, x_2, x_3\}$, and v is a contradicting vertex. Thus no vertex $v \in V(G) \setminus (N(x_1) \cup N(x_2))$ is adjacent to x_3.

We now prove that w and w' are not adjacent to x_3. Suppose w is adjacent to x_3. By Lemma 3.17, w has a neighbor u_1 adjacent to only one of $\{x_1, x_2\}$ (say x_1) such that $[u_1x_1w]$ is facial. (Thus u_1 is also adjacent to x_3 and $[ww_1x_3]$ is facial, since it separates x_3 from x_1 and x_2.) Again by Lemma 3.17, u_1 has a neighbor v_1 in M adjacent to only one of $\{x_1, x_3\}$. Suppose first v_1 is adjacent to x_3 (and not to x_1). Then v_1 is also adjacent to x_2. Following Observation 3.16(iii), w has other neighbors. So there is a vertex t such that $[x_2tw]$ is facial, and since t is separated from x_1 by $(x_2v_1x_3w)$, t is adjacent to x_3. Applying Lemma 3.17 on t, we get a contradiction. So v_1 is adjacent to x_1 but not to x_3, and thus $v_1 = w'$ (and w' is not adjacent to x_3). But x_3 has degree at least three, so there is a vertex v_2 adjacent to x_2 and x_3. Again, $[u_1x_3w]$, $[v_2x_2w]$ and $[v_2x_3w]$ must be facial. But then there is no vertex that may have propagated to w. Thus w and w' are not adjacent to x_3. (□)

Let us now consider the neighbors of x_1 and x_2 in $M \setminus \{w, w'\}$. Let $(u_1, \ldots, u_k)$ and $(v_1, \ldots, v_\ell)$ be the paths from w to w' among respectively $N(x_1) \cap M$ and $N(x_2) \cap M$. Since x_3 has degree at least 3, then by Claim 2, $k + \ell \geq 3$.

First observe that k and ℓ both are at most 2. Otherwise, say $k \geq 3$, then by Claim 2, each u_i is adjacent to x_3, and the triangles $[u_iu_{i+1}x_3]$ are facial, in particular $[u_1u_2x_3]$ and $[u_2u_3x_3]$. But then u_2 contradicts Observation 3.16(iii).

We thus have two cases:

- $k + \ell = 3$, say u_1 is the only neighbor of x_1 and v_1, v_2 are the only two neighbors of x_2 in $M \setminus \{w, w'\}$. By Claim 2, u_1, v_1 and v_2 are neighbors of x_3. Moreover, since none of $\{w, w'\}$ is adjacent to x_3, u_1 is adjacent to v_1 and v_2. By Claim 2, triangles $[u_1v_1x_3]$, $[v_1v_2x_3]$ and $[u_1v_2x_3]$ are facial, and G is isomorphic to the first graph depicted in Figure 3.19.
- x_1 and x_2 both have exactly two neighbors in $M \setminus \{w, w'\}$. By Claim 2, u_1, u_2, v_1 and v_2 are neighbors of x_3. Again, u_1 is adjacent to v_1 and u_2 is adjacent to v_2 since neither w nor w' is adjacent to x_3. By Claim 2, triangles $[u_1v_1x_3]$, $[v_1v_2x_3]$, $[u_1u_2x_3]$ and $[u_2v_2x_3]$ are facial and G is isomorphic to the second graph depicted in Figure 3.19.

This concludes the proof. □

Lemma 3.22. *Let G and M satisfy the assumptions of Lemma 3.14. If an induced triangulation G' is such that $\overline{M} \cap V(G')$ is an independent set, then G' is isomorphic to one of the splitting structures depicted in Figure 3.20.*

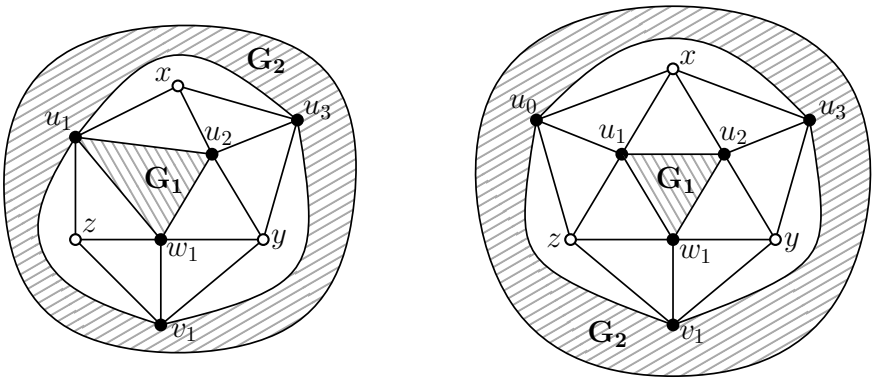

Figure 3.20: The two possible configurations of a graph G if $G[\overline{M}]$ is an independent set. G_1 and G_2 are triangulations. All other triangles of the drawings are facial.

Proof. Let G satisfy the assumptions of the lemma.

Claim 1. There exists a vertex $u \in M$ with only two neighbors in $\overline{M}$.

Proof. Suppose by way of contradiction that every vertex in M with non-monitored neighbors has exactly three neighbors in $\overline{M}$. Note first that no two vertices in M have exactly two common neighbors in $\overline{M}$, or they would be contradicting vertices.

Suppose first that all vertices in M with a common neighbor in $\overline{M}$ have exactly one such common neighbor. We define an auxiliary graph H as follows: the vertices of H are the vertices in $\overline{M}$, and two vertices in H are adjacent if they have a common neighbor in G. Observe that from a planar drawing of G, we can easily build a planar drawing of H: we keep the position of the vertices, and for each edge (uv) in H, u and v have a common neighbor x in G and we can have the edge (uv) follow closely the edges (ux) and (xv) (that would not create crossings since $N_G(x) \cap \overline{M} = 3$). By our assumption that no two vertices in M have more than one common neighbor in $\overline{M}$, the degree of a vertex in H is precisely twice its degree in G. Since every vertex in $\overline{M}$ has degree at least 3 and every vertex in M has three neighbors in $\overline{M}$, that implies H has minimum degree at least 6. But this contradicts Euler's formula for planar graphs.

So there are at least two vertices u and v in M with three common neighbors in $\overline{M}$, say x_1, x_2 and x_3 forming an induced $K_{2,3}$. Consider such an induced $K_{2,3}$ such that the subgraph G' induced by the vertices within its outer face does not contain the same structure. Denote x_1 and x_3 the vertices of the outer face. Since x_1, x_2 and x_3 are pairwise non adjacent, there is another neighbor w of x_2 in M, which has at least two other neighbors in $\overline{M}$. By minimality of the selected $K_{2,3}$, now all vertices in G' that belong to M and share a neighbor in $\overline{M}$ do share exactly one. Building the

graph H on G' the same way as above, we get a planar graph H where every vertex has degree at least six except for x_1, x_2 and x_3 that have respectively degree at least 2, 4 and 2. Therefore, we get that the sum of the degrees of the vertices in H is at least $6|V(H)| - 10$, again a contradiction with Euler's formula. This concludes the proof. (□)

Claim 2. If a vertex u of M has degree 2 in $\overline{M}$, then all the vertices of M sharing a neighbor in $\overline{M}$ with u also have degree 2 in $\overline{M}$.

Proof. Let u_1 be a vertex of M with two neighbors v_1, v_2 in $\overline{M}$. Suppose that there exists a vertex u_2 in M adjacent to v_1 or v_2 (say v_1) and with degree 3 in $\overline{M}$. If u_2 is not adjacent to v_2, then u_2 is a contradicting vertex. So assume u_2 is also adjacent to v_2 and let v_3 be the third neighbor of u_2 in $\overline{M}$. Applying Lemma 3.17 to vertex u_1, let t be a vertex adjacent to only one of v_1 and v_2, say v_1, and such that $[u_1v_1t]$ is facial. There is another vertex adjacent to t in $\overline{M}$. If this vertex is not v_3, then t is a contradicting vertex (as u_1 propagates to v_2 then u_2 to v_3). So t has only two neighbors in $\overline{M}$, v_1 and v_3.

Now, every other vertex in the graph is separated from v_1, v_2 or v_3 by one of the three separating cycles $(u_1v_1u_2v_2)$, $(tv_1u_2v_3)$ and $(tu_1v_2u_2v_3)$. The monitored vertex u_2 necessarily has more neighbors (by Observation 3.16(iii)). Suppose there is a neighbor of u_2 in the cycle $(tu_1v_2u_2v_3)$. Then there is a neighbor w to u_2 and v_2 forming a face $[u_2v_2w]$. If w is not adjacent to v_3, then w has some extra neighbors in $\overline{M}$, and is a contradicting vertex (u_1 propagates to v_1 then u_2 to v_3). If w is also adjacent to v_3, by Lemma 3.17 it has a neighbor adjacent to only one of v_2 and v_3, also separated from v_1 by the cycle $(tu_1v_2u_2v_3)$, and the same argument applies. The same arguments apply also if u_2 has neighbors in the other separating cycles. Thus there is no vertex adjacent to v_1 or v_2 with degree 3 in $\overline{M}$. This concludes the proof. (□)

Let u_1 be a vertex with exactly two neighbors in $\overline{M}$, denoted x and z. By Lemma 3.17, there is a neighbor of u_1 adjacent to only one of x and z, say u_2 is adjacent to x but not z (and $[xu_1u_2]$ is facial). By Claim 2, u_2 has only one other neighbor in $\overline{M}$, denote it y. Note that we now have the property **(P)** : any neighbor $v \in M$ of x, y or z has at least two neighbors in $\{x, y, z\}$ and is not adjacent to any vertex of $\overline{M} \setminus \{x, y, z\}$. Otherwise v would be a contradicting vertex. Consider the two paths from u_2 to z that partition $N(u_1)$. Let w_1 be the last vertex before z in the path that does not go through x. Since u_2 is not adjacent to z, then $w_1 \neq u_2$. By the above property (P), w_1 is adjacent to y. Moreover, y may not have a neighbor separated from x and z by $(u_1u_2yw_1)$, so $[u_2w_1y]$ is a facial triangle.

Suppose first that x is of degree three, and let u_3 denote its third neighbor, adjacent to both u_1 and u_2. It has one other neighbor among y and z, say y. Observe that $[u_2u_3y]$ is necessarily a facial triangle, and that by Claim 2, u_3 is not adjacent to z. Since z is of degree at least 3, it has a neighbor $v_1 \neq u_3$ such that $[u_1v_1z]$ is facial. By property (P), v_1 is adjacent to y. Now z has no other neighbor within the cycle (v_1yw_1z), or it would be a common neighbor to y and z, but applying Lemma 3.17 would lead to a contradiction. So w_1 is adjacent to v_1, and $[v_1w_1y]$ and $[v_1w_1z]$ are facial triangles. In addition, y cannot have a neighbor separated from x and z by $(u_1u_3yv_1)$ so $[u_3v_1y]$ is a facial triangle. Thus we are in the first configuration of

Figure 3.20.

Assume now that each of x, y and z have degree at least 4. Let u_3 form a facial triangle with x and u_2. If u_3 is adjacent to z, then the fourth neighbor of x is also adjacent to z. By Lemma 3.17, it has a neighbor adjacent to only one of x and z, which is separated from y by $(u_1 x u_3 z)$, a contradiction. So u_3 is adjacent to y forming a facial triangle $[u_2 u_3 x]$. By the same argument, we infer the existence of u_0 and v_1, common neighbors of x and z and of y and z respectively, and that the corresponding triangle are facial. If x was of degree 5, then we would get similarly a contradiction applying Lemma 3.17 on u_3 or u_0. By the same reasoning on y and z, we obtain the second configuration of Figure 3.20, which concludes the proof of Lemma 3.22. □

The results from the four Lemmas 3.19, 3.20, 3.21 and 3.22 conclude the section: after Algorithm 3.2, each induced triangulation of G is isomorphic to one of the graphs depicted in Figure 3.16.

3.2 Power domination in triangular grids

We now turn to another class of graphs, namely triangular grid graphs. A *triangular grid* T_k has vertex set $V(T_k) = \{(x, y, z) \mid x, y, z \in [0..2k-2], x - y + z = k - 1\}$. Two vertices (x, y, z) and (x', y', z') are adjacent if and only if $|x'-x|+|y'-y|+|z'-z| = 2$. A triangular grid T_k has a regular hexagonal shape, and k is the number of vertices on each edge of the hexagon. Figure 3.21 shows the two triangular grids T_2 and T_3. Note that T_k appears as a subgraph of T_{k+1} (where $(1, 1, 1)$ has been added to the coordinates of each vertex in T_k).

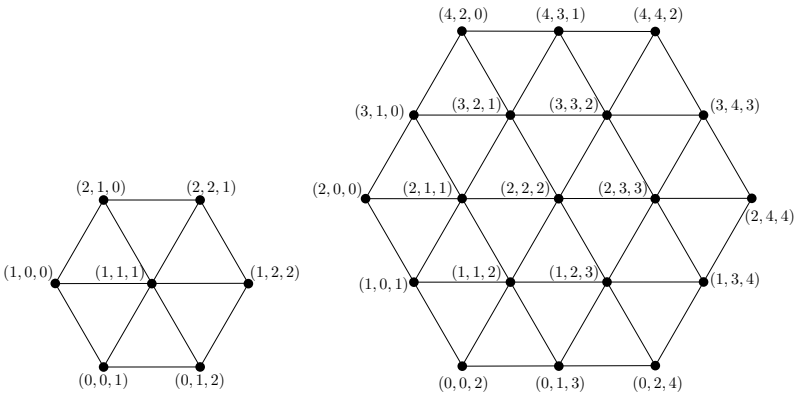

Figure 3.21: The graphs T_2 and T_3.

An inner vertex v with coordinates (x, y, z) has 6 neighbors with the following coordinates: $(x, y + 1, z + 1)$, $(x - 1, y, z + 1)$, $(x - 1, y - 1, z)$, $(x, y - 1, z - 1)$, $(x + 1, y, z - 1)$ and $(x + 1, y + 1, z)$ (see Figure 3.22a). The coordinates of a vertex v are denoted by (v_1, v_2, v_3). The *line* $l_{v_j=i}$ is the set of vertices $\{(v_1, v_2, v_3) \mid v_j = i\}$ (see Figure 3.22b).

One interesting property of the triangular grids is that if an equilateral triangle having one side of the hexagonal border as base is monitored, then the border allows

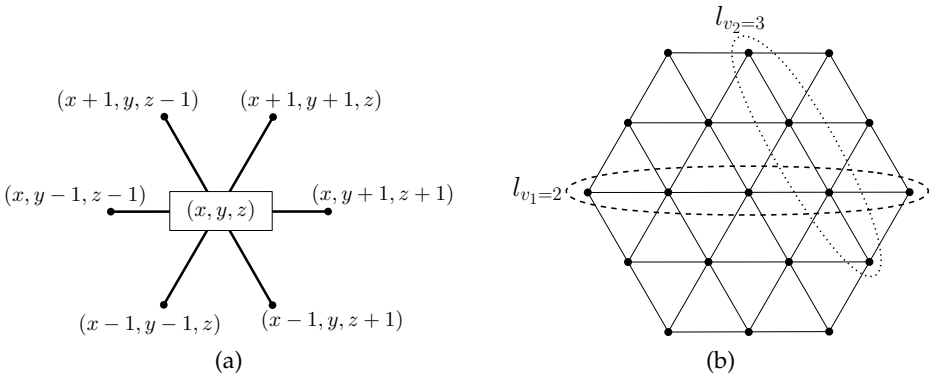

Figure 3.22: (a) The coordinates of the neighbors around an inner vertex $v = (x, y, z)$. (b) The lines $l_{v_1=2}$ and $l_{v_2=3}$ in T_3.

the propagation until the whole graph is monitored. For example, it suffices to monitor the set $\mathcal{T} = \{v = (v_1, v_2, v_3) \in V(G) \mid 0 \leq v_1, v_2 \leq k-1, k-1 \leq v_3 \leq 2k-2\}$ to monitor T_k (see Figure 3.23).

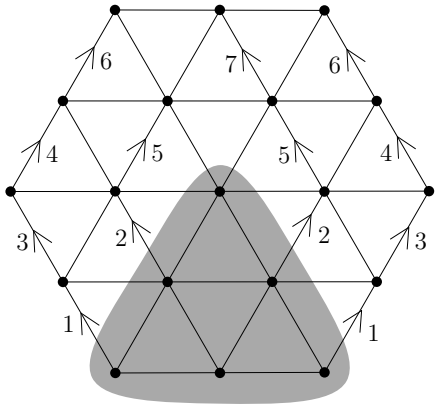

Figure 3.23: The propagation steps to monitor T_3 once the set $\mathcal{T}$ (in the gray area) is monitored. Propagation steps with the same number can be done in parallel.

We assume throughout the section that $k \geq 4$: observe that if $k \leq 3$, then $\gamma_P(T_k) = 1$, with $S = \{(k-2, k-2, k-1)\}$ (for $k = 2, 3$).

We prove the following theorem:

Theorem 3.23. *For $k \in \mathbb{N}^*$, $\gamma_P(T_k) = \lceil \frac{k}{3} \rceil$.*

3.2.1 Upper bound

We begin by giving a construction for the upper bound:

Lemma 3.24. *For $k \in \mathbb{N}^*$, $\gamma_P(T_k) \leq \lceil \frac{k}{3} \rceil$.*

Proof. Let $i = \lfloor \frac{k}{3} \rfloor$, and $d = k-i-1$ if $k \equiv 0, 1 \mod 3$, $d = k-i-2$ otherwise. Let S' be the following set of vertices (see Figure 3.24): $S' = \{(1+3\ell, d+\ell, k+d-2-2\ell), 0 \leq \ell \leq i-1\}$. In other words, S' contains the vertex $v = (1, d, k+d-2)$ and vertices whose coordinates are obtained by adding $(3, 1, -2)$ up to i times to the coordinates of v. If $k \not\equiv 0 \mod 3$, $S = S' \cup \{(k-1, k-1, k-1)\}$. Otherwise, $S = S'$. Then we have, depending on the value of k modulo 3:

- $k = 3i$: $|S| = i = \lceil \frac{3i}{3} \rceil$.
- $k = 3i+1$: $|S| = i+1 = \lceil \frac{3i+1}{3} \rceil$.
- $k = 3i+2$: $|S| = i+1 = \lceil \frac{3i+2}{3} \rceil$.

In each case, S is a set with cardinality $\lceil \frac{k}{3} \rceil$, and S progressively power dominates the set $\mathcal{T}$ (see Figure 3.24), and thus the whole triangular grid T_k. □

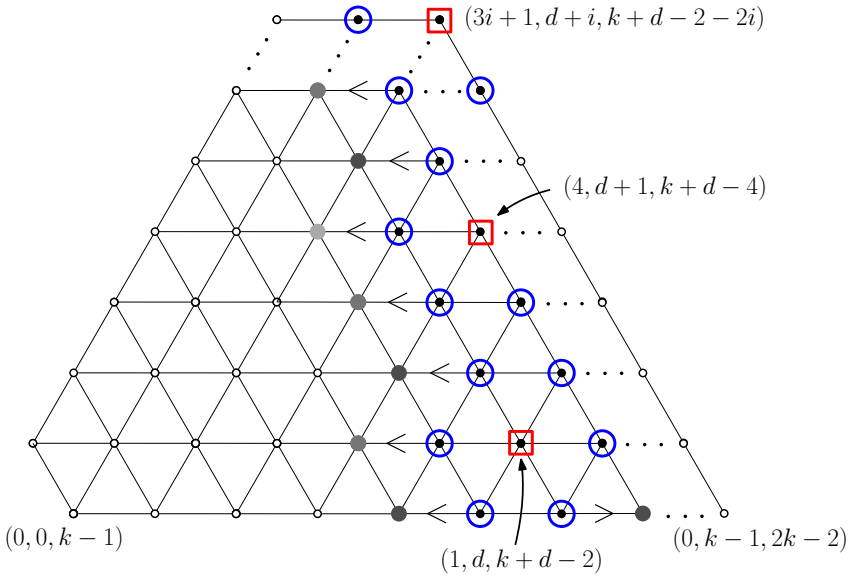

Figure 3.24: Construction and propagation of the set S': $d = k-i-1$ if $k \equiv 0, 1 \mod 3$, $d = k-i-2$ if $k \equiv 2 \mod 3$. Red square-framed vertices are in S', blue circle-framed vertices are in $N[S]$. Dark gray vertices are monitored in the first propagation round, gray ones in the second round, and the light gray one in the third round. Observe how the pattern of monitored vertices repeats.

3.2.2 Lower bound

Let $A \subset V(T_k)$ be a set of vertices of the graph. We call $\mathcal{B}_A \subseteq A$ the *border* of A defined as follows: $\mathcal{B}_A = \{v \in A, N(v) \setminus A \neq \emptyset\}$. Let $A_{v_j=i}$ denote the set of vertices

of A in a given line $l_{v_j=i}$. We define the *j-shifted set* $A' = A^{(j)}$ of A as follows (see Figure 3.25): $|A'| = |A|$, and for each line $l_{v_j=i}$, A' contains the $|A_{v_j=i}|$ vertices with smallest coordinates v_{j+1} (for example, the 1-shifted set of A contains only left-most vertices on each horizontal line). More formally,

$$A'_{v_j=i} = \{(v_1, v_2, v_3) \mid v_j = i, v_{j+1} = \begin{cases} \ell & 0 \leq i \leq k-1 \\ \ell + i - (k-1) & k \leq i \leq 2k-2 \end{cases}, 0 \leq \ell < |A_{v_j=i}|\}.$$

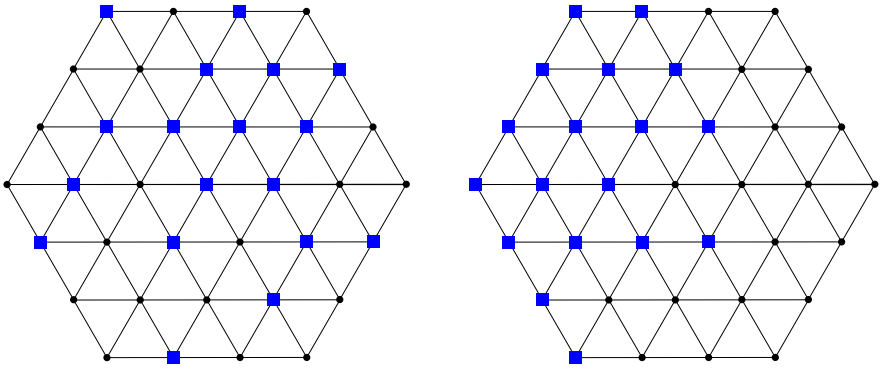

Figure 3.25: (Left) Blue-square vertices are in the set A. (Right) Blue-square vertices are in the 1-shifted set A' of A: the left-most vertices of each line $l_{v_1=i}$ are in A'.

Lemma 3.25. *Let A' be the j-shifted set of A. Then $|\mathcal{B}_{A'}| \leq |\mathcal{B}_A|$.*

Proof. In this proof, since j is fixed, we simplify the notation $l_{v_j=i}$ into l_i. Let a_i be the number of vertices in A (and in A') in line l_i and b_i (resp. b'_i) be the number of vertices in $\mathcal{B}_A$ (resp. $\mathcal{B}_{A'}$) in line l_i. We show that $b_i \geq b'_i$ for every line l_i, $0 \leq i \leq 2k-2$. We consider three cases depending on the value of i (when $0 \leq i < k-1$, when $i = k-1$ and when $k \leq i \leq 2k-2$):

- $0 \leq i < k-1$: we thus have $|l_{i+1}| = |l_i| + 1$ and $|l_i| = |l_{i-1}| + 1$. Let us consider vertices in line l_i which are in A but not in the border of A: there are $a_i - b_i$ such vertices. By definition, we have $a_i - b_i \leq a_i$. Their neighbors (if they exist) in l_{i-1} and l_{i+1} are in A. We have thus $a_{i+1} \geq (a_i - b_i) + 1$, and $a_{i-1} \geq a_i - b_i$. Hence $a_i - b_i \leq \min\{a_{i+1} - 1, a_{i-1}, a_i\}$ for $1 \leq i < k-1$ (for $i = 0$, we have $a_i - b_i \leq \min\{a_{i+1} - 1, a_i\}$). We can do the same reasoning on the vertices which are in A' but not in the border of A': we get that $a_i - b'_i = \min\{a_{i+1} - 1, a_{i-1}, a_i\}$ (for $i = 0$, we have $a_i - b'_i = \min\{a_{i+1} - 1, a_i\}$). Then $a_i - b_i \leq a_i - b'_i$, and thus $b_i \geq b'_i$.
- We have a similar proof when $k-1 < i \leq 2k-2$, for which we have $|l_{i+1}| = |l_i| - 1$ and $|l_i| = |l_{i-1}| - 1$: in that case, we get $a_i - b'_i = \min\{a_{i-1} - 1, a_{i+1}, a_i\} \geq a_i - b_i$.
- $i = k-1$: we thus have $|l_{i+1}| = |l_{i-1}| = |l_i| + 1$. As for the previous case, first consider vertices which are in A but not in the border of A: by definition $a_i - b_i \leq a_i$, and we have $a_{i+1} \geq a_i - b_i$ and $a_{i-1} \geq a_i - b_i$. Thus $a_i - b_i \leq$

$\min\{a_{i+1}, a_{i-1}, a_i\}$. Similarly, we get that $a_i - b'_i = \min\{a_{i+1}, a_{i-1}, a_i\}$. Thus $a_i - b_i \leq a_i - b'_i$, and so $b_i \geq b'_i$. □

We define the *shifting process* of a set $A \subset V(T_k)$ as the following iterative process: $A_{\ell+1} = ((A_\ell^{(1)})^{(2)})^{(3)}$, with $A_0 = A$. In fact, 1-shift, 2-shift and 3-shift are successively applied to the set A until a fixed point A_{ℓ^*} is reached. We show that this fixed point exists and that the vertices of the resulting set form a particular shape:

Lemma 3.26. (i) *This shifting process stops, i.e. there exists ℓ^* such that $A_{\ell^*+1} = A_{\ell^*}$.*

(ii) *Let $A^* = A_{\ell^*}$. If $v = (x, y, z) \in A^*$, then all vertices $v' = (x', y', z')$ with $y' \leq y$ and $z' \leq z$ are also in A^* (see Figure 3.26).*

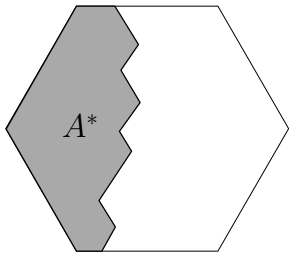

Figure 3.26: The set A^* has a staircase shape.

Proof. (i) We define the *weight* in A of a vertex as follows: $w_A(v) = v_1 + 2v_2 + 2v_3$ if $w \in A$, $w_A(v) = 0$ otherwise. Similarly, the weight of a set S relatively to A is $w_A(S) = \sum_{v \in S} w(v)$. For simplicity, we denote by w_A the *global weight* of the set A: $w_A = w_A(T_k)$.

Let A' be the j-shifted set of A. We show that if $A' \neq A$, then $w_{A'} < w_A$.

Recall that for every vertex $v = (v_1, v_2, v_3)$ of T_k, $v_1 - v_2 + v_3 = k - 1$. We first show that if v and v' are two vertices with $v_j(v') = v_j(v)$ and $v_{j+1}(v') < v_{j+1}(v)$, then $w(v') < w(v)$:

- $j = 1$: $v_1(v') = v_1(v)$ and $v_2(v') < v_2(v)$, so $v_3(v') = k - 1 - v_1(v') + v_2(v') = k - 1 - v_1(v) + v_2(v') < v_3(v)$. Thus $w(v') < w(v)$.
- $j = 2$: $v_2(v') = v_2(v)$ and $v_3(v') < v_3(v)$. Since $v_1(v) - v_2(v) + v_3(v) = v_1(v') - v_2(v') + v_3(v')$, we get $v_1(v) + v_3(v) = v_1(v') + v_3(v')$. Thus $w(v) - w(v') = v_1(v) + 2v_2(v) + 2v_3(v) - v_1(v') - 2v_2(v') - 2v_3(v') = v_3(v) - v_3(v')$. So $w(v') < w(v)$.
- $j = 3$: $v_3(v') = v_3(v)$ and $v_1(v') < v_1(v)$, so $v_2(v') = v_1(v') + v_3(v') - k + 1 = v_1(v') + v_3(v) - k + 1 \leq v_2(v)$. Thus $w(v') < w(v)$.

By definition on a j-shifted set, for each line $l_{v_j=i}$,

$$w'_A(l_{v_j=i}) - w_A(l_{v_j=i}) = \sum_{v' \in A' \setminus A} w(v') - \sum_{v' \in A \setminus A'} w(v)\,,$$

and either $A_{v_j=i} = A'_{v_j=i}$, and this sums to 0, or $A_{v_j=i} \neq A'_{v_j=i}$, and it is strictly negative. Therefore $A' \neq A$ implies $w_{A'} < w_A$. Since w_A is positive, this directly concludes the proof of item (i).

(ii) Let $v = (v_1, v_2, v_3)$ be a vertex in A^*. The vertices $u_1 = (v_1 + 1, v_2, v_3 - 1)$, $u_2 = (v_1, v_2 - 1, v_3 - 1)$ and $u_3 = (v_1 - 1, v_2 - 1, v_3)$ (i.e. the north-west, west and south-west neighbors of v) are also in A^*: otherwise, we could again shift the set A^* and get the set $A^* - \{v\} + \{u_i\}$, which has less weight than A^*, a contradiction. Since this is true for every vertex of A^*, the proposition holds. □

We can now prove the lower bound:

Lemma 3.27. *For $k \in \mathbb{N}^*$, $\gamma_P(T_k) \geq \dfrac{2k-1}{6}$.*

Proof. Let S be a power dominating set of T_k. If $|S| > \frac{k}{3}$, then the result holds. Thus we assume $|S| \leq \lceil \frac{k}{3} \rceil$. In power domination, propagation from a set S is done by rounds. We decide of an arbitrary order on the vertices monitored by S during each round. This defines a (non-unique) total order $m_1, \ldots, m_{|V(G)\setminus N[S]|}$ on the vertices of $V(G) \setminus N[S]$. We then define the set $M[t]$ as follows: $M[0] = N[S]$, and $M[t+1] = M[t] \cup \{m_{t+1}\}$.

The key idea of this proof is to consider the size of the sets $\mathcal{B}_{M[t]}$, to bound it and to deduce a bound on $|S|$. It is a classical way to prove lower bounds for power domination in regular lattices (see for example the lower bound proof on strong products [DMKŠ08]). However, on the contrary to what happens in other cases, the size of the sets $\mathcal{B}_{M[t]}$ is not globally bounded from below: at the end of the propagation, no vertices belong to the border of the monitored set. We thus "stop" the propagation in the middle of the process and reason from there.

Claim 1. For any $0 \leq i \leq |V(G) \setminus N[S]|$, we have $|\mathcal{B}_{M[i]}| \leq 6|S|$.

Proof. We prove it by induction on i: $|\mathcal{B}_{M[0]}| = |\mathcal{B}_{N[S]}| \leq 6|S|$ by definition. If the vertex m_{i+1} becomes monitored by propagation from a vertex v, then v is not in $\mathcal{B}_{M[i+1]}$, and at most one vertex (m_{i+1}) is added to $\mathcal{B}_{M[i+1]}$. Thus $|\mathcal{B}_{M[i+1]}| \leq |\mathcal{B}_{M[i]}|$. Using the induction hypothesis, we conclude that $|\mathcal{B}_{M[i+1]}| \leq 6|S|$. (□)

Let M be the set $M[t]$ containing $\frac{|V(T_k|}{2}$ vertices (as soon as $k \geq 3$, we get $\frac{|V(T_k|}{2} = \frac{3k^2-3k+1}{2} \geq \frac{7(k+1)}{3} \geq 7|S| \geq |M[0]|$, and so M exists), and let M^* be the set defined from M by Lemma 3.26(i).

Claim 2. We have $2k - 1 \leq |\mathcal{B}_{M^*}|$.

Proof. We now prove that for every index $0 \leq i \leq 2k-2$, the line $l_{v_1=i}$ contains at least one vertex of $\mathcal{B}_{M^*}$.

Suppose there exists an index $0 \leq i \leq 2k-2$ such that all vertices of the line $l_{v_1=i}$ are in M^*. If $0 \leq i \leq k-1$, then the vertex $w = (i, k+i-1, 2k-2)$ (i.e. the right-most vertex of the line $l_{v_1=i}$) is in M^*, and so by Lemma 3.26(ii), all vertices of the set $\{(v_1, v_2, v_3) \mid v_2 \leq k+i-1\}$ are also in M^* (see Figure 3.27a). Since $k+i-1 > k-1$, then strictly more than half of the vertices of T_k are in M^*, and so M^* has strictly more than the required number of vertices, a contradiction. Similarly, if $k-1 < i \leq 2k-2$: the vertex $w = (i, 2k-2, 3k-3-i)$ (i.e. the right-most vertex of the line $l_{v_1=i}$) is in M^*, and thus by Lemma 3.26(ii), all vertices of the set $\{(v_1, v_2, v_3) \mid v_3 \leq 3k-3-i\}$ are also in M^*. Since $3k-3-i > k-1$, then strictly

more than half of the vertices of T_k are in M^*, a contradiction. Thus every line $l_{v_1=i}$ contains at least one vertex not in M^*.

Suppose now that one of the lines $l_{v_1=i}$ contains no vertex of M^*. If $0 \leq i \leq k-1$ (see Figure 3.27b), then the vertex $w = (i, 0, k-1-i)$ (i.e. the left-most vertex of the line $l_{v_1=i}$) is not in M^*. By the contrapositive of Lemma 3.26(ii), the line $l_{v_3=k-1-i}$ also contains no vertices of M^*, and so all vertices of M^* are included in the set $\{(v_1, v_2, v_3) \mid v_3 < k-1-i\}$ (they are all on the left and above line $l_{v_3=k-1-i}$). Thus M^* contains strictly less than the half of the vertices of T_k, a contradiction. Similarly, if $k-1 < i \leq 2k-2$, then the vertex $w = (i, i-k+1, 0)$ is not in M^*. By the contrapositive of Lemma 3.26(ii), the line $l_{v_2=i-k+1}$ also contains no vertices of M^*, and so all vertices of M^* are included in the set $\{(v_1, v_2, v_3) \mid v_2 < i-k+1\}$ (they are all on the left and below line $l_{v_2=i-k+1}$). Since in that case $i-k+1 < k-1$, then again, $|M^*| = |M| < \frac{|V(T_k)|}{2}$ vertices, a contradiction.

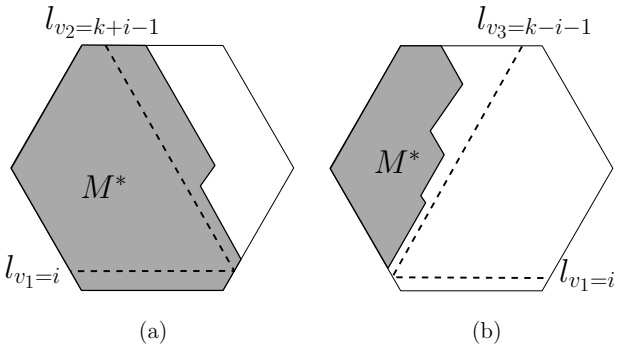

Figure 3.27: (a) If all vertices of a line $l_{v_1=i}$ are in M^* ($0 \leq i \leq k-1$), then all vertices of T_k with $v_2 \leq k+i-1$ are also in M^*. (b) If the line $l_{v_1=i}$ contains no vertices of M^* ($1 \leq i \leq k-1$), then all vertices of M are above and left of line $l_{v_3=k-i-1}$.

We thus get that each line $l_{v_1=i}$ contains at least one vertex of M^* and not all its vertices are in M^*. Thus each line contains at least one vertex of $\mathcal{B}_{M^*}$, and so $2k-1 \leq |\mathcal{B}_{M^*}|$. (□)

By Lemma 3.25, $|\mathcal{B}_{M^*}| \leq |\mathcal{B}_M|$, hence $2k-1 \leq |\mathcal{B}_M|$. Using Claim 1, we get $2k-1 \leq |\mathcal{B}_M| \leq 6|S|$, and so $|S| \geq \dfrac{2k-1}{6}$, which concludes the proof. □

We know that $\gamma_P(T_k)$ is an integer. Since there is no integer between $\frac{2k-1}{6} = \frac{k}{3} - \frac{1}{6}$ and $\lceil \frac{k}{3} \rceil$, then Lemma 3.27 directly implies that $\lceil \frac{k}{3} \rceil \leq \gamma_P(T_k)$.

This then gives our global result:

$$\gamma_P(T_k) = \lceil \frac{k}{3} \rceil \quad ,$$

concluding the proof of Theorem 3.23.

3.3 Conclusion and outlook

In this chapter, we computed bounds for power domination on two different classes of planar graphs: maximal planar graphs, and triangular grids. After exhibiting a family of graphs whose power domination number is at least $\frac{n}{6}$, we proved that any maximal planar graph with n vertices admits a power dominating set of size at most $\frac{n-2}{4}$. Doing so, we proposed a constructive algorithm in three steps computing such a set.

The most interesting question raised by our study is to determine the tight upper bound for the power domination number of maximal planar graphs, i.e. to refine the bound of ε such that for every maximal planar graph G, $\gamma_P(G) \leq \varepsilon n$. We showed in this chapter that $\varepsilon \leq \frac{1}{4}$, and the construction presented in Figure 3.17 proves that $\frac{1}{6} \leq \varepsilon$. However, we also know that there exists graphs with power domination number strictly larger than $\frac{1}{6}$: for example, the triakis octahedron shown in Figure 3.9 has 10 vertices and its power domination number equals two. The question of the value of ε remains thus open.

One can also remark that if the input triangulation G is 4-connected, then Algorithm 3.2 is the only one to apply: G would then contain no special structures, and all splitting structures appearing also have separating triangles. It may thus be interesting to see if the power domination number of 4-connected graphs is at most $\frac{n}{5}$ or even $\frac{n}{6}$.

We carried on with the study of power domination in regular lattices, and examined the value of $\gamma_P(G)$ when G is a triangular grid with hexagonal-shaped border. We showed that $\gamma_P(G) = \lceil \frac{k}{3} \rceil$.

The process of propagation in power domination led to the development of the concept of propagation radius, i.e. the number of propagation steps necessary in order to monitor the whole graph [DK14]. It would be interesting to study the propagation radius of our constructions (in particular in the case of triangular grids) and to try and find a power dominating set minimizing this radius.

It seems that the border plays an important role in the propagation when the grid has an hexagonal shape, and so the next step in the understanding of power domination in triangular grids would be to look into grids with non-hexagonal shape. For example, what is the power domination number of a triangular grid with triangular border?

Finally, the relation of our results with the ones presented for hexagonal grids by Ferrero et al. [FVV11] has to be noted: they show (with techniques different from the ones used in this chapter) that $\gamma_P(H_n) = \lceil \frac{2n}{3} \rceil$, where n is the dimension of the hexagonal grid H_n, and so $\gamma_P(H_n) \geq \gamma_P(T_{2n})$. Moreover, it is interesting to remark that H_n is an induced subgraph of T_{2n}. We already know [DVV16] that in general, the power domination number of an induced subgraph can be either smaller or arbitrarily large compared to the power domination number of the whole graph. It would then be very interesting to investigate further under which conditions induced subgraphs have the same power dominating number as the whole graph.

4

Planar Eulerian orientations

In this chapter, we focus on the enumeration of *planar Eulerian orientations*, i.e. orientations of Eulerian planar maps, and we count them by their number n of edges [1] (see Figure 4.1). From now on, every map is considered planar and rooted, and these precisions are often omitted. As opposed to the previous chapters, the maps may contain loops and multiple edges. An introduction to (or reminder of) the notions of combinatorics used throughout this chapter is given in Section 1.2.

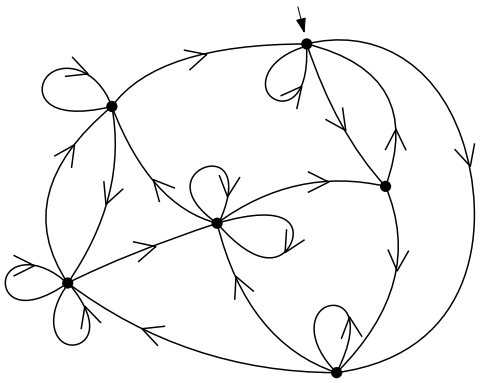

Figure 4.1: A Eulerian orientation with 6 vertices and 19 edges. The arrow indicates the root corner of the map.

Eulerian orientations are specific orientations of Eulerian maps, namely those in which every vertex as equal in- and out-degree (Figure 4.2). *Eulerian maps*, i.e. maps with even degree at each vertex, are well-known combinatorial objects with rich combinatorial connections to other classes. They have been much studied since the work of Tutte in 1963, in which the number of rooted bicubic maps (which are in bijection with Eulerian maps [2]) is crucial to obtain the number of general rooted planar maps. In particular, the number m_n of rooted planar Eulerian maps with n edges is

[1] Beware! In this chapter, n denotes the number of edges of the objects, and not their number of vertices as in the previous chapters.

[2] See e.g. [BMS00, Cor. 2.4] for the dual bijection between face-bicolored triangulations and bipartite maps.

$$m_n = \frac{3 \cdot 2^{n-1}}{(n+1)(n+2)} \binom{2n}{n}. \tag{4.1}$$

The associated generating function $M(t) = \sum_{n \geq 0} m_n t^n$ is known to be algebraic, and its functional equation is

$$t^2 + 11t - 1 - (8t^2 + 12t - 1)M(t) + 16t^2 M(t)^2 = 0.$$

Eulerian maps are equinumerous with several other families of objects (like certain trees [BMS00] and permutations [Bón97; Fus12]), and often related to them by beautiful bijections.

Clearly, a map needs to be Eulerian to admit an Eulerian orientation, and this condition is also sufficient (one can compute an Eulerian cycle of the map, and orient the edges along the cycle).

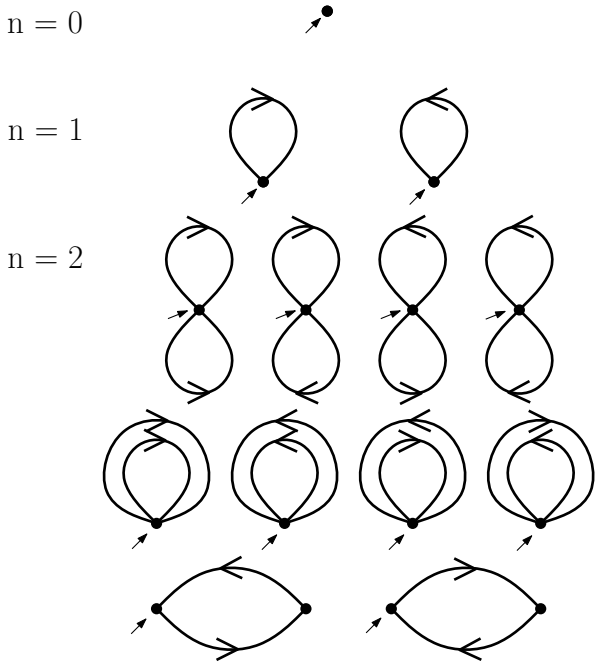

Figure 4.2: The Eulerian orientations with at most two edges.

The enumeration of planar maps has received a lot of attention since the sixties and the seminal work of Tutte in its series of "Census" papers [Tut62a; Tut62b; Tut62c; Tut63a], followed by its major paper on the topic [Tut68]. Two main approaches are used to count maps (and in particular planar maps): the recursive method, successfully used by Tutte, tries to translate a possible recursive construction of the class into a functional equation for the generating function, which one can later try to solve. The second possibility is to look for bijections with other sets of objects for which the enumeration has already been done. Lots of bijections relate maps with specific sets of trees [BDFG02a; BDFG04; CS04; CV81; Sch97] and explain their algebraicity properties.

Beyond their enumerative implications, bijections involving planar maps have many applications, and among them compact coding, generation of random structures and drawing (see for example [BGH05; CADS08; Fus09; PS06]). Random planar maps are particularly of interest to theoretical physicists, since they are considered as a model of random surfaces for two-dimensional quantum gravity [DFGZJ95]. Bijective methods have recently played a key role in proving that they admit a universal scaling limit known as the *Brownian map* [LG13].

Planar maps equipped with an additional structure (e.g. a spanning tree [Mul67], a proper colouring [BBM11; BDFG02b; Tut73; Tut84], a special orientation of the edges ...) are also much studied, including in statistical physics, where the structure can represent particles or spins for example. One of the solved examples consists of maps (in fact, triangulations) equipped with *Schnyder orientations*, derived from the construction of the Schnyder wood of the map [Sch89] [3]. The results obtained there have analogies with those obtained for another class of orientations, called *bipolar*, which are directed acyclic maps with exactly one source and one sink, both on the outer face. Indeed, for both classes of oriented maps:

- they are counted by simple numbers, which are also known to count other combinatorial objects (various lattice paths and permutations, among others);
- there exist nice bijections explaining these equi-enumeration results [Bon05; BBMF08; FFNO11; FPS09];
- for a given map M, the set of Schnyder/bipolar orientations of M has a lattice structure [Fel04; Men94; Pro]. The above bijections, once specialized to maps equipped with their (unique) minimal orientation, coincide with attractive bijections designed for unoriented maps [BB09; BBMF08];
- specializing the bijections further to maps that have only one Schnyder/bipolar orientation also yields interesting combinatorial results [BB09; BBMF08].

One similarity between the sets of Schnyder/bipolar orientations and the set of Eulerian orientations of a given planar map is that the latter can also be equipped with a lattice structure [Fel04; Pro], for which the basic operation consists in reversing the orientation of a clockwise circuit. It then seems interesting to study Eulerian orientations and see if they also have such nice properties.

Our first goal is to compute sufficiently many terms of the sequence (o_n) giving the number of Eulerian orientations with respect to their number of edges. In Section 4.1, we present a simple recursive decomposition of (rooted) Eulerian orientations, based on the contraction of the root edge, and then a variant of this decomposition, which we call *prime decomposition*. Thanks to this variant, we can compute the values o_n for $n \leq 15$ (Figure 4.3), which do not match cardinalities of other sets of combinatorial objects [4].

However, finding a simple formula for the generating function of the Eulerian orientations appears to be a difficult problem. In fact, we even lack an efficient way to compute the corresponding numbers (say, in polynomial time). This leads us to resort to approximation methods that are often used when studying hard counting

[3] For more details on Schnyder woods, see Section 2.1.2

[4] to our present knowledge

n	o_n	n	o_n	n	o_n
0	1	6	37 548	12	37 003 723 200
1	2	7	350 090	13	393 856 445 664
2	10	8	3 380 520	14	4 240 313 009 272
3	66	9	33 558 024	15	46 109 094 112 170
4	504	10	340 670 720		
5	4 216	11	3 522 993 656		

Figure 4.3: First values of o_n, for n from 0 to 15 (entry A277493 of the OEIS [OEI]).

problems, like the widely studied enumeration of self-avoiding walks [AJ90; FS59; GJ09; PT00] (which are sequences of moves on a lattice without visiting the same point twice), or polyominoes [BMRR06; Jen03; KR73].

We adopt the following approach in Sections 4.2 to 4.5: denoting by $\mathcal{O}$ the set of Eulerian orientations, we construct subsets and supersets of $\mathcal{O}$, indexed by an integer parameter k, which converge (monotonously) to $\mathcal{O}$ as k increases, and we count the elements of these sets. Those sets are respectively denoted by $\mathcal{L}^{(k)}$ (and $\mathbb{L}^{(k)}$), $\mathcal{U}^{(k)}$ (and $\mathbb{U}^{(k)}$), as they give *lower* and *upper* bounds on the numbers o_n and their growth rate. Families $\mathcal{L}^{(k)}$ and $\mathbb{L}^{(k)}$ are built on the first recursive decomposition of planar Eulerian orientations, whereas families $\mathcal{U}^{(k)}$ and $\mathbb{U}^{(k)}$ use the prime decomposition. For each set, we give a system of functional equations defining its generating function.

One difference between our study and those dealing with tricky objects on regular lattices (like the above mentioned self-avoiding walks and polyominoes) is worth noting. The subsets and supersets that are defined to approximate lattice objects often have a one-dimensional structure and *rational generating functions* . But our subsets and supersets of orientations belong to the world of maps (or random lattices in the physics terminology), and have *algebraic generating functions*. More precisely, our subsets have a branching, tree-like structure, which yields a system of algebraic equations for their generating functions, and a universal asymptotic behaviour in $\lambda^n n^{-3/2}$ (for a growth rate λ depending on the index k). The generating functions of our supersets are more mysterious. They are bivariate series (i.e. series of two variables) given by systems of equations involving divided differences of the form

$$\frac{F(t;x) - F(t;1)}{x-1},$$

and we have to resort to a deep theorem in algebra, due to Popescu [Swa98], to prove their algebraicity for all k. We conjecture that their asymptotic behaviour is also universal, this time in $\lambda^n n^{-5/2}$, as for planar maps (again, for varying λ).

We solve our systems of equations explicitly for small values of k, and thus obtain Table 4.1. All calculations are supported by MAPLE sessions [5].

The results of this chapter are joint work with Nicolas Bonichon, Mireille Bousquet-Mélou and Paul Dorbec [BBMDP17].

[5] Available at http://www.labri.fr/perso/cpennaru/orientations-web.mw

Table 4.1: Growth rates and cardinalities of subsets ($\mathcal{L}^{(k)}$ and $\mathbb{L}^{(k)}$) and supersets ($\mathcal{U}^{(k)}$ and $\mathbb{U}^{(k)}$) of Eulerian orientations. The table also records the degrees of the associated generating functions, which are systematically algebraic. The symbol $\simeq$ refers to a numerical estimate. The other growth rates are algebraic numbers known exactly via their minimal polynomial.

	degree	growth	1	2	3	4	5	6	7
Eulerian maps	2	8	1	3	12	56	288	1 584	9 152
$\mathcal{L}^{(1)}$	2	$9.68\ldots$	**2**	**10**	**66**	466	3 458	26 650	211 458
$\mathcal{L}^{(2)}$	4	$10.16\ldots$	**2**	**10**	**66**	**504**	4 008	32 834	275 608
$\mathbb{L}^{(1)}$	3	$10.60\ldots$	**2**	**10**	**66**	490	3 898	32 482	279 882
$\mathbb{L}^{(2)}$	6	$10.97\ldots$	**2**	**10**	**66**	**504**	4 148	35 794	319 384
$\mathbb{L}^{(3)}$	20	$11.22\ldots$	**2**	**10**	**66**	**504**	**4 216**	37 172	339 406
$\mathbb{L}^{(4)}$	258	$\simeq 11.41$	**2**	**10**	**66**	**504**	**4 216**	**37 548**	347 850
$\mathbb{L}^{(5)}$	?	$\simeq 11.56$	**2**	**10**	**66**	**504**	**4 216**	**37 548**	**350 090**
Eulerian orientations		$\simeq$ **12.5**	**2**	**10**	**66**	**504**	**4 216**	**37 548**	**350 090**
$\mathbb{U}^{(5)}$	?	$\simeq 13.005$	**2**	**10**	**66**	**504**	**4 216**	**37 548**	**350 090**
$\mathbb{U}^{(4)}$	?	$\simeq 13.017$	**2**	**10**	**66**	**504**	**4 216**	**37 548**	350 538
$\mathbb{U}^{(3)}$	?	$\simeq 13.031$	**2**	**10**	**66**	**504**	**4 216**	37 620	352 242
$\mathbb{U}^{(2)}$	28	$13.047\ldots$	**2**	**10**	**66**	**504**	4 228	37 878	356 252
$\mathbb{U}^{(1)}$	3	$13.065\ldots$	**2**	**10**	**66**	506	4 266	38 418	363 194
$\mathcal{U}^{(2)}$	27	$13.057\ldots$	**2**	**10**	**66**	**504**	4 232	37 970	357 744
$\mathcal{U}^{(1)}$	3	$13.065\ldots$	**2**	**10**	**66**	506	4 266	38 418	363 194
Oriented Eulerian maps	2	16	**2**	12	96	896	9 216	101 376	1 171 456

4.1 Decomposition of Eulerian maps and orientations

In this section we recall the standard recursive decomposition of Eulerian maps based on the contraction of the root edge, which can be traced back to the early papers of Tutte (e.g. [Tut68]). We then adapt it to decompose Eulerian orientations. We also introduce a variant of the standard decomposition of Eulerian maps, based on a notion of *prime* maps, and adapt it again to Eulerian orientations. This variant is slightly more involved, but it allows us to compute the numbers o_n for larger values of n. Prime decomposition also leads to better lower and upper bounds on these numbers, as shown later in Sections 4.3 and 4.5.

4.1.1 Standard decomposition

The recursive decomposition for Eulerian maps is essentially the same as for planar maps (presented in details in Section 1.2.2). If the root edge of the Eulerian map is a loop, we delete it and obtain two orientations, which are both Eulerian (in any oriented map, the sum over all vertices of in-degrees equals the sum of out-degrees, hence one cannot have a single vertex with distinct in- and out-degrees); otherwise

we contract the root edge, which gives a smaller Eulerian map.

Consider an Eulerian map E, not reduced to the atomic map, and its root edge e. If e is a loop, then E is obtained from two smaller maps E_1 and E_2 by joining them at their root vertices and adding a loop around E_1 (Figure 4.4, left). The maps E_1 and E_2 are themselves Eulerian (because the sum of vertex degrees in a map is even, so that one cannot have a single odd vertex in E_1 or E_2). We call this operation the *merge* of E_1 and E_2.

If the root edge e is not a loop, then we contract it, which gives a smaller Eulerian map E'. Note however that several maps give E' after contracting their root edge. All such maps can be obtained from E' as follows (see Figure 4.4, right): we split the root vertex v of E' into two vertices v and v' joined by an edge (which will be the root edge), and distribute the edges adjacent to v between v and v' such that the degrees of v and v' remain even. This operation is called a *split* of E', and more precisely an i-*split* if v has degree $2i$ in the larger map. Note that if v has degree $2d$ in E', then i can be chosen arbitrarily between 1 and d.

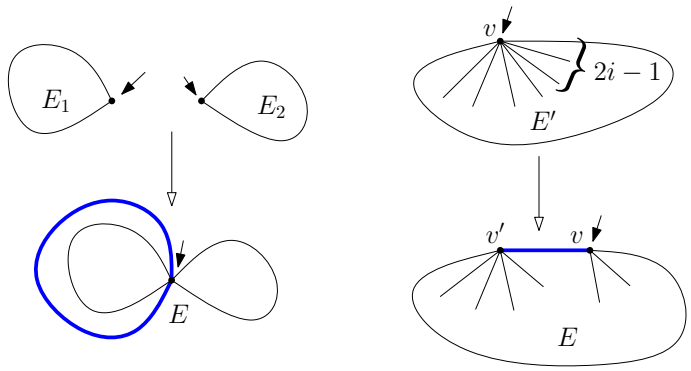

Figure 4.4: Construction of an Eulerian map with n edges: merge an ordered pair of Eulerian maps E_1, E_2 with n_1 and n_2 edges ($n_1+n_2 = n-1$) and add a loop, or make a split on an Eulerian map with $n-1$ edges. The new edge (here thicker) is the root edge of E.

Since the number of possible splits of an Eulerian map depends on the degree of the root vertex v (more precisely, on the half-degree of v, since it is even), then, as for general planar maps, we need a catalytic variable accounting for this half degree.

Let $E(t;x)$ be the generating function of Eulerian maps, counted by number of edges (variable t) and by the half degree of the root vertex (variable x):

$$E(t;x) = \sum_{E\in\mathcal{E}} t^{\mathrm{e}(E)} x^{\mathrm{dv}(E)} = \sum_{d\geq 0} x^d E_d(t)\,,$$

where $\mathcal{E}$ is the set of Eulerian maps and $E_d(t)$ denotes the generating function of Eulerian maps with root vertex degree $2d$, counted by number of edges.

The above construction directly translates into the following functional equation:

$$E(t;x) = 1 + txE(t;x)^2 + t\sum_{d\geq 0} E_d(t)(x + x^2 + \cdots + x^d)$$
$$= 1 + txE(t;x)^2 + \frac{tx}{x-1}(E(t;x) - E(t;1))\,, \tag{4.2}$$

where the first term accounts for the atomic map, the next term for maps obtained by merging two smaller maps, and the third term for maps obtained from a split.

Merge and split operations on Eulerian orientations

We continue in the same approach to decompose Eulerian orientations. As for Eulerian maps, removing the root-edge (either by deletion, when it is a loop, or by contraction, when it is not) causes no particular problem.

However, one must take care when going in the opposite direction, that is, when constructing large orientations from smaller ones. The first type of orientations, obtained by a merge, do not raise any difficulty; the new root edge (the loop) can be oriented in two different ways (Figure 4.5, left). But consider now an Eulerian orientation O', with root vertex v of degree at least $2i$, and perform an i-split on O': is there a way to orient the new edge so as to obtain an orientation O that is still Eulerian? The answer is yes if and only if the numbers of in- and out-edges in the last $2i-1$ edges incident to v in O' differ by ± 1 (edges are visited in counterclockwise order, starting from the root corner). The orientation of the root edge of O is then forced (Figure 4.5, right). In this case, we say that the i-split, performed on O', is *legal*. Note that the 1-split and the d-split are always legal, where $2d$ is the degree of the root vertex of O'.

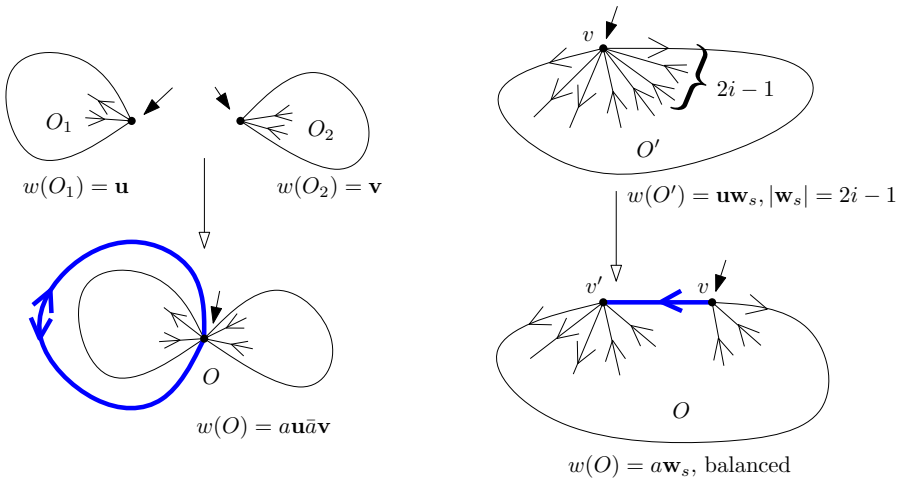

Figure 4.5: Construction of an Eulerian orientation: merge two Eulerian orientations (the loop can be oriented in either way), or split (legally) an Eulerian orientation. Observe how the root word evolves.

The fact that not all splits are legal makes it difficult to write a single functional equation for the generating function of Eulerian orientations. However, we can

write an *infinite system* of equations relating the generating functions of orientations with prescribed orientations at the root.

Let us be more precise. Given an Eulerian orientation O with root vertex v of degree $2d$, the *root word* $w(O)$ of O is a word of length $2d$ on the alphabet $\{0,1\}$ describing the orientation of the edges around v (in counterclockwise order, starting from the root corner): the k-th letter of $w(O)$ is 0 (resp. 1) if the k-th edge around v is an in-edge (resp. out-edge). Note that this word is always *balanced*, meaning that it contains as many 0's as 1's. We call a word $\mathbf{w}$ *quasi-balanced* if the number of 0's and 1's in $\mathbf{w}$ differ by ± 1. The length (number of letters) of $\mathbf{w}$ is denoted by $|\mathbf{w}|$, while the number of occurrences of the letter a in it is denoted by $|\mathbf{w}|_a$. We define the *balance* of $\mathbf{w}$ to be $b(\mathbf{w}) := ||\mathbf{w}|_1 - |\mathbf{w}|_0|$. The empty word is denoted by ε.

Now we can decide from the root word of O' if the i-split of O' is legal: this holds if and only if the last $2i-1$ letters of $w(O')$ form a quasi-balanced word.

Generating function of Eulerian orientations

Given $\mathbf{w}$ a word on $\{0,1\}$, let $O_{\mathbf{w}}(t) \equiv O_{\mathbf{w}}$ be the generating function of Eulerian orientations having $\mathbf{w}$ as root word, counted by their edge number. Clearly, $O_{\mathbf{w}} = 0$ if $\mathbf{w}$ is not balanced and $O_\varepsilon = 1$ (accounting for the atomic map). Now if $\mathbf{w}$ is non-empty and balanced,

$$O_{\mathbf{w}} = t \sum_{a\mathbf{u}\bar{a}\mathbf{v}=\mathbf{w}} O_{\mathbf{u}} O_{\mathbf{v}} + t \sum_{\mathbf{u}} O_{\mathbf{u}\mathbf{w}_s}. \tag{4.3}$$

This identity is illustrated in Figure 4.5. Here, a stands for any of the letters 0, 1, and the first sum runs over all factorizations of $\mathbf{w}$ of the form $a\mathbf{u}\bar{a}\mathbf{v}$, with $\bar{a} := 1-a$. This sum counts orientations obtained by a merge. The second sum runs over all possible words $\mathbf{u}$, and $\mathbf{w}_s$ denotes the suffix of $\mathbf{w}$ of length $|\mathbf{w}|-1$. This sum counts orientations obtained by a (legal) split of an orientation having root word $\mathbf{u}\mathbf{w}_s$. Now the generating function O of Eulerian orientations is

$$\sum_{\mathbf{w}} O_{\mathbf{w}},$$

where the sum runs over all (balanced) words $\mathbf{w}$.

We do not know how to solve this system, but since a map with n edges has a root word of length at most $2n$, we can use our system to compute the numbers o_n for small values of n. This way, we obtain the first 11 values of Figure 4.3.

4.1.2 Prime decomposition

A (non-atomic) map is said to be *prime* if the root vertex appears only once when walking around the root face. A planar map M can be seen as a sequence of prime maps $M_1, \dots, M_\ell$ (Figure 4.6). We say that the M_i are the *prime submaps* of M, and denote $M = M_1 \cdots M_\ell$. Note that if M is Eulerian, then each M_i is Eulerian too.

Now take a *prime* Eulerian map E, and apply the standard decomposition of Section 4.1.1, illustrated in Figure 4.4: either E is an (arbitrary) Eulerian map E_1 surrounded by a loop, or E is obtained by an i-split in a larger Eulerian map E',

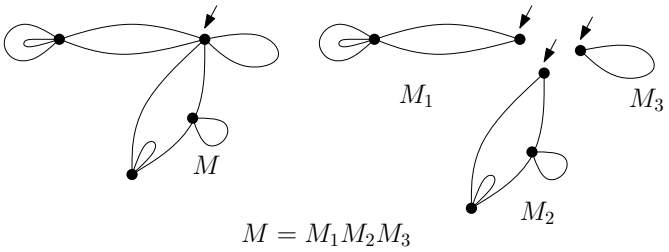

Figure 4.6: Decomposition of a planar (Eulerian) map M into prime (Eulerian) maps M_1, M_2, M_3.

provided the last prime submap of E' (in counterclockwise order) has root degree at least $2i$, (otherwise, the resulting map would not be prime). Alternatively, if $E' = E'_1 \cdots E'_\ell$, we can obtain E by performing an i-split in the prime map E'_ℓ, and attaching the map $E'' := E'_1 \cdots E'_{\ell-1}$ at the new vertex v' created by this split (Figure 4.7).

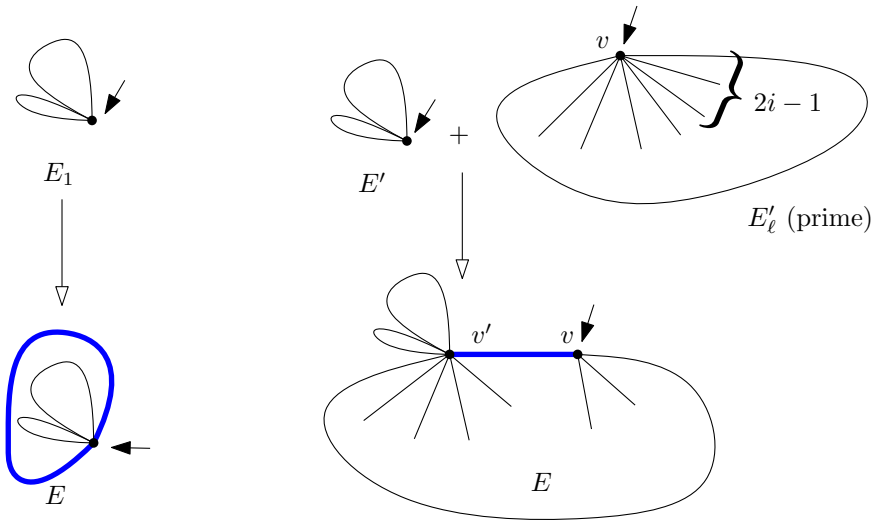

Figure 4.7: Construction of a prime Eulerian map: add a loop around any Eulerian map, or split a prime Eulerian map, and attach an arbitrary Eulerian map at the end of its root edge.

This alternative decomposition of Eulerian maps gives a system of two equations defining the generating function $E(t;x)$ of Eulerian maps (still counted by number of edges and root vertex degree) and its counterpart $E'(t;x)$ for prime maps:

$$\begin{cases} E(t;x) &= 1 + E(t;x)E'(t;x) \\ E'(t;x) &= txE(t;x) + txE(t;1)\dfrac{E'(t;x) - E'(t;1)}{x-1} \end{cases}$$

In the first equation, the term $E'(t;x)$ accounts for the last prime submap attached at the root vertex (denoted by E_ℓ above). In the second equation, the divided difference $\dfrac{E'(t;x) - E'(t;1)}{x-1}$ has the same explanation as in (4.2). This equation is

easily recovered by eliminating $E'(t;x)$ from the above system.

This decomposition can also be applied to Eulerian orientations: an Eulerian orientation is a sequence of prime Eulerian orientations, and a prime orientation is either obtained by adding an oriented loop around another orientation, or by performing a legal split in a prime orientation, and attaching another orientation at the vertex v' created by the split.

Thus, denoting again by $O_{\mathbf{w}}$ the generating function of orientations with root word $\mathbf{w}$, and by $O'_{\mathbf{w}}$ its counterpart for prime orientations, we now have $O_{\mathbf{w}} = O'_{\mathbf{w}} = 0$ if $\mathbf{w}$ is not balanced, $O_\varepsilon = 1$, $O'_\varepsilon = 0$ and finally for $\mathbf{w}$ balanced and non-empty,

$$\begin{cases} O_{\mathbf{w}} = \sum_{\mathbf{uv}=\mathbf{w}} O_{\mathbf{u}} O'_{\mathbf{v}} \\ O'_{\mathbf{w}} = tO_{\mathbf{w}_c} + tO \sum_{\mathbf{u}} O'_{\mathbf{u}\mathbf{w}_s} \end{cases}$$

In the second equation, $\mathbf{w}_c$ denotes the central factor or $\mathbf{w}$ of length $|\mathbf{w}| - 2$, and $O = \sum_{\mathbf{w}} O_{\mathbf{w}}$ is the generating function of all Eulerian orientations. Recall that $\mathbf{w}_s$ is the suffix of $\mathbf{w}$ of length $|\mathbf{w}| - 1$.

Using these equations, we have been able to push further the enumeration of Eulerian orientations of small size, thus obtaining the values of Figure 4.3.

Super-multiplicative property and first approximations

By attaching two orientations at their root vertex, we see that the sequence $(o_n)_{n\geq 0}$ is super-multiplicative, i.e. satisfies $o_{m+n} \geq o_m o_n$.

This classically (see Fekete's Lemma in [LW01, p. 103]) implies that the limit μ of $o_n^{1/n}$ exists and satisfies

$$\mu = \sup_n o_n^{1/n}. \tag{4.4}$$

We call μ the *growth rate* of Eulerian orientations. It is bounded from below by the growth rate 8 of Eulerian maps, and from above by the growth rate 16 of Eulerian maps equipped with an arbitrary orientation. Our data for $n \leq 15$ suggests than μ is around 12.5 (Figure 4.8). Using differential approximants [Gut], Tony Guttmann predicts $\mu = 12.568\ldots$, and an asymptotic behaviour $o_n \sim c\mu^n n^{-\gamma}$ with $\gamma = 2.23\ldots$.

4.2 Subsets with standard decomposition

Recall from Figure 4.5 that planar Eulerian orientations can be obtained recursively from the atomic map by either:

- the merge of two orientations $O_1, O_2 \in \mathcal{O}$,
- or a legal split on an orientation $O' \in \mathcal{O}$.

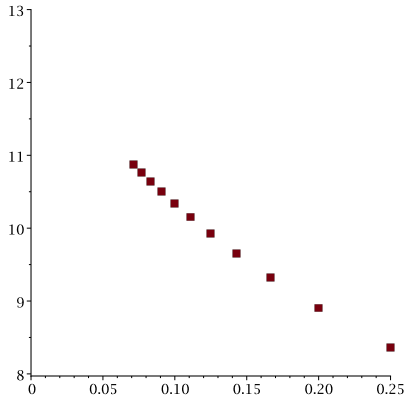

Figure 4.8: A plot of o_{n+1}/o_n vs. $1/n$, for $n = 4, \ldots, 14$, suggests that the growth rate of Eulerian orientations, located at the intercept of the curve and the y-axis, is around 12.5.

Definition 4.1. Let $k \geq 1$. Let $\mathcal{L}^{(k)}$ be the set of planar orientations obtained recursively from the atomic map by either:

- the merge of two orientations $O_1, O_2 \in \mathcal{L}^{(k)}$ (with the root loop oriented in either way),
- or a legal i-split on an orientation $O' \in \mathcal{L}^{(k)}$ such that $i \leq k$ or $i = \mathrm{dv}(O')$.

In other words, the only allowed splits are the *small* splits ($i \leq k$) and the *maximal* split ($i = \mathrm{dv}(O')$).

Obviously, all orientations of $\mathcal{L}^{(k)}$ are Eulerian. Moreover, the sets $\mathcal{L}^{(k)}$ form an increasing sequence since more and more (legal) splits are allowed as k grows. Finally, all Eulerian orientations of size n belong to $\mathcal{L}^{(n)}$ (and even to $\mathcal{L}^{(n-2)}$). Hence the limit of the sets $\mathcal{L}^{(k)}$ is the set $\mathcal{O}$ of all Eulerian orientations.

Figure 4.9 shows a (random) orientation of $\mathcal{L}^{(1)}$.

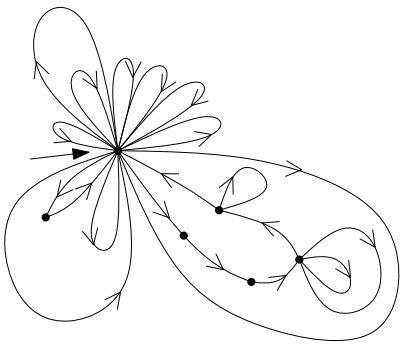

Figure 4.9: An Eulerian orientation in $\mathcal{L}^{(1)}$, taken uniformly at random among those with 20 edges.

4.2.1 An algebraic system for $\mathcal{L}^{(k)}$

In this section, k is a fixed integer.

Definition 4.2. A word $\mathbf{w}$ on $\{0,1\}$ is *valid* (for k) if there exists a balanced word of length $2k$ having $\mathbf{w}$ as a factor. Equivalently, the balance of $\mathbf{w}$ satisfies $b(\mathbf{w}) \leq 2k - |\mathbf{w}|$. This holds automatically if $|\mathbf{w}| \leq k$.

Given a word $\mathbf{w}$, it will be convenient to have notation for several words that differ from $\mathbf{w}$ by one or two letters. We have already defined $\mathbf{w}_c$, the central factor of $\mathbf{w}$ of length $|\mathbf{w}| - 2$, and $\mathbf{w}_s$, the suffix of $\mathbf{w}$ of length $|\mathbf{w}| - 1$. We similarly define $\mathbf{w}_p$ as the prefix of $\mathbf{w}$ of length $|\mathbf{w}| - 1$. Finally, if $\mathbf{w}$ is quasi-balanced, then $\overleftarrow{\mathbf{w}}$ stands for the unique balanced word of the form $a\mathbf{w}$, for $a \in \{0,1\}$.

For any word $\mathbf{w}$, we denote by $L^{(k)}_{\mathbf{w}}(t)$ the generating function of orientations of $\mathcal{L}^{(k)}$ whose root word ends with $\mathbf{w}$, counted by edges. In particular, the generating function counting all orientations of $\mathcal{L}^{(k)}$ is $L^{(k)}_{\varepsilon}(t)$. We denote by $K^{(k)}_{\mathbf{w}}(t)$ the generating function of orientations of $\mathcal{L}^{(k)}$ having root word exactly $\mathbf{w}$. In order to lighten notation, we often omit the dependence of our series in t and the superscript (k).

We now give equations defining the series $L_{\mathbf{w}}$ (for $|\mathbf{w}| \leq 2k-1$) and $K_{\mathbf{w}}$ (for $|\mathbf{w}| \leq 2k$). First, we note that $K_{\mathbf{w}} = 0$ if $\mathbf{w}$ is not balanced, and that $K_{\varepsilon} = 1$. Now for $\mathbf{w}$ balanced of length between 2 and $2k$, we have:

$$K_{\mathbf{w}} = t \sum_{\mathbf{w}=a\mathbf{u}\bar{a}\mathbf{v}} K_{\mathbf{u}} K_{\mathbf{v}} + t L_{\mathbf{w}_s}, \tag{4.5}$$

where, as before, a is any of the letters $0, 1$. This equation is analogous to (4.3): the first term counts orientations obtained from a merge, the second orientations obtained from a split. Now for $L_{\mathbf{w}}$, with $\mathbf{w}$ of length at most $2k-1$, we have:

$$\begin{aligned} L_{\mathbf{w}} = \mathbb{1}_{\mathbf{w}=\varepsilon} + 2tL_{\varepsilon}L_{\mathbf{w}} + t \sum_{\mathbf{w}=\mathbf{u}a\mathbf{v}} L_{\mathbf{u}}K_{\mathbf{v}} + t \sum_{\mathbf{w}=a\mathbf{u}\bar{a}\mathbf{v}} K_{\mathbf{u}}K_{\mathbf{v}} \\ + t\left(L_{\mathbf{w}} - \mathbb{1}_{\mathbf{w}=\varepsilon}\right) + t \sum_{\substack{\mathbf{u}=\mathbf{v}\mathbf{w} \\ 2\leq|\mathbf{u}|\leq 2k \\ \mathbf{u} \text{ balanced}}} (L_{\mathbf{u}_s} - K_{\mathbf{u}}). \end{aligned} \tag{4.6}$$

This equation deserves some explanations. The first line counts the atomic map (if $\mathbf{w} = \varepsilon$), and the orientations obtained by a merge. The second (resp. third, fourth) term of this line counts orientations such that no (resp. one, both) half-edge(s) of the root loop is/are involved in the suffix $\mathbf{w}$ of the root word. Equivalently, denoting by O_1 and O_2 the merged orientations, those three terms respectively correspond to $|\mathbf{w}| \leq 2\,\mathrm{dv}(O_2)$, $2\,\mathrm{dv}(O_2) < |\mathbf{w}| < 2 + 2\,\mathrm{dv}(O_1) + 2\,\mathrm{dv}(O_2)$ and $|\mathbf{w}| = 2 + 2\,\mathrm{dv}(O_1) + 2\,\mathrm{dv}(O_2)$.

The second line counts orientations O obtained by a legal i-split (with $i \leq k$) in a smaller orientation O'. The first term accounts for maximal splits ($i = \mathrm{dv}(O')$), which, we recall, do not change the root word (note also that no split is possible on the atomic map). The second term counts orientations O obtained from a non-maximal split. The word $\mathbf{u}$ stands for the root word of O. The subtraction of $K_{\mathbf{u}}$ comes from the condition that the split is not maximal.

Proposition 4.1. Consider the collection of equations consisting of:

- Equation (4.5), written for all balanced words $\mathbf{w}$ of length ℓ, $2 \leq \ell \leq 2k$,
- Equation (4.6), written for all valid words $\mathbf{w}$ of length at most $2k-1$.

In this collection, replace all trivial K-series by their value: $K_{\mathbf{w}} = 0$ when $\mathbf{w}$ is not balanced, $K_\varepsilon = 1$. Let S_0 denote the resulting system. The number of series it involves is

$$f(k) = \binom{2k+2}{k+1} - 1 + \sum_{i=1}^{k-1} \binom{2i}{i}. \tag{4.7}$$

The system S_0 defines uniquely these $f(k)$ series. Its size can be (roughly) divided by two upon noticing that replacing all 0's by 1's, and vice-versa, in a word $\mathbf{w}$, does not change the series $L_{\mathbf{w}}$ nor $K_{\mathbf{w}}$.

Proof. To see that S_0 defines all the series it involves, it suffices to note the factor t in the right-hand sides of (4.5) and (4.6), and to check that each series occurring in the right-hand side of some equation also occurs as the left-hand side of another. This is easy to check, as any factor of a valid word is also valid.

Let us now count the equations of the system. The number of non-empty balanced words of length at most $2k$ is

$$\sum_{i=1}^{k} \binom{2i}{i}.$$

Then, all words of length at most k are valid, while the number of valid words of length $k+i$, for $1 \leq i \leq k-1$, is

$$\sum_{j=i}^{k} \binom{k+i}{j}.$$

(One can interpret j as the number of occurrences of 0 in the word.) Hence the number of equations in the system is

$$f(k) = \sum_{i=1}^{k} \binom{2i}{i} + \sum_{i=0}^{k} 2^i + \sum_{i=1}^{k-1} \sum_{j=i}^{k} \binom{k+i}{j}.$$

The second sum evaluates to $2^{k+1} - 1$. The third one is

$$\begin{aligned}
\sum_{j=1}^{k} \sum_{i=1}^{\min(j,k-1)} \binom{k+i}{j} &= \sum_{j=1}^{k-1} \sum_{i=1}^{j} \binom{k+i}{j} + \sum_{i=1}^{k-1} \binom{k+i}{k} \\
&= \left(1 + \binom{2k+1}{k} - 2^{k+1}\right) + \left(\frac{k}{k+1}\binom{2k}{k} - 1\right) \\
&= \frac{3k+1}{k+1}\binom{2k}{k} - 2^{k+1}.
\end{aligned}$$

The sums are evaluated using classical summation identities, or Gosper's algorithm [PWZ96]. The expression of $f(k)$ is then given by

$$\begin{aligned} f(k) &= \sum_{i=1}^{k} \binom{2i}{i} + 2^{k+1} - 1 + \frac{3k+1}{k+1}\binom{2k}{k} - 2^{k+1} \\ &= \sum_{i=1}^{k-1} \binom{2i}{i} + \binom{2k}{k}\frac{4k+2}{k+1} - 1 \\ &= \sum_{i=1}^{k-1} \binom{2i}{i} + 2\binom{2k+1}{k} - 1 \\ &= \sum_{i=1}^{k-1} \binom{2i}{i} + \binom{2k+2}{k+1} - 1\,, \end{aligned}$$

which completes the proof. □

Remark 4.2. If $\mathbf{w}$ is such that $0\mathbf{w}$ and $1\mathbf{w}$ are both valid of length less than $2k$, we can define $L_{\mathbf{w}}$ by a simpler "forward" equation, without increasing the size of the system:

$$L_{\mathbf{w}} = K_{\mathbf{w}} + L_{0\mathbf{w}} + L_{1\mathbf{w}}. \tag{4.8}$$

This is obviously smaller than (4.6), and possibly better suited to feed a computer algebra system. However, mixing equations of type (4.6) and (4.8) makes some proofs of Section 4.2.3 heavier.

4.2.2 Examples

The case $k = 1$.

When $k = 1$, the system S_0 contains $f(1) = 5$ equations and reads

$$\begin{cases} K_{01} &= tK_\varepsilon K_\varepsilon + tL_1 \\ K_{10} &= tK_\varepsilon K_\varepsilon + tL_0 \\ L_\varepsilon &= 1 + 2tL_\varepsilon L_\varepsilon + t(L_\varepsilon - 1) + t(L_0 - K_{10} + L_1 - K_{01}) \\ L_0 &= 2tL_\varepsilon L_0 + tL_\varepsilon K_\varepsilon + tL_0 + t(L_0 - K_{10}) \\ L_1 &= 2tL_\varepsilon L_1 + tL_\varepsilon K_\varepsilon + tL_1 + t(L_1 - K_{01})\,, \end{cases} \tag{4.9}$$

with $K_\varepsilon = 1$. Using the $0/1$ symmetry, this system can be compacted into the following one:

$$\begin{cases} K_{01} &= t + tL_0 \\ L_\varepsilon &= 1 + 2tL_\varepsilon L_\varepsilon + t(L_\varepsilon - 1) + 2t(L_0 - K_{01}) \\ L_0 &= 2tL_\varepsilon L_0 + tL_\varepsilon + tL_0 + t(L_0 - K_{01})\,. \end{cases}$$

The variant mentioned in Remark 4.2 consists in replacing the second equation by $L_\varepsilon = 1+2L_0$. Eliminating L_0 and K_{01} from the system gives a quadratic equation for the generating function $L_\varepsilon = L_\varepsilon^{(1)}$ of Eulerian orientations in $\mathcal{L}^{(1)}$:

$$2tL_\varepsilon^2 - L_\varepsilon(1-t)^2 - t^2 - 2t + 1 = 0\,. \tag{4.10}$$

We defer to Section 4.2.3 the study of the asymptotic behaviour of its coefficients.

The case $k = 2$.

When $k = 2$, the system S_0 of Proposition 4.1 contains $f(2) = 21$ equations, or 11 if we exploit the $0/1$ symmetry:

$$\begin{cases}
K_{10} = K_{01} &= t + tL_0 \\
K_{1100} &= tK_{10} + tL_{100} \\
K_{1010} &= t(K_{10} + K_{01}) + tL_{010} \\
K_{0110} &= tK_{10} + tL_{110} \\
L_\varepsilon &= 1 + 2tL_\varepsilon L_\varepsilon + t(L_\varepsilon - 1) + 2t(L_0 - K_{10} + L_{100} - K_{1100} \\
&\qquad + L_{010} - K_{1010} + L_{110} - K_{0110}) \\
L_0 = L_1 &= 2tL_\varepsilon L_0 + tL_\varepsilon + tL_0 + t(L_0 - K_{10} + L_{100} - K_{1100} \\
&\qquad + L_{010} - K_{1010} + L_{110} - K_{0110}) \\
L_{00} = L_{11} &= 2tL_\varepsilon L_{00} + tL_0 + tL_{00} + t(L_{100} - K_{1100}) \\
L_{10} = L_{01} &= 2tL_\varepsilon L_{10} + tL_1 + t + tL_{10} + t(L_0 - K_{10} + L_{010} \\
&\qquad - K_{1010} + L_{110} - K_{0110}) \\
L_{100} &= 2tL_\varepsilon L_{100} + tL_{10} + tL_{100} + t(L_{100} - K_{1100}) \\
L_{010} &= 2tL_\varepsilon L_{010} + t(L_{01} + L_\varepsilon K_{10}) + tL_{010} + t(L_{010} - K_{1010}) \\
L_{110} &= 2tL_\varepsilon L_{110} + t(L_{11} + L_\varepsilon K_{10}) + tL_{110} + t(L_{110} - K_{0110})\,.
\end{cases} \tag{4.11}$$

The variant mentioned in Remark 4.2 consists in replacing the equations defining L_ε, L_0 and L_{10} by $L_\varepsilon = 1 + 2L_0$, $L_0 = L_{00} + L_{10}$ and $L_{10} = K_{10} + L_{010} + L_{110}$ respectively.

Eliminating all series but L_ε gives a quartic functional equation for the generating function $L_\varepsilon = L_\varepsilon^{(2)}$ of Eulerian orientations in $\mathcal{L}^{(2)}$:

$$\begin{aligned}
&8t^3L_\varepsilon^4 - 4t^2(3t^3 + 4t^2 - 6t + 3)L_\varepsilon^3 + 2t(3t^5 - 12t^4 - 10t^3 + 14t^2 - 10t + 3)L_\varepsilon^2 \\
&+(t-1)(11t^5 - 10t^4 - 6t^3 - 3t^2 - t + 1)L_\varepsilon + (t-1)(5t^5 - 4t^4 + 6t^3 - 7t^2 + 5t - 1) = 0\,.
\end{aligned} \tag{4.12}$$

Once again, we defer to Section 4.2.3 the study of the asymptotic behaviour of its coefficients.

4.2.3 Asymptotic analysis

Here, we have to apply the theory of *positive irreducible polynomial systems* [FS09, Sec. VII.6] to get some information on the asymptotic behaviour of the series L_ε.

Theorem 4.3. *[Drmota-Lalley-Woods (DLW) Theorem, [FS09, Thm VII.6]] Consider a nonlinear polynomial system $\{y_j = \Phi_j(z, y_1, \cdots, y_m)\}$, $j = 1, \cdots, m$, that is positive, proper, and irreducible. Then, all component solutions y_j have the same radius of convergence $\rho < \infty$, and there exist functions h_j analytic at the origin such that, in a neighbourhood of ρ:*

$$y_j = h_j(\sqrt{1 - z/\rho}\,).$$

If furthermore the system is aperiodic, all y_j have ρ as unique dominant singularity. In that case, the coefficients admit a complete asymptotic expansion

$$[z^n]y_j(z) \sim \rho^{-n}\Big(\sum_{i\geq 0} d_i n^{-3/2-i}\Big)$$

for computable d_i.

We now apply the DLW Theorem to System S_0 and get the following result:

Proposition 4.4. For $k \geq 1$, let ρ_k denote the radius of convergence of the series $L_\varepsilon^{(k)}$, which counts orientations of $\mathcal{L}^{(k)}$. Then ρ_k is the only singularity of $L_\varepsilon^{(k)}$ of minimal modulus, and it is of the square root type: as t tends to ρ_k from below,

$$L_\varepsilon^{(k)}(t) = \alpha - \beta\sqrt{1 - t/\rho_k}\,(1 + o(1))$$

for non-zero constants α and β depending on k [a].

The number $\ell_n^{(k)}$ of orientations of size n in $\mathcal{L}^{(k)}$ satisfies, as n tends to infinity:

$$\ell_n^{(k)} \sim c\lambda_k^n n^{-3/2},$$

where $\lambda_k = 1/\rho_k$ and $c = -\beta/\Gamma(-1/2)$.

[a] The positivity of β is not directly stated in the DLW Theorem, but can be deduced in step *c1)* of its proof by the positivity property of the system S_0.

Proof. We use the terminology of [FS09, Sec. VII.6.3]. In order to apply DLW Theorem, we have to prove that the system S_0 has four properties: positivity, properness, aperiodicity, and irreducibility. Each of these notions are briefly explained as the proof goes along. For more details on these properties and their implications in other cases, we refer the reader to Section VII.6.3 of Flajolet and Sedgewick's book [FS09].

Our first objective is to transform the system S_0 of Proposition 4.1 into a positive one, i.e. a system with only positive terms. The obstructions to positivity come from the expression (4.6) of $L_{\mathbf{w}}$, and more precisely from the terms $L_\varepsilon - 1$ (when $\mathbf{w} = \varepsilon$) and $L_{\mathbf{u}_s} - K_{\mathbf{u}}$, where $\mathbf{u}$ is balanced. These terms can be written $L_{\mathbf{w}} - K_{\overleftarrow{\mathbf{w}}}$, where $\mathbf{w} = \mathbf{u}_s$ is quasi-balanced and $\overleftarrow{\mathbf{w}}$ is the unique balanced word of the form $a\mathbf{w}$, for

$a \in \{0, 1\}$.

This leads us to define, for $\mathbf{w}$ quasi-balanced of length less than $2k$, the series $L^+_{\mathbf{w}} := L_{\mathbf{w}} - K_{\overleftarrow{\mathbf{w}}}$. We also need to define, for $\mathbf{w}$ balanced, $L^+_{\mathbf{w}} := L_{\mathbf{w}} - K_{\mathbf{w}}$. Both these series have a natural combinatorial interpretation: they represent orientations whose root word ends *strictly* with $\mathbf{w}$ (if $\mathbf{w}$ is balanced) or $\overleftarrow{\mathbf{w}}$ (if $\mathbf{w}$ is quasi-balanced). We alter the original system S_0 as follows:

(i) For $\mathbf{w}$ balanced or quasi-balanced, we replace the equation (4.6) defining $L_{\mathbf{w}}$ by an equation defining $L^+_{\mathbf{w}}$:

$$L^+_{\mathbf{w}} = 2tL_\varepsilon L_{\mathbf{w}} + t \sum_{\mathbf{w}=\mathbf{u}a\mathbf{v}} (L_{\mathbf{u}} - K_{\mathbf{u}})K_{\mathbf{v}} + tL^+_{\mathbf{w}} + t \sum_{\substack{\mathbf{u}=\mathbf{v}\mathbf{w}, \mathbf{u}\neq\mathbf{w} \\ |\mathbf{u}|\leq 2k-1 \\ \mathbf{u} \text{ quasi-balanced}}} L^+_{\mathbf{u}}\,. \tag{4.13}$$

To obtain it, either we get back to the explanation of (4.6) and remove from its right-hand side the terms that count orientations with root word exactly $\mathbf{w}$ (if $\mathbf{w}$ is balanced) or $\overleftarrow{\mathbf{w}}$ (if $\mathbf{w}$ is quasi-balanced), or we simply subtract from (4.6) Equation (4.5), written for $\mathbf{w}$ if $\mathbf{w}$ is balanced, for $\overleftarrow{\mathbf{w}}$ if $\mathbf{w}$ is quasi-balanced.

(ii) In the new system obtained, we replace every series $K_{\mathbf{w}}$ such that $\mathbf{w}$ is not balanced by 0, every series $L_{\mathbf{w}}$ such that $\mathbf{w}$ is balanced by $K_{\mathbf{w}} + L^+_{\mathbf{w}}$, and every series $L_{\mathbf{w}}$ such that $\mathbf{w}$ is quasi-balanced by $K_{\overleftarrow{\mathbf{w}}} + L^+_{\mathbf{w}}$. In particular, the series $L_{\mathbf{u}} - K_{\mathbf{u}}$ occurring in (4.13) becomes $L^+_{\mathbf{u}}$ when $\mathbf{u}$ is balanced, $L_{\mathbf{u}}$ otherwise. The only series $L_{\mathbf{w}}$ that remain in the system are such that the balance of $\mathbf{w}$ is at least 2.

We obtain a positive system, denoted S_1, defining the following series:

- $K_{\mathbf{w}}$, for $\mathbf{w}$ balanced of length between 2 and $2k$,
- $L^+_{\mathbf{w}}$, for $\mathbf{w}$ balanced or quasi-balanced of length less than $2k$,
- $L_{\mathbf{w}}$, for $\mathbf{w}$ valid of length less than $2k$ and balance at least 2.

For instance, when $k = 1$, the system (4.9) becomes (after exploiting the $0/1$ symmetry):

$$\begin{cases} K_{01} &= t + t(K_{01} + L^+_0) \\ L^+_\varepsilon &= 2t(1 + L^+_\varepsilon)^2 + tL^+_\varepsilon + 2tL^+_0 \\ L^+_0 &= 2t(1 + L^+_\varepsilon)(K_{01} + L^+_0) + tL^+_\varepsilon + tL^+_0\,. \end{cases}$$

Similarly, when $k = 2$, the system (4.11) is replaced by:

$$\begin{cases} K_{10} = K_{01} &= t + t(K_{10} + L_0^+) \\ K_{1100} &= tK_{10} + t(K_{1100} + L_{100}^+) \\ K_{1010} &= t(K_{10} + K_{01}) + t(K_{1010} + L_{010}^+) \\ K_{0110} &= tK_{01} + t(K_{0110} + L_{110}^+) \\ L_\varepsilon^+ &= 2t(1 + L_\varepsilon^+)^2 + tL_\varepsilon^+ + 2t(L_0^+ + L_{100}^+ + L_{010}^+ + L_{110}^+) \\ L_0^+ = L_1^+ &= 2t(1 + L_\varepsilon^+)(K_{10} + L_0^+) + tL_\varepsilon^+ + tL_0^+ + t(L_{100}^+ + L_{010}^+ + L_{110}^+) \\ L_{00} = L_{11} &= 2t(1 + L_\varepsilon^+)L_{00} + t(K_{10} + L_0^+) + tL_{00} + tL_{100}^+ \\ L_{10}^+ = L_{01}^+ &= 2t(1 + L_\varepsilon^+)(K_{10} + L_{10}^+) + t(K_{01} + L_1^+) + tL_{10}^+ + t(L_{110}^+ + L_{010}^+) \\ L_{100}^+ &= 2t(1 + L_\varepsilon^+)(K_{1100} + L_{100}^+) + tL_{10}^+ + tL_{100}^+ \\ L_{010}^+ &= 2t(1 + L_\varepsilon^+)(K_{1010} + L_{010}^+) + t(L_{01}^+ + L_\varepsilon^+ K_{10}) + tL_{010}^+ \\ L_{110}^+ &= 2t(1 + L_\varepsilon^+)(K_{0110} + L_{110}^+) + t(L_{11} + L_\varepsilon^+ K_{10}) + tL_{110}^+ . \end{cases}$$

The second condition that we need is *properness* (again, in the sense of [FS09, Sec. VII.6.3]). A system is said to be proper if it has a unique solution which can be obtained iteratively. But the system S_1 that we just obtained is proper, thanks to the factor t occurring in the right-hand side of (4.5), (4.6) and (4.13).

Now let us prove that S_1 is irreducible. Recall that in such a polynomial system, a series F *depends* on a series G if G occurs in the right-hand side of the equation defining F. Irreducibility means that the directed graph of dependences is strongly connected. Recall that S_1 involves two families of series: the series $K_{\mathbf{w}}$, for $\mathbf{w}$ balanced of length between 2 and $2k$, and $L_{\mathbf{w}}$ (or $L_{\mathbf{w}}^+$) for any valid $\mathbf{w}$ of length at most $2k-1$. To lighten notation, for any $\mathbf{w}$ we denote by $\tilde{L}_{\mathbf{w}}$ the corresponding L-series, be it $L_{\mathbf{w}}$ or $L_{\mathbf{w}}^+$.

Let us first prove that every series in S_1 depends on $\tilde{L}_\varepsilon = L_\varepsilon^+$. By (4.6) and (4.13), this holds for every $\tilde{L}_{\mathbf{w}}$. Now, by (4.5), each $K_{\mathbf{w}}$ depends on at least one $\tilde{L}$-series, and thus by transitivity on L_ε^+.

Conversely, let us prove that L_ε^+ depends on all other series occurring in S_1.

- First, Equation (4.13) applied to $\mathbf{w} = \varepsilon$ shows that L_ε^+ depends on all series $\tilde{L}_{\mathbf{u}}$ such that $\mathbf{u}$ is quasi-balanced.
- We now prove by induction on the balance $b(\mathbf{u})$ that L_ε^+ depends on $\tilde{L}_{\mathbf{u}}$ for each valid word $\mathbf{u}$ of length at most $2k-1$. We have already seen this for $b(\mathbf{u}) = 1$. If $b(\mathbf{u}) = 0$, then $|\mathbf{u}| \leq 2k-2$, and for any letter a the word $\mathbf{w} := \mathbf{u}a$ is valid and quasi-balanced. The second term in (4.13) shows that $\tilde{L}_{\mathbf{w}}$ depends on $\tilde{L}_{\mathbf{u}}$. By transitivity, this implies that L_ε^+ depends on $\tilde{L}_{\mathbf{u}}$. We have thus set the initial cases of our induction, for balances 0 and 1. Now assume $b(\mathbf{u}) \geq 2$. There exists a letter a such that $\mathbf{w} := \mathbf{u}a$ is valid and has balance $b(\mathbf{u}) - 1$. If $b(\mathbf{w}) = 1$ (resp. $b(\mathbf{w}) > 1$), the second (resp. third) term in the equation (4.13) (resp. (4.6)) defining $\tilde{L}_{\mathbf{w}}$ shows that $\tilde{L}_{\mathbf{w}}$ depends on $\tilde{L}_{\mathbf{u}}$. By the induction hypothesis, L_ε^+ depends on $\tilde{L}_{\mathbf{w}}$, and thus by transitivity on $\tilde{L}_{\mathbf{u}}$.
- Finally, let $\mathbf{u}$ be balanced of length between 2 and $2k$. Then $\mathbf{w} := \mathbf{u}_s$ is quasi-balanced. The first term of the equation (4.13) defining $\tilde{L}_{\mathbf{w}}$ involves $L_{\mathbf{w}} = K_{\mathbf{u}} + \tilde{L}_{\mathbf{w}}$, so that by transitivity, L_ε^+ depends on $K_{\mathbf{u}}$.

The last condition to check is aperiodicity. The aperiodicity of an irreducible system is equivalent to the aperiodicity of at least one of the series it contains [FS09, p. 483]. We recall the definition of aperiodicity of a series [FS09, Definition IV.5, p. 266]: For a sequence (f_n) with generating function $f(z)$, the *support* of f, denoted $Supp(f)$, is the set of all n such that $f_n \neq 0$. The sequence f_n, as well as $f(z)$, is said to admit a *span* d if for some r, there holds $Supp(f) \subseteq r+d\mathbb{Z}_{\geq 0} \equiv \{r, r+d, r+2d, \cdots\}$. The largest span, p, is the *period*. If p is equal to 1, the sequence f_n and $f(z)$ are said to be aperiodic. The coefficients of t^1 and t^2 in the series $L_\varepsilon^+(t)$ are both non-zero. This implies that this series is aperiodic, and thus the system S_1 is aperiodic too.

We have now checked all conditions of Theorem VII.6 of [FS09, p. 489]. Applying it gives our proposition. The asymptotic behaviour of the coefficients $\ell_n^{(k)}$ is given by a direct application of the "transfer theorem" [FS09, Thm. VI.4, p.393]. □

The $-3/2$ exponent in the asymptotic expansion of the coefficients is typical of "branching-like" classes, which can be seen as classes whose structure is close from the one of planar trees. This is not that surprising, since the orientations of the sets $\mathcal{L}^{(k)}$ are built through operations with a small number of splits allowed.

4.2.4 Back to examples

We now return to the cases $k = 1$ and $k = 2$ studied in Section 4.2.2.

When $k = 1$, we have obtained for L_ε the quadratic equation (4.10). Its dominant coefficient only vanishes at $t = 0$, and its discriminant is $\Delta_1(t) := t^4 + 4t^3 + 22t^2 - 12t + 1$. The radius ρ_1 must be one of the roots of Δ_1. The only real positive roots are around 0.1032 and 0.3998. By solving (4.10) explicitly, we see that the smallest of these roots is indeed a singularity of L_ε. Hence $\rho_1 = 0.1032\ldots$ and the corresponding growth rate is $\lambda_1 = 1/\rho_1 = 9.684\ldots$, which improves on the lower bound 8 coming from Eulerian maps.

When $k = 2$, we have obtained for L_ε the quartic equation (4.12). Its dominant coefficient does not vanish away from 0, and its discriminant is

$$\begin{aligned}\Delta_2(t) := 64t^{12}(t-1)(81t^{21} + 1863t^{20} + 11322t^{19} + 38592t^{18} + 101105t^{17} + \\ 226631t^{16} + 393423t^{15} + 532907t^{14} + 665167t^{13} + 719797t^{12} + 454804t^{11} + \\ 355710t^{10} + 360159t^9 - 262135t^8 - 239969t^7 + 723151t^6 - 1106764t^5 + \\ 820832t^4 - 316644t^3 + 65424t^2 - 6780t + 268)\,.\end{aligned}$$

The only roots strictly between 0 and 1 are $0.0984\ldots$ and $0.2714\ldots$. The radius ρ_2 is the first one (the other would give a growth rate smaller than 8). Hence the corresponding growth rate is $\lambda_2 = 1/\rho_2 = 10.16\ldots$, which improves on the previous bound λ_1.

We do not push our study to larger values of k, as we will obtain better bounds with the prime decomposition in the next section.

4.3 Subsets with prime decomposition

In this section, we combine the restriction on allowed splits of the previous section with the prime decomposition of Section 4.1.2 to obtain a new family of subsets of Eulerian orientations. The results and proofs are similar to those of the previous section, and we give fewer details. The new subsets $\mathbb{L}^{(k)}$ satisfy $\mathcal{L}^{(k)} \subset \mathbb{L}^{(k)}$ (Proposition 4.6), hence they give better lower bounds on the growth rate μ than those obtained in the previous section. Moreover these bounds increase to μ as k increases (Proposition 4.5).

Recall from Section 4.1.2 that an Eulerian orientation is a sequence of prime Eulerian orientations, and that a prime (Eulerian) orientation can be obtained recursively from the atomic map by either:

- adding a loop, oriented in either way, around an orientation O_1,
- or performing a legal split on a prime orientation $O' \in \mathcal{O}$, followed by the concatenation of an arbitrary Eulerian orientation O'' at the new vertex created by the split (Figure 4.7).

Definition 4.3. Let $k \geq 1$. Let $\mathbb{L}^{(k)}$ be the set of planar orientations obtained recursively from the atomic map by either:

- concatenating a sequence of prime orientations of $\mathbb{L}^{(k)}$,
- or adding a loop, oriented in either way, around an orientation O_1 of $\mathbb{L}^{(k)}$,
- or performing a legal i-split on a prime orientation $O' \in \mathbb{L}^{(k)}$, with $i = \mathrm{dv}(O')$ or $i \leq k$, followed by the concatenation of an arbitrary orientation of $\mathbb{L}^{(k)}$ at the new vertex created by the split.

Clearly, the sets $\mathbb{L}^{(k)}$ increase to the set $\mathcal{O}$ of all Eulerian orientations as k increases, hence their growth rates $\bar{\lambda}_k$ form a non-decreasing sequence of lower bounds on μ. But we have in this case a stronger result.

Proposition 4.5. For $k \geq 1$, the sequence $(\bar{\ell}_n^{(k)})_{n\geq 0}$ that counts orientations of $\mathbb{L}^{(k)}$ by their size is super-multiplicative. Consequently, the associated growth rate

$$\bar{\lambda}_k := \lim_n (\bar{\ell}_n^{(k)})^{1/n} = \sup_n (\bar{\ell}_n^{(k)})^{1/n} \tag{4.14}$$

increases to μ as k tends to infinity.

Proof. By definition of $\mathbb{L}^{(k)}$, concatenating two orientations of $\mathbb{L}^{(k)}$ at their root vertex gives a new element of $\mathbb{L}^{(k)}$, which implies super-multiplicativity and the identity (4.14) (by Fekete's Lemma [LW01, p. 103]).

Now since $\mathbb{L}^{(k)}$ converges to $\mathcal{O}$, for any n, there exists k such that $o_n = \ell_n^{(k)}$ (one can take $k = n$, or even $k = n - 2$). Hence

$$o_n^{1/n} = (\bar{\ell}_n^{(k)})^{1/n} \leq \bar{\lambda}_k \leq \lim_k \bar{\lambda}_k \,,$$

and from (4.4), $\mu \leq \lim_k \bar{\lambda}_k$. Since $\bar{\lambda}_k \leq \mu$, the proposition follows. □

Proposition 4.6. For $k \geq 1$, the subset of orientations $\mathbb{L}^{(k)}$ includes the subset $\mathcal{L}^{(k)}$ defined in Section 4.2.

Proof. We prove this by induction on the number of edges. The inclusion is obvious for orientations with no edge. Let $O \in \mathcal{L}^{(k)}$, having at least one edge.

If O is the merge of two orientations O_1 and O_2, then the induction hypothesis implies that O_1 and O_2 are in $\mathbb{L}^{(k)}$. The structure of $\mathbb{L}^{(k)}$ implies that every prime sub-orientation of O_2 (attached at the root of O_2) also belongs to $\mathbb{L}^{(k)}$. Then O can be obtained as an orientation of $\mathbb{L}^{(k)}$ by first adding a loop around O_1 (this is the second construction in Definition 4.3), then concatenating one by one the prime sub-orientations of O_2 (first construction in Definition 4.3).

Otherwise, O is obtained by a legal split in an orientation O' formed of the prime sub-orientations $P_1, \ldots, P_\ell$. By the induction hypothesis, O', and its prime sub-orientations $P_1, \ldots, P_\ell$, belong to $\mathbb{L}^{(k)}$. Let us say that the split occurs in P_i (this means that the sub-orientations $P_1, \ldots, P_{i-1}$ are attached to the new created vertex v', while $P_{i+1}, \ldots, P_\ell$ remain attached to the original vertex v, the root vertex of O). Then the orientation O_1 obtained by deleting from O the sub-orientations $P_{i+1}, \ldots, P_\ell$ can be obtained by a legal split in the prime orientation P_i, followed by the concatenation of $P_1, \ldots, P_{i-1}$ at the new created vertex. This is the third construction in Definition 4.3, hence O_1 belongs to $\mathbb{L}^{(k)}$. It remains to concatenate $P_{i+1}, \ldots, P_\ell$ at the root (first construction in Definition 4.3), and we recover O as an element of $\mathbb{L}^{(k)}$. □

4.3.1 An algebraic system for $\mathbb{L}^{(k)}$

We now fix $k \geq 1$. For $\mathbf{w}$ a word on $\{0,1\}$, let $\mathsf{L}^{(k)}_{\mathbf{w}}(t) \equiv \mathsf{L}_{\mathbf{w}}$ denote the generating function of orientations of $\mathbb{L}^{(k)}$ whose root word ends with $\mathbf{w}$. Let $\mathsf{K}_{\mathbf{w}}$ be the generating function of those that have root word exactly $\mathbf{w}$. Let $\mathsf{L}'_{\mathbf{w}}$ and $\mathsf{K}'_{\mathbf{w}}$ be the corresponding series for *prime* orientations of $\mathbb{L}^{(k)}$. We are especially interested in the series L_ε that counts all orientations of $\mathbb{L}^{(k)}$.

If $\mathbf{w}$ is not balanced, $\mathsf{K}_{\mathbf{w}} = \mathsf{K}'_{\mathbf{w}} = 0$, while if $\mathbf{w} = \varepsilon$, $\mathsf{K}_{\mathbf{w}} = 1$ and $\mathsf{K}'_{\mathbf{w}} = 0$. For $\mathbf{w}$ non-empty and balanced, of length at most $2k$, we have

$$\mathsf{K}_{\mathbf{w}} = \sum_{\mathbf{w}=\mathbf{uv}} \mathsf{K}_{\mathbf{u}}\mathsf{K}'_{\mathbf{v}}, \tag{4.15}$$

since an orientation of $\mathbb{L}^{(k)}$ is a sequence of orientations of $\mathbb{L}^{(k)}$. Now the description of prime orientations of $\mathbb{L}^{(k)}$ (Definition 4.3) gives

$$\mathsf{K}'_{\mathbf{w}} = t\mathsf{K}_{\mathbf{w}_c} + t\mathsf{L}_\varepsilon\mathsf{L}'_{\mathbf{w}_s}. \tag{4.16}$$

The first term corresponds to adding a loop, and the second to a legal i-split, where $i \leq k$ is the half-length of $\mathbf{w}$. The factor L_ε accounts for the orientation O'' attached at the end of the root edge.

Now let $\mathbf{w}$ be a valid word of length at most $2k-1$, and let us write equations for the series $\mathsf{L}_{\mathbf{w}}$ and $\mathsf{L}'_{\mathbf{w}}$. For $\mathsf{L}_{\mathbf{w}}$, the sequential structure of orientations of $\mathbb{L}^{(k)}$ gives

$$\mathsf{L}_{\mathbf{w}} = \mathbb{1}_{\mathbf{w}=\varepsilon} + \mathsf{L}_\varepsilon\mathsf{L}'_{\mathbf{w}} + \sum_{\mathbf{w}=\mathbf{uv},\mathbf{v}\neq\mathbf{w}} \mathsf{L}_{\mathbf{u}}\mathsf{K}'_{\mathbf{v}}. \tag{4.17}$$

The second (resp. third) term counts orientations in which the root word of the last prime component ends with $\mathbf{w}$ (resp. is shorter than $\mathbf{w}$). Finally, for the series $\mathsf{L}'_{\mathbf{w}}$ we obtain the following counterpart of (4.6):

$$\mathsf{L}'_{\mathbf{w}} = 2t\mathsf{L}_{\varepsilon}\mathbb{1}_{\mathbf{w}=\varepsilon} + t\mathsf{L}_{\mathbf{w}_p}\mathbb{1}_{\mathbf{w}\neq\varepsilon} + t\mathsf{K}_{\mathbf{w}_c}\mathbb{1}_{\mathbf{w}\neq\varepsilon} \text{ balanced} + t\mathsf{L}_{\varepsilon}\left(\mathsf{L}'_{\mathbf{w}} + \sum_{\substack{\mathbf{u}=\mathbf{v}\mathbf{w}\\ 0<|\mathbf{u}|\leq 2k\\ \mathbf{u}\text{ balanced}}} (\mathsf{L}'_{\mathbf{u}_s} - \mathsf{K}'_{\mathbf{u}})\right). \quad (4.18)$$

The first three terms count orientations in which the root edge is a loop, and the last one those obtained by a split.

Proposition 4.7. Consider the collection of equations consisting of:
- Equation (4.15), written for all balanced words $\mathbf{w}$ of length ℓ, $2 \leq \ell \leq 2k-2$,
- Equation (4.16), written for all balanced words $\mathbf{w}$ of length ℓ, $2 \leq \ell \leq 2k$,
- Equation (4.17), written for all valid words $\mathbf{w}$ of length at most $2k-2$,
- Equation (4.18), written for all valid words $\mathbf{w}$ of length at most $2k-1$.

In this collection, replace all trivial K- and K'-series by their value: $\mathsf{K}_{\mathbf{w}} = \mathsf{K}'_{\mathbf{w}} = 0$ when $\mathbf{w}$ is not balanced, $\mathsf{K}_{\varepsilon} = 1$, $\mathsf{K}'_{\varepsilon} = 0$. Let S_0 denote the resulting system. The number of series it involves is $2f(k) - 2\binom{2k}{k}$, where $f(k)$ is given by (4.7). Moreover, S_0 defines uniquely all these series. Its size can be (roughly) divided by two upon exploiting the $0/1$ symmetry.

Proof. To prove that all series are well defined by the system, we first check that every series occurring in the right-hand side of some equation is the left-hand side of another equation. Then we note that:

- the equations for prime orientations, namely (4.16) and (4.18), have a factor t in their right-hand sides,
- for the other two equations, (4.15) and (4.17), every non-trivial term in the right-hand side has a series of prime orientations as a factor.

Now the number of equations: every series that was occurring in the system S_0 of Proposition 4.1 now has two copies (one with a prime, one without), except for the series $K_{\mathbf{w}}$, for $\mathbf{w}$ balanced of length $2k$, and $L_{\mathbf{w}}$, for $\mathbf{w}$ quasi-balanced of length $2k-1$, which have only one copy. Since there are $\binom{2k}{k}$ balanced words of length $2k$, and $2\binom{2k-1}{k} = \binom{2k}{k}$ quasi-balanced words of length $2k-1$, the result follows. □

Remark 4.8. As in Remark 4.2, if $\mathbf{w}$ is such that $0\mathbf{w}$ and $1\mathbf{w}$ are both valid of length less than $2k-2$ (resp. $2k-1$), we can replace (4.17) (resp. (4.18)) by the simpler forward equation:

$$\mathsf{L}_{\mathbf{w}} = \mathsf{K}_{\mathbf{w}} + \mathsf{L}_{0\mathbf{w}} + \mathsf{L}_{1\mathbf{w}} \qquad (\text{resp. } \mathsf{L}'_{\mathbf{w}} = \mathsf{K}'_{\mathbf{w}} + \mathsf{L}'_{0\mathbf{w}} + \mathsf{L}'_{1\mathbf{w}}).$$

This does not increase the size of the system.

4.3.2 Examples

The case $k = 1$.

When $k = 1$, the system S_0 contains $2(f(1) - 2) = 6$ equations, or 4 by exploiting the $0/1$ symmetry:

$$\begin{cases} \mathsf{K}'_{10} &= t + t\mathsf{L}_\varepsilon \mathsf{L}'_0 \\ \mathsf{L}_\varepsilon &= 1 + \mathsf{L}_\varepsilon \mathsf{L}'_\varepsilon \\ \mathsf{L}'_\varepsilon &= 2t\mathsf{L}_\varepsilon + t\mathsf{L}_\varepsilon(\mathsf{L}'_\varepsilon + 2\mathsf{L}'_0 - 2\mathsf{K}'_{10}) \\ \mathsf{L}'_0 &= t\mathsf{L}_\varepsilon + t\mathsf{L}_\varepsilon(\mathsf{L}'_0 + \mathsf{L}'_0 - \mathsf{K}'_{10})\,. \end{cases}$$

Eliminating all series but L_ε gives a cubic equation for the generating function $\mathsf{L}_\varepsilon \equiv \mathsf{L}_\varepsilon^{(1)}$ of Eulerian orientations in $\mathbb{L}^{(1)}$:

$$t^2\mathsf{L}_\varepsilon^3 + t(t-4)\mathsf{L}_\varepsilon^2 + (2t+1)\mathsf{L}_\varepsilon - 1 = 0. \tag{4.19}$$

The case $k = 2$.

When $k = 2$, the system S_0 contains $2(f(2) - 6) = 30$ equations, or 16 if we exploit the $0/1$ symmetry:

$$\begin{cases} \mathsf{K}_{01} = \mathsf{K}_{10} &= \mathsf{K}'_{01} \\ \mathsf{K}'_{10} = \mathsf{K}'_{01} &= t + t\mathsf{L}_\varepsilon \mathsf{L}'_1 \\ \mathsf{K}'_{1100} &= t\mathsf{K}_{10} + t\mathsf{L}_\varepsilon \mathsf{L}'_{100} \\ \mathsf{K}'_{1010} &= t\mathsf{K}_{01} + t\mathsf{L}_\varepsilon \mathsf{L}'_{010} \\ \mathsf{K}'_{0110} &= t\mathsf{L}_\varepsilon \mathsf{L}'_{110} \\ \mathsf{L}_\varepsilon &= 1 + \mathsf{L}_\varepsilon \mathsf{L}'_\varepsilon \\ \mathsf{L}_0 = \mathsf{L}_1 &= \mathsf{L}_\varepsilon \mathsf{L}'_0 \\ \mathsf{L}_{00} = \mathsf{L}_{11} &= \mathsf{L}_\varepsilon \mathsf{L}'_{00} \\ \mathsf{L}_{01} = \mathsf{L}_{10} &= \mathsf{L}_\varepsilon \mathsf{L}'_{01} \\ \mathsf{L}'_\varepsilon &= 2t\mathsf{L}_\varepsilon + t\mathsf{L}_\varepsilon(\mathsf{L}'_\varepsilon + 2(\mathsf{L}'_0 - \mathsf{K}'_{10} + \mathsf{L}'_{100} - \mathsf{K}'_{1100} \\ &\qquad + \mathsf{L}'_{010} - \mathsf{K}'_{1010} + \mathsf{L}'_{110} - \mathsf{K}'_{0110})) \\ \mathsf{L}'_0 = \mathsf{L}'_1 &= t\mathsf{L}_\varepsilon + t\mathsf{L}_\varepsilon(\mathsf{L}'_0 + \mathsf{L}'_0 - \mathsf{K}'_{10} + \mathsf{L}'_{100} - \mathsf{K}'_{1100} + \mathsf{L}'_{010} \\ &\qquad - \mathsf{K}'_{1010} + \mathsf{L}'_{110} - \mathsf{K}'_{0110}) \\ \mathsf{L}'_{00} &= t\mathsf{L}_0 + t\mathsf{L}_\varepsilon(\mathsf{L}'_{00} + \mathsf{L}'_{100} - \mathsf{K}'_{1100}) \\ \mathsf{L}'_{10} = \mathsf{L}'_{01} &= t\mathsf{L}_1 + t + t\mathsf{L}_\varepsilon(\mathsf{L}'_{10} + \mathsf{L}'_1 - \mathsf{K}'_{01} + \mathsf{L}'_{010} - \mathsf{K}'_{1010} + \mathsf{L}'_{110} - \mathsf{K}'_{0110}) \\ \mathsf{L}'_{100} &= t\mathsf{L}_{10} + t\mathsf{L}_\varepsilon(\mathsf{L}'_{100} + \mathsf{L}'_{100} - \mathsf{K}'_{1100}) \\ \mathsf{L}'_{010} &= t\mathsf{L}_{01} + t\mathsf{L}_\varepsilon(\mathsf{L}'_{010} + \mathsf{L}'_{010} - \mathsf{K}'_{1010}) \\ \mathsf{L}'_{110} &= t\mathsf{L}_{11} + t\mathsf{L}_\varepsilon(\mathsf{L}'_{110} + \mathsf{L}'_{110} - \mathsf{K}'_{0110})\,. \end{cases} \tag{4.20}$$

Eliminating all series but L_ε gives an equation of degree 6 for the generating function $\mathsf{L}_\varepsilon \equiv \mathsf{L}_\varepsilon^{(2)}$ of Eulerian orientations in $\mathbb{L}^{(2)}$:

$$2t^5\mathsf{L}_\varepsilon^6 - t^4(t+8)\mathsf{L}_\varepsilon^5 - t^3(3t^2-16)\mathsf{L}_\varepsilon^4 + t^2(2t+3)(2t-5)\mathsf{L}_\varepsilon^3 \\ - t(2t^2-7t-7)\mathsf{L}_\varepsilon^2 - (5t+1)\mathsf{L}_\varepsilon + 1 = 0\,. \qquad (4.21)$$

4.3.3 Asymptotic analysis

We now prove for the polynomial system of Proposition 4.7 an analogue of Proposition 4.4.

Proposition 4.9. For $k \geq 1$, let $\bar\rho_k$ denote the radius of convergence of the series $\mathsf{L}_\varepsilon^{(k)}$ that counts orientations of $\mathbb{L}^{(k)}$. Then $\bar\rho_k$ is the only singularity of $\mathsf{L}_\varepsilon^{(k)}$ of minimal modulus, and it is of the square root type. Consequently, there exists a constant c such that the number $\bar\ell_n^{(k)}$ of orientations of size n in $\mathbb{L}^{(k)}$ satisfies, as n tends to infinity:

$$\bar\ell_n^{(k)} \sim c\bar\lambda_k^n n^{-3/2},$$

with $\bar\lambda_k = 1/\bar\rho_k$.

Proof. Again, we apply the theory of positive irreducible polynomial systems [FS09, Sec. VII.6].

The system of Proposition 4.7 is not positive. To correct this, we replace the series $\mathsf{L}_\mathbf{w}$ (for $\mathbf{w}$ balanced) and $\mathsf{L}'_\mathbf{w}$ (for $\mathbf{w}$ balanced or quasi-balanced) by their "positive" versions:

$$\mathsf{L}^+_\mathbf{w} := \mathsf{L}_\mathbf{w} - \mathsf{K}_\mathbf{w}\,, \qquad \mathsf{L}'^+_\mathbf{w} := \mathsf{L}'_\mathbf{w} - \mathsf{K}'_\mathbf{w} \qquad (\mathbf{w} \text{ balanced}),$$

$$\mathsf{L}'^+_\mathbf{w} := \mathsf{L}'_\mathbf{w} - \mathsf{K}'_{\overleftarrow{\mathbf{w}}} \qquad (\mathbf{w} \text{ quasi-balanced}).$$

In particular, L_ε is replaced by $\mathsf{L}^+_\varepsilon := \mathsf{L}_\varepsilon - 1$ and $\mathsf{L}'^+_\varepsilon$ coincides with L'_ε. We alter the original system S_0 as follows:

(i) For $\mathbf{w}$ balanced, we replace the equation (4.17) defining $\mathsf{L}_\mathbf{w}$ by the difference between (4.17) and (4.15):

$$\mathsf{L}^+_\mathbf{w} = \mathsf{L}^+_\varepsilon \mathsf{L}'_\mathbf{w} + \mathsf{L}'^+_\mathbf{w} + \sum_{\mathbf{w}=\mathbf{uv},\mathbf{v}\neq\mathbf{w}} \mathsf{L}_\mathbf{u}\mathsf{K}'_\mathbf{v}\,. \qquad (4.22)$$

(ii) For $\mathbf{w}$ balanced or quasi-balanced, we replace the equation (4.18) defining $\mathsf{L}'_\mathbf{w}$ by the difference between (4.18) and (4.16) (written for $\mathbf{w}$ if $\mathbf{w}$ is balanced, for $\overleftarrow{\mathbf{w}}$ otherwise):

$$\mathsf{L}'^+_\mathbf{w} = 2t\mathsf{L}_\varepsilon \mathbb{1}_{\mathbf{w}=\varepsilon} + t(\mathsf{L}_{\mathbf{w}_p} - \mathsf{K}_{\mathbf{w}_p})\mathbb{1}_{\mathbf{w}\neq\varepsilon} + t\mathsf{L}_\varepsilon \left(\mathsf{L}'^+_\mathbf{w} + \sum_{\substack{\mathbf{u}=\mathbf{vw},\mathbf{u}\neq\mathbf{w} \\ |\mathbf{u}|\leq 2k-1 \\ \mathbf{u} \text{ quasi-balanced}}} \mathsf{L}'^+_\mathbf{u} \right). \qquad (4.23)$$

(iii) In the new system thus obtained, we replace every series $\mathsf{K}_{\mathbf{w}}$ such that $\mathbf{w}$ is not balanced by 0, every series $\mathsf{L}_{\mathbf{w}}$ (resp. $\mathsf{L}'_{\mathbf{w}}$) such that $\mathbf{w}$ is balanced by $\mathsf{K}_{\mathbf{w}} + \mathsf{L}^+_{\mathbf{w}}$ (resp. $\mathsf{K}'_{\mathbf{w}} + \mathsf{L}'^+_{\mathbf{w}}$), and every series $\mathsf{L}'_{\mathbf{w}}$ such that $\mathbf{w}$ is quasi-balanced by $\mathsf{K}'_{\overline{\mathbf{w}}} + \mathsf{L}'^+_{\mathbf{w}}$. In particular, the series $L_{\mathbf{w}_p} - K_{\mathbf{w}_p}$ occurring in (4.23) becomes $L^+_{\mathbf{w}_p}$ when $\mathbf{w}_p$ is balanced, $L_{\mathbf{w}_p}$ otherwise. The series $\mathsf{L}_{\mathbf{w}}$ (resp. $\mathsf{L}'_{\mathbf{w}}$) that remain in the system are such that $\mathbf{w}$ has balance at least 1 (resp. 2).

We thus obtain a positive system, denoted S_1, defining the following series:

- $\mathsf{K}_{\mathbf{w}}$, for $\mathbf{w}$ balanced of length between 2 and $2k-2$,
- $\mathsf{K}'_{\mathbf{w}}$, for $\mathbf{w}$ balanced of length between 2 and $2k$,
- $\mathsf{L}_{\mathbf{w}}$ for $\mathbf{w}$ valid of balance at least 1 and length at most $2k-2$,
- $\mathsf{L}'_{\mathbf{w}}$ for $\mathbf{w}$ valid of balance at least 2 and length at most $2k-1$,
- $\mathsf{L}^+_{\mathbf{w}}$, for $\mathbf{w}$ balanced of length at most $2k-2$,
- $\mathsf{L}'^+_{\mathbf{w}}$, for $\mathbf{w}$ balanced or quasi-balanced of length at most $2k-1$.

For instance, when $k=1$ we obtain the following system:

$$\begin{cases} \mathsf{K}'_{10} &= t + t(1+\mathsf{L}^+_\varepsilon)(\mathsf{K}'_{10} + \mathsf{L}'^+_0) \\ \mathsf{L}^+_\varepsilon &= \mathsf{L}^+_\varepsilon \mathsf{L}'^+_\varepsilon + \mathsf{L}'^+_\varepsilon \\ \mathsf{L}'^+_\varepsilon &= 2t(1+\mathsf{L}^+_\varepsilon) + t(1+\mathsf{L}^+_\varepsilon)(\mathsf{L}'^+_\varepsilon + 2\mathsf{L}'^+_0) \\ \mathsf{L}'^+_0 &= t\mathsf{L}^+_\varepsilon + t(1+\mathsf{L}^+_\varepsilon)\mathsf{L}'^+_0 \,. \end{cases}$$

Recall that the series we are interested in is L^+_ε. But then we can drop the first equation of the above system. This size reduction occurs for any value of k, and the positive system S_2 that we will study is finally obtained by performing one last change:

(iv) Delete the equations defining the series $\mathsf{K}'_{\mathbf{w}}$, for $\mathbf{w}$ of length $2k$.

Observe that all the series involved in S_2 are well-defined by this system. This comes from the fact that all the series $\mathsf{K}'_{\mathbf{u}}$, for $\mathbf{u}$ of length $2k$, that occurred in S_0 came from the term $\mathsf{L}'_{\mathbf{u}_s} - \mathsf{K}'_{\mathbf{u}}$ of (4.18), which now reads $\mathsf{L}'^+_{\mathbf{u}_s}$.

Here is for instance the system obtained for $k=2$, which has three equations

less than (4.20):

$$\begin{cases} \mathsf{K}_{01} = \mathsf{K}_{10} &= \mathsf{K}'_{01} \\ \mathsf{K}'_{10} = \mathsf{K}'_{01} &= t + t(1+\mathsf{L}^+_\varepsilon)(\mathsf{K}'_{01} + \mathsf{L}'^+_1) \\ \mathsf{L}^+_\varepsilon &= \mathsf{L}^+_\varepsilon \mathsf{L}'^+_\varepsilon + \mathsf{L}'^+_\varepsilon \\ \mathsf{L}_0 &= (1+\mathsf{L}^+_\varepsilon)(\mathsf{K}'_{10} + \mathsf{L}'^+_0) \\ \mathsf{L}_{00} = \mathsf{L}_{11} &= (1+\mathsf{L}^+_\varepsilon)\mathsf{L}'_{00} \\ \mathsf{L}^+_{01} &= \mathsf{L}^+_\varepsilon(\mathsf{K}'_{01} + \mathsf{L}'^+_{01}) + \mathsf{L}'^+_{01} \\ \mathsf{L}'^+_\varepsilon &= 2t(1+\mathsf{L}^+_\varepsilon) + t(1+\mathsf{L}^+_\varepsilon)(\mathsf{L}'^+_\varepsilon + 2(\mathsf{L}'^+_0 + \mathsf{L}'^+_{100} + \mathsf{L}'^+_{010} + \mathsf{L}'^+_{110})) \\ \mathsf{L}'^+_0 = \mathsf{L}'^+_1 &= t\mathsf{L}^+_\varepsilon + t(1+\mathsf{L}^+_\varepsilon)(\mathsf{L}'^+_0 + \mathsf{L}'^+_{100} + \mathsf{L}'^+_{010} + \mathsf{L}'^+_{110}) \\ \mathsf{L}'_{00} &= t\mathsf{L}_0 + t(1+\mathsf{L}^+_\varepsilon)(\mathsf{L}'_{00} + \mathsf{L}'^+_{100}) \\ \mathsf{L}'^+_{10} = \mathsf{L}'^+_{01} &= t\mathsf{L}_1 + t(1+\mathsf{L}^+_\varepsilon)(\mathsf{L}'^+_{10} + \mathsf{L}'^+_{010} + \mathsf{L}'^+_{110}) \\ \mathsf{L}'^+_{100} &= t\mathsf{L}^+_{10} + t(1+\mathsf{L}^+_\varepsilon)\mathsf{L}'^+_{100} \\ \mathsf{L}'^+_{010} &= t\mathsf{L}^+_{01} + t(1+\mathsf{L}^+_\varepsilon)\mathsf{L}'^+_{010} \\ \mathsf{L}'^+_{110} &= t\mathsf{L}_{11} + t(1+\mathsf{L}^+_\varepsilon)\mathsf{L}'^+_{110}\,. \end{cases}$$

Let us now discuss properness [FS09, p. 489]. The system S_2 that we have just obtained is not proper. However, the right-hand sides of the equations that define series with a prime (K', L' and L'^+) are multiples of t (see (4.16), (4.18) and (4.23)). In the remaining equations, that is (4.15), (4.17) (for $\mathbf{w}$ not balanced) and (4.22) (for $\mathbf{w}$ balanced), each term on the right-hand side involves a series with a prime: hence after one iteration of S_2, one obtains a new system S_3 which is positive and proper.

Aperiodicity holds as in the previous section, and we are left with irreducibility. Note that proving irreducibility for S_2 or its iterated version S_3 is equivalent, so we focus on S_2. As in the previous section, we denote by $\tilde{\mathsf{L}}_\mathbf{w}$ the series $\mathsf{L}^+_\mathbf{w}$ or $\mathsf{L}_\mathbf{w}$, depending on whether $\mathbf{w}$ is balanced or not. Similarly, $\tilde{\mathsf{L}}'_\mathbf{w}$ denotes $\mathsf{L}'^+_\mathbf{w}$ if $\mathbf{w}$ is balanced or quasi-balanced, and $\mathsf{L}'_\mathbf{w}$ otherwise. Let us prove that all series depend on $\tilde{\mathsf{L}}_\varepsilon$. We first observe that this holds for every K'- or $\tilde{\mathsf{L}}$- or $\tilde{\mathsf{L}}'$-series (see (4.16), (4.17), (4.18), (4.22), (4.23)). We are left with the series $\mathsf{K}_\mathbf{w}$: but it depends on $\mathsf{K}'_\mathbf{w}$ (see (4.15)), and hence on $\tilde{\mathsf{L}}_\varepsilon$.

Conversely, let us prove that $\tilde{\mathsf{L}}_\varepsilon$ depends on every other series in the system. By (4.22), it depends on L'_ε. Then by (4.23) applied to $\mathbf{w} = \varepsilon$, it depends on every series $\mathsf{L}'_\mathbf{u}$, where $\mathbf{u}$ is quasi-balanced. Going back and forth between the equations defining the L- series and the L'-series (see (4.17), (4.18), (4.22), (4.23)), and using an induction on the balance, we then see that $\tilde{\mathsf{L}}_\varepsilon$ depends on all series $\tilde{\mathsf{L}}_\mathbf{u}$ (for $|\mathbf{u}| \leq 2k-2$) and all series $\tilde{\mathsf{L}}'_\mathbf{u}$ (for $|\mathbf{u}| \leq 2k-1$). Then the first term of (4.22), written as $\mathsf{L}^+_\varepsilon(\mathsf{K}'_\mathbf{w} + \mathsf{L}'^+_\mathbf{w})$, shows that $\tilde{\mathsf{L}}_\varepsilon$ depends on all series $\mathsf{K}'_\mathbf{v}$ with $|\mathbf{v}| \leq 2k-2$. It remains to prove that $\tilde{\mathsf{L}}_\varepsilon$ depends on the K-series. Let $\mathbf{u} = a\mathbf{u}_s$ be balanced of length at most $2k-2$, and define $\mathbf{w} = \mathbf{u}_s\bar{a}$. This word has balance 2. The second term of (4.18) involves $\mathsf{L}_{\mathbf{w}_p} = \mathsf{L}_{\mathbf{u}_s} = \mathsf{K}_\mathbf{u} + \mathsf{L}^+_{\mathbf{u}_s}$. Hence $\mathsf{L}'_\mathbf{w}$ depends on $\mathsf{K}_\mathbf{u}$, and by transitivity, $\tilde{\mathsf{L}}_\varepsilon$ depends on $\mathsf{K}_\mathbf{u}$. This proves the irreducibility of the system and concludes the proof of the proposition. □

4.3.4 Back to examples

We first return to the cases $k = 1$ and $k = 2$ studied in Section 4.3.2.

When $k = 1$, we obtained the cubic equation (4.19) for $\mathsf{L}_\varepsilon^{(1)}$. The discriminant has three positive roots, which are 1, (approximately) 0.094, and 15.9. The second one is the radius of convergence, and we obtain the lower bound $\bar{\lambda}_1 \simeq 10.603$ on the growth rate of Eulerian orientations. This improves significantly on the growth rate $\lambda_1 = 9.68\ldots$ obtained from the set $\mathcal{L}^{(1)}$.

For $k = 2$, we obtained the equation (4.21) satisfied by $\mathsf{L}_\varepsilon^{(2)}$. The discriminant has two roots in $(0, 1)$, which are approximately 0.0911 and 0.414. The first one is the radius of convergence, and we obtain the lower bound $\bar{\lambda}_2 \simeq 10.9759$ on the growth rate of Eulerian orientations.

When $k = 3$, we find that $\mathsf{L}_\varepsilon^{(3)}$ satisfies an equation of degree 20 (see the Maple sessions available on our web pages). The dominant coefficient only vanishes at $t = 8$, and the discriminant has only one relevant root, around 0.089. This gives the lower bound $\bar{\lambda}_3 \simeq 11.2289$ on the growth rate of Eulerian orientations.

For $k = 4$, we did not compute the equation satisfied by $\mathsf{L}_\varepsilon^{(4)}$, but we estimated $\bar{\lambda}_4$ from the first 30 coefficients of $\mathsf{L}_\varepsilon^{(4)}$ using quadratic approximants [BG90]. We predict $\bar{\lambda}_4 \simeq 11.41$. This value has then been confirmed by Bruno Salvy using the Maple package NewtonGF [PSS12], with which he obtained 10 digits of $\bar{\lambda}_4$. This package also allows us to compute more coefficients in $\mathsf{L}_\varepsilon^{(4)}$. Moreover, Jean-Charles Faugère [Fau16] has been able to determine the equation for $\mathsf{L}_\varepsilon^{(4)}$, which has degree 258 in $\mathsf{L}_\varepsilon^{(4)}$.

Similarly, we predict

$$\bar{\lambda}_5 \simeq 11.56, \qquad \bar{\lambda}_6 \simeq 11.68\,.$$

4.4 Supersets with standard decomposition

We now want to define and count supersets of Eulerian orientations. Their generating functions will be described by functional equations involving divided differences (as in (4.2)). The proof of their algebraicity is non-trivial and rely on a deep result from Artin's approximation theory (Theorem 4.13).

Recall that Eulerian orientations can be obtained recursively from the atomic map by either:

- the merge of two orientations $O_1, O_2 \in \mathcal{O}$ (with the root loop oriented in either way),
- or a legal split on an orientation $O' \in \mathcal{O}$.

We now define the sets $\mathcal{U}^{(k)}$. The idea is that we allow illegal i-splits, provided i is larger than k.

Definition 4.4. Let $k \geq 1$. Let $\mathcal{U}^{(k)}$ be the set of planar orientations obtained recursively from the atomic map by either:

- the merge of two orientations $O_1, O_2 \in \mathcal{U}^{(k)}$ (with the root loop oriented in either way),
- or a legal i-split on a map $O' \in \mathcal{U}^{(k)}$ with $i \leq k$ (small split),
- or an arbitrary split on a map $O' \in \mathcal{U}^{(k)}$ with $i > k$ (large split). If the split is legal, the root edge is oriented in the only way that makes the new orientation Eulerian. Otherwise, it is oriented away from the root vertex.

Observe that all Eulerian orientations belong to $\mathcal{U}^{(k)}$. Moreover, the sets $\mathcal{U}^{(k)}$ form a decreasing sequence, as fewer illegal splits are performed as k grows. Finally, for $k \geq n$ (and even for $k \geq n-2$), all orientations of size n in $\mathcal{U}^{(k)}$ are Eulerian. Hence the limit of the sets $\mathcal{U}^{(k)}$ is the set $\mathcal{O}$ of all Eulerian orientations.

Another important observation is that, if the root vertex of an orientation of $\mathcal{U}^{(k)}$ has degree at most $2k$, then the root word of this orientation is balanced.

4.4.1 Functional equations for $\mathcal{U}^{(k)}$

We now fix an integer k. For a word $\mathbf{w}$ on $\{0,1\}$, let $U^{(k)}_{\mathbf{w}}(t;x) \equiv U_{\mathbf{w}}(x)$ denote the generating function of orientations of $\mathcal{U}^{(k)}$ whose root word ends with $\mathbf{w}$, counted by the edge number (variable t) and the half-degree of the root vertex (variable x). Let $T^{(k)}_{\mathbf{w}}(t) \equiv T_{\mathbf{w}}$ denote the generating function of orientations of $\mathcal{U}^{(k)}$ having root word exactly $\mathbf{w}$. We do not record in this series the root degree (which is the length of $\mathbf{w}$). To lighten notation, we often denote simply by $U_{\mathbf{w}}$ the edge generating function $U_{\mathbf{w}}(1) \equiv U_{\mathbf{w}}(t,1)$, and by $U^x_{\mathbf{w}}$ the refined generating function $U_{\mathbf{w}}(x) \equiv U_{\mathbf{w}}(t;x)$.

Note that $T_{\mathbf{w}} = 0$ if $\mathbf{w}$ is not balanced and that $T_\varepsilon = 1$. Now, for $\mathbf{w}$ balanced of length between 2 and $2k$, we have

$$T_{\mathbf{w}} = t \sum_{a\mathbf{u}\bar{a}\mathbf{v}=\mathbf{w}} T_{\mathbf{u}} T_{\mathbf{v}} + t U_{\mathbf{w}_s}. \tag{4.24}$$

The first term counts orientations obtained by a merge. The second one counts those obtained by a split, which is necessarily small since we have assumed $|\mathbf{w}| \leq 2k$. Note the analogy with (4.5).

For $\mathbf{w}$ valid of length at most $2k-1$, let us now prove the following identity:

$$\begin{aligned} U^x_{\mathbf{w}} = \mathbb{1}_{\mathbf{w}=\varepsilon} + 2txU^x_\varepsilon U^x_{\mathbf{w}} + tx \sum_{\mathbf{w}=\mathbf{u}a\mathbf{v}} U^x_{\mathbf{u}} x^{|\mathbf{v}|/2} T_{\mathbf{v}} + tx^{|\mathbf{w}|/2} \sum_{\mathbf{w}=a\mathbf{u}\bar{a}\mathbf{v}} T_{\mathbf{u}} T_{\mathbf{v}} \\ + t \sum_{\substack{\mathbf{u}=\mathbf{v}\mathbf{w} \\ 2\leq|\mathbf{u}|\leq 2k \\ \mathbf{u}\text{ balanced}}} x^{|\mathbf{u}|/2} U_{\mathbf{u}_s} + \frac{tx}{x-1}\left(U^x_{\mathbf{w}} - x^k U_{\mathbf{w}}\right) - \frac{tx}{x-1} \sum_{\substack{\mathbf{u}=\mathbf{v}\mathbf{w} \\ |\mathbf{u}|\leq 2k-2}} T_{\mathbf{u}}(x^{|\mathbf{u}|/2} - x^k). \end{aligned} \tag{4.25}$$

The first line is similar to the first line of (4.6): it counts the atomic map and orientations obtained from a merge. The only difference is that we now record the root degree. On the second line, the first sum counts orientations obtained by a

small split (with root word $\mathbf{u}$). Let us explain the remaining terms, which count orientations obtained by a large split, legal or not, of an orientation O' whose root word ends (necessarily) with $\mathbf{w}$. Given an orientation O' with root vertex degree $2d$, with $d > k$, the generating function of orientations obtained from O' by a large split is

$$t^{1+\mathrm{e}(O')}\left(x^{k+1}+x^{k+2}+\cdots+x^{d}\right) = t^{1+\mathrm{e}(O')}\,\frac{x^{d+1}-x^{k+1}}{x-1}\,.$$

Let us underline that we cannot apply a large split to an orientation O' whose root word $\mathbf{u}$ satisfies $|\mathbf{u}| \leq 2k$. Hence the generating function of orientations obtained by a large split is

$$\frac{tx}{x-1}\left(\left(U^x_{\mathbf{w}} - \sum_{\mathbf{u}=\mathbf{vw},|\mathbf{u}|\leq 2k} x^{|\mathbf{u}|/2}T_{\mathbf{u}}\right) - x^k\left(U_{\mathbf{w}} - \sum_{\mathbf{u}=\mathbf{vw},|\mathbf{u}|\leq 2k} T_{\mathbf{u}}\right)\right),$$

which gives the last two terms of (4.25) (the terms $T_{\mathbf{u}}$ with $|\mathbf{u}| = 2k$ do not contribute).

Remark 4.10. In the proof of (4.25), we have tried to follow the same steps as in the proof of (4.6). However, comparing (4.24) and (4.25) suggests to replace (4.25) by a lighter equation:

$$U^x_{\mathbf{w}} = x^{|\mathbf{w}|/2}T_{\mathbf{w}} + 2txU^x_\varepsilon U^x_{\mathbf{w}} + tx\sum_{\mathbf{w}=\mathbf{u}a\mathbf{v}} U^x_{\mathbf{u}}x^{|\mathbf{v}|/2}T_{\mathbf{v}} + t\sum_{\substack{\mathbf{u}=\mathbf{vw}\\ |\mathbf{u}|\leq 2k-1\\ \mathbf{u}\text{ quasi-balanced}}} x^{(1+|\mathbf{u}|)/2}U_{\mathbf{u}}$$
$$+\frac{tx}{x-1}\left(U^x_{\mathbf{w}} - x^kU_{\mathbf{w}}\right) - \frac{tx}{x-1}\sum_{\substack{\mathbf{u}=\mathbf{vw}\\ |\mathbf{u}|\leq 2k-2}} T_{\mathbf{u}}(x^{|\mathbf{u}|/2}-x^k). \quad (4.26)$$

Proposition 4.11. Consider the collection of equations consisting of:

- Equation (4.24), written for all balanced words $\mathbf{w}$ of length between 2 and $2k-2$,
- Equation (4.26), written for all valid words $\mathbf{w}$ of length at most $2k-1$.

In this collection, replace all trivial T-series by their value: $T_{\mathbf{w}} = 0$ when $\mathbf{w}$ is not balanced, $T_\varepsilon = 1$. Let R_0 denote the resulting system. The number of series it involves is $f(k) - \binom{2k}{k}$, where $f(k)$ is given by (4.7). Moreover, R_0 defines uniquely these series. Its size can be (roughly) divided by two upon exploiting the $0/1$ symmetry.

The proof is similar to the proof of Proposition 4.1.

Remark 4.12. As in Remark 4.2, if $\mathbf{w}$ is such that $0\mathbf{w}$ and $1\mathbf{w}$ are both valid of length less than $2k$, we can replace (4.26) by the simpler forward equation:

$$U^x_{\mathbf{w}} = x^{|\mathbf{w}|/2}T_{\mathbf{w}} + U^x_{0\mathbf{w}} + U^x_{1\mathbf{w}}\,.$$

This does not increase the size of the system.

4.4.2 Algebraicity

Since the early work of Brown in the sixties on the *quadratic method* [Bro65], a lot has been known about equations involving divided differences of the form $\dfrac{F(t;x)-F(t;1)}{x-1}$. However, most of the literature deals with a single equation, not with a system [BMJ06; GJ83b]. In order to prove that the series $U_\varepsilon^{(k)}(t;x)$ that counts orientations of $\mathcal{U}^{(k)}$ is algebraic, we use a deep theorem from Artin's approximation theory, due to Popescu [Swa98]. The form we will need is given below. We recall that $\mathbb{C}[[z_1,\dots,z_\ell]]$ is the ring of formal power series in the variables $z_1,\dots,z_\ell$, with complex coefficients, and that a series Z in this ring is *algebraic* if it satisfies a non-trivial polynomial equation $\mathrm{Pol}(z_1,\dots,z_\ell,Z)=0$.

Theorem 4.13 ([Swa98]). *Consider a polynomial system of n equations in $\ell+n$ variables over $\mathbb{C}$, written as $P_i(z_1,\dots,z_\ell,y_1,\dots,y_n)=0$, for $1\le i\le n$. Let $(d_1,\dots,d_n)$ be a sequence of integers in $\{0,1,\dots,\ell\}$. Assume that there exists an n-tuple $\mathcal{Y}=(Y_1,\dots,Y_n)$ of series in $\mathbb{C}[[z_1,\dots,z_\ell]]$ that satisfies the following conditions:*

- *the n-tuple $\mathcal{Y}$ solves this system, that is,*

$$P_i(z_1,\dots,z_\ell,Y_1,\dots,Y_n)=0 \qquad \text{for } 1\le i\le n,$$

- *for $1\le i\le n$, the series Y_i does not depend on the variables z_j such that $j>d_i$ (if $d_i=\ell$, then there is no condition on the series Y_i).*

Then there exists an n-tuple $(Z_1,\dots,Z_n)$ of algebraic *series in $\mathbb{C}[[z_1,\dots,z_\ell]]$ that solves the system and satisfies the same dependence conditions as $\mathcal{Y}$.*

In particular, if the system has a unique solution satisfying the dependence conditions, then this solution is algebraic.

An application. To our knowledge, this theorem has not been applied yet in a combinatorial context. So, before we use it to prove the algebraicity of $U_\varepsilon^{(k)}(t;x)$, let us examine its application to a simple equation, namely (4.2), which we recall now:

$$M(t;x)=1+txM(t;x)^2+\frac{tx}{x-1}(M(t;x)-M(t;1))\,. \tag{4.2}$$

First, observe that the algebraicity of $M(t;x)$ is not obvious. Clearly, if we could prove that $M(t;1)$ is algebraic, we would be done with $M(t;x)$ as well, but why should $M(t;1)$ be algebraic? We can apply the above theorem as follows. Let us denote $t=z_1$ and $x=1+z_2$ (we shall explain later why we need to translate the variable x). We now consider the system in z_1, z_2, y_1 and y_2 consisting of the following (single) equation:

$$z_2y_2=z_2+z_1z_2(1+z_2)y_2^2+z_1(1+z_2)(y_2-y_1).$$

Take $d_1=1$ and $d_2=2$. Then (4.2) shows that the pair $(Y_1,Y_2):=(M(t;1),M(t;x))$ solves the above equation. Moreover $Y_1=M(t;1)$ is independent of $z_2=x-1$,

while $Y_2 = M(t;x)$ depends on both variables z_1 and z_2, in accordance with $d_1 = 1$ and $d_2 = 2$.

Let us now prove that there cannot be another solution of this system in the ring $\mathbb{C}[[z_1, z_2]]$ such that Y_1 is independent of z_2. First, setting $z_2 = 0$ in the equation shows that Y_1 must be the specialization of Y_2 at $z_2 = 0$. This, combined with the factor z_1 occurring in every non-initial term in the right-hand side, implies that the coefficient of z_1^n in Y_2 can be computed by induction of n, starting from the constant coefficient 1. Hence the uniqueness of (Y_1, Y_2). The algebraicity of $M(t;x)$ now follows from the above theorem.

Note that, if we had used $z_2 = x$ instead of $z_2 = x - 1$, we could not apply the last part of Theorem 4.13. The equation would read

$$(z_2 - 1)y_2 = (z_2 - 1) + z_1(z_2 - 1)z_2y_2^2 + z_1z_2(y_2 - y_1),$$

but this equation has many solutions in the ring $\mathbb{C}[[z_1, z_2]]$ of formal power series in $z_1 = t$ and $z_2 = x$. For instance, one can take $Y_1 = 0$ and

$$Y_2 = \frac{1 - x + tx - \sqrt{(1 - x + tx)^2 - 4tx(1 - x)^2}}{2tx(1 - x)}.$$

Theorem 4.13 tells us that at least one of these solutions is algebraic, but we need uniqueness to conclude that *our* solution is algebraic. The key point is that a series in $\mathbb{C}[[z_1, z_2]]$ can always be specialized at $z_2 = 0$, but not at $z_2 = 1$.

We now apply Theorem 4.13 to the larger example of orientations of $\mathcal{U}^{(k)}$.

Proposition 4.14. For any $k \geq 1$, the generating function $U_\varepsilon^{(k)}(t;x)$ that counts orientations of $\mathcal{U}^{(k)}$ is algebraic.

Proof. Again, we take as variables $z_1 = t$ and $z_2 = x - 1$. For short, we denote z_2 by z. We consider the polynomial system consisting of the following equations, which mimic (4.24) and (4.26). For $\mathbf{w}$ balanced of length between 2 and $2k - 2$,

$$A_{\mathbf{w}} = t \sum_{a\mathbf{u}\bar{a}\mathbf{v}=\mathbf{w}} A_{\mathbf{u}}A_{\mathbf{v}} + tC_{\mathbf{w}_s},$$

and for $\mathbf{w}$ valid of length at most $2k - 1$,

$$\begin{aligned} zB_{\mathbf{w}} = z(1+z)^{|\mathbf{w}|/2}A_{\mathbf{w}} + 2tz(1+z)B_\varepsilon B_{\mathbf{w}} + tz(1+z)\sum_{\mathbf{w}=\mathbf{u}a\mathbf{v}} B_{\mathbf{u}}(1+z)^{|\mathbf{v}|/2}A_{\mathbf{v}} \\ + tz \sum_{\substack{\mathbf{u}=\mathbf{v}\mathbf{w}\,|\mathbf{u}|\leq 2k-1 \\ \mathbf{u} \text{ quasi-balanced}}} (1+z)^{(1+|\mathbf{u}|)/2}C_{\mathbf{u}} + t(1+z)\left(B_{\mathbf{w}} - (1+z)^k C_{\mathbf{w}}\right) \\ - t(1+z) \sum_{\substack{\mathbf{u}=\mathbf{v}\mathbf{w} \\ |\mathbf{u}|\leq 2k-2}} A_{\mathbf{u}}\left((1+z)^{|\mathbf{u}|/2} - (1+z)^k\right), \end{aligned} \tag{4.27}$$

where $A_\varepsilon = 1$. The variables $A_{\mathbf{w}}$, $B_{\mathbf{w}}$ and $C_{\mathbf{w}}$ play the role of the y_i in Theorem 4.13. By construction, the series

$$A_{\mathbf{w}} := T_{\mathbf{w}}(t), \qquad B_{\mathbf{w}} := U_{\mathbf{w}}(t; 1+z), \quad C_{\mathbf{w}} := U_{\mathbf{w}}(t; 1)$$

solve the system. Moreover, $A_{\mathbf{w}}$ and $C_{\mathbf{w}}$ do not depend on $z_2 = z$.

By Theorem 4.13, it suffices to prove that the system in A, B, C has a unique solution in $\mathbb{C}[[t, z]]$ satisfying these dependence relations to conclude that all our series T and U counting orientations are algebraic.

So assume that $A_{\mathbf{w}}$, $B_{\mathbf{w}}$ and $C_{\mathbf{w}}$ solve the system and satisfy the required dependences. Then by setting $z = 0$ in (4.27), we see that $C_{\mathbf{w}}$ must be the specialization of $B_{\mathbf{w}}$ at $z = 0$, for all $\mathbf{w}$ valid of length at most $2k - 1$. Then the form of the system implies that the coefficient of t^n in all series can be computed by induction on n, the initial values being $B_\varepsilon = C_\varepsilon = 1 + O(t)$ and $A_{\mathbf{w}} = B_{\mathbf{w}} = C_{\mathbf{w}} = O(t)$ for $\mathbf{w}$ non-empty (recall that we have set $A_\varepsilon = 1$). This proves the uniqueness of the solution (with the required dependences) and concludes the proof. □

4.4.3 Examples

The case $k = 1$.

When $k = 1$, the system of Proposition 4.11 contains $f(1) - 2 = 3$ equations. Upon exploiting the $0/1$ symmetry, it reads:

$$\begin{cases} U_\varepsilon^x &= 1 + 2tx(U_\varepsilon^x)^2 + 2txU_0 + \frac{tx}{x-1}(U_\varepsilon^x - xU_\varepsilon) + tx \\ U_0^x &= 2txU_\varepsilon^x U_0^x + txU_\varepsilon^x + txU_0 + \frac{tx}{x-1}(U_0^x - xU_0)\,. \end{cases} \tag{4.28}$$

Replace U_0 by $(U_\varepsilon - 1)/2$ to obtain a single equation involving only $U_\varepsilon^x = U_\varepsilon(x)$ and $U_\varepsilon = U_\varepsilon(1)$ (the second equation of System (4.28) can be removed). For simplicity, we now drop the index ε. This equation reads:

$$\mathrm{Pol}(U(x), U(1), t, x) = 0\,,$$

with

$$\begin{aligned} \mathrm{Pol}(x_0, x_1, t, x) = (x-1)(-x_0 + 1 + 2txx_0^2 + tx(x_1 - 1)) \\ + tx(x_0 - xx_1) + tx(x-1)\,. \end{aligned} \tag{4.29}$$

We apply Brown's *quadratic method*. Its principle is the following: if there exists a formal power series $X \equiv X(t)$ such that

$$\mathrm{Pol}_{x_0}(U(X), U(1), t, X) = 0\,, \tag{4.30}$$

then this series X must be a double root of the discriminant $\Delta(U(1), t, x)$ of $\mathrm{Pol}(x_0, U(1), t, x)$ with respect to x_0 (the notation Pol_{x_0} stands for the derivative of Pol with respect to its first variable). The proof can be found in [GJ83b, Sec. 2.9] or [BMJ06]. Equation (4.30) thus reads

$$X = 1 + tX + 4tX(X-1)U(X)\,,$$

and has a unique power series solution $X(t)$, whose coefficients can be computed by induction from those of $U(x)$ (we do not need to determine X, just to know that it exists). Thus X is a double root of $\Delta(U(1), t, x)$, and hence the discriminant in x

of Δ must vanish. This gives the following cubic equation for $U(1)$ (see our Maple sessions):

$$64t^3U(1)^3 + 2t(24t^2 - 36t + 1)U(1)^2 + (-15t^3 + 9t^2 + 19t - 1)U(1) \\ + t^3 + 27t^2 - 19t + 1 = 0\,. \qquad (4.31)$$

The series $U(1)$ has a unique positive singularity τ_1, around 0.0765, which is a root of $216t^3 - 81t^2 + 18t - 1$. This gives the upper bound $\mu_1 = 1/\tau_1 = 13.0659\cdots$ on the growth rate of Eulerian orientations. Expanding the series near τ_1 (using for instance the Maple function `algeqtoseries` [SZ94]) shows that it has a singularity in $(1-\mu_1 t)^{3/2}$, as the generating function of many families of planar maps.

The case $k = 2$.

When $k = 2$, the system of Proposition 4.11 contains $f(2) - 6 = 15$ equations. Upon exploiting the $0/1$ symmetry and (some) forward equations, it reads:

$$\begin{cases} T_{10} &= t + tU_0 \\ U^x_\varepsilon &= 1 + 2U^x_0 \\ U^x_0 = U^x_1 &= 2txU^x_\varepsilon U^x_0 + txU^x_\varepsilon + txU_0 + tx^2(U_{100} + U_{010} + U_{110}) \\ &\qquad + \tfrac{tx}{x-1}(U^x_0 - x^2U_0) + tx^2T_{10} \\ U^x_{10} = U^x_{01} &= xT_{10} + U^x_{110} + U^x_{010} \\ &= xT_{10} + 2txU^x_\varepsilon U^x_{10} + txU^x_1 + tx^2(U_{010} + U_{110}) \\ &\qquad + \tfrac{tx}{x-1}(U^x_{10} - x^2U_{10}) + tx^2T_{10} \\ U^x_{00} = U^x_{11} &= 2txU^x_\varepsilon U^x_{00} + txU^x_0 + tx^2U_{100} + \tfrac{tx}{x-1}(U^x_{00} - x^2U_{00}) \\ U^x_{100} &= 2txU^x_\varepsilon U^x_{100} + txU^x_{10} + tx^2U_{100} + \tfrac{tx}{x-1}(U^x_{100} - x^2U_{100}) \\ U^x_{010} &= 2txU^x_\varepsilon U^x_{010} + tx\,(U^x_{01} + U^x_\varepsilon xT_{10}) + tx^2U_{010} + \tfrac{tx}{x-1}(U^x_{010} - x^2U_{010}) \\ U^x_{110} &= 2txU^x_\varepsilon U^x_{110} + tx\,(U^x_{11} + U^x_\varepsilon xT_{10}) + tx^2U_{110} + \tfrac{tx}{x-1}(U^x_{110} - x^2U_{110})\,. \end{cases} \qquad (4.32)$$

Observe that we can reduce it to a system of three equations defining the series $U^x_\varepsilon, U^x_{10}$ and U^x_{100}:

$$\begin{cases} U^x_\varepsilon &= 1 + 4txU^x_\varepsilon U^x_0 + 2txU^x_\varepsilon + 2txU_0 + 2tx^2(U_{100} + U_{10}) + \tfrac{2tx}{x-1}(U^x_0 - x^2U_0) \\ U^x_{10} &= xt(1 + U_0) + 2txU^x_\varepsilon U^x_{10} + txU^x_0 + tx^2U_{10} + \tfrac{tx}{x-1}(U^x_{10} - x^2U_{10}) \\ U^x_{100} &= 2txU^x_\varepsilon U^x_{100} + txU^x_{10} + tx^2U_{100} + \tfrac{tx}{x-1}(U^x_{100} - x^2U_{100})\,, \end{cases} \qquad (4.33)$$

in which we still need to plug

$$U_0 = \frac{U_\varepsilon - 1}{2} \qquad \text{and} \qquad U^x_0 = \frac{U^x_\varepsilon - 1}{2}\,. \qquad (4.34)$$

To solve this system, we could develop a matrix analogue of the quadratic method, where (4.30) would be replaced by the cancellation of the Jacobian of the system. However, we prefer a step by step approach here, among other reasons because our system is not generic (its Jacobian has a multiple root).

From now on, we lighten notation by denoting $A = U_\varepsilon^x$, $A_1 = U_\varepsilon$, $B = U_{10}^x$, $B_1 = U_{10}$, $C = U_{100}^x$ and $C_1 = U_{100}$. We will determine three polynomial equations relating the one-variable series A_1, B_1 and C_1, and then eliminate B_1 and C_1 to obtain a polynomial equation satisfied by $A_1 = U_\varepsilon$.

We now describe the various steps of our calculation, without giving the intermediate equations: we refer to our web pages for a Maple session where the calculations are performed.

The first equation of (4.33), after injecting (4.34), involves only one x-dependent series, namely $A = U_\varepsilon^x = U_\varepsilon(x)$. Once the denominators are cleared out, the degree in A is 2, and we can apply the quadratic method of Section 4.4.3: the discriminant (in x) of a certain discriminant (in x_0) vanishes, and this gives a first equation between A_1, B_1 and C_1.

We then move to the second equation of (4.33), which (after injecting (4.34)) involves two x-dependent series, namely A and B. It is linear in the latter series, with coefficient:

$$1 - x + tx + 2tx(x-1)A\,. \tag{4.35}$$

This coefficient vanishes for a (unique) series in t, denoted X, satisfying

$$X = 1 + tX + 2tX(X-1)A_2, \qquad \text{with } A_2 := U_\varepsilon(X)\,.$$

Replacing x by X in the second equation of (4.33) gives another equation between X and A_2, from which we compute

$$2t(A_1 - 2B_1)X^2 + (1 - t - 2tA_1)X = 1\,, \tag{4.36}$$

$$A_2 = \frac{2XB_1}{X-1} - A_1\,.$$

We now eliminate X and A_2 between the last two identities and the first equation of (4.33), specialized at $x = X$. This gives a second equation between our three main unknown series A_1, B_1 and C_1.

We finally consider the third equation of (4.33) (after injecting (4.34)), which now involves all three x-dependent series. It is linear in C, again with coefficient (4.35). Setting $x = X$ in this equation gives an expression of $U_{10}(X)$:

$$B_2 := U_{10}(X) = XC_1/(X-1)\,.$$

We now get back to the second equation of (4.33), differentiate it with respect to x and set $x = X$. Replacing B_2 and A_2 by the above expressions gives:

$$\begin{aligned} A_2' &:= \frac{\partial U_\varepsilon}{\partial x}(X) \\ &= \frac{2}{t(X-1)^2(4C_1X + X - 1)}\big\{2C_1t(2X-1)(X-1)A_1 - 4Xt(2X-1)B_1C_1 \\ &\qquad\qquad - B_1t(X-1) - (t-1)(X-1)C_1\big\}\,. \end{aligned} \tag{4.37}$$

It remains to differentiate the first equation of (4.33) with respect to x, specialize it at $x = X$, and plug the above values of A_2', B_2 and A_2 to obtain one more equation

between A_1, B_1, C_1 and X. Eliminating X thanks to (4.36) gives our third and last equation between A_1, B_1 and C_1.

From this system, we eliminate B_1 and C_1, and obtain an equation of degree 27 for $A_1 = U_\varepsilon$. Its dominant coefficient does not vanish away from 0, and its discriminant has three roots in $[1/10, 1/16]$ (where we know that the radius must be found), respectively located around 0.07509, 0.07658 and 0.07727. Following numerically the branches that start from 1 at $t = 0$ shows that the radius of U_ε is the second one, giving the upper bound $\mu_2 = 13.057\ldots$ on the growth rate μ of Eulerian orientations. From numerical estimates of the singular exponent, we predict that the series has again a "planar map" singularity in $(1 - \mu_2 t)^{3/2}$. This is known to hold for many series satisfying an equation with divided differences [DN11]. This leads us to complete Proposition 4.14 as follows.

Conjecture 4.15. For every k, the algebraic series $U_\varepsilon^{(k)}(t; 1)$ that counts orientations of $\mathcal{U}^{(k)}$ has a unique dominant singularity $\tau_k = 1/\mu_k$ which is of the planar map type: as t approaches τ_k from below,

$$U_\varepsilon^{(k)}(t; 1) = c_0 + c_1(1 - \mu_k t) + c_2(1 - \mu_k t)^{3/2}\big(1 + o(1)\big)$$

with $c_2 \neq 0$.

4.5 Supersets with prime decomposition

In this section, we combine the illegal large splits of the previous section with the prime decomposition of Section 4.1.2 to obtain a new family of supersets of Eulerian orientations. These new supersets $\mathbb{U}^{(k)}$ satisfy $\mathbb{U}^{(k)} \subset \mathcal{U}^{(k)}$ (Proposition 4.16), hence they give better bounds on the growth rate μ than those obtained from the standard decomposition. Many arguments are similar to those of the previous section, and we give fewer details.

Recall from Section 4.1.2 that an Eulerian orientation is a sequence of prime Eulerian orientations, and that a prime (Eulerian) orientation can be obtained recursively from the atomic map by either:

- adding a loop, oriented in either way, around an orientation O_1,
- or a legal split on a prime orientation $O' \in \mathcal{O}$, followed by the concatenation of an arbitrary Eulerian orientation O'' at the new vertex created by the split (Figure 4.7).

Definition 4.5. Let $k \geq 1$. Let $\mathbb{U}^{(k)}$ be the set of planar orientations obtained recursively from the atomic map by either:

- concatenating a sequence of prime orientations of $\mathbb{U}^{(k)}$,
- or adding a loop, oriented in either way, around an orientation O_1 of $\mathbb{U}^{(k)}$,
- or performing a legal i-split on a prime orientation $O' \in \mathbb{U}^{(k)}$, with $i \leq k$, followed by the concatenation of an arbitrary orientation O'' of $\mathbb{U}^{(k)}$ at the new vertex created by the split (small split),
- or performing an arbitrary i-split on a prime orientation $O' \in \mathbb{U}^{(k)}$, with $i > k$, followed by the concatenation of an arbitrary orientation $O''$of $\mathbb{U}^{(k)}$ at the new vertex created by the split (large split). If the split is legal, then the new edge is given the only orientation that makes the root word balanced, otherwise the root edge is oriented away from the root vertex.

Again, the sets $\mathbb{U}^{(k)}$ decrease to the set $\mathcal{O}$ of all Eulerian orientations as k increases, hence their growth rates $\bar{\mu}_k$ form a non-increasing sequence of upper bounds on μ. We do not know if this sequence converges to μ. At any rate, the convergence appears to be rather slow, as shown by the estimates of $\bar{\mu}_k$ in Table 4.1.

Proposition 4.16. For $k \geq 1$, the superset of orientations $\mathbb{U}^{(k)}$ is contained in the superset $\mathcal{U}^{(k)}$ defined in Section 4.4.

Proof. We prove this by induction on the number of edges. The inclusion is obvious for orientations with no edges. Now let $O \in \mathbb{U}^{(k)}$, having at least one edge.

If O is prime and is obtained by adding a loop around a smaller orientation O_1 of $\mathbb{U}^{(k)}$ (second construction in Definition 4.5), then O_1 belongs to $\mathcal{U}^{(k)}$ by the induction hypothesis, and so does O (first construction in Definition 4.4).

Assume now that O is prime and is obtained by an i-split in a prime orientation O' of $\mathbb{U}^{(k)}$, followed by the concatenation of an orientation O'' of $\mathbb{U}^{(k)}$ at the new vertex (third or fourth construction in Definition 4.5). Then the orientation $\tilde{O}$ obtained by concatenating O' and O'' at their root belongs to $\mathbb{U}^{(k)}$ (first construction in $\mathbb{U}^{(k)}$) and hence to $\mathcal{U}^{(k)}$ by the induction hypothesis. But then one can recover O by performing an i-split in $\tilde{O}$, which is allowed in $\tilde{O}$ as it was allowed in O'. This is the second construction in Definition 4.4, hence O is in $\mathcal{U}^{(k)}$.

Assume finally that O is obtained by concatenating a prime orientation P of $\mathbb{U}^{(k)}$ and another orientation O_2 of $\mathbb{U}^{(k)}$ (first construction in Definition 4.5). By the induction hypothesis, both P and O_2 are in $\mathcal{U}^{(k)}$. If the root edge of P is a loop, deleting it from P leaves an orientation O_1 which is in $\mathcal{U}^{(k)}$. Then we can reconstruct O by a merge of O_1 and O_2 as in the first construction of Definition 4.4. If the root edge of P is not a loop (Figure 4.10), then P was obtained by the third or fourth construction in Definition 4.5: allowed split in a prime orientation P' of $\mathbb{U}^{(k)}$, followed by the concatenation of some $O'' \in \mathbb{U}^{(k)}$ at the new vertex. Let $\tilde{O}$ be obtained by concatenating O'', P' and O_2 (in counterclockwise order) at their roots. Then $\tilde{O}$ is in $\mathbb{U}^{(k)}$, but also in $\mathcal{U}^{(k)}$ by the induction hypothesis. Then O can be recovered by a split in $\tilde{O}$, which is allowed in $\tilde{O}$ as it was allowed in P' (the split may have been small in P' and become large in $\tilde{O}$, because of the orientation O_2, but

the converse is not possible). This is the second construction in Definition 4.4, hence O is in $\mathcal{U}^{(k)}$. □

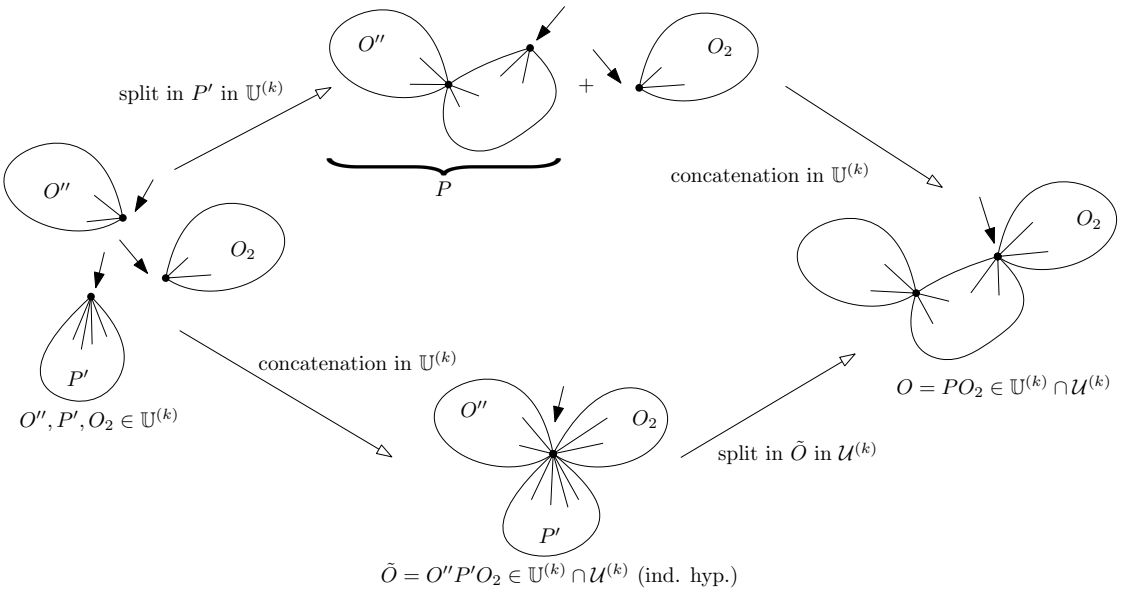

Figure 4.10: Two constructions of the orientation O: (top) in $\mathbb{U}^{(k)}$, via an i-split, (bottom) in $\mathcal{U}^{(k)}$, via a j-split, with $j = i + \mathrm{dv}(O_2)$.

4.5.1 Functional equations for $\mathbb{U}^{(k)}$

We now fix an integer k. For a word $\mathbf{w}$ on $\{0, 1\}$, let $\mathsf{U}^{(k)}_{\mathbf{w}}(t; x) \equiv \mathsf{U}_{\mathbf{w}}(x)$ denote the generating function of orientations of $\mathbb{U}^{(k)}$ whose root word ends with $\mathbf{w}$, counted by the edge number (variable t) and the half-degree of the root vertex (variable x). Let $\mathsf{T}^{(k)}_{\mathbf{w}}(t) \equiv \mathsf{T}_{\mathbf{w}}$ denote the generating function of orientations of $\mathbb{U}^{(k)}$ having root word exactly $\mathbf{w}$. We define analogous generating functions $\mathsf{U}'_{\mathbf{w}}(x)$ and $\mathsf{T}'_{\mathbf{w}}$ for prime orientations. As in the previous section, we often denote simply by $\mathsf{U}_{\mathbf{w}}$ (resp. $\mathsf{U}'_{\mathbf{w}}$) the edge generating function $\mathsf{U}_{\mathbf{w}}(t; 1)$ (resp. $\mathsf{U}'_{\mathbf{w}}(t; 1)$), and by $\mathsf{U}^x_{\mathbf{w}}$ (resp. $\mathsf{U}'^x_{\mathbf{w}}$) the refined generating function $\mathsf{U}_{\mathbf{w}}(t; x)$ (resp. $\mathsf{U}'_{\mathbf{w}}(t; x)$).

Note that $\mathsf{T}_{\mathbf{w}} = \mathsf{T}'_{\mathbf{w}} = 0$ if $\mathbf{w}$ is not balanced and that $\mathsf{T}_\varepsilon = 1$, $\mathsf{T}'_\varepsilon = 0$. For $\mathbf{w}$ balanced of length between 2 and $2k$, we have both a sequential equation

$$\mathsf{T}_{\mathbf{w}} = \sum_{\mathbf{w}=\mathbf{uv}} \mathsf{T}_{\mathbf{u}}\mathsf{T}'_{\mathbf{v}} \tag{4.38}$$

analogous to (4.15), and an equation for prime orientations:

$$\mathsf{T}'_{\mathbf{w}} = t\mathsf{T}_{\mathbf{w}_c} + t\mathsf{U}_\varepsilon\mathsf{U}'_{\mathbf{w}_s}, \tag{4.39}$$

analogous to (4.16). The factor U_ε accounts for the orientation concatenated after a split.

For $\mathbf{w}$ valid of length at most $2k-1$, we have a sequential equation, analogous to (4.17) but taking care of the root degree:

$$\mathsf{U}^x_{\mathbf{w}} = \mathbb{1}_{\mathbf{w}=\varepsilon} + \mathsf{U}^x_\varepsilon \mathsf{U}'^x_{\mathbf{w}} + \sum_{\mathbf{w}=\mathbf{uv},\mathbf{v}\neq\mathbf{w}} \mathsf{U}^x_{\mathbf{u}} x^{|\mathbf{v}|/2}\mathsf{T}'_{\mathbf{v}}. \tag{4.40}$$

Finally, we have the following equation for prime orientations, which is the counterpart of (4.18) and involves ingredients of (4.25) for orientations obtained by a split:

$$\begin{aligned}\mathsf{U}'^x_{\mathbf{w}} &= 2tx\mathsf{U}^x_\varepsilon \mathbb{1}_{\mathbf{w}=\varepsilon} + tx\mathsf{U}^x_{\mathbf{w}_p}\mathbb{1}_{\mathbf{w}\neq\varepsilon} + tx^{|\mathbf{w}|/2}\mathsf{T}_{\mathbf{w}_c}\mathbb{1}_{\mathbf{w}\neq\varepsilon} \text{ balanced}\\ &+t\mathsf{U}_\varepsilon\left(\sum_{\substack{\mathbf{u}=\mathbf{vw}\\ 2\le|\mathbf{u}|\le 2k\\ \mathbf{u}\text{ balanced}}} x^{|\mathbf{u}|/2}\mathsf{U}'_{\mathbf{u}_s} + \frac{x}{x-1}\left(\mathsf{U}'^x_{\mathbf{w}} - x^k\mathsf{U}'_{\mathbf{w}}\right) - \frac{x}{x-1}\sum_{\substack{\mathbf{u}=\mathbf{vw}\\ |\mathbf{u}|\le 2k-2}} \mathsf{T}'_{\mathbf{u}}(x^{|\mathbf{u}|/2}-x^k)\right).\end{aligned} \tag{4.41}$$

The first line counts orientations obtained by adding a loop, and the second those obtained by a split.

Remark 4.17. As in the previous section, we can use (4.39) to replace (4.41) by a slightly lighter equation:

$$\begin{aligned}\mathsf{U}'^x_{\mathbf{w}} = x^{|\mathbf{w}|/2}\mathsf{T}'_{\mathbf{w}} &+ 2tx\mathsf{U}^x_\varepsilon\mathbb{1}_{\mathbf{w}=\varepsilon} + tx\mathsf{U}^x_{\mathbf{w}_p}\mathbb{1}_{\mathbf{w}\neq\varepsilon} + t\mathsf{U}_\varepsilon\left(\sum_{\substack{\mathbf{u}=\mathbf{vw}\\ |\mathbf{u}|\le 2k-1\\ \mathbf{u}\text{ quasi-balanced}}} x^{(1+|\mathbf{u}|)/2}\mathsf{U}'_{\mathbf{u}}\right.\\ &\left.+\frac{x}{x-1}\left(\mathsf{U}'^x_{\mathbf{w}} - x^k\mathsf{U}'_{\mathbf{w}}\right) - \frac{x}{x-1}\sum_{\substack{\mathbf{u}=\mathbf{vw}\\ |\mathbf{u}|\le 2k-2}} \mathsf{T}'_{\mathbf{u}}(x^{|\mathbf{u}|/2}-x^k)\right).\end{aligned} \tag{4.42}$$

Proposition 4.18. Consider the collection of equations consisting of:

- Equation (4.38), written for all balanced words $\mathbf{w}$ of length between 2 and $2k-4$,
- Equation (4.39), written for all balanced words $\mathbf{w}$ of length between 2 and $2k-2$,
- Equation (4.40), written for all valid words $\mathbf{w}$ of length at most $2k-2$,
- Equation (4.42), written for all valid words $\mathbf{w}$ of length at most $2k-1$.

In this collection, replace all trivial T- and T'-series by their value: $\mathsf{T}_{\mathbf{w}} = \mathsf{T}'_{\mathbf{w}} = 0$ when $\mathbf{w}$ is not balanced, $\mathsf{T}_\varepsilon = 1$, $\mathsf{T}'_\varepsilon = 0$. Let R_0 denote the resulting system. The number of series it involves is $2f(k) - 3\binom{2k}{k} - \binom{2k-2}{k-1}\mathbb{1}_{k>1}$, where $f(k)$ is given by (4.7). Moreover, R_0 defines uniquely all these series. Its size can be (roughly) divided by two upon exploiting the $0/1$ symmetry.

The proof is similar to the proofs of Propositions 4.1 and 4.7.

Remark 4.19. As always, we can alternatively write forward equations:

$$\mathsf{U}^x_{\mathbf{w}} = x^{|\mathbf{w}|/2}\mathsf{T}_{\mathbf{w}} + \mathsf{U}^x_{0\mathbf{w}} + \mathsf{U}^x_{1\mathbf{w}}, \qquad \mathsf{U}'^x_{\mathbf{w}} = x^{|\mathbf{w}|/2}\mathsf{T}'_{\mathbf{w}} + \mathsf{U}'^x_{0\mathbf{w}} + \mathsf{U}'^x_{1\mathbf{w}}.$$

4.5.2 Algebraicity

The analogue of Proposition 4.14 holds for the supersets obtained via the prime decomposition.

> **Proposition 4.20.** For any $k \geq 1$, the generating function $\mathsf{U}^{(k)}_\varepsilon(t;x)$ that counts orientations of $\mathbb{U}^{(k)}$ is algebraic.

Proof. Again, the idea is to apply Theorem 4.13 to the system of Proposition 4.18, after writing $x = 1+z$. The proof is roughly the same as that of Proposition 4.14: we define a polynomial system involving two variables, t and z, and six families of unknowns $A_{\mathbf{w}}$, $A'_{\mathbf{w}}$, $B_{\mathbf{w}}$, $B'_{\mathbf{w}}$, $C_{\mathbf{w}}$, $C'_{\mathbf{w}}$. The equations they satisfy are those of Proposition 4.18, rewritten with

$$\mathsf{T}_{\mathbf{w}} \to A_{\mathbf{w}}, \qquad \mathsf{T}'_{\mathbf{w}} \to A'_{\mathbf{w}}, \qquad \mathsf{U}^x_{\mathbf{w}} \to B_{\mathbf{w}},$$
$$\mathsf{U}'^x_{\mathbf{w}} \to B'_{\mathbf{w}}, \qquad \mathsf{U}_{\mathbf{w}} \to C_{\mathbf{w}}, \qquad \mathsf{U}'_{\mathbf{w}} \to C'_{\mathbf{w}}.$$

In fact, the only series $\mathsf{U}_{\mathbf{w}}$ occurring in our system is U_ε, so that the polynomial system we construct involves C_ε, but no other C-series. The prescribed dependences are that the A, A', C and C' series are independent of z. For instance, when $k=1$ we convert (4.43) into:

$$\begin{cases} B_\varepsilon &= 1 + B_\varepsilon B'_\varepsilon, \\ B'_\varepsilon &= 2t(1+z)B_\varepsilon + tC_\varepsilon\left(2(1+z)C'_0 + \frac{1+z}{z}(B'_\varepsilon - (1+z)C'_\varepsilon)\right), \\ B'_0 &= t(1+z)B_\varepsilon + tC_\varepsilon\left((1+z)C'_0 + \frac{1+z}{z}(B'_0 - (1+z)C'_0)\right). \end{cases}$$

However, this is not sufficient, because this system does not imply that C_ε is B_ε at $z=0$ (it does however imply that C'_ε is B'_ε at $z=0$, and similarly for C'_0 and B'_0). Hence, in order to apply Popescu's theorem, we need to add to our collection of equations the case $x=1$, $\mathbf{w}=\varepsilon$ of (4.40), namely $C_\varepsilon = 1 + C_\varepsilon C'_\varepsilon$. The rest of the argument mimics the proof of Proposition 4.14. □

4.5.3 Examples

The case $k=1$.

When $k=1$, the system of Proposition 4.18 contains $2f(1) - 3\cdot 2 = 4$ equations. Upon exploiting the $0/1$ symmetry, it reads:

$$\begin{cases} \mathsf{U}^x_\varepsilon &= 1 + \mathsf{U}^x_\varepsilon \mathsf{U}'^x_\varepsilon, \\ \mathsf{U}'^x_\varepsilon &= 2tx\mathsf{U}^x_\varepsilon + t\mathsf{U}_\varepsilon\left(2x\mathsf{U}'_0 + \frac{x}{x-1}(\mathsf{U}'^x_\varepsilon - x\mathsf{U}'_\varepsilon)\right), \\ \mathsf{U}'^x_0 &= tx\mathsf{U}^x_\varepsilon + t\mathsf{U}_\varepsilon\left(x\mathsf{U}'_0 + \frac{x}{x-1}(\mathsf{U}'^x_0 - x\mathsf{U}'_0)\right). \end{cases} \tag{4.43}$$

The second equation can be replaced by the forward equation $\mathsf{U}'^x_\varepsilon = 2\mathsf{U}'^x_0$.

In the second equation, replace U^x_ε by $1/(1-\mathsf{U}'^x_\varepsilon)$, U_ε by $1/(1-\mathsf{U}'_\varepsilon)$ and U'_0 by $\mathsf{U}'_\varepsilon/2$. This gives a polynomial equation involving only $\mathsf{U}'^x_\varepsilon$ and U'_ε, which can be solved by the quadratic method already used in Section 4.4.3. This gives for U'_ε a cubic equation. Getting back to $\mathsf{U}_\varepsilon = 1/(1-\mathsf{U}'_\varepsilon)$, we obtain for the generating function $\mathsf{U}^{(1)}_\varepsilon$ of orientations in $\mathbb{U}^{(1)}$ the same cubic equation (4.31) as for orientations of $\mathcal{U}^{(1)}$. In fact, one can check that $\mathbb{U}^{(1)} = \mathcal{U}^{(1)}$. Of course, the upper bound on μ is $\bar{\mu}_1 = \mu_1 = 13.0659\ldots$

The case $k = 2$.

When $k = 2$, the system of Proposition 4.18 contains $2f(2) - 3\cdot 6 - 2 = 22$ equations. Upon exploiting the $0/1$ symmetry and the forward equations, it reads:

$$\begin{cases}
\mathsf{T}'_{01} &= t + t\mathsf{U}_\varepsilon\mathsf{U}'_1\\
\mathsf{U}^x_\varepsilon &= 1 + \mathsf{U}^x_\varepsilon\mathsf{U}'^x_\varepsilon\\
\mathsf{U}^x_0 &= \mathsf{U}^x_\varepsilon\mathsf{U}'^x_0\\
\mathsf{U}^x_{10} = \mathsf{U}^x_{01} &= \mathsf{U}^x_\varepsilon\mathsf{U}'^x_{10}\\
\mathsf{U}^x_{00} = \mathsf{U}^x_{11} &= \mathsf{U}^x_\varepsilon\mathsf{U}'^x_{00}\\
\mathsf{U}'^x_\varepsilon &= 2\mathsf{U}'^x_0\\
\mathsf{U}'^x_0 = \mathsf{U}'^x_1 &= tx\mathsf{U}^x_\varepsilon + t\mathsf{U}_\varepsilon\Big(x\mathsf{U}'_0 + x^2(\mathsf{U}'_{100}+\mathsf{U}'_{010}+\mathsf{U}'_{110})\\
&\qquad\qquad + \tfrac{x}{x-1}(\mathsf{U}'^x_0 - x^2\mathsf{U}'_0) + x^2\mathsf{T}'_{10}\Big)\\
\mathsf{U}'^x_{10} = \mathsf{U}'^x_{01} &= x\mathsf{T}'_{10} + \mathsf{U}'^x_{110} + \mathsf{U}'^x_{010}\\
&= x\mathsf{T}'_{10} + tx\mathsf{U}^x_1 + t\mathsf{U}_\varepsilon\Big(x^2\mathsf{U}'_{010} + x^2\mathsf{U}'_{110}\\
&\qquad\qquad + \tfrac{x}{x-1}(\mathsf{U}'^x_{10} - x^2\mathsf{U}'_{10}) + x^2\mathsf{T}'_{10}\Big)\\
\mathsf{U}'^x_{00} &= tx\mathsf{U}^x_0 + t\mathsf{U}_\varepsilon\left(x^2\mathsf{U}'_{100} + \tfrac{x}{x-1}(\mathsf{U}'^x_{00} - x^2\mathsf{U}'_{00})\right)\\
\mathsf{U}'^x_{100} &= tx\mathsf{U}^x_{10} + t\mathsf{U}_\varepsilon\left(x^2\mathsf{U}'_{100} + \tfrac{x}{x-1}(\mathsf{U}'^x_{100} - x^2\mathsf{U}'_{100})\right)\\
\mathsf{U}'^x_{010} &= tx\mathsf{U}^x_{01} + t\mathsf{U}_\varepsilon\left(x^2\mathsf{U}'_{010} + \tfrac{x}{x-1}(\mathsf{U}'^x_{010} - x^2\mathsf{U}'_{010})\right)\\
\mathsf{U}'^x_{110} &= tx\mathsf{U}^x_{11} + t\mathsf{U}_\varepsilon\left(x^2\mathsf{U}'_{110} + \tfrac{x}{x-1}(\mathsf{U}'^x_{110} - x^2\mathsf{U}'_{110})\right).
\end{cases} \tag{4.44}$$

It can be reduced to a system of three equations defining the series U'_ε, U'_{10} and U'_{100}:

$$\begin{cases}
\mathsf{U}'^x_\varepsilon &= 2tx\mathsf{U}^x_\varepsilon + t\mathsf{U}_\varepsilon\left(x\mathsf{U}'_\varepsilon + 2x^2(\mathsf{U}'_{100}+\mathsf{U}'_{10}) + \tfrac{x}{x-1}(\mathsf{U}'^x_\varepsilon - x^2\mathsf{U}'_\varepsilon)\right)\\
\mathsf{U}'^x_{10} &= xt(1+\mathsf{U}_\varepsilon\mathsf{U}'_\varepsilon/2) + tx(\mathsf{U}^x_\varepsilon - 1)/2 + t\mathsf{U}_\varepsilon\left(x^2\mathsf{U}'_{10} + \tfrac{x}{x-1}(\mathsf{U}'^x_{10} - x^2\mathsf{U}'_{10})\right)\\
\mathsf{U}'^x_{100} &= tx\mathsf{U}^x_{10} + t\mathsf{U}_\varepsilon\left(x^2\mathsf{U}'_{100} + \tfrac{x}{x-1}(\mathsf{U}'^x_{100} - x^2\mathsf{U}'_{100})\right),
\end{cases} \tag{4.45}$$

in which we inject

$$\mathsf{U}_\varepsilon = \frac{1}{1-\mathsf{U}'_\varepsilon}, \qquad \mathsf{U}^x_\varepsilon = \frac{1}{1-\mathsf{U}'^x_\varepsilon} \qquad \text{and} \qquad \mathsf{U}^x_{10} = \frac{\mathsf{U}'^x_{10}}{1-\mathsf{U}'^x_\varepsilon}. \tag{4.46}$$

We lighten notation by denoting $A = \mathsf{U}'^{x}_{\varepsilon}$, $A_1 = \mathsf{U}'_{\varepsilon}$, $B = \mathsf{U}'^{x}_{10}$, $B_1 = \mathsf{U}'_{10}$, $C = \mathsf{U}'^{x}_{100}$ and $C_1 = \mathsf{U}'_{100}$, and we follow the steps used in Section 4.4.3 to solve System (4.32). Again, we refer to our web pages for the corresponding Maple session. The intermediate steps are as follows. We first apply the quadratic method to the first equation. We then turn to the second one. The equation satisfied by X is

$$X = 1 + \frac{t}{1 - t - A_1},$$

(Note that it gives X explicitly in terms of A_1, whereas we had a quadratic equation (4.36) in the previous case.) We then derive

$$A_2 := \mathsf{U}'_{\varepsilon}(X) = 1 + t\,\frac{1 - A_1}{t - 2B_1(1 - A_1)}.$$

We finally consider the third equation of (4.45) (after injecting (4.46)), and derive:

$$B_2 := \mathsf{U}'_{10}(X) = (1 - A_2)C_1/t\,.$$

Then it follows from the second equation that:

$$A'_2 := \frac{\partial \mathsf{U}'_{\varepsilon}}{\partial x}(X) = \frac{2(1 - A_1)(1 - t - A_1)^2((1 - t - A_1)C_1 + 2(-1 + A_1)B_1^2 + tB_1)}{(t - 2B_1(1 - A_1))^3}.$$

At the end, we obtain an equation of degree 28 for $A_1 = \mathsf{U}'_{\varepsilon}$, and then for U_{ε}. Its dominant coefficient does not vanish away from 0, and its discriminant has only one root in $[1/10, 1/16]$ (where we know that the radius must be found), around 0.0766. This gives the upper bound $\bar{\mu}_2 = 13.047\ldots$ on the growth rate μ of Eulerian orientations. From numerical estimates of the singular exponent, we predict that the series has again a "planar map" singularity in $(1 - \bar{\mu}_2 t)^{3/2}$.

For $k = 3$, 4 and 5, we have generated our systems of equations and computed the first 100 coefficients of $\mathsf{U}^{(k)}_{\varepsilon}(t; x)$. From this we get the estimates of the growth rates $\bar{\mu}_k$ shown in Table 4.3. The singularity still appears to be in $(1 - \bar{\mu}_k t)^{3/2}$. We conjecture that this holds for any k.

Conjecture 4.21. For every k, the algebraic series $\mathsf{U}^{(k)}_{\varepsilon}(t; 1)$ that counts orientations of $\mathbb{U}^{(k)}$ has a unique dominant singularity $\bar{\tau}_k = 1/\bar{\mu}_k$ which is of the planar map type: as t approaches $\bar{\tau}_k$ from below,

$$\mathsf{U}^{(k)}_{\varepsilon}(t; 1) = c_0 + c_1(1 - \mu_k t) + c_2(1 - \bar{\mu}_k t)^{3/2}\big(1 + o(1)\big)$$

for $c_2 \neq 0$.

4.6 Conclusion and outlook

In this chapter, we studied the enumeration of particular orientations, namely planar Eulerian orientations. Despite the apparent complexity of the question, we used

a variant of the standard decomposition of orientations allowing us to compute exactly the number o_n of Eulerian orientations having n edges for $n \leq 15$. We defined subsets and supersets of planar Eulerian orientations, each time based on two different decompositions. For each set, we give a system of functional equations defining its generating function, and we prove that the resulting series are all algebraic. The coefficients of the subsets have a tree-like asymptotic behaviour in $\lambda^n n^{-3/2}$, whereas we are reduced to conjecture a map-like asymptotic behaviour in $\lambda^n n^{-5/2}$ for the supersets. This way, we show that the growth rate of planar Eulerian orientations is between 11.56 and 13.005.

The enumeration of planar Eulerian orientations seems difficult, but another decomposition (which is yet to be found) of the orientations may lead to a simpler algorithm to generate the sequence of numbers o_n. Moreover, we did not find any equi-enumeration between planar Eulerian orientations and other known combinatorial classes. Finding such equi-enumerations (or even bijections!) would lead to a better understanding of the structure of these objects. A third interesting way to apprehend planar Eulerian orientations would be to specialize them to maps equipped with their minimal Eulerian orientation and to see if this set is simpler to count or has bijections with known combinatorial objects.

We also think that counting Eulerian orientations of 4-regular (or 4-valent) maps might be simpler than Eulerian ones. In such orientations, each vertex has two in-edges and two out-edges, so that counting Eulerian orientations means solving the so-called *ice-model* on (random) 4-regular maps [Bax82, Chap. 8]. The number of Eulerian orientations of a 4-regular map is known to be a third of the number of proper 3-colorings of its dual [Wel99], so counting these orientations is equivalent to counting 3-colored planar quadrangulations. It is known that 3-colored maps and 3-colored maximal planar graphs have algebraic generating functions [BBM11; BDFG02b; Tut95; Tut63a], so this could also hold for 3-colored quadrangulations, and for Eulerian orientations of 4-regular maps. Several results on this problem appear in the physics literature, but there does not seem to be an explicit exact solution at the moment [Kos00; ZJ00].

Conclusion

Throughout this thesis, we studied various problems on planar graphs and used their properties, in an algorithmical, enumerative, as well as structural point of view. We now recall our main results and present some global perspectives.

In Chapter 2, we studied *non-aligned planar drawings*. Although they appear as a step in the construction of other types of drawings, their properties had not been considered per se. We present a characterization of maximal planar graphs with minimal straight-line planar non-aligned drawings, as well as two polynomial algorithms for minimal polyline planar non-aligned drawings (creating respectively $n-3$ and at most $\frac{2n-5}{3}$ bends). In particular, 4-connected graphs have minimal non-aligned drawings with at most one bend. We also give upper bounds on the size of a minimal grid for straight-line planar non-aligned drawings, with two constructions reaching $O(n^4)$ area.

One interesting research direction would be to try and apply the non-aligned property to other kinds of planar drawings, such as *convex drawings*, in which each face of the graph must be drawn in a convex way (strictly or not). As Andrews [And63] showed, a strictly convex straight-line grid drawing of a cycle with n vertices requires area $\Omega(n^3)$. Since a minimal non-aligned drawing uses area $O(n^2)$, there is no strictly convex minimal straight-line non-aligned drawing of the cycle C_n for large n. However, we can ask what is the minimal size of a grid supporting a convex (or strictly convex) straight-line non-aligned drawing for any planar graph.

Non-aligned drawings originally appeared in the context of visualization of large graphs (not necessarily planar ones). For these graphs, the main feature of the final drawing we are interested in is not planarity. There are many parameters one may want to take into account, such as minimizing the total length of edges in the drawing (following what has been done for L-drawings [Ang+16]) or making topological structures appear. For example, we know that small-world graphs [BA99; WS98] have a high clustering coefficient, meaning that the vertices tend to form "communities", or clusters. It would be interesting to look for an algorithm computing the best arrangement of the vertices of a small-world graph in a non-aligned drawing in order to visualize these clusters.

Chapter 3 deals first with *power domination*, both on maximal planar graphs and on triangular grids. We first show that every maximal planar graph with n vertices has a power dominating set of order at most $\frac{n-2}{4}$. Our proof relies on different

properties of (maximal) planar graphs, and although going through tedious case analysis, it provides useful ingredients for further study of power domination in maximal planar graphs. We also show that the power domination number of a triangular grid with dimension k is $\lceil \frac{k}{3} \rceil$.

One natural continuity of our studies would be to try and apply the methods used on triangular grids to other grids, like n-dimensional grids or other kinds of lattices. It would also be interesting to study power domination in general products of graphs (other than paths), and this way extend the results already known [VV16], in particular by finding sharp lower bounds.

There are also questions still open about the complexity of POWER DOMINATING SET (and DOMINATING SET) in maximal planar graphs. In particular, it would be interesting to look for the existence of a PTAS for POWER DOMINATING SET on planar graphs.

Another avenue of research is the further examination of other variants of power domination, in particular generalized power-domination [CDMR12] (in which a monitored vertex can propagate as soon as less than k of its vertices are not monitored).

Chapter 4 relates to the enumeration of planar Eulerian orientations. This problem proves to be tough, and even if we do not exhibit a recurrence equation on the number of Eulerian orientations with a finite number of parameters, we used many different techniques to try and better understand the combinatorial properties of these objects. In particular, we propose a so-called prime decomposition of maps which we use to compute the first terms of the counting sequence. We then approximate the growth rate μ of planar Eulerian orientations by generating algebraic systems of series for supersets and subsets of the original family, and we subsequently show that $11.56 \leq \mu \leq 13.005$.

The general method used in our studies may be used to approximate the behaviour of counting sequences of other combinatorial classes that are known to be difficult to study. For instance, we could try to put our method into practice on the enumeration of meanders, which we crossed paths with when working on planar Eulerian orientations.

In Sections 4.2.3 and 4.3.3, we use a general result about positive irreducible systems of polynomial equations to prove that the generating functions of our subsets of Eulerian orientations have a square-root singularity. Could one define a notion of positive irreducible system of polynomial equations *with divided differences* whose solutions would systematically exhibit a singularity in $(1-\mu t)^{3/2}$? Hopefully this would apply to our supersets of orientations and prove Conjectures 4.15 and 4.21. A first step in this direction, applicable to a single equation, is achieved in [DN11].

Finally, the original goal of the enumeration of planar Eulerian orientations was to discover equi-enumerations between this family and other combinatorial classes, and later to build bijections. We did not achieve this goal, but finding bijections is one of the research perspectives we would like to follow in later work.

Bibliography

References for Introduction and Preliminaries

[AABB11] Y.-Y. Ahn, S. E. Ahnert, J. P. Bagrow, and A.-L. Barabási. "Flavor network and the principles of food pairing". *Scientific reports* 1 (2011) (cit. on pp. 2, 10).

[DFPP90] H. De Fraysseix, J. Pach, and R. Pollack. "How to draw a planar graph on a grid". *Combinatorica* 10.1 (1990), pp. 41–51 (cit. on pp. 5, 12, 30, 33, 44, 55, 58, 62).

[Eul41] L. Euler. "Solutio problematis ad geometriam situs pertinentis (The solution of a problem relating to the geometry of position)". *Commentarii academiae scientiarum Petropolitanae* 8 (1741), pp. 128–140 (cit. on pp. 7, 14).

[FS09] P. Flajolet and R. Sedgewick. *Analytic combinatorics*. Cambridge University Press, 2009 (cit. on pp. 27, 28, 114, 116, 117, 122, 124).

[Fá48] I. Fáry. "On straight-line representing of planar graphs". *Acta Sci. Math. Szeged* 11 (1948), pp. 229–233 (cit. on pp. 3, 11, 30).

[GNR08] J. Guo, R. Niedermeier, and D. Raible. "Improved algorithms and complexity results for power domination in graphs". *Algorithmica* 52.2 (2008), pp. 177–202 (cit. on pp. 5, 12, 68).

[HHHH02] T. W. Haynes, S. M. Hedetniemi, S. T. Hedetniemi, and M. A. Henning. "Domination in graphs applied to electric power networks". *SIAM Journal on Discrete Mathematics* 15.4 (2002), pp. 519–529 (cit. on pp. 5, 13, 66–68).

[HW73] C. Hierholzer and C. Wiener. "Ueber die Möglichkeit, einen Linienzug ohne Wiederholung und ohne Unterbrechung zu umfahren". *Math. Ann.* 6.1 (1873), pp. 30–32 (cit. on p. 14).

[Kur30] C. Kuratowski. "Sur le problème des courbes gauches en topologie". *Fundamenta mathematicae* 15.1 (1930), pp. 271–283 (cit. on p. 21).

[MT96] L. R. Matheson and R. E. Tarjan. "Dominating sets in planar graphs". *European J. Combin.* 17.6 (1996), pp. 565–568 (cit. on pp. 5, 66, 68, 70).

[Pui50] V. Puiseux. "Recherches sur les fonctions algébriques." *Journal de Mathématiques Pures et Appliquées* (1850), pp. 365–480 (cit. on p. 28).

[Sch89] W. Schnyder. "Planar graphs and poset dimension". *Order* 5.4 (1989), pp. 323–343 (cit. on pp. 5, 12, 36, 101).

[Sch90] W. Schnyder. "Embedding planar graphs on the grid". *Symposium on Discrete Algorithms*. Vol. 90. 1990, pp. 138–148 (cit. on pp. 3, 5, 11, 12, 31, 33, 36, 58–61).

[Ste51] S. K. Stein. "Convex maps". *Proceedings of the American Mathematical Society* 2.3 (1951), pp. 464–466 (cit. on pp. 3, 11, 30).

[Tut68] W. T. Tutte. "On the enumeration of planar maps". *Bull. Amer. Math. Soc.* 74 (1968), pp. 64–74 (cit. on pp. 6, 13, 100, 103).

[Tut63a] W. T. Tutte. "A census of planar maps". *Canad. J. Math* 15.2 (1963), pp. 249–271 (cit. on pp. 6, 13, 100, 140).

[Wag36] K. Wagner. "Bemerkungen zum Vierfarbenproblem." *Jahresbericht der Deutschen Mathematiker-Vereinigung* 46 (1936), pp. 26–32 (cit. on pp. 3, 11, 21, 30).

[Zei00] D. Zeilberger. "The Umbral Transfer-Matrix Method: I. Foundations". *J. Comb. Theory, Ser. A* 91 (2000), pp. 451–463 (cit. on p. 26).

References for Chapter 2

[AB12] S. Alamdari and T. Biedl. "Planar Open Rectangle-of-Influence Drawings with Non-aligned Frames". *Graph Drawing (GD'11)*. Vol. 7034. LNCS. Springer-Verlag, 2012, pp. 14–25 (cit. on p. 32).

[Ang+16] P. Angelini, G. Da Lozzo, M. Di Bartolomeo, V. Di Donato, M. Patrignani, V. Roselli, and I. G. Tollis. "L-drawings of directed graphs". *International Conference on Current Trends in Theory and Practice of Informatics*. Springer. 2016, pp. 134–147 (cit. on pp. 32, 141).

[AH77] K. Appel and W. Haken. "Every planar map is four colorable. I. Discharging." *Illinois J. Math.* 21.3 (1977), pp. 429–490 (cit. on p. 53).

[AP13] D. Archambault and H. C. Purchase. "Mental map preservation helps user orientation in dynamic graphs". *Graph Drawing*. Springer. 2013, pp. 475–486 (cit. on p. 31).

[ABDP15] D. Auber, N. Bonichon, P. Dorbec, and C. Pennarun. "Rook-drawing for Plane Graphs". *Proceedings of the* 23^{rd} *International Symposium on Graph Drawing and Network Visualization (GD 2015)*. Volume 9411 of Lecture Notes in Computer Science. 2015, pp. 180–191 (cit. on p. 33).

[ABDP17] D. Auber, N. Bonichon, P. Dorbec, and C. Pennarun. "Rook-drawings for plane graphs". *Journal of Graph Algorithms and Applications* 21.1 (2017), pp. 103–120 (cit. on p. 33).

[BGETT99] D. Battista G, P. Eades, I. G. Tollis, and R. Tamassia. *Graph drawing: algorithms for the visualization of graphs*. 1999 (cit. on p. 29).

[BRSG07] C. Bennett, J. Ryall, L. Spalteholz, and A. Gooch. "The aesthetics of graph visualization." *Computational Aesthetics* 2007 (2007), pp. 57–64 (cit. on p. 29).

[BBDL01] T. Biedl, P. Bose, E. Demaine, and A. Lubiw. "Efficient Algorithms for Petersen's theorem". *J. Algorithms* 38.1 (2001), pp. 110–134 (cit. on pp. 52, 53).

[BBM99] T. Biedl, A. Bretscher, and H. Meijer. "Rectangle of Influence Drawings of Graphs without Filled 3-Cycles". *Graph Drawing (GD'99)*. Vol. 1731. LNCS. Springer-Verlag, 1999, pp. 359–368 (cit. on pp. 45, 49).

[BKK97] T. Biedl, G. Kant, and M. Kaufmann. "On Triangulating Planar Graphs under the Four-Connectivity Constraint". *Algorithmica* 19.4 (1997), pp. 427–446 (cit. on p. 48).

[BD16] T. Biedl and M. Derka. "The (3,1)-ordering for 4-connected planar triangulations". *Journal of Graph Algorithms and Applications* 20.2 (2016), pp. 347–362 (cit. on p. 45).

[BK97] T. Biedl and M. Kaufmann. "Area-efficient static and incremental graph drawings". *European Symposium on Algorithms*. Springer. 1997, pp. 37–52 (cit. on p. 32).

[BP] T. Biedl and C. Pennarun. *Non-aligned drawings for planar graphs*. In press (cit. on p. 33).

[BP16] T. Biedl and C. Pennarun. "Non-aligned drawings for planar graphs". *Proceedings of the* 24^{th} *International Symposium on Graph Drawing and Network Visualization (GD 2016)*. Volume 9801 of Lecture Notes in Computer Science. 2016, pp. 131–143 (cit. on p. 33).

[BGH11] N. Bonichon, C. Gavoille, and N. Hanusse. "An information-theoretic upper bound on planar graphs using well-orderly maps". *Towards an Information Theory of Complex Networks*. Springer, 2011, pp. 17–46 (cit. on p. 37).

[BLSM02] N. Bonichon, B. Le Saëc, and M. Mosbah. "Optimal area algorithm for planar polyline drawings". *Graph-Theoretic Concepts in Computer Science*. Springer. 2002, pp. 35–46 (cit. on pp. 31, 36, 37, 62).

[Car+15] J. Cardinal, M. Hoffmann, V. Kusters, C. Tóth, and M. Wettstein. "Arc Diagrams, Flip Distances, and Hamiltonian Triangulations". *Symp. Theoretical Aspects of Computer Science, STACS 2015*. Vol. 30. LIPIcs. 2015, pp. 197–210 (cit. on pp. 50, 54).

[CLL01] Y.-T. Chiang, C.-C. Lin, and H.-I. Lu. "Orderly spanning trees with applications to graph encoding and graph drawing". *Proceedings of the twelfth annual ACM-SIAM symposium on Discrete Algorithms, SODA 2001*. Society for Industrial and Applied Mathematics. 2001, pp. 506–515 (cit. on p. 36).

[CYN84] N. Chiba, T. Yamanouchi, and T. Nishizeki. "Linear algorithms for convex drawings of planar graphs". *Progress in graph theory* (1984), pp. 153–173 (cit. on p. 30).

[CK97] M. Chrobak and G. Kant. "Convex grid drawings of 3-connected planar graphs". *Internat. J. Comput. Geom. Appl.* 7.3 (1997), pp. 211–223 (cit. on p. 58).

[CN98] M. Chrobak and S.-I. Nakano. "Minimum-width grid drawings of plane graphs". *Computational Geometry* 11.1 (1998), pp. 29–54 (cit. on pp. 31, 44).

[CP96] M. K. Coleman and D. S. Parker. "Aesthetics-based Graph Layout for Human Consumption". *Software: Practice and Experience* 26.12 (1996), pp. 1415–1438 (cit. on pp. 29, 31).

[DFPP90] H. De Fraysseix, J. Pach, and R. Pollack. "How to draw a planar graph on a grid". *Combinatorica* 10.1 (1990), pp. 41–51 (cit. on pp. 5, 12, 30, 33, 44, 55, 58, 62).

[DG+14] E. Di Giacomo, W. Didimo, M. Kaufmann, G. Liotta, and F. Montecchiani. "Upward-rightward planar drawings". *Information, Intelligence, Systems and Applications, IISA 2014, The 5th International Conference on*. IEEE. 2014, pp. 145–150 (cit. on p. 33).

[DMPT14] W. Didimo, F. Montecchiani, E. Pallas, and I. G. Tollis. "How to visualize directed graphs: a user study". *Information, Intelligence, Systems and Applications, IISA 2014, The 5th International Conference on*. IEEE. 2014, pp. 152–157 (cit. on p. 32).

[DLT84] D. Dolev, F. Leighton, and H. Trickey. "Planar embedding of planar graphs". *Advances in Computing Research* 2 (1984), pp. 147–161 (cit. on pp. 31, 61, 62).

[ELMS91] P. Eades, W. Lai, K. Misue, and K. Sugiyama. *Preserving the mental map of a diagram*. Tech. rep. Technical Report IIAS-RR-91-16E, Fujitsu Laboratories, 1991 (cit. on p. 31).

[Fá48] I. Fáry. "On straight-line representing of planar graphs". *Acta Sci. Math. Szeged* 11 (1948), pp. 229–233 (cit. on pp. 3, 11, 30).

[GT91] H. Gabow and R. Tarjan. "Faster Scaling Agorithms for General Graph Matching Problems". *Journal of the ACM* 38 (1991), pp. 815–853 (cit. on p. 54).

[GJ83a] M. R. Garey and D. S. Johnson. "Crossing number is NP-complete". *SIAM Journal on Algebraic Discrete Methods* 4.3 (1983), pp. 312–316 (cit. on p. 29).

[He97] X. He. "Grid embedding of 4-connected plane graphs". *Discrete & Computational Geometry* 17.3 (1997), pp. 339–358 (cit. on p. 44).

[IS85] M. Ichino and J. Sklansky. "The relative neighborhood graph for mixed feature variables". *Pattern recognition* 18.2 (1985), pp. 161–167 (cit. on p. 44).

[Kan97] G. Kant. "A more compact visibility representation". *Internat. J. Comput. Geom. Appl.* 7.3 (1997), pp. 197–210 (cit. on p. 53).

[KW02] M. Kaufmann and R. Wiese. "Embedding Vertices at Points: Few Bends suffice for Planar Graphs". *Journal of Graph Algorithms and Applications* 6.1 (2002), pp. 115–129 (cit. on p. 50).

[KW03] M. Kaufmann and D. Wagner. *Drawing graphs: methods and models*. Vol. 2025. Springer, 2003 (cit. on p. 29).

[KT11] E. M. Kornaropoulos and I. G. Tollis. "Overloaded orthogonal drawings". *Graph Drawing*. Springer. 2011, pp. 242–253 (cit. on p. 32).

[KT12] E. M. Kornaropoulos and I. G. Tollis. "DAGView: an approach for visualizing large graphs". *Graph Drawing*. Springer. 2012, pp. 499–510 (cit. on p. 32).

[LLY03] C.-C. Liao, H.-I. Lu, and H.-C. Yen. "Compact floor-planning via orderly spanning trees". *Journal of Algorithms* 48.2 (2003), pp. 441–451 (cit. on p. 36).

[LLS04] C.-C. Lin, H.-I. Lu, and I.-F. Sun. "Improved compact visibility representation of planar graph via Schnyder's realizer". *SIAM Journal on Discrete Mathematics* 18.1 (2004), pp. 19–29 (cit. on p. 36).

[LLMW98] G. Liotta, A. Lubiw, H. Meijer, and S. Whitesides. "The rectangle of influence drawability problem". *Comput. Geom.* 10.1 (1998), pp. 1–22 (cit. on p. 45).

[MELS95] K. Misue, P. Eades, W. Lai, and K. Sugiyama. "Layout adjustment and the mental map". *Journal of visual languages and computing* 6.2 (1995), pp. 183–210 (cit. on p. 31).

[MNN01] K. Miura, S.-I. Nakano, and T. Nishizeki. "Grid drawings of 4-connected plane graphs". *Discrete & Computational Geometry* 26.1 (2001), pp. 73–87 (cit. on p. 44).

[MNRA11] D. Mondal, R. I. Nishat, M. S. Rahman, and M. J. Alam. "Minimum-area drawings of plane 3-trees". *Journal of Graph Algorithms and Applications* 15.2 (2011), pp. 177–204 (cit. on p. 63).

[PT90] F. N. Paulisch and W. F. Tichy. "EDGE: An extendible graph editor". *Software: Practice and Experience* 20.S1 (1990) (cit. on p. 31).

[Pet91] J. Petersen. "Die Theorie der regulären graphs (The theory of regular graphs)." *Acta Mathematica* 15 (1891), pp. 193–220 (cit. on p. 52).

[Pur97] H. C. Purchase. "Which aesthetic has the greatest effect on human understanding?" *International Symposium on Graph Drawing*. Springer. 1997, pp. 248–261 (cit. on p. 29).

[Pur02] H. C. Purchase. "Metrics for graph drawing aesthetics". *Journal of Visual Languages & Computing* 13.5 (2002), pp. 501–516 (cit. on p. 29).

[PCJ95] H. C. Purchase, R. F. Cohen, and M. James. "Validating graph drawing aesthetics". *International Symposium on Graph Drawing*. Springer. 1995, pp. 435–446 (cit. on p. 29).

[Rea87] R. C. Read. "A new method for drawing a planar graph given the cyclic order of the edges at each vertex". *Congressus Numerantium* 56 (1987), pp. 31–44 (cit. on p. 30).

[RSST97] N. Robertson, D. Sanders, P. Seymour, and R. Thomas. "The four-colour theorem". *J. Combin. Theory Ser. B* 70.1 (1997), pp. 2–44 (cit. on p. 54).

[Sch89] W. Schnyder. "Planar graphs and poset dimension". *Order* 5.4 (1989), pp. 323–343 (cit. on pp. 5, 12, 36, 101).

[Sch90] W. Schnyder. "Embedding planar graphs on the grid". *Symposium on Discrete Algorithms*. Vol. 90. 1990, pp. 138–148 (cit. on pp. 3, 5, 11, 12, 31, 33, 36, 58–61).

[Ste51] S. K. Stein. "Convex maps". *Proceedings of the American Mathematical Society* 2.3 (1951), pp. 464–466 (cit. on pp. 3, 11, 30).

[TDBB88] R. Tamassia, G. Di Battista, and C. Batini. "Automatic graph drawing and readability of diagrams". *IEEE Transactions on Systems, Man, and Cybernetics* 18.1 (1988), pp. 61–79 (cit. on p. 29).

[Tut63b] W. T. Tutte. "How to draw a graph". *Proc. London Math. Soc* 13.3 (1963), pp. 743–768 (cit. on p. 30).

[Ull84] J. D. Ullman. *Computational aspects of VLSI*. Computer Science Press, 1984 (cit. on p. 30).

[Val81] L. G. Valiant. "Universality considerations in VLSI circuits". *IEEE Transactions on Computers* 100.2 (1981), pp. 135–140 (cit. on p. 30).

[Wag36] K. Wagner. "Bemerkungen zum Vierfarbenproblem." *Jahresbericht der Deutschen Mathematiker-Vereinigung* 46 (1936), pp. 26–32 (cit. on pp. 3, 11, 21, 30).

References for Chapter 3

[AS09] A. Aazami and K. Stilp. "Approximation algorithms and hardness for domination with propagation". *SIAM Journal on Discrete Mathematics* 23.3 (2009), pp. 1382–1399 (cit. on p. 68).

[Bak94] B. Baker. "Approximation Algorithms for NP-Complete Problems on Planar Graphs". *J. ACM* 41.1 (1994), pp. 153–180 (cit. on p. 66).

[BMBA93] T. L. Baldwin, L. Mili, M. B. Boisen, and R. Adapa. "Power system observability with minimal phasor measurement placement". *IEEE Transactions on Power Systems* 8.2 (1993), pp. 707–715 (cit. on p. 66).

[BF11] R. Barrera and D. Ferrero. "Power domination in cylinders, tori, and generalized Petersen graphs". *Networks* 58.1 (2011), pp. 43–49 (cit. on p. 68).

[Ber62] C. Berge. *The Theory of Graphs and Its Applications*. Ed. by Methuen. London, 1962 (cit. on p. 65).

[BPV17] P. Bose, C. Pennarun, and S. Verdonschot. *Power domination in triangular grids*. 2017, accepted to the Canadian Conference on Computational Geometry (cit. on p. 69).

[BH05] D. J. Brueni and L. S. Heath. "The PMU placement problem". *SIAM Journal on Discrete Mathematics* 19.3 (2005), pp. 744–761 (cit. on p. 66).

[DGP17] P. Dorbec, A. González, and C. Pennarun. *Power domination in triangulations*. 2017, manuscript (cit. on p. 69).

[DK14] P. Dorbec and S. Klavžar. "Generalized Power Domination: Propagation Radius and Sierpiński Graphs". *Acta Applicandae Mathematicae* 134.1 (2014), pp. 75–86 (cit. on p. 97).

[DMKŠ08] P. Dorbec, M. Mollard, S. Klavžar, and S. Špacapan. "Power domination in product graphs". *SIAM J. Discrete Math.* 22.2 (2008), pp. 554–567 (cit. on pp. 68, 95).

[DVV16] P. Dorbec, S. Varghese, and A. Vijayakumar. "Heredity for generalized power domination". *Discrete Mathematics & Theoretical Computer Science* Vol. 18 no. 3 (Apr. 2016) (cit. on p. 97).

[Dor+13] P. Dorbec, M. A. Henning, C. Löwenstein, M. Montassier, and A. Raspaud. "Generalized power domination in regular graphs". *SIAM Journal on Discrete Mathematics* 27.3 (2013), pp. 1559–1574 (cit. on p. 68).

[DH06] M. Dorfling and M. A. Henning. "A note on power domination in grid graphs". *Discrete Applied Mathematics* 154.6 (2006), pp. 1023–1027 (cit. on p. 68).

[FVV11] D. Ferrero, S. Varghese, and A Vijayakumar. "Power domination in honeycomb networks". *Journal of Discrete Mathematical Sciences and Cryptography* 14.6 (2011), pp. 521–529 (cit. on pp. 68, 97).

[GJ79] M. R. Garey and D. S. Johnson. *Computers and intractability: a guide to the theory of NP-completeness*. Ed. by W. H. Freeman. San Francisco, 1979 (cit. on p. 66).

[GPRT11] D. Gonçalves, A. Pinlou, M. Rao, and S. Thomassé. "The domination number of grids". *SIAM Journal on Discrete Mathematics* 25.3 (2011), pp. 1443–1453 (cit. on p. 68).

[GNR08] J. Guo, R. Niedermeier, and D. Raible. "Improved algorithms and complexity results for power domination in graphs". *Algorithmica* 52.2 (2008), pp. 177–202 (cit. on pp. 5, 12, 68).

[HHHH02] T. W. Haynes, S. M. Hedetniemi, S. T. Hedetniemi, and M. A. Henning. "Domination in graphs applied to electric power networks". *SIAM Journal on Discrete Mathematics* 15.4 (2002), pp. 519–529 (cit. on pp. 5, 13, 66–68).

[HHS98a] T. W. Haynes, S. T. Hedetniemi, and P. J. Slater. *Domination in graphs: advanced topics*. Vol. 209. Monographs and Textbooks in Pure and Applied Mathematics. Marcel Dekker Inc., New York, 1998 (cit. on p. 66).

[HHS98b] T. W. Haynes, S. T. Hedetniemi, and P. J. Slater. *Fundamentals of domination in graphs*. Vol. 208. Monographs and Textbooks in Pure and Applied Mathematics. Marcel Dekker Inc., New York, 1998 (cit. on p. 66).

[Jae62] C. F. de Jaenisch. *Traité des applications de l'analyse mathématique au jeu des échecs. (Treatise on the applications of mathematical analysis to chess)*. St. Petersburg, 1862 (cit. on p. 65).

[KP10] E. L. King and M. J. Pelsmajer. "Dominating sets in plane triangulations". *Discrete Mathematics* 310.17 (2010), pp. 2221–2230 (cit. on p. 66).

[KMRR06] J. Kneis, D. Mölle, S. Richter, and P. Rossmanith. "Parameterized power domination complexity". *Information Processing Letters* 98.4 (2006), pp. 145–149 (cit. on p. 68).

[LL05] C.-S. Liao and D.-T. Lee. "Power domination problem in graphs". *Computing and Combinatorics*. Springer, 2005, pp. 818–828 (cit. on p. 68).

[LL13] C.-S. Liao and D.-T. Lee. "Power domination in circular-arc graphs". *Algorithmica* 65.2 (2013), pp. 443–466 (cit. on p. 68).

[MT96] L. R. Matheson and R. E. Tarjan. "Dominating sets in planar graphs". *European J. Combin.* 17.6 (1996), pp. 565–568 (cit. on pp. 5, 66, 68, 70).

[MBA90] L Mili, T Baldwin, and R Adapa. "Phasor measurement placement for voltage stability analysis of power systems". *Decision and Control, 1990., Proceedings of the 29th IEEE Conference on*. IEEE. 1990, pp. 3033–3038 (cit. on p. 66).

[Ore62] O. Ore. *Theory of graphs*. Ed. by A. M. Society. Vol. XXXVIII. American Mathematical Society Colloquium Publications. 1962 (cit. on p. 65).

[PTK86] A. Phadke, J. Thorp, and K. Karimi. "State estimation with phasor measurements". *IEEE Transactions on Power Systems* 1.1 (1986), pp. 233–238 (cit. on p. 66).

[Ree96] B. Reed. "Paths, stars and the number three". *Combinatorics, Probability and Computing* 5.3 (1996), pp. 277–295 (cit. on p. 66).

[SX09] M. Y. Sohn and Y. Xudong. "Domination in graphs of minimum degree four". *J. Korean Math. Soc* 46.4 (2009), pp. 759–773 (cit. on p. 66).

[XSC06] H.-M. Xing, L. Sun, and X.-G. Chen. "Domination in graphs of minimum degree five". *Graphs and Combinatorics* 22.1 (2006), pp. 127–143 (cit. on p. 66).

[XKSZ06] G. Xu, L. Kang, E. Shan, and M. Zhao. "Power domination in block graphs". *Theoretical Computer Science* 359.1 (2006), pp. 299–305 (cit. on p. 68).

[ZK07] M. Zhao and L. Kang. "Power domination in planar graphs with small diameter". *Journal of Shanghai University* 11 (2007), pp. 218–222 (cit. on p. 68).

[ZKC06] M. Zhao, L. Kang, and G. J. Chang. "Power domination in graphs". *Discrete Math.* 306.15 (2006), pp. 1812–1816 (cit. on p. 68).

References for Chapter 4

[AJ90] S. E. Alm and S. Janson. "Random self-avoiding walks on one-dimensional lattices". *Comm. Statist. Stochastic Models* 6.2 (1990), pp. 169–212 (cit. on p. 102).

[BMRR06] G. Barequet, M. Moffie, A. Ribó, and G. Rote. "Counting polyominoes on twisted cylinders". *Integers* 6 (2006), A22 (cit. on p. 102).

[Bax82] R. J. Baxter. *Exactly solved models in statistical mechanics*. London: Academic Press, Inc., 1982 (cit. on p. 140).

[BB09] O. Bernardi and N. Bonichon. "Intervals in Catalan lattices and realizers of triangulations". *J. Combin. Theory Ser. A* 116.1 (2009), pp. 55–75 (cit. on p. 101).

[BBM11] O. Bernardi and M. Bousquet-Mélou. "Counting colored planar maps: algebraicity results". *J. Combin. Theory Ser. B* 101.5 (2011), pp. 315–377 (cit. on pp. 101, 140).

[Bón97] M. Bóna. "Exact enumeration of 1342-avoiding permutations: a close link with labeled trees and planar maps". *J. Combin. Theory Ser. A* 80.2 (1997), pp. 257–272 (cit. on p. 100).

[Bon05] N. Bonichon. "A bijection between realizers of maximal plane graphs and pairs of non-crossing Dyck paths". *Discrete Math.* 298.1-3 (2005), pp. 104–114 (cit. on p. 101).

[BBMF08] N. Bonichon, M. Bousquet-Mélou, and E. Fusy. "Baxter permutations and plane bipolar orientations". *Sém. Lothar. Combin.* 61A (2008), Art. B61Ah (cit. on p. 101).

[BGH05] N. Bonichon, C. Gavoille, and N. Hanusse. "Canonical Decomposition of Outerplanar Maps and Application to Enumeration, Coding and Generation". *J. Graph Algorithms Appl.* 9.2 (2005), pp. 185–204 (cit. on p. 101).

[BBMDP17] N. Bonichon, M. Bousquet-Mélou, P. Dorbec, and C. Pennarun. "On the number of planar Eulerian orientations". *European Journal of Combinatorics* 65 (2017), pp. 59–91 (cit. on p. 102).

[BMJ06] M. Bousquet-Mélou and A. Jehanne. "Polynomial equations with one catalytic variable, algebraic series and map enumeration". *J. Combin. Theory Ser. B* 96 (2006), pp. 623–672 (cit. on pp. 128, 130).

[BMS00] M. Bousquet-Mélou and G. Schaeffer. "Enumeration of planar constellations". *Adv. in Appl. Math.* 24.4 (2000), pp. 337–368 (cit. on pp. 99, 100).

[BDFG02a] J. Bouttier, P. Di Francesco, and E. Guitter. "Census of planar maps: from the one-matrix model solution to a combinatorial proof". *Nuclear Phys. B* 645.3 (2002), pp. 477–499 (cit. on p. 100).

[BDFG02b] J. Bouttier, P. Di Francesco, and E. Guitter. "Counting Colored Random Triangulations". *Nucl.Phys. B* 641 (2002), pp. 519–532 (cit. on pp. 101, 140).

[BDFG04] J. Bouttier, P. Di Francesco, and E. Guitter. "Planar maps as labeled mobiles". *Electron. J. Combin.* 11.1 (2004), R69 (cit. on p. 100).

[BG90] R. Brak and A. J. Guttmann. "Algebraic approximants: a new method of series analysis". *J. Phys. A* 23.24 (1990), pp. L1331–L1337 (cit. on p. 125).

[Bro65] W. G. Brown. "On the existence of square roots in certain rings of power series". *Math. Ann.* 158 (1965), pp. 82–89 (cit. on p. 128).

[CADS08] L. Castelli Aleardi, O. Devillers, and G. Schaeffer. "Succinct representations of planar maps". *Theoret. Comput. Sci.* 408.2-3 (2008), pp. 174–187 (cit. on p. 101).

[CS04] P. Chassaing and G. Schaeffer. "Random planar lattices and integrated superBrownian excursion". *Probability Theory and Related Fields* 128.2 (2004), pp. 161–212 (cit. on p. 100).

[CV81] R. Cori and B. Vauquelin. "Planar maps are well-labeled trees". *Canad. J. Math* 33.5 (1981), pp. 1023–1042 (cit. on p. 100).

[DFGZJ95] P. Di Francesco, P. Ginsparg, and J. Zinn-Justin. "2D gravity and random matrices". *Phys. Rep.* 254.1-2 (1995), pp. 1–133 (cit. on p. 101).

[DN11] M. Drmota and M. Noy. "Universal exponents and tail estimates in the enumeration of planar maps". *Elec. Notes Discrete Math.* 38 (2011), pp. 309–317 (cit. on pp. 133, 142).

[Fau16] J.-C. Faugère. *Personal communication*. 2016 (cit. on p. 125).

[Fel04] S. Felsner. "Lattice structures from planar graphs". *Electron. J. Combin.* 11.1 (2004), R15 (cit. on p. 101).

[FFNO11] S. Felsner, É. Fusy, M. Noy, and D. Orden. "Bijections for Baxter families and related objects". *J. Combin. Theory Ser. A* 118.3 (2011), pp. 993–1020 (cit. on p. 101).

[FS59] M. E. Fisher and M. F. Sykes. "Excluded-volume problem and the Ising model of ferromagnetism". *Phys. Rev. (2)* 114 (1959), pp. 45–58 (cit. on p. 102).

[FS09] P. Flajolet and R. Sedgewick. *Analytic combinatorics*. Cambridge University Press, 2009 (cit. on pp. 27, 28, 114, 116, 117, 122, 124).

[Fus09] É. Fusy. "Transversal structures on triangulations: a combinatorial study and straight-line drawings". *Discrete Math.* 309.7 (2009), pp. 1870–1894 (cit. on p. 101).

[FPS09] É. Fusy, D. Poulalhon, and G. Schaeffer. "Bijective counting of plane bipolar orientations and Schnyder woods". *European J. Combin.* 30.7 (2009), pp. 1646–1658 (cit. on p. 101).

[Fus12] É. Fusy. "Bijective Counting of Involutive Baxter Permutations". *Fundamenta Informaticae* 117.1-4 (2012), pp. 179–188 (cit. on p. 100).

[GJ83b] I. P. Goulden and D. M. Jackson. *Combinatorial enumeration*. Wiley-Interscience Series in Discrete Mathematics. New York: John Wiley & Sons Inc., 1983 (cit. on pp. 128, 130).

[Gut] A. J. Guttmann. *Personal communication*. March 2016 (cit. on p. 108).

[GJ09] A. J. Guttmann and I. Jensen. "Effect of confinement: polygons in strips, slabs and rectangles". *Polygons, polyominoes and polycubes*. Vol. 775. Lecture Notes in Phys. Springer, 2009, pp. 235–246 (cit. on p. 102).

[Jen03] I. Jensen. "Counting polyominoes: A parallel implementation for cluster computing". *Computational Science—Proc. ICCS 2003, Part III*. Ed. by P. M. A. S. et al. Vol. 2659. Lecture Notes in Computer Science. 2003 (cit. on p. 102).

[KR73] D. A. Klarner and R. L. Rivest. "A procedure for improving the upper bound for the number of n-ominoes". *Canad. J. Math.* 25 (1973), pp. 585–602 (cit. on p. 102).

[Kos00] I. K. Kostov. "Exact solution of the six-vertex model on a random lattice". *Nuclear Phys. B* 575.3 (2000), pp. 513–534 (cit. on p. 140).

[LG13] J.-F. Le Gall. "Uniqueness and universality of the Brownian map". *The Annals of Probability* 41.4 (2013), pp. 2880–2960 (cit. on p. 101).

[LW01] J. H. van Lint and R. M. Wilson. *A Course in Combinatorics*. Cambridge University Press, 2001 (cit. on pp. 108, 118).

[Men94] P. Ossona de Mendez. "Orientations bipolaires". PhD thesis. Paris: École des Hautes Études en Sciences Sociales, 1994 (cit. on p. 101).

[Mul67] R. C. Mullin. "On the enumeration of tree-rooted maps". *Canad. J. Math.* 19 (1967), pp. 174–183 (cit. on p. 101).

[OEI] OEIS Foundation Inc. "The On-Line Encyclopedia of Integer Sequences". http://oeis.org (cit. on p. 102).

[PWZ96] M. Petkovšek, H. S. Wilf, and D. Zeilberger. $A = B$. Wellesley, MA: A K Peters Ltd., 1996, pp. xii+212 (cit. on p. 112).

[PSS12] C. Pivoteau, B. Salvy, and M. Soria. "Algorithms for Combinatorial Structures: Well-founded systems and Newton iterations". *Journal of Combinatorial Theory, Series A* 119 (2012), pp. 1711–1773 (cit. on p. 125).

[PT00] A. Pönitz and P. Tittmann. "Improved upper bounds for self-avoiding walks in $\mathbf{Z}^d$". *Electron. J. Combin.* 7 (2000), R21 (cit. on p. 102).

[PS06] D. Poulalhon and G. Schaeffer. "Optimal coding and sampling of triangulations". *Algorithmica* 46.3-4 (2006), pp. 505–527 (cit. on p. 101).

[Pro] J. Propp. "Lattice structure for orientations of graphs". 1993. arXiv: math/0209005 (cit. on p. 101).

[SZ94] B. Salvy and P. Zimmermann. "Gfun: a Maple package for the manipulation of generating and holonomic functions in one variable". *ACM Transactions on Mathematical Software* 20.2 (1994), pp. 163–177 (cit. on p. 131).

[Sch97] G. Schaeffer. "Bijective Census and Random Generation of Eulerian Planar Maps with Prescribed Vertex Degrees". *The Electronic Journal of Combinatorics* 4.1 (1997), R20 (cit. on p. 100).

[Sch89] W. Schnyder. "Planar graphs and poset dimension". *Order* 5.4 (1989), pp. 323–343 (cit. on pp. 5, 12, 36, 101).

[Swa98] R. G. Swan. "Néron-Popescu desingularization." *Proceedings of the international conference on algebra and geometry, Taipei, Taiwan, 1995*. Cambridge, MA: International Press, 1998, pp. 135–192 (cit. on pp. 102, 128).

[Tut62a] W. T. Tutte. "A census of Hamiltonian polygons". *Canad. J. Math.* 14 (1962), pp. 402–417 (cit. on p. 100).

[Tut62b] W. T. Tutte. "A census of planar triangulations". *Canad. J. Math.* 14 (1962), pp. 21–38 (cit. on p. 100).

[Tut68] W. T. Tutte. "On the enumeration of planar maps". *Bull. Amer. Math. Soc.* 74 (1968), pp. 64–74 (cit. on pp. 6, 13, 100, 103).

[Tut73] W. T. Tutte. "Chromatic sums for rooted planar triangulations: the cases $\lambda = 1$ and $\lambda = 2$". *Canad. J. Math.* 25 (1973), pp. 426–447 (cit. on p. 101).

[Tut84] W. T. Tutte. "Map-colourings and differential equations". *Progress in graph theory (Waterloo, Ont., 1982)*. Toronto, ON: Academic Press, 1984, pp. 477–485 (cit. on p. 101).

[Tut95] W. T. Tutte. "Chromatic sums revisited". *Aequationes Math.* 50.1-2 (1995), pp. 95–134 (cit. on p. 140).

[Tut62c] W. T. Tutte. "A census of slicings". *Canad. J. Math* 14.4 (1962), pp. 708–722 (cit. on p. 100).

[Tut63a] W. T. Tutte. "A census of planar maps". *Canad. J. Math* 15.2 (1963), pp. 249–271 (cit. on pp. 6, 13, 100, 140).

[Wel99] D. Welsh. "The Tutte polynomial". *Random Structures Algorithms* 15.3-4 (1999). Statistical physics methods in discrete probability, combinatorics, and theoretical computer science (Princeton, NJ, 1997), pp. 210–228 (cit. on p. 140).

[ZJ00] P. Zinn-Justin. "The six-vertex model on random lattices". *Europhys. Lett.* 50.1 (2000), pp. 15–21 (cit. on p. 140).

References for Conclusion

[And63] G. E. Andrews. "A lower bound for the volume of strictly convex bodies with many boundary lattice points". *Transactions of the American Mathematical Society* (1963), pp. 270–279 (cit. on p. 141).

[Ang+16] P. Angelini, G. Da Lozzo, M. Di Bartolomeo, V. Di Donato, M. Patrignani, V. Roselli, and I. G. Tollis. "L-drawings of directed graphs". *International Conference on Current Trends in Theory and Practice of Informatics*. Springer. 2016, pp. 134–147 (cit. on pp. 32, 141).

[BA99] A.-L. Barabási and R. Albert. "Emergence of Scaling in Random Networks". *Science* 286.5439 (1999), pp. 509–512 (cit. on p. 141).

[CDMR12] G. J. Chang, P. Dorbec, M. Montassier, and A. Raspaud. "Generalized power domination of graphs". *Discrete Applied Mathematics* 160.12 (2012), pp. 1691–1698 (cit. on p. 142).

[DN11] M. Drmota and M. Noy. "Universal exponents and tail estimates in the enumeration of planar maps". *Elec. Notes Discrete Math.* 38 (2011), pp. 309–317 (cit. on pp. 133, 142).

[VV16] S. Varghese and A. Vijayakumar. "On the power domination number of graph products". *Conference on Algorithms and Discrete Applied Mathematics*. Springer. 2016, pp. 357–367 (cit. on p. 142).

[WS98] D. J. Watts and S. H. Strogatz. "Collective dynamics of 'small-world' networks". *Nature* 393.6684 (June 1998), pp. 440–442 (cit. on p. 141).